Nanofiltration of multi-solute systems: Solute interactions and theory.

Mandale, Stephen John

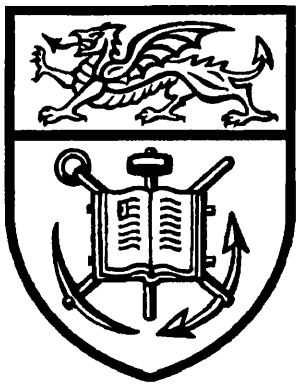

School of Engineering
University of Wales Swansea

Nanofiltration of Multi-Solute Systems: Solute Interactions and Theory

by

Stephen John Mandale
M. Eng. (Wales)

A Thesis Submitted in Fulfilment of the Requirement
for the Degree

DOCTOR OF PHILOSOPHY
Philosophiae Doctor (Ph.D.)

May 2005

SUMMARY

From the outset, membrane researchers have studied the behaviour and governing processes of membrane separations. Theoretical representation of membrane transport systems is central to membrane research and the most recent investigations have considered single and binary solute systems of charged and uncharged species. A gap in the research was detected with respect to systems of combined charged (dissociated) and uncharged (non-dissociated) species. Thus these systems were explored from both a practical-experimental and theoretical perspective.

The result of experimental investigation into combined systems of charged/uncharged solutes, was an observation of negative rejections for uncharged solutes in the presence of high salt concentrations. This is a phenomenon that was not observed elsewhere and in general the rejection of uncharged solutes was attributed to steric factors hence a direct interaction between salts and neutral solutes was not suggested.

The reliability of the negative rejection observations was established through a discussion of experimental error and a consideration of concentration polarisation. It was found that the error was negligible and that the measured negative rejections (approximately -10% in some cases) were not attributable to variation in the results caused by external influences. An analysis of concentration polarisation only served to amplify the negative rejection observed, since real rejection (that at the membrane surface) exhibited greater negativity than the observed rejection.

The observed phenomenon was discussed with respect to current forms of membrane transport theories. The semi-black box technique proposed by Spiegler and Kedem and later modified by Van der Bruggen and co-workers was found to provide a reasonable fit of the experimental data where valance was taken to be a non-integer fitting parameter. Errors in the Fortran implementation of the Bowen and Welfoot development of the Donnan Steric Partitioning Model (DSPM) prevented this transport theorem from being explored in relation to the measured phenomenon. Thus it was a recommendation of this work that this theory should be considered in more depth.

DECLARATION

This work has not previously been accepted in substance for any degree and is not being concurrently submitted in candidature for any degree.

Signed: .....(*Candidate*: Stephen John Mandale)
Date: .....21/12/05.....

STATEMENT 1

This thesis is the result of my own investigation, except where otherwise stated. Other sources are acknowledged by footnotes giving explicit references. A bibliography is appended.

Signed: .....(*Candidate*: Stephen John Mandale)
Date: .....21/12/05.....

Signed: .....(*Supervisor*: Dr M. G. Jones)
Date: .....

STATEMENT 2

I hereby give consent for my thesis, if accepted, to be available for photocopying and inter-library loan, and for the title and summary to be made available to outside organisations.

Signed: .....(*Candidate*: Stephen John Mandale)
Date: .....21/12/05.....

ACKNOWLEDGEMENTS

My acknowledgment, thanks and appreciation go to the following people:

My PhD Supervisor Meirion Jones for his continuous support, guidance and insight throughout the project.

Steven Moss who helped develop the control and data-logging program used on the filtration apparatus and provided material assistance and discussion during the research.

The Head of Department for Chemical and Biochemical Process Engineering at the University of Wales Swansea, Professor Paul Preece.

Professor Richard Bowen and all academic staff in the Department of Chemical and Biochemical Process Engineering

Darren Oatley and Julian Welfoot, who developed the Fortran based modelling programs discussed in this work.

The department technical staff,

Gary Tucket
Glyn Phillips
Adrian Jenkins

I would also like to give special thanks to my family, especially my Mum and Dad for supporting me through University and friends both in and outside of the Department.

I would also like to give special thanks to Michelle for her love, support, understanding and above all, patience!

Stephen Mandale

Contents

SUMMARY II

DECLARATION III

ACKNOWLEDGEMENTS IV

1 INTRODUCTION 6

1.1 HISTORY AND DEVELOPMENT OF FILTRATION 6

1.1.1 HISTORIC 6

1.1.2 MODERN WATER TREATMENT AND FILTRATION 8

1.1.3 MEMBRANE FILTRATION AND CONVENTIONAL FILTRATION – A COMPARISON 9

1.2 HISTORY AND DEVELOPMENT OF MEMBRANE FILTRATION 10

1.3 PRESENT STATE OF MEMBRANE FILTRATION TECHNOLOGY 12

1.3.1 APPLICATIONS 12

1.3.2 COMMERCIAL MEMBRANES 13

1.4 FUNDAMENTAL CONCEPTS IN PRESSURE DRIVEN MEMBRANE SEPARATIONS 13

1.4.1 MEMBRANE FORMATS 15

1.4.2 MEMBRANE PLANT CONFIGURATION 17

1.5 OBJECTIVES OF THE PRESENT WORK 18

2 LITERATURE REVIEW 20

2.1 MEMBRANE RESEARCH – EXPERIMENTAL INVESTIGATION 20

2.1.1 INTRODUCTION 20

2.2 SOLUTE TYPE AND NANOFILTRATION TRANSPORT BEHAVIOUR 34

2.2.1 WHY NANOFILTRATION? 34

2.2.2 INORGANIC SALTS 35

2.2.3 UN-DISSOCIATED ORGANIC COMPOUNDS 35

2.2.4 DISSOCIATED COMPOUNDS 36

2.2.5 UN-DISSOCIATED COMPOUNDS AND SALTS 39

2.2.6 CONCLUSION 40

2.3 TRANSPORT THEORY AND MODELLING DEVELOPMENT 41

2.3.1 EARLY DEVELOPMENTS 41

2.3.2 IRREVERSIBLE THERMODYNAMICS 42
2.3.3 MODELS BASED ON THE EXTENDED NERNST-PLANCK EQUATION 49

3 MATERIALS AND METHODS 60

3.1 INTRODUCTION 60
3.2 MEMBRANE FILTRATION APPARATUS 60
3.2.1 FILTER HOLDER 61
3.2.2 PUMP 64
3.2.3 MEASUREMENT AND CONTROL INPUT/OUTPUT DEVICES 66
3.3 EXPERIMENTAL PROCEDURE 79
3.3.1 MEMBRANE PREPARATION 79
3.3.2 PRE-FILTRATION 81
3.3.3 FILTRATION START-UP AND OPERATING CONDITIONS 81
3.3.4 FILTRATION AND DATA COLLECTION 83
3.3.5 TERMINATION OF EXPERIMENTS AND CLEANING 83
3.4 MEMBRANES 84
3.4.1 SELECTION AND ACQUISITION 84
3.5 CHEMICALS 85
3.5.1 SPECIAL PROPERTIES AND HANDLING OF COMPOUNDS USED 87
3.6 CHEMICAL ANALYSIS 87
3.6.1 UV SPECTROPHOTOMETERY 88
3.6.2 VISIBLE SPECTROPHOTOMETERY 89
3.6.3 INDUCTIVELY COUPLED PLASMA – OPTICAL EMISSION SPECTROSCOPY 93
3.6.4 CONDUCTIVITY MEASUREMENT 94

4 MEMBRANE SELECTION AND CHARACTERISATION 96

4.1 INTRODUCTION 96
4.2 MEMBRANE SELECTION CRITERIA 97
4.2.1 MEMBRANE PERFORMANCE 100
4.3 TRISEP XN45 108
4.3.1 TRISEP XN45 – THEORETICAL CHARACTERISATION 108
4.4 RESULTS 115

4.4.1 TRISEP XN45 MEMBRANE EXPERIMENTAL DATA 116
4.4.2 THREE ION SOLUTION SYSTEMS 116
4.4.3 ORGANIC COMPOUND REJECTION AND PH 118
4.4.4 THE INFLUENCE OF SALT CONCENTRATION ON UNCHARGED ORGANIC SOLUTE REJECTION 120
4.4.5 SALT REJECTION 129
4.5 CONCLUSIONS 130

5 THE NEGATIVE REJECTION PHENOMENON 132

5.1 INTRODUCTION 132
5.2 ERROR 132
5.2.1 GLUCOSE 132
5.2.2 CAFFEINE AND BENZYL ALCOHOL 134
5.2.3 GLYCEROL 134
5.3 REAL REJECTION 138
5.3.1 THEORETICAL EVALUATION OF REAL REJECTION 140
5.3.2 METHOD APPLICATION 144
5.3.3 RESULTS 144
5.4 OSMOTIC PRESSURE – MEASUREMENT AND THEORETICAL ASSESSMENT 149
5.4.1 THE IMPORTANCE OF OSMOTIC PRESSURE 149
5.4.2 EVALUATION OF OSMOTIC PRESSURE 150
5.4.3 OSMOTIC PRESSURE - THEORETICAL EVALUATION, PRACTICAL MEASUREMENT OR USE OF LITERATURE VALUES 158
5.5 CONCLUSION 160

6 NEGATIVE REJECTION THEORY 162

6.1 INTRODUCTION 162
6.2 NEGATIVE REJECTION MODELS 163
6.2.1 PERRY AND LINDER 163
6.2.2 DEY, RAMACHANDHRAN AND MISRA 168
6.2.3 SCHIRG AND WIDMER 169
6.2.4 EXTENDED NERNST PLANCK MODELS 171

6.3 PATTERNS OF SALT REJECTION **174**
6.4 MODELLING THE NEGATIVE REJECTION PHENOMENA **180**
6.4.1 MODEL APPLICATION – GENERAL METHOD 180
6.4.2 THE VALENCE ASSUMPTION 183
6.4.3 MODEL PARAMETERS 183
6.4.4 CHARGE PROPERTIES OF NEUTRAL MOLECULES 184
6.5 MODEL PERFORMANCE **186**
6.5.1 MODEL PARAMETERS AND DATA TRENDS 190
6.6 IMPORTANCE OF THE PHENOMENA **191**
6.7 CONCLUSIONS **192**

7 CONCLUSIONS AND RECOMMENDATIONS **194**

7.1 CONCLUSIONS **194**
7.2 RECOMMENDATIONS **196**

NOMENCLATURE **197**

BIBLIOGRAPHY **202**

APPENDIX **A-1**

A.1 ERROR IN GLUCOSE ANALYSIS **A-1**
A.1.1 ACCUMULATED ERROR A-1
A.1.2 STATISTICAL ERROR ANALYSIS A-2
A.2 INSTRUMENT CALIBRATION CURVES **A-5**
A.2.1 PRESSURE TRANSDUCERS A-5
A.2.2 TEMPERATURE MEASUREMENT A-6
A.2.3 FLOW MEASUREMENT A-7
A.3 CHEMICAL ANALYSIS CALIBRATION CURVES **A-8**
A.3.1 SACCHARIDES A-8
A.3.2 SUBSTANCES WITH ABSORPTIONS IN THE UV REGION A-9
A.4 PUMP PERFORMANCE CURVES **A-18**
A.4.1 ROTAFLOW PUMP A-18

A.5 CONTROL AND DATA LOGGING PROGRAM **A-19**

A.5.1 QBASIC 4.5 A-19

A.6 CIRCUIT AND WIRING DIAGRAMS FOR EXPERIMENTAL EQUIPMENT **A-39**

A.6.1 SIGNAL CONDITIONER A-39

A.6.2 RELAY POWER CONTROL UNIT A-40

A.7 HEAT EXCHANGER DESIGN **A-41**

1 Introduction

Membrane filtration is one of several operations that form the collection of separation techniques available to Chemical Engineers. Unlike other methods, membrane separations do not involve aggressive procedures such as the introduction of heat or additional process chemicals (e.g. solvents in extraction processes). As such membrane separation provides a means by which solutes that are sensitive to changes in their environment or cannot be contaminated through the addition of new chemicals, may be separated and concentrated as required.

As an introduction to this study relating to membrane filtration, the history and development of filtration technology was considered, paying close attention to the recent development of synthetic membranes. There was also an examination of the present state of the art with respect to membrane technology and fundamental concepts and definitions relating to membranes were investigated and ultimately the objectives of the present work were indentified.

1.1 History and development of filtration

1.1.1 Historic

One of the driving forces behind the development of filtration and membrane filtration technologies has been the provision of water for domestic consumption. Early development in the supply and improvement of water for domestic purposes, was clearly advanced by the interest and investment made by the Roman civilisation. Indeed it would appear that the Romans developed the forerunner to water rates and water metering:

> "No person shall draw water from the public supply without official permission, i.e. an imperial licence, nor shall he draw more than he has been granted."
>
> Frontinus, De Aquaducta II, 103

Romans also applied their attentions to drainage and sewerage as well as the supply of appropriate quantities of fresh water via a system of aqueducts. Water treatment methods used by the Romans that are more pertinent to this thesis were the use of filtration for water improvement. On a more industrial scale there is evidence of the use of two techniques of filtration. One such technique was the transfer of water through a large but permeable barrier in the line of flow, though rare, evidence of such a device suggests that sand bags were used in the filter's construction. An alternative device found at Ampurius utilised charcoal and sand that had been packed into amphorae, these vessels arranged in a circle were used to filter rainwater (Hodge, 1992).

Not only does this evidence of early technology indicate an interest in filtration techniques but also a desire to improve the quality of water for domestic purposes. However, in the time of the Roman Empire liquids for direct oral consumption were strictly limited to spring water (which had a certain religious value) and wine.

Following the fall of the Roman Empire, interest in the development of water treatment and supply systems dropped. Although London had had a system of pipes for the distribution of non-purified water since 1560 it was not until the late eighteenth century, in France, that there was a resurgence of interest in domestic supply of water and sanitation. However, there was not too much concern over the purification of water. It was the work of Louis Pasteur that triggered concern with respect to the microbial quality of water and the need for boiling or filtration (Goubert, 1986).

Between the eighteenth and twentieth centuries there was a period of rapid technological evolution. This allowed for the development of more useful techniques of water analysis, both chemical and bacteriological. As a guiding principle it was stated that drinking water should not contain any harmful mineral, organic or inorganic substances. Indeed the more affluent residents of French society became less keen on the water they consumed as they considered it to be of rather ambiguous source. Though ground water was preferred, it was not the only source and some water was drawn from surface supplies (rivers and lakes). Although the process of nitrification largely dissipated organic-matter, this was not considered to be totally

acceptable and so some means of sand filtration was recommended. On these grounds small private companies set up filtration plants using sand and gravel filters and charged customers for the product.

In France the use of household filters spread from 1840 onwards and even around 1900, in cities endowed with a water supply network, their usefulness was not questioned. The filters were seen as a means of supplementing the central filtration process, the water supply was said to reach the town in more or less the same state as it left the watercourse. Construction of these filters varied between two types, clarifying filters that used sandstone, sand, gravel and porous wool and purifying filters that made use of charcoal.

The use and effectiveness of conventional sand bed filters was demonstrated in 1892 when a cholera epidemic killed 8500 people in the city of Hamburg. The water that was supplied to the area was drawn from the River Elbe and was largely untreated. One suburb, Altara, treated the water with sedimentation and sand filtration and did not experience the cholera epidemic. This instance highlighted the importance of pathogen removal and that it can be achieved with sand filters (Kiely, 1997).

1.1.2 Modern water treatment and filtration

In areas of the developed world, where supplies of fresh surface and ground water are plentiful there are accepted processes for water treatment. These processes depend on the water source but might incorporate such steps as extraction, screening, neutralisation, aeration, chemical pre-treatment, sedimentation, coagulation and flocculation as well as filtration and disinfection (Kiely, 1997). This combination of steps produces highly acceptable potable water.

In arid countries or on small densely populated islands where demand for water far exceeds the amount of fresh water available, desalination processes are used to produce drinking water from seawater. These processes are now being superseded by Reverse Osmosis (RO) as a method for producing clean potable water (Marsh et al., 1998) and in some cases this technology has been exploited for as much as thirty

years (Baig and Al Kutbi, 1998). Development with respect to seawater RO plants included the incorporation of additional membranes, e.g. Microfiltration (MF) and Ultrafiltration (UF) where surface seawater quality was poor (Glueckstern and Priel, 1998).

1.1.3 Membrane filtration and conventional filtration – a comparison

The filter medium used in conventional filtration is defined as a barrier that lets the liquid pass while retaining most of the solids; it may be a screen, cloth, paper, or bed of solids. The liquid that passes through the filter medium is called the filtrate. In membrane filtration the nature of the retentate ranges from solids to solute molecules whereas, as already stated, normal filtration deals only with suspended solids.

The mechanism that operates in conventional filtration is either *cake filtration* where solids form a layer on the filter and they themselves act to retain other particles, or *depth filtration* where the actual material becomes caught in the media of the filter. In membrane processes, mechanisms similar to those described for standard filtration occur, however a filtration cake will only form where solids are being separated and only then when there is insufficient hydraulic action (brought about by cross-flow or some other form of agitation) to prevent a build-up. A similar result occurs for solutes but this time the layer at the membrane is referred to as either a *gel* layer or the *concentration polarization* layer. Unlike the cake layer the concentrated level of solute molecules that form the gel layer do not further exclude solute molecules on a size basis but there is a concentration driving force that opposes the direction of flux and is attributable to the concentration difference (Laros, 1999).

The operation of filters in conventional filtration is in some cases comparable to membrane techniques. Membranes are operated in both plate and frame (Bowen, 1997) and dead-end arrangements (Koenders et al., 2000). However, the most effective means of operation are unique to membrane technology.

From this comparison of technologies it can be seen that the fundamental mechanisms and attributes of both conventional and membrane filtration are very similar and thus one technology leads to the other. However, there are additional properties relating to membranes, particular at the low end of size separation that are unique to this technology and will be discussed later.

1.2 History and Development of membrane filtration

Every cell in nature is surrounded by a complex membrane. These membranes regulate the conditions within the cell by a process of osmosis. In producing synthetic membranes an attempt is being made to replicate natural membranes. However, these artificial membranes are far less sophisticated (Eykamp, 1998).

A review of membrane development provided by Lonsdale gave a useful insight into the technological milestones (Lonsdale, 1987). The first commercially viable synthetic membrane was comprised of cellulose acetate and was developed in the late 1950s by Loeb and Sourirajan. This membrane was produced using an innovative technique termed "phase inversion" where a polymer film, dissolved in an appropriate solvent, was immersed in water, which in turn drove the solvent away and caused the polymer to set. The original technique, where membranes were produced by drying films of polymer-solvent solutions in air, resulted in relatively thick membranes that did not lend themselves to industrial application.

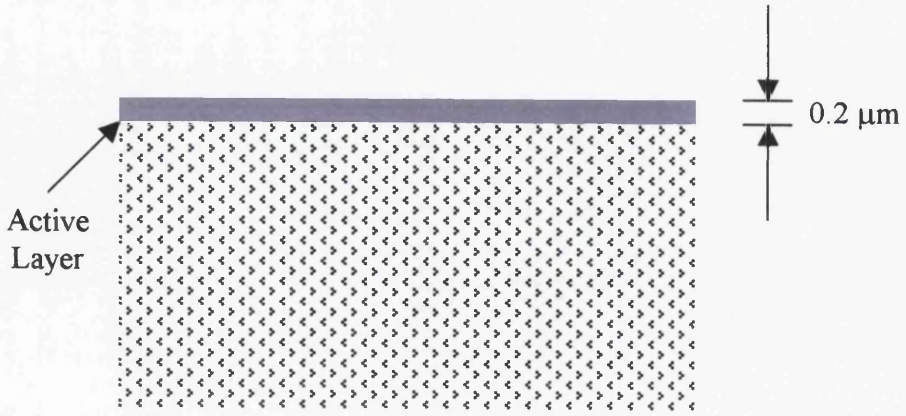

Figure 1-1 Schematic representation of membrane composition

These Reverse Osmosis CA membranes had a (*now*) characteristic structure as schematically represented by Figure 1-1. This characteristic structure consists of a

thin layer of dense membrane about 0.2 μm thick supported on a substrate of micro-porous membrane many times thicker.

Other innovations in membrane technology included the consideration of dynamically formed membranes (colloidal gel-layers on ceramic supports), dip-coated thin membranes, plasma polymerisation, thin liquid membranes, water cast membranes (cast on the surface of the water), and interfacial polymerisation. However, with the exception of dip coating and interfacial polymerisation, most of these discussions represent experimental developments and not techniques suitable for commercial membrane manufacture or exploitation.

Membranes produced by dip coating and interfacial polymerisations are further productionised by the introduction of a support material. The resultant membranes are referred to as thin film composite (TFC) membranes.

Since the development of the TFC membranes the most significant advances in membrane technology have been with respect to the polymers used in their construction and adjustments to the conditions prevailing during membrane manufacture. The most recent focus has been on composite membranes made of aromatic polyamide material (Matsuura, 2001).

The most recent and significant development in membrane technology is the nanofiltration membrane. This type of membrane was identified by Eriksson with Dow-Filmtec being amongst the first producers of membranes of this kind (Eriksson, 1988). The nanofiltration membrane is considered to fall between RO and UF and share properties of both. Thus nanofiltration membranes are charged and possess the Donnan exclusion properties of RO membranes and yet are assumed to retain pores, hence their similarity to UF.

1.3 Present state of membrane filtration technology

1.3.1 Applications

Although it could be argued that the development of the synthetic membrane was born out from the desire to efficiently desalinate water through filtration, the technology surrounding membranes has been considered and applied to numerous separation scenarios. Table 1-1 provides a list of recent uses for reverse osmosis and nanofiltration membranes.

Membrane application	Source
Effluent water treatment in a paper recycling plant	(Ahn et al., 1998)
Treatment of cheese whey effluent	(Alkhatim et al., 1998)
Sea water desalination	(Baig and Al Kutbi, 1998)
Removal of pesticides from surface water	(Berg et al., 1997)
Water treatment in the soft drinks industry	(Holden, 1998)
Recycling water for space missions	(Lee and Lueptow, 2001)
Dye recovery	(Levenstein et al., 1995)
	(Sojka-Ledakowicz et al., 1998)
Boron reduction in sea water desalination	(Magara et al., 1998)
Purification of land fill leachate	(Peters, 1998)

Table 1-1 Some industrial applications of membrane processes

Table 1-1 provides examples of the uses for which membranes are employed. The majority of the processes are centred on the recovery of water and water quality with the exception of a few applications where solute recovery is the aim. The number of examples of membrane use in water treatment underlines the importance of the relation and interaction between conventional water treatment techniques and membrane separations.

1.3.2 Commercial membranes

The number of manufacturers who produce membranes for commercial exploitation underlines the success of the pressure driven membrane process, as a legitimate separation technique.

Membranes are often developed for specific end uses, for example the Dow-Filmtec NF200 membrane was developed for treating surface water drawn from the River Oise in France (Ventresque et al., 2000) and the SR90 membrane by the same manufacturer was used for sulphur recovery from sea water at oil platforms (Dow-Filmtec, 1999).

Manufacturers who retain a large catalogue of membranes include Dow-Filmtec, Osmonics (GEWater), Hydranautics, Nitto Denko, Koch membranes and Trisep. Although these are commercial organisations whose basic technical data cannot be relied upon since it was neither independently refereed nor detailed in nature, they do supply the majority of membranes used in research and some of their products are investigated in this study.

1.4 Fundamental concepts in pressure driven membrane separations

Already, four classes of membrane, as used in pressure driven processes, have been mentioned in this chapter. These four categories are:

- Microfiltration
- Ultrafiltration
- Nanofiltration
- Reverse osmosis

The diagram in Figure 1-2 provides a simple illustration of the characteristic transport behaviour for each membrane type indicating the defining properties (Raman et al., 1994).

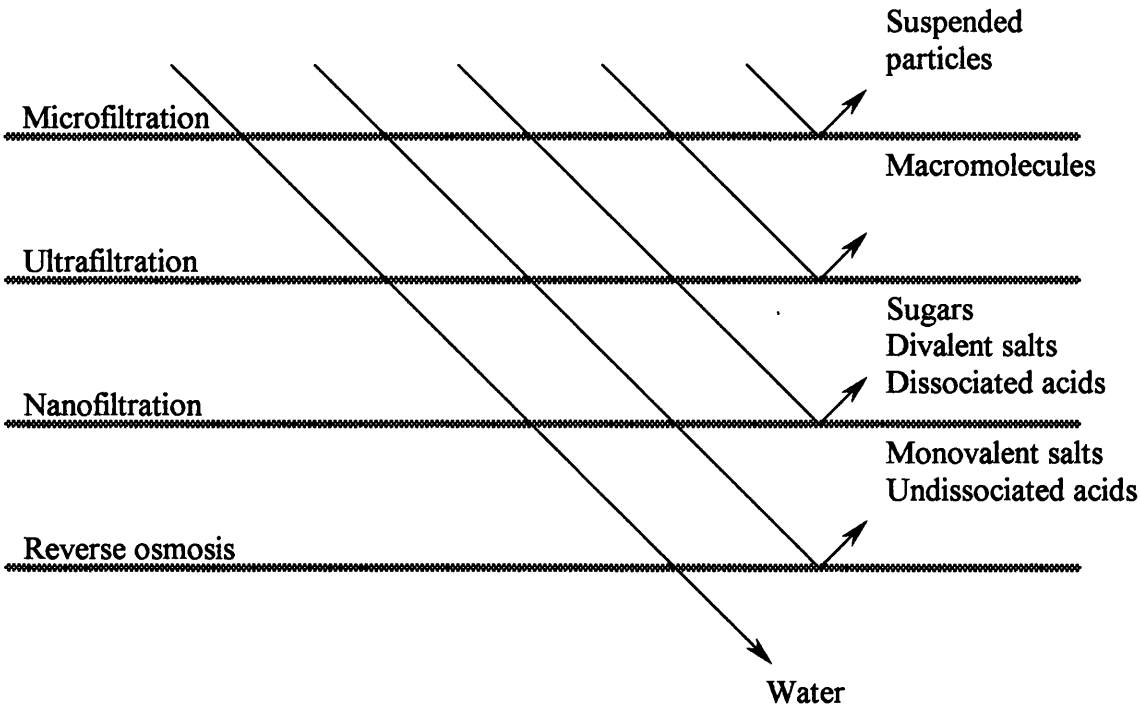

Figure 1-2 Defining rejection behaviours of the four pressure-driven membrane technologies

The mechanisms controlling rejection have been defined by Yaroshchuk as (Yaroshchuk, 2002):

- Steric partitioning; the most basic mechanism in membrane separation is a result of the size exclusion that occurs when solute molecules are larger than channel or pore available for permeation.
- Donnan partitioning; the process where ions with a charge the same as the membrane (coions) are repelled and therefore rejected to degree far greater than steric properties would indicate. In single salt systems, due to the requirement for electroneutrality, the counter ion is also rejected. In systems containing more than one salt or ionic compound a polarisation of charge around the membrane can lead to the negative rejection of an ion.
- Dielectric exclusion; this phenomenon is caused by the interactions of ions with the polarisation charges induced by them at the pore surface. In the simple case of single ion located in the centre of an aqueous medium bounded by a polymer, the polarisation charges induced at the solution/membrane interface show the same sign as the single reference ion. As a consequence the interactions always cause the repulsion of each ion, independent of the sign (Bandini and Vezzani, 2003).

- Hydration mechanism; charged ions in solution with water become hydrated thus promoting enhanced steric rejection.

For the four membrane classifications discussed, not all of the mechanisms are relevant. Indeed, for MF and to an extent UF only steric partitioning may take place. For NF and RO one mechanism may be dominant but none are mutually exclusive since all electrical effects influence one another and steric properties can influence the extent to which each charge property affects the rejections.

1.4.1 Membrane formats

When operated industrially, membranes are used in a number of orientations. As previously mentioned membranes can be used as flat sheets in dead-end cells or plate frame arrangements (similar to conventional filter presses). However, it is only plate and frame operation that is significantly viable for industrial use of flat sheet membranes. Figure 1-3 presents a schematic of a flat sheet system, a specific flow regime is created using membrane sheets interspersed with spacers or frames (Bowen, 1997). Although this arrangement is effective in creating a flow pattern that demotes concentration polarisation it is limited by the effective membrane area that can be made available. This is in sharp contrast with the other three membrane arrangements that are widely used; Spiral wound, hollow-fibre and tubular membranes.

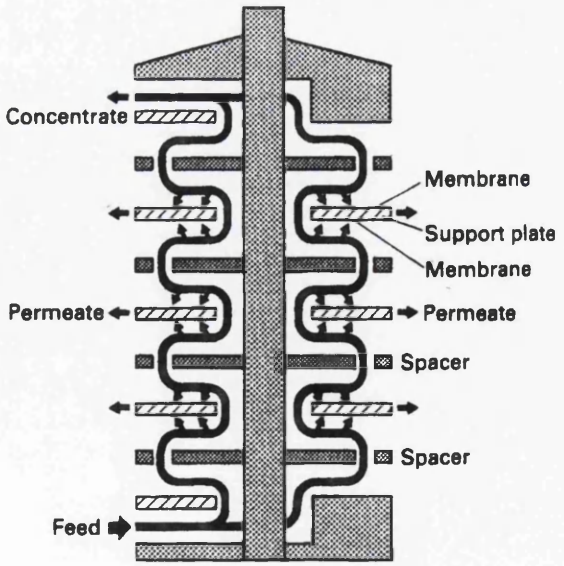

Figure 1-3 Schematic diagram of a flat sheet module (Bowen, 1997)

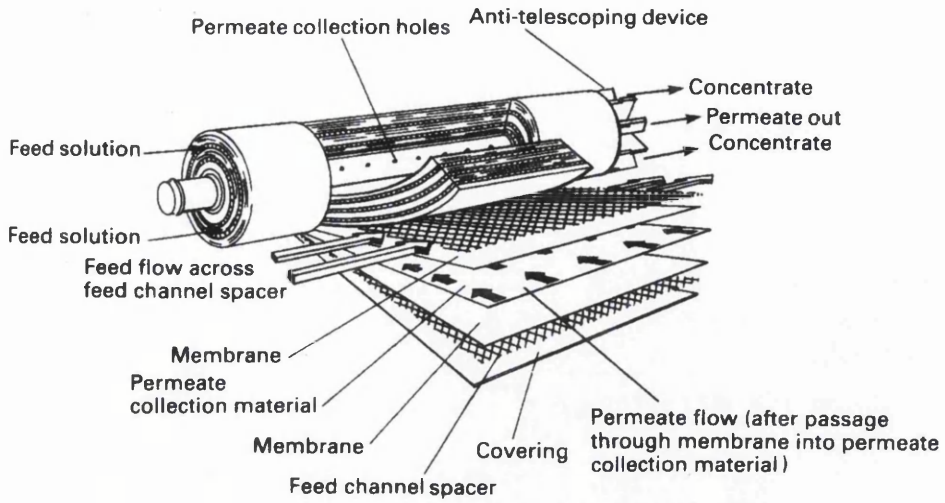

Figure 1-4 Schematic diagram of a Spiral-wound module (Eykamp, 1998)

Figure 1-4 demonstrates the technology behind spiral modules, which utilises membrane envelopes wound around a central permeate tube (Eykamp, 1998). The solution permeates into these envelopes from where it is transported to the central permeate tube. This arrangement allows a large area of flat-sheet membrane to be operated in a small physical volume.

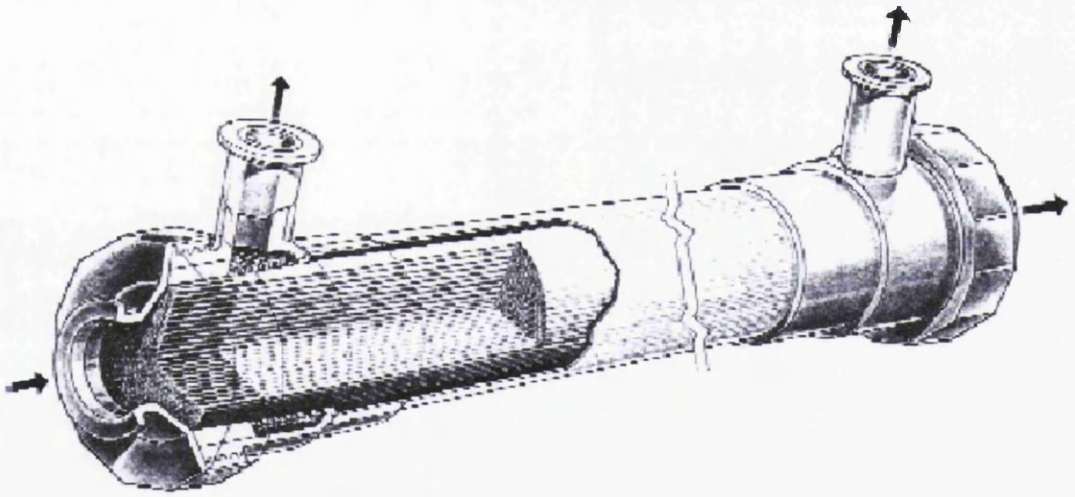

Figure 1-5 Cutaway view of low-pressure capillary-membrane module (Eykamp, 1998)

Figures 1-5 and 1-6 illustrate the Hollow-Fibre and Tubular membranes respectively (Eykamp, 1998). In concept the operation of both membrane types is the same, but hollow-fibre modules contain capillary membranes with diameters of the order of 1 mm whereas tubular membranes are generally greater than 10 mm in diameter. In both cases the ends of the tubes or capillaries are sealed into a resin block that separates the feed from the permeate side of the membrane.

Figure 1-6 End views of two tubular membrane modules (Dow Filmtec)

1.4.2 Membrane plant configuration

A typical equipment configuration for a membrane plant is shown in Figure 1-7 (Bowen, 1997). The key features are the pump, the heat exchanger, the membrane and the feed tank. Very often a second pump is used such that one is available to supply the pressure head required to promote transport across the membrane and the other maintains the volumetric flow rate around the system.

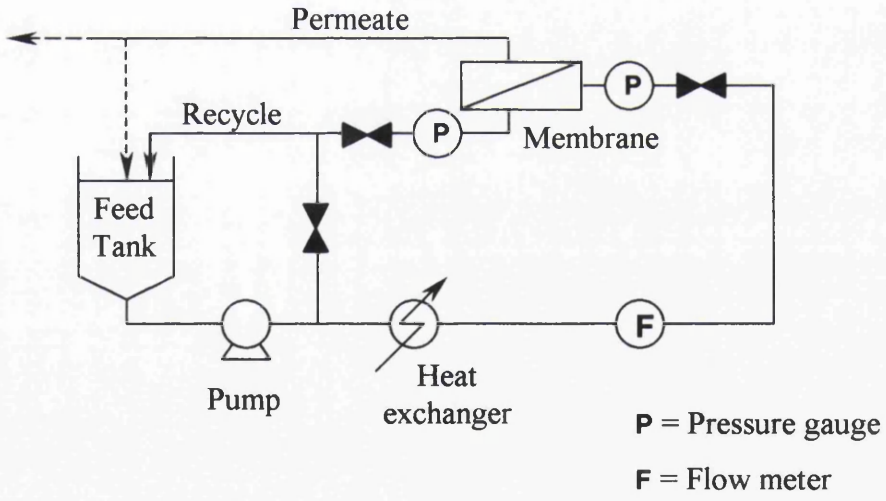

Figure 1-7 Flow diagram for a simple batch membrane process (Bowen, 1997)

The pumps in the process provide a heating effect that can lead to damage of sensitive process fluids; consequently all systems are fitted with a heat exchanger to remove heat energy. Figure 1-7 illustrates a cross flow membrane system and many commercial membrane modules make this possible by having both an inlet and an outlet for the feed side of the membrane. The valve fitted after the membrane on the recycle is used to create a backpressure, this can be essential for membranes that have

a low pressure-drop such as tubular membranes but it is not such a necessity in SPW modules.

1.5 Objectives of the present work

The aim of the study reported here was to extend the boundaries of knowledge with respect to pressure-driven membrane filtration with particular reference to nanofiltration. Nanofiltration was selected due to it being a relatively new class of membrane. Nanofiltration is of additional interest to the researcher as it retains properties intermediate between those of reverse osmosis membranes and ultrafiltration membranes. Where reverse osmosis membranes can be considered simplistic as the rejection is almost total for the majority of solutes and ultrafiltration separation is mainly a result of steric factors, nanofiltration membranes show intermediate rejections for small organic and inorganic substance and are strongly influenced by the chemistry of the membrane/solution system.

This thesis set out to extend knowledge in the field of nanofiltration by identifying an area of research that has not been explored, considering the importance and worth of the knowledge that can be gained from a resultant study and if deemed valuable commencing on course of practical and theoretical discussion in the area of interest. To achieve this aim required a thorough evaluation and understanding of material already published with regard to the field of nanofiltration research.

Once an area of the research was identified that merited investigation it was explored both practically and theoretically and the results were discussed in relation to contemporary reports and conventional understanding. To achieve this an apparatus appropriate for membrane experimentation was constructed and ancillary laboratory techniques were exploited as necessary. The relevance of the membrane apparatus was supported through replication of seminal experiments and new experiments were devised and conducted in order further explore the field of research.

The next objective was to discuss the findings of the experimental work with respect to the legitimacy of the observations and to relate these observations to contemporary theories and models. The final aim was to consider how these observations affect the

practical application of membrane separation processes, what practical benefit might be gained from them and where research both theoretical and experimental should be taken in the future.

2 Literature Review

2.1 Membrane Research – Experimental Investigation

2.1.1 Introduction

Discussion of previous studies with respect to their experimental focus provides a convenient basis for their consideration. It was thus beneficial to conduct a study of publications relating to membrane technology and make a qualitative assessment of the type of practical studies undertaken and how they influence the course of research detailed in this report. To achieve an analysis of this kind it was useful to split the research into categories and then discuss the individual investigations that fit each category.

The categories of investigation were defined as:

i) Investigation of solution/system properties: investigation of the influence of variables such as pH, ionic strength, major cation valence, molecular size, polarity, charge, temperature, pressure, cross-flow rate, location with respect to the membrane surface, concentration and concentration ratios.

ii) Pilot experiments: filtration of specific and often unusual feed streams, targeting specific solutes for removal/separation, optimisation of operating techniques.

iii) Membrane properties and membrane chemistry: pore size, charge, structural properties, investigations of new membranes that claim to possess useful properties, experimentation with membranes (lab generated) according to their surface properties and composition, membrane fouling, solute surface interactions.

iv) Interrogation of theoretical techniques: transport model assessment, concentration polarisation analysis.

The published research relating to these categories is summarised below, with the intention providing a background to the direction taken in the research reported in this document.

Solution and system properties

This category of experimental research is focussed on investigating the affects that extra-membrane variables have on membrane transport and separations. As such, a publication may be solely concerned with the effect of, for example, pressure or the variation of concentration ratios of two solutes or the relation of a solute size characteristic to rejection. Although there are instances where work was solely focussed on the influence of solution properties, it was common for experimental work conducted on a basis of one or more variables to be carried out for other purposes (see points (ii) to (iv) above). However, the work that falls precisely into this category is given here.

Van der Bruggen and co-workers are amongst a small number of researchers who have devoted time to the consideration of organic solutes in nanofilter membrane separations (Van der Bruggen et al., 1999). Prior to this authors were mostly concerned with inorganic salts in single solute solutions. The extent of their work was such that it covered a large range of organic compounds and enabled a discussion of their rejection in terms of size characteristic, polarity and charge. Twenty five solutes were used and, amongst others, they included alcohols, saccharides and dye compounds.

They also considered ways in which the reflection coefficient (the maximal rejection of a solute at infinite pressure) might be estimated and they compared a number of descriptions (based on a pore/solute size relationship) with output from a range of membranes and an array of solutes. This provided an informed selection of a model to describe the process (Van der Bruggen et al., 2000).

Kiso and co-workers had also completed a study of the influence of molecular size on rejection. However, this was completed using just one cellulose acetate RO membrane. The rejections of 36 different organic compounds were measured and their rejections were then plotted as a function of various size descriptors. The work also considered the influence of molecular shape and orientation at the membrane surface. Strong correlations between molecular width and Stokes radius were observed (Kiso et al., 1992).

Investigation was continued with the nanofiltration of non-phenolic pesticides (Kiso et al., 2000). The driving force behind this work was the perceived risk posed by the presence of pesticides in drinking water and the need for a means of removal. But it also provided a basis upon which the influence of solute chemistry on rejection could be studied. As well as molecular size factors the authors introduced the concept of hydrophobicity for further consideration. Following this, the rejection of alkyl phthalates and other solutes such as mono-substituted benzenes, alcohols and saccharides was investigated (Kiso et al., 2001). Alcohol and saccharide rejections were found to be controlled by steric factors whereas the other compounds were found to be dependent on hydrophobic properties. In all 27 compounds were studied in relation to 4 membranes. This constitutes a significant piece of membrane research that was led by experiment and it both reveals and confirms basic understandings of membrane transport.

The work of Soltanieh and Sahebdelfar is important in that it is one of few publications that detail an attempt to acquire some insight into the complex issue of multicomponent systems (Soltanieh and Sahebdelfar, 2001). Most significantly it considers multicomponent interactions. The authors suggest that there are potentially two processes occurring that lead to a change in the transport of one solute in the presence of another. The first was a coupling of fluxes, which was the possibility of a more permeable solute pulling the less permeable component through the membrane and reducing its retention. The second was the interaction of the solute component(s) with the membrane resulting in charge changes in the membrane. The work compared the influence of varied acetic acid/NaCl and oxalic acid/NaCl concentration ratios with respect to a salt permeability coefficient determined from a theoretical model.

Zander and Curry undertook experimental work to gain a deeper understanding of the performance of NF membranes and thus their potential for application in the drinking water treatment (Zander and Curry, 2001). They considered the effects of solution pH, ionic strength and cation valence (Na^+ or Ca^{2+}) on humic acid rejection and found that rejection was the result of a complex interaction of steric hindrance, electrostatic repulsion, solution effects on the membrane and solute shape, and thickness of the double layer surrounding the membrane in solution.

From this work it was concluded that research, driven purely by experiment, is sparse. This is probably a consequence of the variety of scenarios that are available for exploration, only some of which might provide useful insight into membrane transport.

Pilot experiments and specific process streams

Perhaps the most relevant motive for practical investigation was the consideration of membrane separations for commercial exploitation. Under these circumstances the process fluid was very specific and often complex in nature, and the separation demands sometimes great. This category was also concerned with application of membranes to solutes that are of particular environmental or anthropological concern, even though there was no real intention, by the authors, to commercially develop a process.

A common application for nanofiltration was the treatment of wastewaters from paper manufacture. Ahn and co-workers investigated the performance of five nanofiltration membranes measuring the reduction of TOC and colour. Particular attention was paid to the cause of flux decay, and resistances to flow were apportioned to fouling and concentration polarisation effects (Ahn et al., 1998).

Almost certainly one of the first major municipal applications of membrane filtration was the production of potable water from sea or brackish water. Desalination, as a means of producing domestic water, normally finds demand in arid areas of the world such as the Middle East. However, drought conditions in the UK prompted a feasibility study on producing clean water from the North Sea (Murrer and Rosberg, 1998). For this purpose, pilot rigs were developed that could be operated on location and utilised a two-stage system of UF followed by RO.

Much work has been published on the subject of desalination and the latest writings were concerned with the idiosyncrasies of commercial processes. As an example Vrowenvelder and co-workers focussed on biofouling (Vrouwenvelder et al., 1998). Three pilot plants operating both RO and NF membranes were studied. An unusual step was to destructively autopsy the membranes after use. It was observed that cleaning agents occasionally promoted a fouling increase rather than a reduction.

Indeed one of the variables studied was the cleaning agent used, they also considered fouling according to stage and element number.

The increase in attention to detail with respect to water treatment was illustrated by the consideration of boron removal from drinking water. It has been observed that desalinated water contains levels of boron that are potentially adverse to human health (Magara et al., 1998). It was also noted that the rejection of boron was far less than that of other salts in RO. The solution was to employ a multistage RO desalination process. In attaining this solution the affects of pH, feed concentration and operating pressure were also considered.

Since fouling is deemed to be inevitable in industrial membrane applications, this was an aspect that many authors give consideration, to one extent or another. To this end experiments have been devised that replicate systems that typically suffer from high fouling. Cho and co-workers, endeavoured to assess the way in which membrane characteristics were modified by the presence of foulants (Cho et al., 1998). The process fluids used were a variety of surface waters from rivers and lakes; eight membranes were employed in the study. To assess the affect of fouling, measurement was made of contact angles to determine hydrophobicity and zeta potential, and a spectroscopic technique was used to evaluate the functional groups on the membrane surface and those on the foulants.

A well-known water quality descriptor is hardness and in some cases consumers prefer water of a softer nature than available from source. Nanofiltration has been considered as a means of reducing hardness and because hardness can be caused by a number of compounds, these represent specific solutes suitable for experimental study (Schaep et al., 1998). Investigations conducted using three membranes, illustrated the influence of pressure, temperature and ion type on rejection and also demonstrated the influence of viscosity on permeate flux. Nanofiltration was found to be very effective in reducing hardness.

Schaep and co-workers also observed fouling; this is a common occurrence where compounds contributing to hardness are present. The concentration polarisation phenomenon that occurs at the membrane surface leads to saturation and thence

precipitation of the solute. The result is either scale formation directly on the surface of the membrane or the formation of a "cake" layer of crystals.

One of the more significant areas of research with respect to specific solutes is indeed the removal of pesticides from water intended for domestic supply. This has come about due to the relatively recent innovation that has been presented in form of nanofiltration membranes. Because NF membranes bridge the gap between RO and UF with respect to pore size and surface chemistry, they are ideal for separating relatively small organic molecules from smaller salts. As a consequence they are ideal for use in pesticide removal. The work of Van der Bruggen and co-workers constitutes an important contribution to this area of study (Van der Bruggen et al., 1998). They identified that pesticide compounds tend to remain in water sources, including ground waters and require removal in the processing stage of drinking water production. Traditionally, activated carbon is employed for this purpose but it was deemed to be expensive and limited so the authors wanted to establish the eligibility of nanofiltration for the same task.

Pesticides have been used as a measure of membrane performance as they represent micropollutants of some concern. In recent work three membranes were used for the purpose of evaluating a new "Ultra-low pressure" reverse osmosis membrane (Hofman et al., 1997). Rejection performance of the new membranes was reported to be comparable if not better than conventional membranes.

As mentioned earlier, Kiso and co-workers also gave extensive consideration to pesticide rejection (Kiso et al., 2000). They considered four membranes with a range of desalting abilities and measured the rejections of 14 non-phenolic pesticides. The rejection of uncharged organic compounds was found to be largely dependent on molecular size and pore size distributions. The dipole moment of the molecule is also implicated and discussion illustrated how this aids the transport of a molecule through the membrane. Four membranes were used in the experimental part of the study one of which was positively charged at the pH of the system and another had a pore size significantly larger than the other three. These differences between the membranes clearly demonstrated the importance of molecular size on rejection. There was some charge influence exhibited by the pesticide molecules, which was not evident when

compared to the rejections of non-polar saccharides. Clearly, therefore, polarity of certain pesticides was significant.

The importance of both pesticide and hardness removal was further emphasised by a study that examined the performance of a membrane plant employed at a conventional water works. This work displayed that Nanofiltration was highly suitable for this application (Wittmann et al., 1998).

The effective MWCO of nanofiltration membranes makes them ideal for separating solutes in a multicomponent solution where the components fall either side of the cut-off, on a size basis. A study on whey effluents in the dairy industry (Alkhatim et al., 1998) inspected the potential for demineralising and deacidifying acid cheese whey and assessed the influence of pH, temperature and pressure on this separation. Both experimental and commercially manufactured membranes were found to be suitable for this application.

The work discussed so far is a representative sample of the studies that were initiated by an interest in the filtration of a predefined solute. It is shown that there are several subjects that are popular sources of research, namely: water desalination, pesticide removal, hardness removal and various aspects of potable water processes. The conclusion can be made that pilot level experimental work is of significant value, where process stream components are known and the applicability of membrane filtration is required. Pilot work is also shown to be important for optimising the operating conditions, particularly in terms of membrane module combinations and arrangements.

Membrane properties and membrane chemistry

In the desire to characterise the behaviour and performance of membranes some insight is required into the relation between membrane surface properties and membrane performance with regard to rejection/separation and fouling effects. For this purpose, attempts have been made to relate performance to: pore size, pore size distributions, porosity, membrane charge, membrane charge density, surface topography, membrane thickness and the concentration and type of active groups on

the membrane. To correlate membrane performance to membrane chemistry requires experimental investigation.

The simplest of membrane properties is that of the membrane module type termed here as "orientation". There are a number of orientations including "flat sheet", "spiral wound", "tubular" and "hollow fibre", each of which lends itself to certain filtration scenarios. Module type is important when considered in relation to fouling and some insight into the effect has been obtained for calcium sulphate ($CaSO_4$) fouling (Lee et al., 1999). The conclusion of this work was that spiral wound membranes are most effective at minimising scale formation.

Peremate flux reduction is considered to be a function of fouling. Although perhaps indirectly related, fouling can be considered to be a property of the membrane. Contact angles, zeta potentials and IR spectra of clean and natural organic matter fouled membranes have been evaluated and compared to demonstrate the differences in hydrophobicity, surface charge and functional groups (Cho et al., 1998). This work represented a novel consideration of fouling in that it effectively viewed permeate flux reduction as an inevitability and as such aimed to understand how it changes the properties of the membrane. The conclusion of this work was that (depending on the foulants) the presence of foulant could change the hydrophobicity, hydrophilicity and charge of the membrane. However, the authors did not specifically comment on the factors that may promote or discourage fouling.

Separation or membrane selectivity is clearly dependent on specific membrane properties. Linder and Kedem studied asymmetric mosaic membranes to determine the relationship between internal structure and separation properties. During the work seven membranes were fabricated each with a different composition and preparation regime. The membranes produced were investigated using a Scanning Electron Microscope and through evaluating their rejection of sulphate and chloride salts, DNS and Procion blue. Polymer solution compositions were shown to affect the structure and behaviour of the membrane (Linder and Kedem, 2000).

Membrane fabrication constitutes an important part of membrane research and when new membranes are formed, investigation and discussion of their chemistry in relation

to performance must follow. Recent work has been involved with polysulphone – sulphonated (ether-ether) ketone blend membranes (Bowen et al., 2001a). In that study membranes were manufactured with a range of compositions, experimentally characterised and their properties evaluated using the Donnan Steric Partitioning Model (DSPM) (detailed in section 2.3.3). This model enabled evaluation of pore size, permeabilties and charge density. Some characterisation was also achieved using an atomic force microscope.

Workers have also considered the preparation and characterisation of polyetherimide nanofiltration membranes (Kim et al., 2001). It was implied that polyetherimide is preferable to polyamide, as composite polyamide membranes are susceptible to free chlorine and alkaline attack. Thus membranes were prepared and evaluated by solvent flux and solute rejection experiments with 600 Da PEG and inspection with a scanning electron microscope. This enabled correlation to be drawn between preparation techniques, structural properties and performance.

Poly-Ethylene Glycol (PEG) has often been used to characterise membranes. Lab produced membranes prepared from the sodium form of sulphonated polysulphone were found to have various charge densities and were assessed using PEG-600 – 6000 Da (Jitsuhara and Kimura, 1983a). Since these were ultrafiltration membranes PEG, in this size range, was used to evaluate reflection coefficient and permeability of the membrane. In the work, these two parameters were determined using the modelling of Spiegler and Kedem (Spiegler and Kedem,1966).

New, commercially developed membranes that claimed to possess specific properties were also the subject of investigation. A study made of an ultra-low pressure reverse osmosis membrane examined the influences of solute size and solution pH on the rejection by the membrane (Ozaki and Li, 2002). In essence this work was also a study of the properties of membrane materials. Others, who considered the application of "ultra-low pressure" RO membranes, studied the performance of three membranes with respect to the rejection of a series of pesticide compounds (Hofman et al., 1997).

In another case an attempt was made to consider the influence of membrane materials when evaluating performance data (Tu et al., 2001). A discussion of surface chemistry

was included which attributed flux variation between two membranes to differences in hydrophobicity. Fouling potential was stated as being influenced by surface characteristics due to sorption of organic molecules, and chemical and electrostatic interactions between the organic molecules and the membrane. On consideration of membrane fouling with tannic acid it was noted that hydrogen bonds between the carbonyl groups on the membrane and charged phenolic groups on the tannic acid were formed and were preferential to hydrogen bonds formed with water. Although both membranes contain carboxyl groups the difference in their observed fouling potentials was attributed to hydrolysability of carboxyl groups in differing polymer blocks.

Membrane fouling with tannic acid was noted to have a marked influence on the hydrophobicity of the membrane, something that was commented on by Cho and co-workers (Cho et al., 1998) other authors also noted that hydrophobicity played a key role in rejection (Kiso et al., 2001). Hydrophobicity is a property of the membrane that is influenced by the functional groups on the polymer and it is a characteristic that has been investigated experimentally by studying the permeation of a variety of solutes.

External influences are important on membrane properties, as they have been known to affect the structure or surface properties of the membrane. For example, solution concentration has been seen to modify surface charge. Childress and co-workers discussed the impact of humic substances and ionic surfactants on the charge of RO membranes (Childress and Deshmukh, 1998). Zeta potential was measured relative to pH and solute type, the effect was found to be significant. The inverse situation was studied by Yeom and co-workers and entailed the use of three membranes negatively charged, neutral and positively charged. The work investigated the rejections of a number of anionic solutes and reported the charge to be highly relevant (Yeom et al., 2000).

Temperature has also been shown to influence the performance of a membrane and it has been suggested that observed trends might be due to changes in the physical properties of the polymeric membrane e.g. pore radius (Goosen et al., 2002). Schaep and co-workers also considered the affect of temperature, when considering

nanofiltration for the softening of potable groundwater (Schaep et al., 1998). The observation was made that laboratory experiments were carried out by preference at 25°C, but in practical situations operating temperatures were in the range of 10-15 °C. Experiments were carried out in the range of 10-30 °C, however, in this case variations in flux were attributed to the influence of temperature on viscosity.

Evaluation of membrane transport theory

The most important area of membrane research is the formulation of transport models. The significance of this work is in the insight that modelling provides to all aspects of the work. As a consequence a great deal of research has been devoted to theoretical descriptions of the phenomena that are either witnessed or assumed to exist in filtration processes. In sum, the aim of model development is either to calculate rejection from an ab initio basis or to evaluate characteristics of the membrane-solution system.

Bowen and associates have further developed the extended Nernst-Planck equation based transport model. Through experimental investigation each enhancement or consolidation of the theory has been either evaluated or used to interpret the results. In one case six NF membranes were experimentally studied and modelling was used to characterise them by evaluating membrane thickness and charge density (Bowen and Mukhtar, 1996). Experimental work was mainly concerned with rejection variation with flux for three ions. A later study used the model to predict rejections of salts and dye compounds in normal batch and diafiltration systems (Bowen and Mohammed, 1998). Experiments were used to verify the model such that it could be used for optimisation of processing conditions in a diafiltration system.

Further development of the extended Nernst-Planck based modelling was completed with the aim of reducing the number of ambiguous membrane property coefficients (Bowen and Welfoot, 2002). Process data were again used to test agreement of new models with real results. Modelling and experiment was conducted on the basis of rejection variation with applied pressure for various mono- and divalent salts.

The "black-box" transport models of Spiegler and Kedem were further developed through a theoretical analysis of processes governing separation (Van der Bruggen et

al., 2000). Experimentally derived values of the Reflection Coefficient, σ, and Permeability, P_s, (for 16 organic compounds) were compared with modelled values therefore allowing identification of the most appropriate theory for the determination of these two parameters.

The two parameters upon which the Spiegler and Kedem model was based have been described in various ways by different authors. The permeability and reflection coefficients were ascribed relationships based on solution concentrations, membrane charge densities and other charge properties of the membrane and solution (Tsuru et al., 1990). Experimental data was again used to compare values determined from calculation and measurable properties of the membrane, with values obtained from curve fitting exercises. In the work of Tsuru and co-workers, filtration experiments were conducted using ultrafiltration membranes and various molecular weights of PEG.

Jitsuhara and Kimura derived the reflection coefficient using a frictional interpretation; that is the thermodynamic force acting on each ion is balanced by the frictional force (Jitsuhara and Kimura, 1983b). The result of this approach was the reflection coefficient defined as a function of solute concentration, an osmotic coefficient, a dimensionless *transport* number and charge density. Similarly a relation was derived for solute permeability that was drawn from osmotic pressure, concentration and chemical potential considerations. Experimentation was then used to determine values of reflection coefficient and permeability, for two membranes, that were compared to theoretically determined values.

Lonsdale and Pusch considered the effect that a membrane impermeable ion could have on the transport of coions in membrane processes and derived a series of models based upon the solution-diffusion model (Lonsdale et al., 1974). Experimental data were used to determine how well each model derivation described real scenarios. As with much work the models are fitted to the data through adjustment of key coefficients, which are often related to properties of the membrane.

Probstein and co-workers derived a theory that was based on the concept of rejection driven by a build up of charge inside membranes due to the presence of an electrolyte. The model considered charge distribution across the pore on a basis of the Debye length that could be assessed from streaming potential measurements. The aim of the experiments was to map out the dependence of the salt (KCl) rejection on the model parameters. The authors considered the influence on rejection of Peclet number (a dimensionless number related to hindered pore flow) and Debye ratio (the ratio of Debye length to pore radius).

A model referred to as the Electrostatic Steric Hindrance model was developed from the Teorell-Meyer-Sievers model and the Steric Hindrance pore model (Wang et al., 1997). The workers then conducted a series of permeation experiments to determine pore radius, porosity to membrane thickness ratio and membrane charge density. These parameters were then used to predict the performance of the membrane with respect to permeation of known solutes and the results compared with experimental data.

Geraldes and co-workers made the relatively unusual step of modelling the transport processes on a basis of the cross flow condition and the related hydrodynamic affects (boundary layer formation and concentration gradient adjacent to the membrane surface) (Geraldes et al., 2001). As a result the authors paid particular attention to the way that permeate composition varied over the length of the membrane. Experiment was used to obtain values of osmotic pressure for various PEG molecular weights and to provide supporting evidence for the theoretical discussion that followed. The filtration equipment used in this work was unique as it allowed the authors to investigate the relation between permeation point and the permeate condition. This was possible because of the regular sample ports along the length of the membrane channel.

Perhaps one of the most powerful modelling tools available is the Artificial Neural Network (ANN) (Bowen et al., 2000). The ANN's strength was derived from its predefined structure, such that no special knowledge of the membrane system was required before the model could be exploited. ANNs are therefore ideal for use upon complex systems such as membrane transport modelling. The study reported that a

hybrid ANN was used, implying that network inputs are influenced by more detailed theoretical approaches. In the development of the ANN, experimental data was required for three roles: training, testing and validation. The data used related pH and trans-membrane pressure to rejection. This modelling approach was shown to perform well on this data.

In one membrane transport modelling treatment, important phenomenological aspects such as concentration polarisation and gel layer formation are accounted for (Tu et al., 2001). The model developed in this work combined diffusion and convection through the membrane inhibited by a series of resistances. Each resistance was then described on a theoretical basis. Since fouling factors were central to the study, modelling and practical investigations were concerned with the fall off of permeate flux with filtration time.

Pontalier and co-workers developed a model based on standard transport theory of diffusion and convection terms with added consideration of factors influencing transport in narrow pores (Pontalier et al., 1999). The resultant equation for solute flux accounted for velocity profile, friction forces between solute and solvent/membrane as well as chemical potential and electrostatic interactions. Experimental work was necessary in this case, as it provided the data required for the estimation of model parameters using rejection rate and permeate flux. Experiment was then used to validate the model.

2.2 Solute type and nanofiltration transport behaviour

2.2.1 Why nanofiltration?

Nanofiltration membranes represent a recent and significant development in membrane filtration research. The term nanofiltration was coined to describe the region of membranes between RO and UF that reject molecules which have a size in the order of one nanometer (MW range 200-1000) (Eriksson, 1988). As the molecular weight cut-off (MWCO) of nanofiltration membranes allows small monovalent salts to permeate but retains multi-valent salts and organics, they are found to be very useful in water treatment situations and in any applications where solute separation is desired. It is because of these characteristic properties that the nanofiltration membrane is the object of much scrutiny.

In the previous Section, the various facets of membrane research have been presented and the variables and scenarios relating to membrane filtration are found to be numerous. However, to achieve a greater understanding of membrane transport behaviour there are only a few avenues of research that are relevant and it is those that allow quantitative conclusions to be drawn on the basis of a fully quantifiable system. Arguably then, research that examines the membrane separation of complex feed solutions such as the by-products of cheese manufacture (Alkhatim et al., 1998) or the removal of pesticides from natural waters (Hofman et al., 1993), are of low value for development of transport theory as it is very difficult to evaluate what are the factors influencing separation as there are so many. Thus, it can be concluded that the most effective course of study is to commence from very simple and idealised feed solutions.

For the purpose of investigating transport through nanofiltration membranes it was possible to categorise the solutes used. These categories were defined as: inorganic salts, un-dissociated organic compounds, dissociated organics in the presence or otherwise of inorganic salts and un-dissociated organic substances in the presence of charged compounds.

2.2.2 Inorganic salts

Salt transport at RO, NF and UF membranes is well documented and Bowen and co-workers have completed some of the most recent studies to this effect (Bowen and Mukhtar, 1996), (Bowen and Mohammed, 1998), (Bowen et al., 2000). These studies have all related to deriving and improving theories relating to transport across the membrane and since these models are largely phenomenological it is essential that mechanisms are well observed and understood. Discussion of salt transport in binary and ternary systems (where charge effects become important) at synthetic membranes extends back to some of the seminal works of early membrane workers (Donnan, 1995),(Hoffer and Kedem, 1967), (Dresner, 1972), (Probstein et al., 1972), (Lonsdale et al., 1974) thus salt rejection is an area of the technology that is supported by a breadth of knowledge.

2.2.3 Un-dissociated organic compounds

The rejection of un-dissociated organic compounds is generally considered to be a function of their size. Nakao and Kimura used six organic solutes (PRG #4000, Vitamin B12, Raffinose, Sucrose, Glucose and Glycerine) to investigate transport modelling in relation to ultrafiltration membranes (Nakao and Kimura, 1981). These six solutes were selected on the basis of their different molecular weights. The authors were able to produce a curve of reflection coefficient as a function of pore radius that was approximated well by the Spiegler and Kedem model (Spiegler and Kedem, 1966). Three parameters: solvent permeability, L_p, solute permeability, P and reflection coefficient, σ, were determined and were provided as characteristics of the membrane. Nakao and Kimura then used a "pore theory" to relate these parameters to a value of pore radius.

Van der Bruggen and co-workers commenced on a course of research investigating the retention of a series of organic compounds with four commercial nanofiltration membranes (Van der Bruggen et al., 1999). The four membranes were designated as having molecular weight cut-offs ranging from 180 to 2500 and the solutes used, of which there were 25, varied in molecular weight from 32 to 697 g/mol. The compounds selected were alcohols, phenolics, dyes and saccharides. Retention was

found to be strongly governed by size. The authors reported that although the strength of the relationship between molecular size and rejection was increased when using size parameters with a physical meaning such as Stokes diameter, equivalent molecular diameter or calculated molecular size, they concluded that improvement was not significant enough to use these measurements instead of molecular weight.

In a further development of the work, Van der Bruggen and co-workers made a comparison of the model theories available for describing the retention of organic molecules (Van der Bruggen et al., 2000). They evaluated theoretical descriptions of the "black-body" parameter σ, the reflection coefficient. Rejection data was obtained for a series of organic compounds at very high pressures (> 20 bar) such that maximal retention was achieved. Maximal retention, taken as an approximation of reflection coefficient, was plotted as a function of solute size and the parameters of four models, central to the discussion, were fitted to the data using a least-squares method. A theory that treated the membranes as having pores with a log-normal size distribution, was found to provide the best fit to the experimental data. Thus reflection coefficient was determined to be a property of the relation between solute and pore sizes (Van der Bruggen and Vandecasteele, 2002).

2.2.4 Dissociated compounds

Organic

Discussion with respect to the transport of organic ions through membranes, is more prevalent since they provide a more distinct set of characteristics i.e. charge, valence and size. Molecular size has been given a more precise definition, by considering the orientation of molecules as they approach the membrane surface and therefore what dimension (width or length) is most critical (Kiso et al., 1992). Molecular orientation is dependent on the interactions between the membrane and the solute.

When evaluating the rejection behaviour of organic compounds, Van der Bruggen also considered polar and charged molecules at the same time as uncharged non-polar compounds (Van der Bruggen et al., 1999). They found that both polar and charged

molecules did not fit well with the transport theory at the centre of the discussion and had to be omitted to improve the results of statistical analysis.

Trace organic molecules that are increasingly prevalent in surface and ground waters, such as pesticides, are a target for removal by nanofiltration (Berg et al., 1997). A comparison of both charged and uncharged pesticide rejections has been made for a series of nanofiltration membranes. At neutral pH values, nanofiltration membranes and dissociated pesticides are negatively charged thus observed rejections are high (greater than 70% in most cases). Since uncharged compounds are only influenced by steric effects, their rejections vary widely (0 to 90%). This underlines the importance of charge (where it is a factor) as a governing property in rejection. The adjustment of system pH and therefore the degree of solute dissociation, acts to further illustrate the importance of charge on rejection.

By the same token Ozaki and Li considered the effect of pH on the rejection of dissociated organic compounds and concluded that it far outweighed the importance of size factors (Ozaki and Li, 2002). Although it was conceded that neither property could be wholly relied upon when predicting the rejection of solutes. The authors took the unusual step of measuring the rejection of un-dissociated organic compounds while adjusting pH. Seven compounds were chosen (methyl alcohol, ethyl alcohol, benzyl alcohol, urea, ethylene glycol, tri(ethylene glycol) and glucose) and pH was varied from 3 to 9. Some slight variation was present in the results but none that could not be explained as experimental error. With regard to the dependence of rejection on charge, this study went into greater depth than any other work by examining rejection as a function of the pKa value. A sequence of similar compounds (e.g. phenols) was assessed with respect to their rejection at one pH. A strong linear relationship was found to exist between the two properties.

Organic and inorganic salt mixtures

The systems previously mentioned have all been limited to one solute species (e,g a salt or an organic compound) or, at most, two salts with a common counter ion. Thus, the next development was the study of solutions containing two individual compounds or an inorganic salt and a comparatively large organic ion. It is relatively common to find organic solutes in solution with a salt and one particular study

considered the effect of salt concentration (NaCl) on the rejection of a charged organic solute (lactic acid/sodium lactate) (Freger et al., 2000). An increase in salt concentration was shown to reduce flux across the membrane. More unexpected was an observed variation of solution flux with pH, for water and low lactate concentration. However, both behaviours were put down to change in osmotic pressure that results from the change in salt concentration and pH. The authors commented that the possible occurrence of shrinkage in the skin-layer of the membrane, brought about by a reduction of water activity and thus hydration swelling, might explain flux attenuation in the presence of increased salt concentrations where osmotic pressure and viscosity are insufficient. They also observed that the screening of charge on the membrane surface might also be an explanation for this behaviour. All the mechanisms outlined here were considered to play some part in membrane transport, thus highlighting the complexity of membranes systems. To summarise the complex interactions observed and proposed mechanisms taking place the following diagram (Figure 2-1) was provided.

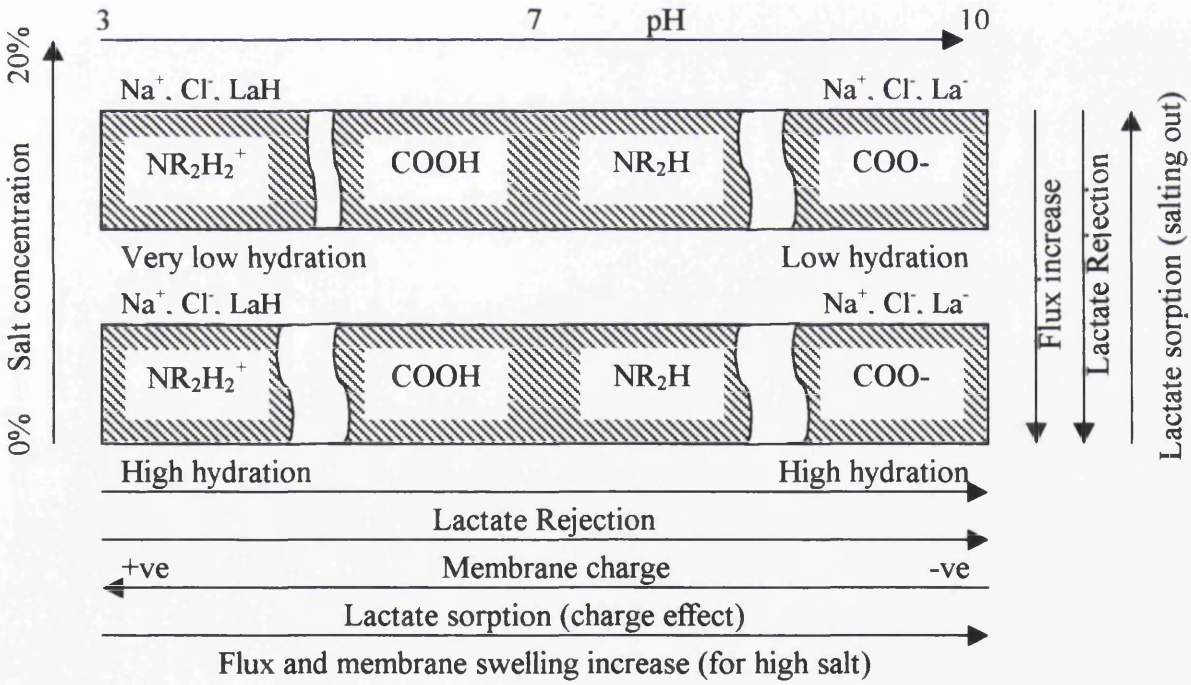

Figure 2-1 A schematic representation of the complex interactions between the different physicochemical effects on membrane performance for salt/lactate solutions (Freger et al., 2000)

A study published in 2001 observed only a few reports investigated the effect of interactions on the retention behaviour in aqueous organic solutions (Weiβbrodt et al.,

2001). To address this imbalance the authors investigated the transport of propan-1-ol across a reverse osmosis membrane in the presence of a series of acids, alcohols, ketones and aldehydes. Propan-1-ol was chosen as it exhibited an intermediate value of rejection. Some modelling work was undertaken and polarity and size were accounted for as parameters in the model. However, although the presence of a second solute was shown to influence transport of propan-1-ol the authors ignored conventional effects such as osmotic pressure and concentration polarisation when discussing the results.

2.2.5 Un-dissociated compounds and salts

Very few investigations have been made into the interactions between un-dissociated organic compounds and salts. This is surprising as it superficially represents a simpler system for investigation than that of charged organic solutes and salts or charged organic and uncharged organic compounds. Two studies that did explore this combination investigated the treatment of combined salt and sugar solutions by nanofiltration.

Vellenga and Tragardh observed that the presence of sugar influenced the rejection of salt at the membrane. Unfortunately they could not make any observations about the influence of salt on sucrose rejection, as the value in all cases was very high (greater than 99%). The change in salt rejection with sugar concentration was attributed to the fact that viscosity at the membrane surface was sufficiently modified to effect salt flux. They did not consider charge effects or possible modifications to the membrane surface (Vellenga and Tragardh, 1998).

In the study by Wang and co-workers permeation experiments were carried out for single component solutions of salts and neutral organic solutes and mixtures of NaCl and glucose or sucrose (Wang et al., 2002). The effects of pressure and concentration as well as coupling interactions between salt and glucose and sucrose were investigated. Some change in glucose and sucrose rejection was observed for increased salt concentrations although the work was not extensive. This change in

rejection was attributed to the phenomena of membrane shrinkage proposed by Vellenga and Tregardh.

2.2.6 Conclusion

To advance knowledge of transport processes in nanofiltration membranes it is beneficial to initially study their performance with respect to the permeation of simple and quantifiable solutions. Studies to this effect have investigated single component solutions of salts, neutral organic compounds and charged organic compounds and combined solutions with two examples of these three solute groups. Transport of charged species across nanofiltration membranes is well-understood relative to systems where neutral solutes are present in combination with charged solutes. Some investigations have been completed for neutral solutes in the presence of salts that indicate coupling effects, but these studies have been secondary only to the main investigation and the authors have not made any attempt to quantify the results in relation to current or advanced model theories.

It is concluded that solute systems comprised of neutral organic solutes in the presence of one or more charged species are worthy of further investigation and it is the aim of this thesis to discover any potential patterns of behaviour in such systems and through theoretical discussion identify mechanisms that cause this behaviour.

2.3 Transport theory and modelling development

A summary of contemporary transport theories and their development is essential to enable a deeper understanding of the mechanisms that exist in membrane transport processes.

In general, there are two approaches to deriving theoretical descriptions the first considers membranes as a "black-box" and models are derived from irreversible thermodynamics. The second method is phenomenological and aims to provide a transport theory that incorporates a description of each governing mechanism.

What follows is a development history of the two principle models that are widely used and generally considered to be the definitive articles of their respective approaches.

2.3.1 Early developments

A leading pioneer in membrane theory and modelling, Ferry, introduced some important key concepts with his theory of ultrafiltration (Ferry, 1936). At this time the principles of sieving, adsorption and the influence of long pores were being considered. However, pore size was determined using the flow of pure water through the membrane. Ferry decided that such a characteristic would be most usefully presented through the definition of a property termed Molecular Weight Cut-Off (MWCO). MWCO was defined as the molecular weight of a compound that was 50% rejected by the membrane and in accepting the notion of partial rejection implied that membrane pores had a size distribution.

As a response to the concept of partial rejection, R, a simple model was developed that considered the statistical likelihood of a molecule colliding with a pore entrance.

$$R = \frac{C_p}{C_f} = 2\left(\frac{d_p - d_s}{d_p}\right)^2 - \left(\frac{d_p - d_s}{d_p}\right)^4 \qquad (2.1)$$

Where C_f and C_p were the feed and permeate concentrations respectively and $\boldsymbol{R}$, the rejection, was a function of the largest particulate species that fails to pass, d_p, and the particle diameter, d_s.

2.3.2 Irreversible thermodynamics

Kedem and Katchalsky conducted a thermodynamic analysis of membrane permeability (Kedem and Katchalsky, 1958). Prior to this there had been treatments of solute and solvent flow based Fick's law analogies and considerations of osmotic pressure represented by

$$\frac{dN_s^i}{dt} = k_s A_m \left(C_f - C_p\right) \tag{2.2}$$

and,

$$\frac{dV_p}{dt} = k_w' A_m \left(\Delta p - \Delta \pi\right) \tag{2.3}$$

Where k_s and k_w' were the solute and solvent permeability coefficients respectively, N_s^i the molar concentration of solute in the permeate, A_m the membrane area, V_p the volume permeated and Δp and $\Delta \pi$ were the applied and osmotic pressures. These equations were found to be deficient in that no distinction was made between permeable and non-permeable solutes and that the relation between diffusion and filtration flows was ignored. Thus permeability equations were derived on the basis of irreversible thermodynamics, which lead to the following

$$J_v = L_p \left(\Delta p - \sigma RT \Delta c\right) \tag{2.4}$$

and

$$j_s = \omega RT \Delta c_s + \left(1-\sigma\right) c_s J_v \tag{2.5}$$

Where J_v was the total permeate volumetric flux, L_p was the hydraulic permeability, σ the reflection coefficient, ω mobility of the solute, c_s was the concentration of the

solute and j_s the solute flux. This treatment considers that three interactions are occurring: those between solvent and solute, the solvent and membrane and the solute and membrane.

The equations derived by Kedem and Katchalsky for solvent and solute flux, (2.4) and (2.5), can be more neatly presented as

$$J_v = L_p(\Delta p - \sigma\Delta\pi) \tag{2.6}$$

and,

$$J_s = \omega\Delta\pi + (1-\sigma)J_v C \tag{2.7}$$

Spiegler and Kedem showed that the above equations can be integrated across the membrane assuming the constancy of three coefficients: the specific hydraulic permeability $\mathscr{P}_1$, the local solute permeability, $\bar{P}$, and the reflection factor, σ; (Spiegler and Kedem, 1966) hence

$$J_v = -\mathscr{P}_1\left(\frac{dp}{dx} - \sigma\frac{d\pi}{dx}\right) \tag{2.8}$$

$$J_s = -\bar{P}\frac{dc_s}{dx} + (1-\sigma)c_s J_v \tag{2.9}$$

The approximate constancy of these three coefficients is brought about by the consideration of local membrane flux. The relationship between local and overall permeabilties can be illustrated by, $L_p \equiv \mathscr{P}_1/\Delta x$ and $\omega \equiv \bar{P}/(2RT\Delta x)$ hence they are normalised for unit membrane thickness.

By stipulating the following conditions (where superscripts ′ and ″ designate the feed and permeate sides of the membrane respectively)

$$c_s'' = J_s/J_v \tag{2.10}$$

and

$$R = 1 - \frac{c''}{c'} \tag{2.11}$$

Salt rejection was defined as

$$R = \frac{(1-F)\sigma}{1-\sigma F} \tag{2.12}$$

Where,

$$F = e^{-J_v A}, A = \frac{1-\sigma}{P_s} \tag{2.13}$$

Equation (2.12) allows calculation of the salt rejection curve using values of reflection coefficient, σ, and solute permeability P_s, determined from suitable apparent osmotic pressure and diffusion measurements. Equations (2.6), (2.7), (2.12) and (2.13) comprise what is commonly referred as the Spiegler-Kedem Model (S-K).

S-K and a membrane impermeable ion

Lonsdale and Pusch observed that the presence of a membrane impermeable ion in the feed solution significantly influences the transport of co-ions through the membrane (Lonsdale et al., 1974). Lonsdale demonstrated this experimentally and then preceded to develop a simple model, an extension of the model developed by Donnan that described the observations. Lonsdale defined the rejection in a simple salt solution as,

$$R_s = 1 - c_s''/c_s' \tag{2.14}$$

If the fluxes of salt and water are assumed to be uncoupled the solution-diffusion model predicts that salt flux is given by:

$$j_s = D_{i,p} K_s (\Delta c/\Delta x) \tag{2.15}$$

Where $D_{i,p}$ was the diffusivity of the salt in the membrane and K_s the diffusion coefficient.

And so, it was found that,

$$\boldsymbol{R}_s = \left(1 + B/J_v\right)^{-1} \tag{2.16}$$

Where $B = D_{i,p}K_s/\Delta x$ was a function of diffusion coefficient, membrane/water partition coefficient and the membrane effective thickness, Δx. Lonsdale continued further to investigate the case of a salt mixture containing an impermeable ion (*i*) and a salt mixture containing a partially-membrane-impermeable ion. Finding that in the case of a membrane-impermeable ion

$$\boldsymbol{R}_- = 1 - \left\{B'/\left(B' + J_v\right)\right\}\sqrt{\left(1 + c_I'/c_-'\right)} \tag{2.17}$$

Where c_-' designated the cation concentration and c_I' the impermeable ion concentration.

And for the condition of a partially-membrane-impermeable ion

$$\begin{aligned} &\left(1-\boldsymbol{R}_-\right)^2\left\{\left(J_v/B''\right)^2 - 1\right\} \\ &-\left\{2\left(J_v/B''\right)\sqrt{\left(1+c_I'/c_-'\right)} + c_I'/c_-'\left(1-\boldsymbol{R}_I\right)\right\}\left(1-\boldsymbol{R}_-\right) + 1 + c_I'/c_-' = 0 \end{aligned} \tag{2.18}$$

The derivation of these equations is assisted by observing the concentrations of ions (anion, cation and impermeable ion) on either side of the membrane, from which a description of the driving force can be drawn. In the case of an impermeable ion, the solute concentration on the upstream side of the membrane can be described by,

$$c_s' = \sqrt{\left(c_+'c_-'\right)} = \sqrt{\left[\left(c_-' + c_I'\right)c_-'\right]} \tag{2.19}$$

and concentration on the downstream side is given by,

$$c_s'' = \sqrt{\left(c_+''c_-''\right)} = c_-'' \tag{2.20}$$

where c_+'' was the anion concentration in the permeate.

If the "impermeable" ion were partially permeable then equation (2.20) would resemble equation (2.19) as the less permeable ion would also be present on the downstream side.

Definitions of transport parameters in the S-K model

Nakao and Kimura considered that the use of non-equilibrium thermodynamics as a basis for the derivation of phenomenological equations was reasonable based on their applicability to experimental data (Nakao and Kimura, 1982). In models derived from irreversible thermodynamics the characteristics of the membrane are expressed by three transport parameters, but it is impossible to clarify the mechanism of permeation as the membrane is treated as a black box.

In this work Nakao and Kimura compared the "frictional model" and the "pore model". These two models are mathematical descriptions of the transport parameters. In the case of the frictional interpretation, developed by Spiegler and Kedem, the driving forces provided by the chemical potential are counterbalanced by mechanical friction effects. Thus pure water permeability, L_p, solute permeability, P_s, and reflection coefficient, σ, are defined. The basis of the pore model was an analysis of solute transport described by a sphere travelling within a cylinder.

Nakao and Kimura compared the two modelling approaches and removed a discrepancy that existed between them. This discrepancy was the result of ignoring the pressure term in the development of the pore model, thus it was eliminated by an exact derivation.

Nakao and Kimura concluded by eliminating wall correction factors from the pore model thus expressing solutes flux as

$$j_s = D_\infty S_d \left(\frac{A_k}{\Delta x}\right) \Delta C_s + J_v \bar{C}_s S_c \left\{1 + (16/9)\lambda^2\right\} \qquad (2.21)$$

Where D_∞ was the bulk diffusivity, S_d and S_c were steric hindrance factors for diffusion and convection respectively, A_k was the porosity, and λ was the ratio of pore to solute radius.

Comparison with (2.8) gives

$$\sigma = 1 - S_c\left\{1 + (16/9)\lambda^2\right\} \tag{2.22}$$

$$P_s = D_\infty S_d\left(\frac{A_k}{\Delta x}\right) \tag{2.23}$$

Equations (2.22) and (2.23) denote the parameter definitions of the steric-hindrance pore model.

Parameter definition was also provided by Jitsuhara and Kimura who carried out an in-depth analysis of the parameters used by the Spiegler-Kedem model (Jitsuhara and Kimura, 1983b). Values for these parameters were determined experimentally, but Kimura and co-workers endeavoured to define them theoretically. As for the above work, a frictional discussion was employed incorporating Donnan equilibrium. As a result reflection coefficient was defined as

$$\sigma = 1 + \frac{\pi_c X_d}{\Delta c_s}\left\{Z^{II} - Z^{I} - (2t_{n1} - 1)\ln\frac{Z^{II} + 2t_{n1} - 1}{Z^{I} + 2t_{n1} - 1}\right\} \tag{2.24}$$

Where $Z = \sqrt{1+B}$, $B = \left(2c_s/\phi X_d\right)^2$, $t_{n1} = \dfrac{\omega_1}{\omega_1 + \omega_2}$, X_d was the charge density, ϕ was the osmotic coefficient and ω was the mobility.

Permeability was defined by

$$P = \frac{RT\pi_c X_d \phi_w}{\tau F^2 \Delta x} \frac{\int_{c_s^I}^{c_s^{II}} \left\{\left(\sqrt{1+B} - 1\right)/c_s\right\} dc_s}{\int_{c_s^I}^{c_s^{II}} \left(\dfrac{\sqrt{1+B} - 1}{\sqrt{1+B} + 1}\dfrac{1}{\Lambda_1^{\,0}} + \dfrac{1}{\Lambda_2^{\,0}}\right) dc_s} \tag{2.25}$$

Where τ was the tortuosity factor, F was the Faraday constant and Λ was the ionic equivalent conductivity.

Comparison of the values obtained using these equations and those determined experimentally using equation (2.12) and (2.13) showed that equation (2.24) provides a good approximation of the reflection coefficient but equation (2.25) provides a weaker correlation although the general trends are reflected.

Inspection of the above definitions of reflection coefficient and permeability shows that they are dependent on membrane characteristics such as, charge density, pore tortuosity, membrane thickness, osmotic coefficient and solution properties such as concentration, ionic equivalent conductivity and mobility.

Van der Bruggen and co-workers also provided the parameters used in the S-K model with physical descriptions. Models suitable for organic molecule rejection by nanofiltration membranes were compared (Van der Bruggen et al., 2000).

It was found that a log-normal model provided the most useful prediction of reflection coefficient and was given by:

$$\sigma(r_s) = \int_0^{r_s} \frac{1}{S_p\sqrt{2\pi}} \frac{1}{r} \exp\left(-\frac{\left[\ln(r) - \ln(r^*)\right]^2}{2S_p^2} \right) dr \qquad (2.26)$$

Where r was the pore radius, r^* was the mean pore radius, r_s was the radius of the solute molecule and S_p was the pore size standard deviation ($\pi = 3.14$). This equation indicates that reflection coefficient is a function of the pore-size distribution and solute radius.

Later on the definition of solute permeability was discussed and was shown to be given by $P_s = D_p / \Delta x$ (Van der Bruggen and Vandecasteele, 2002). Stokes-Einstein's law predicts an inverse relationship between the diffusion coefficient and the pore size:

$$D_p = \frac{kT}{6\pi\eta r} \tag{2.27}$$

Where k was Boltzmann's constant and η was the solution viscosity. If diffusion coefficient $D_s = a/d_s$, where a was a constant and d_s the effective diameter of the molecule then the equation for permeability becomes:

$$P_s = \frac{a}{\Delta x}\frac{1}{d_s} \tag{2.28}$$

or $P_s = \rho/d_s$ where $\rho = a/\Delta x$.

These three sets of parameter definitions derived by Nakao, Jitsuhara and Van der Bruggen all attempt to quantify the controlling mechanisms taking place within the membrane. The work is beneficial as it helps to provide an increased understanding of quantitative experimental data through providing extra meaning to previously undefined parameters.

2.3.3 Models based on the extended Nernst-Planck equation

Schlogl detailed another treatment, not dissimilar to that defined by Kedem and Katchalsky in that the thermodynamics of irreversible processes was discussed. Schlogl stated that thermodynamics of irreversible processes have to be formulated in differential form (Schlogl, 1966). Planck used this method in 1890 to treat convection free liquid layers, and this approach was later extended to cover transport through membranes.

Under the assumption of a small pore membrane, the phenomenological relations of the thermodynamics of irreversible processes reduce to give the flux through the membrane of a dissolved constituent as:

$$j_i = c_i - D_{i,p} \times \left\{ \frac{dc_i}{dx} + z_i c_i \frac{F}{RT}\frac{d\bar{\varphi}}{dx} + c_i \frac{d}{dx}\ln\gamma_i + \frac{c_i}{RT}\left(V_i - \frac{M_i}{M_w}V_w\right)\frac{dP}{dx} \right\} \tag{2.29}$$

and

$$J_v = P_m\left(-\rho_{el}\frac{d\bar{\varphi}}{dx} - \frac{dP}{dx}\right) \tag{2.30}$$

It should be noted that there are four terms operating in the main equation. The first deals with the diffusion contribution due to the concentration gradient where c_i was the concentration of constituent i in the membrane and x was a distance coordinate perpendicular to the surface of the membrane. The second term describes that part of the ion transport that was due to electrical transference, where z_i was the valence of ion i, F was the Faraday constant and $\bar{\varphi}$ the electric potential of the membrane. The term proportional to $d/dx \ln \gamma_i$ accounts for a gradient in the activity coefficient (γ_i). The final term describes the contribution to transport that was due to a pressure gradient $\left(d\bar{P}/dx\right)$ where V_i was the partial molar volume of constituent i, V_w the partial molar volume of the solvent, M_i and M_w are the molecular weights of constituent i and the solvent respectively. Equation (2.30) presents total volume flux as a function of hydrostatic pressure gradient, membrane permeability P_m, electrical space charge, $-\rho_{el}$, and electric potential of the membrane.

If the terms in the equation that do not significantly contribute to the overall transport of ions are removed, then the above expression is, according to Schlogl, reduced to the "extended Nernst-Planck equations".

Thus:

$$j_i = c_i v - D_{i,p}\frac{dc_i}{dx} - D_{i,p} z_i c_i \frac{d\bar{\psi}}{dx} \tag{2.31}$$

Where

$$\bar{\psi} \equiv \frac{F}{RT}\bar{\varphi} \tag{2.32}$$

$$j_v = P_m\left(RTqX_d\frac{d\bar{\psi}}{dx} - \frac{dP}{dx}\right) \tag{2.33}$$

Equation (2.31) represents the solute flux and (2.33) the volume flux where q was the charge sign of ion sites on the membrane and X_d was the concentration of those sites. The key differences between these definitions and those provided by Kedem and Katchalsky are the inclusion of charge properties for both the membrane and solute.

Dresner, proposed a method of integrating the extended Nernst-Planck equation based on the assumption of good co-ion exclusion. Dresner suggested that the extended Nernst-Planck equations are attractive as phenomenological descriptions of membrane transport, since they represent a highly simplified version of the equations of thermodynamics. Yet they still account for the three main mechanisms of ionic transport: diffusion, migration in an electric field and convection (Dresner, 1972).

The space-charge model

Probstein and co-workers stated that salt rejection can be analysed in terms of a relatively simple physical model, where the fluid is assumed to flow through the porous material via a series of uniformly distributed, straight, cylindrical pores (Probstein et al., 1972). The effects of the surface charge of the pore are clearly described. Extending a distance approximately equal to the Debye length into the pore, the result of this charge is a build up of counterions. However, to fulfil the condition of electroneutrality the flow of counterions is reduced (and co-ions increased) such that there is an overall rejection of salt. So the rejection performance of the porous material is dependant on the Debye length described as a dimensionless wall potential related to the zeta potential (ζ) and the Peclet number; a velocity term for flow in the pore.

The resultant modelling is generally based on the Nernst-Planck equation with particular attention paid to the distribution of charge within the pore.

Probstein and co-workers furthered their work with respect to charge capillary modelling by making advanced considerations of solutions containing salt mixtures (Probstein et al., 1973). It was stated that ion flux could be represented by

$$J_i = c_i Q_p K_i' - A D_{i,\infty} K_i'' \frac{dc_i}{dx} - A D_{i,\infty} K_i' c_i \frac{d\bar{\phi}_i}{dx} \qquad (2.34)$$

Where Q_p was the total water flux in the pore, A was the pore cross-sectional area and $\overline{\phi}_i = Z_i F\phi/RT$ a dimensionless potential, and

$$K_i' = 4\int_0^1 \exp\left(-\frac{z_i}{z}\overline{\psi}\right)\left(1-\overline{r}^2\right)\overline{r}d\overline{r}$$
$$K_i'' = 2\int_0^1 \exp\left(-\frac{z_i}{z}\overline{\psi}\right)\overline{r}d\overline{r} \qquad (2.35)$$

The two constants K_i' and K_i'' were defined as being radially dependant on ion charge (valence) and potential. These values therefore act as hindrance factors.

Deen also gave consideration to the filtration of charged solutes and developed a model based on the following assumptions (Deen et al., 1980):

a) All ions obey the Nernst-Planck equation
b) The membrane wall has a homogeneous distribution of charge
c) Donnan equilibria exist at the surface of the membrane

The diagram in Figure 2-2 illustrates the situation, where E' and E represent the electric potential at and within the membrane, δ is the effective membrane thickness.

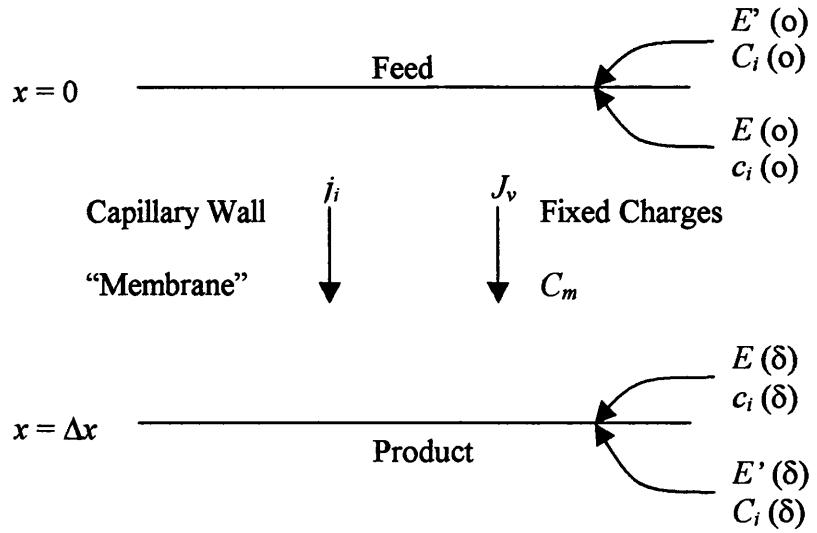

Figure 2-2 Idealised view of the active membrane layer (after Deen et al., 1980)

The assumption was made that fluxes of all charged species are related to local values of solute concentration and electric potential within the membrane, represented by an equation of the form,

$$j_i = -A_k K_{i,d} D_{i,p} \left(\frac{dc_i}{dx} + z_i c_i \frac{d\psi}{dx} \right) + K_{i,c} J_v c_i \qquad (2.36)$$

Where $\psi = FE/RT$ and $\psi' = FE'/RT$ are dimensionless electric potentials and $K_{i,d}$ and $K_{i,c}$ are hinderance factors for diffusion and convection, respectively, which are functions of molecular size, shape and molecular structure. This was, again, a modified form of the Nernst-Planck equation for solute flux.

Deen also described an equilibrium relationship at the membrane solution interface. This was represented by

$$C_i(j) = C_i(j) \Phi_i(\lambda_i) \exp\left\{ z_i \left[\psi(j) - \psi'(j) \right] \right\} \qquad (2.37)$$

Where $\Phi_i(\lambda_i)$ was a term relating to steric partitioning and the exponential term represent the electrostatic contribution to solute partitioning (Donnan Equilibrium).

Combination and successive integration of equations (2.36) and (2.37) gave the following,

$$j_i = \frac{J_v C_i(0) K_{i,c} \Phi_i \exp\left[z_i \left(\psi(0) - \psi'(0) \right) \right]}{1 - \exp(-P_e) \left\{ 1 - K_{i,c} \Phi_i \exp\left[z_i \left(\psi(\Delta x) - \psi'(\Delta x) \right) \right] \right\}} \qquad (2.38)$$

Where

$$P_e = \frac{K_{i,c} J_v \Delta x}{A_k K_{i,d} D_{i,\infty}} \qquad (2.39)$$

Inspection of equation (2.38) reveals that solute flux was a function of the solvent flux, partitioning effects at the two interfaces and other transport properties of the membrane such as hindrance to diffusion and convection, solute diffusivity, porosity and membrane thickness.

Fluid movement across the membrane results from an imbalance between hydraulic and osmotic pressure differences, which may be expressed as

$$J_v = P_m\left(P_R - P_P - \pi_R\right) \tag{2.40}$$

Where P_R and P_P were hydraulic pressures in the retentate and permeate respectively and π_R was the retentate osmotic pressure. P_m was the apparent hydraulic permeability of the membrane wall.

Where membrane pore dimensions are of the same order as solute molecules, it has been observed that the diffusivity of a solute is much lower than in bulk solution. Thus the hindrance effects of fundamental system properties such as the size, shape and electrical charge of both pores and molecules need to be accounted for.

Hinderance factors and the N-P model

Deen reviewed research regarding the hindered transport of solutes in pores, commencing with the transport of rigid molecules depicted by the following diagram (Figure 2-3) where U was the velocity of a sphere radius r_s travelling down a capillary of radius r_o where solvent flow rate was $V_{(r)}$ (Deen, 1987).

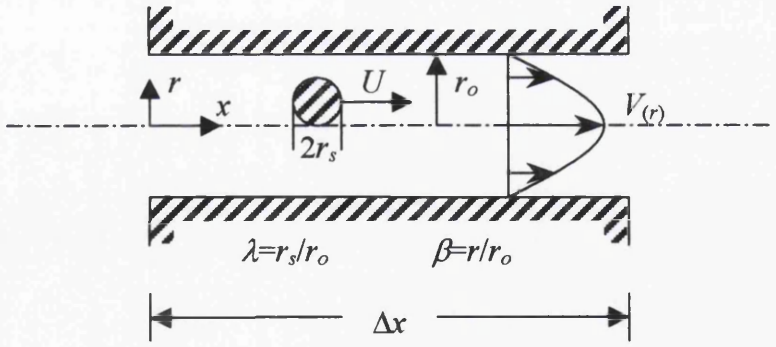

Figure 2-3 Spherical solute in a cylindrical pore (Deen, 1987)

The balance of diffusion force on the molecule and hydrodynamic force combined with considerations of long-range interactions (electrostatic forces) leads to the following definition for local flux.

$$\langle j_i \rangle = -K_d D_{i,\infty} \frac{d\langle D \rangle}{dx} + K_c \langle V \rangle \langle c_i \rangle \tag{2.41}$$

Where,

$$K_d = \frac{\int_0^{1-\lambda} K^{-1} e^{-\psi/kT} \beta d\beta}{\int_0^{1-\lambda} e^{-\psi/kT} \beta d\beta} \tag{2.42}$$

$$K_c = \frac{2\int_0^{1-\lambda} G(1-\beta^2) e^{-\psi/kT} \beta d\beta}{\int_0^{1-\lambda} e^{-\psi/kT} \beta d\beta} \tag{2.43}$$

Note that K_c and K_d, the hydrodynamic convection and diffusion coefficients, were dependent on the radial distribution of solute molecules. G was a coefficient of lag related to the transport of a particle in a fluid filled capillary. Deen focussed on the radial variations of various properties and hence the average values are used in some cases (average values are identified by the use of $\langle\ \rangle$ *angle* brackets).

Relating steady state fluxes to the concentrations in external solutions (C' at $x = 0$ and C" at $x = \Delta x$) requires equation (2.41) be integrated over the pore length. Averaging over the pore cross section it was found that

$$\Phi = \frac{\langle C \rangle_0}{C_0} = \frac{\langle C \rangle_{\Delta x}}{C_{\Delta x}} = 2\int_0^{1-\lambda} e^{-\psi/kT} \beta d\beta \tag{2.44}$$

Where Φ was the partitioning coefficient, the ratio of the average intrapore concentration to that in bulk solution at equilibrium.

The desired macroscopic flux equation is obtained by integration of (2.41), with boundary conditions from (2.44),

$$\langle j_i \rangle = K_{i,c} \langle V \rangle C_0 \frac{\left[1-(C_{\Delta x}/C_0)e^{-Pe}\right]}{\left[1-e^{-Pe}\right]} \tag{2.45}$$

where Peclet number,

$$P_e = \frac{K_{i,c}\langle V \rangle \Delta x}{K_{i,c} D_{i,\infty}} \tag{2.46}$$

Hindrance factor for diffusion,

$$K_{i,d} = \Phi_i K_d = 2\int_0^{1-\lambda} K^{-1} e^{-\psi/kT} \beta d\beta \tag{2.47}$$

and hindrance factor for convection

$$K_{i,c} = \Phi K_c = 4\int_0^{1-\lambda} G\left(1-\beta^2\right) e^{-\psi/kT} \beta d\beta \tag{2.48}$$

Deen concluded the discussion with a review of the hydrodynamic coefficients $K_{i,d}$ and $K_{i,c}$, consideration of pore size, solute shape and concentration, and charge effects.

Mixed electrolyte solutions

Tsuru and co-workers used the extended Nernst-Planck equation to calculate rejection of single and mixed electrolyte solutions. Rejections were found to be strongly dependent upon volume flux, mole fraction of the mixture and the ratio of fixed charge density to feed concentration. For the consideration of mixed electrolyte solutions, the extended Nernst Planck equation was applied by considering the effective charge densities to describe the non-ideality of ion activity in charged membranes (Tsuru et al., 1991).

Probstein had already demonstrated that radial charge distribution was uniform when the Debye length was greater than the pore radius. Steric hindrance could also be ignored on the basis of pore radius being much larger than the ion radius.

Electrochemical potential of the i^{th} ion was expressed as:

$$\mu_i = RT \ln a_i + v_i P + z_i F \psi + \text{const} \tag{2.49}$$

where a_i was the activity of ion i, v_i was the partial molar volume and P was the hydraulic pressure.

Incorporation into the extended Nernst-Planck equation lead to

$$j_i = -c_i \omega_i RT \frac{d}{dx} \ln a_i - z_i c_i \omega_i F \frac{d}{dx} \psi + \beta_i c_i j_v \tag{2.50}$$

where ω_i was the molar mobility. By multiplying equation (2.50) through by z_i / u_i^o and assuming neutrality the following resulted

$$\frac{d}{dx}\psi = \frac{\sum_i \left(\frac{z_i}{\omega_i^o} (c_i - C_{i,p}) j_v \right)}{F \sum_i \left(z_i^2 c_i \right)} \tag{2.51}$$

$$\frac{d}{dx} c_i = \frac{c_i - C_{i,p}}{\omega_i^o RT} j_v - \frac{z_i c_i F}{RT} \frac{d}{dx} \psi \tag{2.52}$$

These could then be solved either analytically or numerically, depending on the complexity of the system, to give a value of permeate concentration. Tsuru compared the performance of this model with those derived from irreversible thermodynamics. Both models showed good agreement.

The Donnan-Steric Partitioning Model

The most recent steps in Nernst-Planck based modelling work have been taken by Bowen and co-workers. They considered a situation of combined Donnan and steric transport effects and hence formulated the Donnan-Steric Partitioning Model (DSPM). Again the extended Nernst-Planck model forms the basis for this description of ion/solute transport in porous membrane, the now widely used representation of the model being:

$$j_i = -D_{i,p} \frac{dc_i}{dx} - \frac{z_i c_i D_{i,p}}{RT} F \frac{d\psi_m}{dx} + K_{i,c} c_i V \tag{2.53}$$

This can be rearranged to give the concentration gradient

$$\frac{dc_i}{dx} = \frac{J_v}{D_{i,p}} \left(K_{i,c} c_i - C_{i,p} \right) - \frac{z_i c_i}{RT} F \frac{d\psi_m}{dx} \tag{2.54}$$

Similarly, the potential gradient term can be expressed as

$$\frac{d\psi_m}{dx} = \frac{\sum_{i=1}^{n} \frac{z_i - J_v}{D_{i,p}} \left(K_{i,c} c_i - C_{i,p} \right)}{\frac{F}{RT} \sum_{i=1}^{n} \left(z_i^2 c_i \right)} \tag{2.55}$$

Note that $D_{i,p} = K_{i,d} D_{i,\infty}$, $K_{i,d} = K^{-1}(\lambda, 0)$ and $K_{i,c} = (2 - \Phi) G(\lambda, 0)$ where K and G were the hydrodynamic coefficients: enhanced drag and lag coefficient respectively. The values of K and G have been studied by Deen and were defined as functions of the ratio of solute to pore radius (Deen, 1987).

Thence, the DSPM was improved by incorporation of concentration polarisation effects (Bowen and Mohammed, 1998) and later on the effects of pore size distributions (Bowen and Welfoot, 2002). Prior to this Bowen and co-workers critically assessed the nature of various contemporary models and found that they were dependent on an arbitrary fitting parameter; the ratio of effective membrane thickness to porosity, $\Delta x / A_k$ (Bowen and Welfoot, 2002). They proceeded to develop a model that was dependant on one membrane parameter – pore radius and also considered the variation of solvent viscosity in small pores. Further to this a second parameter was introduced, the membrane charge.

Through consideration of ion flux and electrochemical potential, the concentration gradient was given as

$$\frac{dc_i}{dx} = \frac{V}{D_{i,p}} \left(\left\{ K_{i,c} - Y_i \right\} c_i - C_{i,p} \right) - \frac{z_i c_i}{RT} F \frac{d\psi}{dx} \tag{2.56}$$

and,

$$\frac{d\psi}{dx} = \frac{\sum_{i=1}^{n} \frac{z_i V}{D_{i,p}} \left(\left\{ K_{i,c} - Y_i \right\} c_i - C_{i,p} \right)}{\frac{F}{RT} \sum_{i=1}^{n} \left(z_i^2 c_i \right)} \tag{2.57}$$

Where,

$$Y = \frac{D_p}{RT} V_s \frac{8\eta}{r_p^2} \tag{2.58}$$

and,

$$V = \frac{r_p^2 \Delta P_e}{8\eta \Delta x} \tag{2.59}$$

Where Y represented the properties of the ion and V was the solvent velocity within the pore, η and D_p were the viscosity and diffusivity in the pore. As for previous studies, equilibrium partitioning at the membrane surface was introduced through use of Donnan equilibrium theory including a steric term. The most commonly use expression is:

$$\frac{\gamma_i c_i}{\gamma_i^0 C_i} = \Phi_i \exp\left(\frac{-z_i F}{RT} \Delta\psi_D\right) \tag{2.60}$$

Where γ_i and γ_i^0 were the pore and bulk fluid ion activities. The assumption was made that a layer of orientated water molecules existed on the pore wall, which reduced the dielectric constant. This reduction in dielectric constant results in an energy barrier to solvation of ions into the pores and can be assumed to be the dominant dielectric exclusion mechanism. Thus it was found that

$$\frac{c_i}{C_i} = \Phi_i \exp\left(\frac{-z_i F}{RT} \Delta\psi_D\right) \exp\left(\frac{-\Delta W_i}{kT}\right) \tag{2.61}$$

Where the solvation energy barrier ΔW_i, is calculated from the Born model:

$$\Delta W_i = \frac{z_i^2 e^2}{8\pi\varepsilon_0 a_s}\left(\frac{1}{\varepsilon_p} - \frac{1}{\varepsilon_b}\right) \tag{2.62}$$

Where e was the electronic charge, ε_b and ε_p were bulk and pore fluid dielectric constants and ε_0 was the permitivity of free space. The steric partitioning coefficient Φ_i must be included otherwise without it equation (2.61) would imply that molecules larger than the pore could enter, which is impossible. The above equations are all determined for ion transport, Bowen and co-workers also made similar considerations for uncharged solutes.

3 Materials and Methods

3.1 Introduction

The aim of this work was to investigate the rejection of solutes in multicomponent organic and inorganic systems. To help achieve this, suitable equipment was necessary for running and monitoring membrane filtration experiments and for analysing the product and feed composition during and after the process.

For the purposes of this work, a number of membrane samples were acquired from several different manufacturers. These membranes were selected on the basis of their publicised performance data. The nanofiltration category of membranes was selected for investigation in this study, as they were known to exhibit rejection properties most suited to this application. However, examples of both RO and UF membranes were also studied. Although commercially supplied in spiral wound (SPW) form, flat sheet samples of the membrane were obtained.

These membranes were used in conjunction with a variety of feed scenarios in the experimental apparatus. These ranged from pure water and single salt solutions to more complex mixtures of compounds, both uncharged and ionic.

3.2 Membrane filtration apparatus

The apparatus constructed for the purpose of membrane filtration experiments had to fulfil a number of requirements. These were:

i. To give high integrity support for the membrane and allow operation in the cross flow orientation.
ii. To provide a known feed at constant concentration, pressure, flow and temperature throughout equipment operation.
iii. To enable control and recording of all experimental variables throughout the course of a filtration experiment.

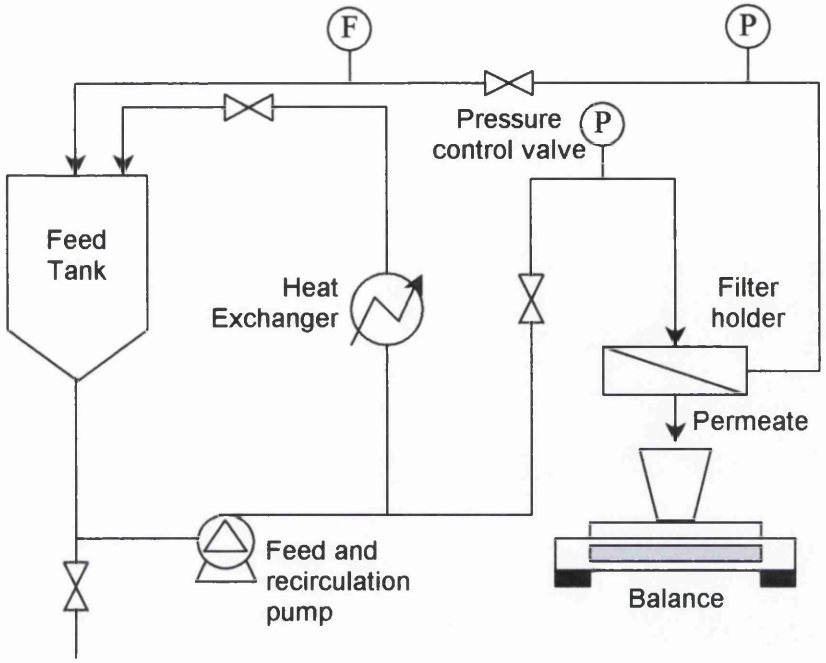

Figure 3-1 Flow diagram of apparatus

3.2.1 Filter holder

The filter holder used in this work was designed and constructed in this laboratory such that it could provide a wide variety of pressures and flow rates to the membrane. Employing relatively small areas of flat sheet membrane the layout was such that feed was directed to and across the membrane surface by means of a spiral shaped channel. The benefit of this design was the establishment of a cross-flow filtration regime without the cost associated with the use of spiral wound modules or similar.

Although the holder used in this work was specifically constructed and is unique, there are commercially available experimental membrane holders that achieve the same effect. In these holders the membrane is again used in flat sheet form but is sandwiched in the module with a gauze like spacer material. It is this spacer material that promotes an even flow of feed over the area of the membrane.

Detailed description

The filter holder was machined from stainless steel and was comprised of two parts, the base and the lid. At its thickest point the base was 33.6 mm deep and was circular in shape with a diameter of 177.6 mm. A recess exists in the base to facilitate location of the membrane. This recess measures 148.3mm in diameter and 8.5 mm deep. Into this were cut circular channels designed to remove and drain product from the underside of the membrane. These channels are laid out as concentric circles, each consecutive channel deeper than the last as they draw closer to the central drain hole.

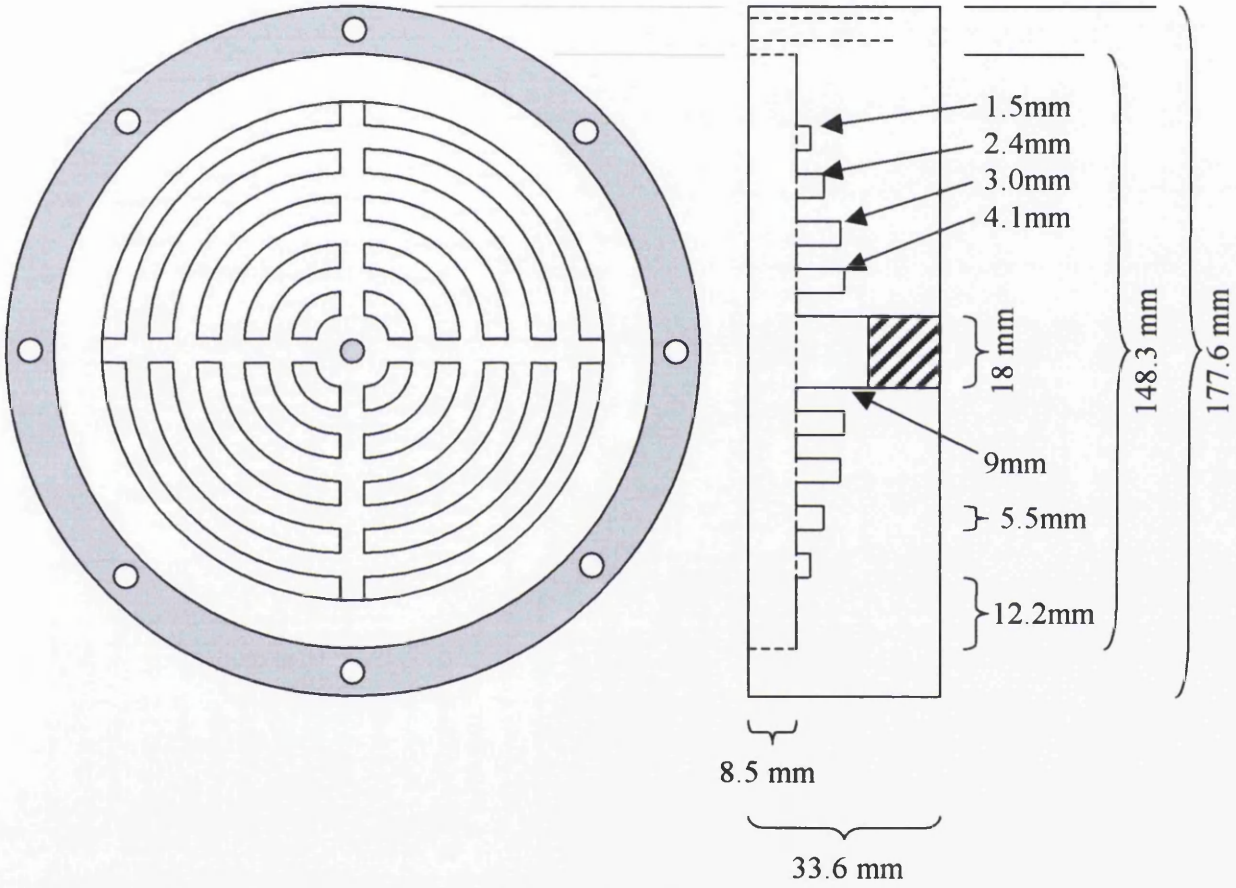

Figure 3-2 The filter holder base section showing the pattern of drainage channels under the filter

The circular lid of the holder (Figure 3-3) measured 18 mm at its thickest point. On the underside of the lid was a protrusion 139.6 mm in diameter that sat in the recess provided by the base part of the module. This protrusion had a spiral shaped groove machined into its face such that when the lid was pressed against the membrane an enclosed channel was formed. This enclosed channel provided a route for feed flow across the membrane.

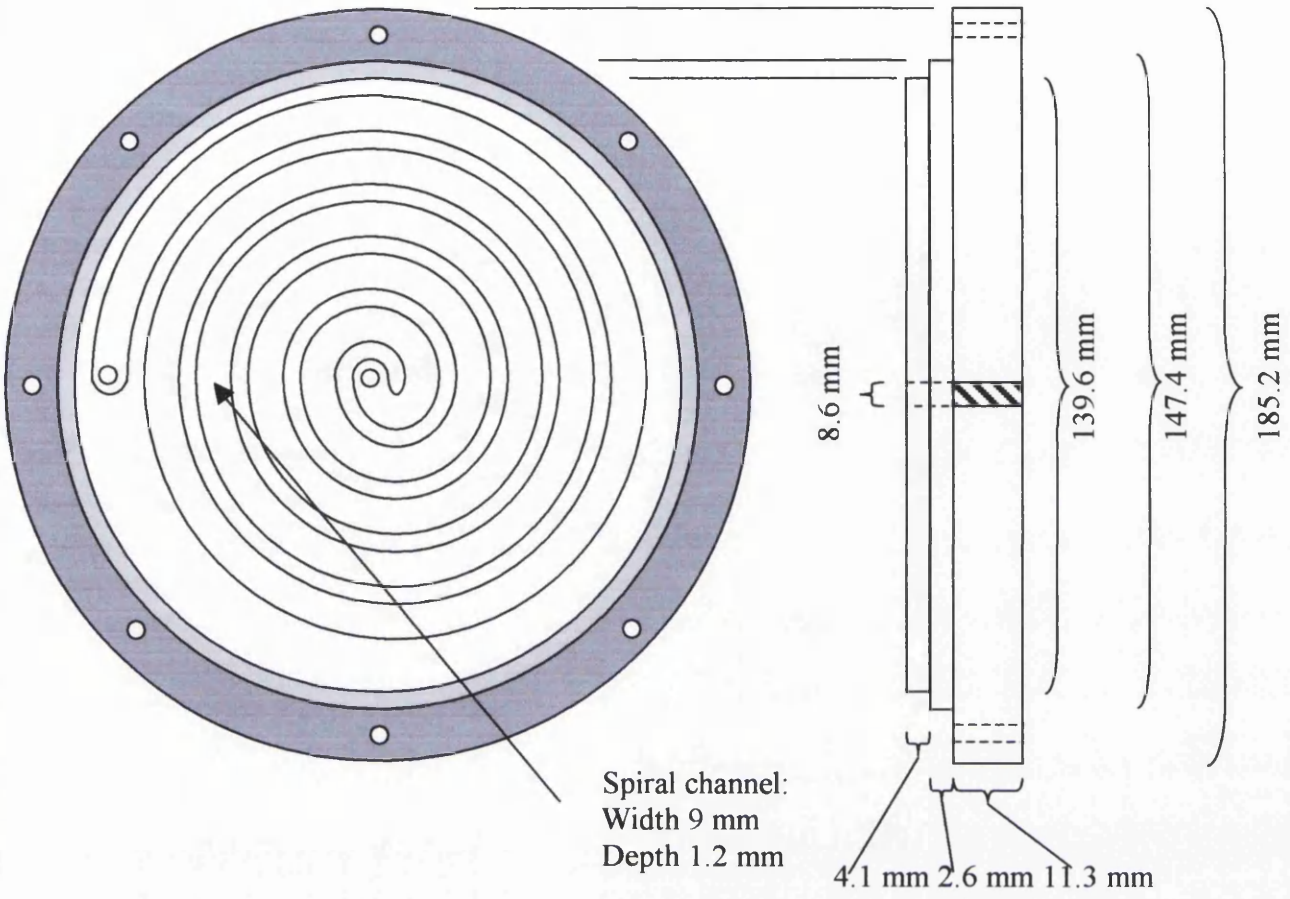

Figure 3-3 The filter lid section illustrating the spiral patterned flow channel

A circular piece of sintered PTFE (diameter 148.3 mm, thickness 2.4 mm) was used as a support for the membrane and fitted precisely into the void that remained between top and base parts of the unit when they were joined. A butyl rubber o-ring, located around the membrane edge, formed a seal against egress of feed around the edge of the membrane and PTFE support, to the product side. The module was sealed using six symmetrically spaced screws located around the edge of the membrane module; these provided the force required to create an even and effective seal between the lid, the O-ring and thus the membrane. Feed was delivered to a central port and the cross flow was collected from a port near the edge of the vessel, both of which used ¼" 316 stainless steel tube compression fittings.

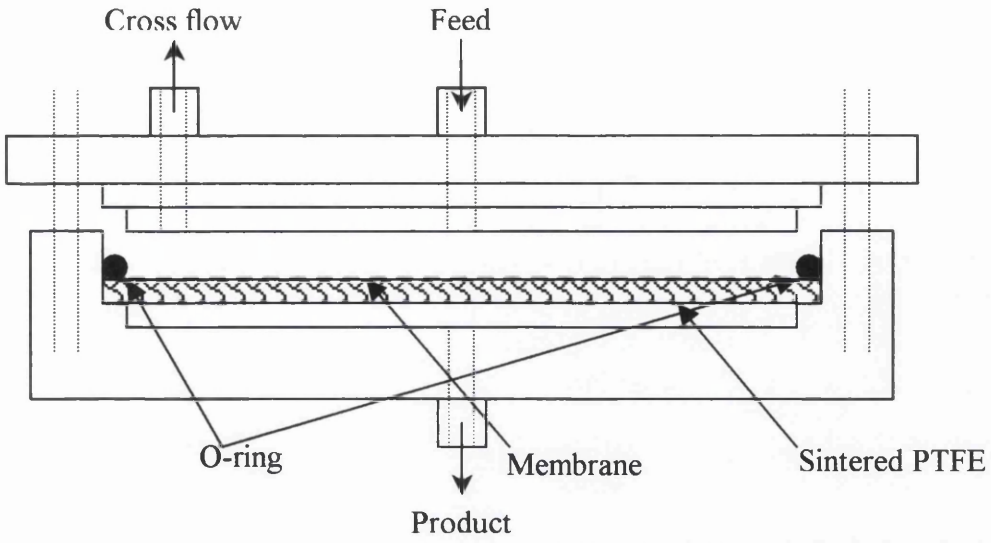

Figure 3-4 Location of the membrane in relation to the sintered PTFE plate and the filter holder

3.2.2 Pump

All membrane filtration systems are pressure dependent and as such require a means by which a positive head can be provided and maintained. In the laboratory several means were available to achieve this:

i. Bench compressed air. Typically available as a range up to 6 bar and limited only by the condition of the supply. Pressure delivered to the membrane was controllable by a reducing valve. Head provided by this means would have been steady and transient free, and promised a smooth flow of liquid.

ii. Cylinder gas. Compressed nitrogen gas, provides a clean source of pressure head and would have allowed development of a system that was sealed from atmosphere thus avoiding potential contamination issues. When delivered the cylinder pressure is usually around 220 bar in the gas cylinder. This is many times higher than required, so a suitable reducer would have enabled a wide range of operating pressures.

iii. Positive displacement pump. This can be fitted in line between the feed tank and membrane module, with feed pressure being controlled either through use of a bypass, or an inverter that controls the speed of the pump motor. The pressure range is dependent only on the pump used.

Compressed gas membrane systems would require a complex design and layout in order to operate them in the desired cross flow format. This therefore precluded the first two options, given above, for use in this study. There were also safety and supply concerns associated with the frequent use of compressed gas. Hence the third option, a positive displacement pump, was selected for use.

The pump

The pump that was used in this work was a positive displacement rotary type unit manufactured by Fluid-o-tech. Specified as being suitable for reverse osmosis applications, replacements and further technical and performance data were found to be available from the manufacturer.

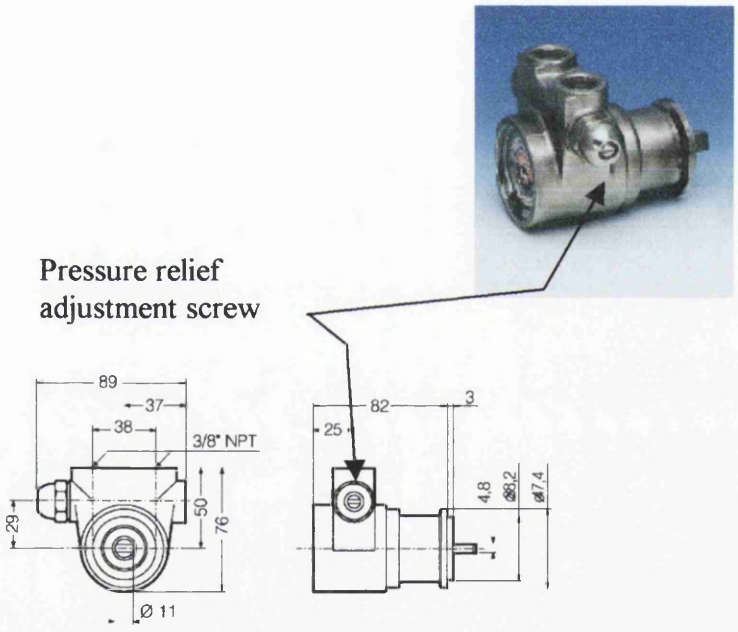

Figure 3-5 Pump head

The pump, cast and machined from AISI 303 stainless steel was of a rotary vane design. The vanes and flow chamber were manufactured from graphitic carbon. The head had 3/8" NPT inlet and outlet ports, these enabled the pump to be incorporated into the system through the use of two Swagelok reducers. Some control of delivery pressure was possible though use of a bypass (pressure relief screw, see Figure 3-5) built onto the pump.

The drive for the pump was a GEC machines limited electric motor. The unit required a 220-240 V single-phase supply and the power output was 180 W at 2.3 A. Output power was not variable as there was no inverter.

The motor ran continuously at 1425 rpm thus according to the performance curves available for the pump (Appendix A-4), output ranged from 345 l/h at 2 bar to 315 l/h at 14 bar (95 ml/s at 29 psi to 87.5 ml/s at 200 psi).

Although capable of operating at very high pressure the apparatus was designed and intended only to be run at low values of pressure and cross flow rate, relative to the maximum output of the pump. This design philosophy allowed a flow as little as 4ml/s at pressures from 0.3 bar to 3.5 bar (5-50 psi) to be achieved.

Pump operation

Power was supplied to the motor via a relay box from the mains supply. The use of a relay enabled remote switching of the pump from the computer that was used for control and data logging. Thus the pump could automatically be brought in and out of use to coincide with beginning and end of experiments.

The bypass built into the pump not only existed as a guard against the dangers associated with blind ending the pump but also enabled a measure of control over the feed supply pressure. Adjustment was made using the screw mounted on top of the pump head (Figure 3-5).

Care was taken in the design of the equipment to ensure that cavitation of the pump was eliminated. This was achieved by ensuring that the tube used in the feed line to the pump was as large as was practicable and that a positive head was provided to the feed side of the pump.

3.2.3 Measurement and control input/output devices

The apparatus had a range of devices for measuring the experimental variables, including temperature, pressure and fluid flow rate. A computer collected and converted data from these devices data via a signal conditioner.

Flow measurement

There were two flows that required continuous measurement. These were the flow of liquid across the membrane – the cross-flow flow rate and the flow of solution through the membrane, the permeate flow rate.

The cross-flow flow rate was measured using a small turbine meter (figure 3-1). This meter was fitted in line with process fluid propelling the turbine. The body of the meter was formed from PVDF and housed a Hall effect switch that was activated by four small magnets in the turbine.

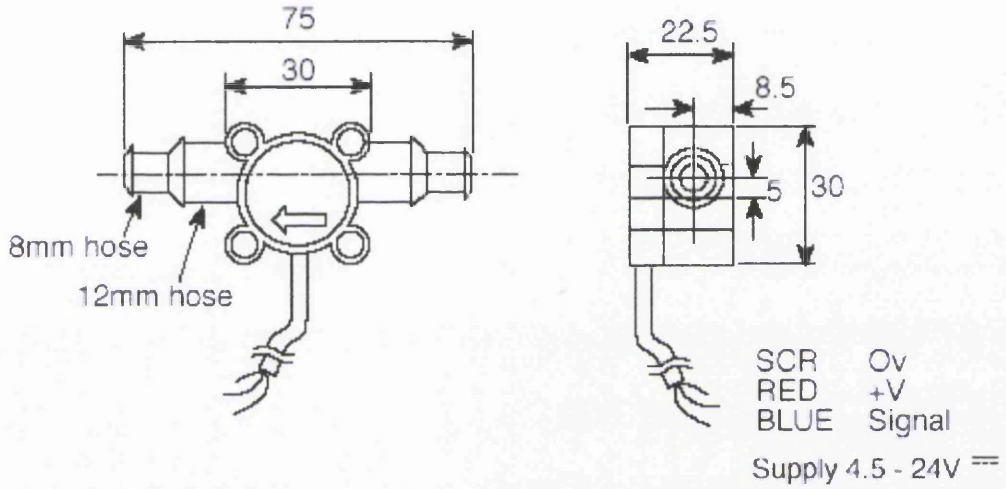

Figure 3-6 The recycle flow meter

The detector had an operating range of - 40°C to + 125°C. Due to the flow meters' utilisation of a Hall Effect system it could not be mounted near any magnetic sources hence a relatively remote location from the pump and the solenoid valves was used. A remote location also helped damp pulses in fluid flow, that were a product of pump operation. The flow meter was attached to the stainless steel piping using flexible hose and Unix clips, making use of the hose connections displayed in Figure 3-6. The power to the meter and the signal it produced were conveyed to and from the signal conditioner through a 9 pin D-type connector.

The flow meter was calibrated using a large measuring cylinder of two-litre capacity and a stopwatch. The resulting calibration curve for flow against signal output (bits)

generated a fourth order polynomial that was incorporated into the data logging and control software. Thus data was converted from an input signal to real values.

The permeate, or product flow rate, was measured using an electronic balance. The balance used was an Ohaus Navigator balance with a total capacity of 410g. It required a 240V mains power supply and a level, stable surface for accurate operation. An RS232 port at the rear of the balance allowed connection to a PC computer. The balance gave a cumulative reading of the product passed through the membrane with time.

The RS232 interface allowed the mass on the balance to be read at the same time as all the other data from the equipment was being logged. Balance accuracy was ± 0.1 g with a precision of 0.1 g.

The balance was located under the outlet for the filter, the filter being suspended above the balance on a frame. A collection vessel was then placed on the pan to collect the filtration product.

Pressure measurement

Pressure was measured at two points in the system, one sensor was located just before the filter housing and one just after. This enabled the pressure drop across the surface of the membrane to be measured.

The pressure gauges used for this task were small low cost electronic devices that relied on a Wheatstone bridge for their operation. In these units the circuitry was printed on a flexible barrier that acts as a seal between the system and the atmosphere. A change in pressure then caused this barrier to flex and a signal to be produced. As with the flow gauge, the pressure sensor received power and outputs a signal to and from the signal-conditioning unit to which it was connected using a DIN plug. The pressure sensor was capable of measuring a pressure in the range 0-6.9 bar (0-100 psi), and was connected to the rest of the system using epoxy resin adhesive and a brass coupling. Both sensors were housed in ABS enclosures to negate the risk of accidental damage.

Fitting each unit in line with an accurate Bourdon tube pressure gauge allowed calibration. Signal output at a sequence of pressures was then depicted as plot of signal versus pressure and an appropriate calibration equation generated. As with the flow sensor, this equation was then used in the software that processed and logged the data.

Temperature measurement

Temperature was measured at the feed tank and at a point just prior to the membrane. For this purpose two platinum resistance (Pt_{100}) thermometers were used. Calibration was not required, as they were known to give a voltage signal that was directly related to temperature. The function relating temperature to voltage was linear between 0 and 2.5 V for 0 to 100°C.

The temperature sensor in the feed tank was suspended centrally in the vessel, care had to be taken to avoid the thermometer "drying out" at anytime during experiment and thus not indicating the true temperature of the fluid. The importance of this was apparent when control of the feed temperature was considered, since the temperature of liquid in the feed taken was used as the measured variable. The robust construction of the device, with the platinum resistance thermometer being encased in a stainless steel sheaf, meant that it would not be damaged in use. The second sensor, located before the filter was inserted into the feed stream by use of a port designed specifically for this purpose. Although the temperature sensor had dimensions similar to that of the tube's internal diameter, insertion into the flow did not create an unacceptable pressure drop.

Heat Exchanger

Membrane filtration was known to be significantly influenced by temperature; therefore some form of control over temperature was required to guard against performance variations due to its fluctuation.

To achieve thermal control a suitable heat exchanger was required. There were two reasons that necessitated a heat exchanger:

- Feed temperature was influenced by ambient conditions and would not necessarily be at the chosen experimental operating temperature (in all cases 25°C). Thus heating or cooling would be required.
- The use of a pump for pressure and flow generation, was accompanied by a heating effect. The heating affect of the pump was determined to be 0.0032 kW.

The presence of a heat exchanger also provided the option of studying the effect of temperature on membrane performance. However, this was not a feature of this study.

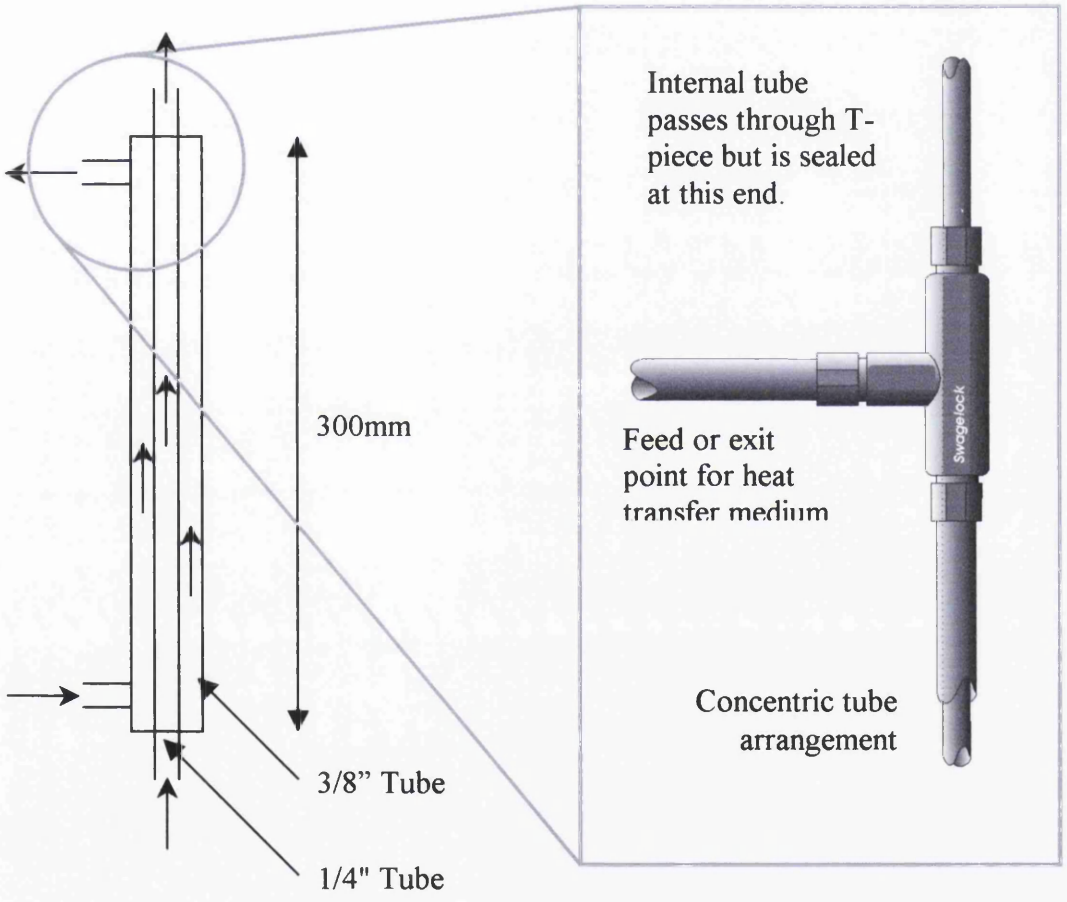

Figure 3-7 concentric tube heat exchanger with connection detail

A specialist fitting available from Swagelok enabling the construction of a concentric tube heat exchanger facilitates this. This fitting resembled a reducing T-piece, where the reduction was on the straight side (not the branch). It differed from a normal reducing T-piece in that it allowed the smaller diameter tube to pass all the way through and onward into the centre of the larger diameter tube. Thus the cooling or heating medium could enter through the branch and flow in the annulus created

between the smaller bore, process-fluid carrying, tube and the larger tube. This is illustrated in Figure (3-7).

Based upon the amount of heat energy produced by the pump (0.0032 kW), a heat exchanger 3.88 cm long was found to be necessary to maintain the process fluid temperature. This was determined on the basis of a typical shell and tube heat transfer coefficient, obtained from literature, of 1.5 $kW/m^2.K$ (see Appendix A-7 for calculations). However, in order to provide a significant amount of heat transfer capability that allowed responsive control and a rapid change of an entire batch of process fluid, a significantly larger heat exchanger was constructed. As can be seen from Figure 3-7, the final unit was 7.5 times the size of that suggested by heat transfer duty calculations.

Figure 3-1 indicates that the heat exchanger was located on the filter by-pass line. This allowed the contents of the feed tank to be heated or cooled without having to expose the membrane to the process fluid. Location in this manner also meant that the overall system temperature would be consistent and steady. Stability was inherent in this layout as the heat exchanger acted to maintain the temperature of fluid in the feed tank and not that of the feed at a point just before the membrane; an arrangement that would have been very sensitive to temperature fluctuations.

Flow of fluids through heat exchanger was co-current. Flow direction was of little importance to the effectiveness of the heat exchanger and co-current flow was selected as it allowed the simplest equipment arrangement with the heat exchanger being located vertically. Both hot and cold water required for heat transfer duty were delivered to the exchanger by way of a simple manifold. Two solenoid valves provided on/off control to the hot and cold streams.

The state of the solenoid valves was controlled via the relay box, which in turn was switched from the software on the PC. The solenoid valves were 240V so could be operated using normal electricity supply if necessary and the use of 240V obviated the need for large low voltage supplies and their associated problems.

Control and data logging

The control and data logging element of the experimental apparatus is composed of five parts:

- A 486 IBM PC with control and data logging software
- An input/output (I/O) data acquisition card
- A signal conditioning unit
- A Relay unit
- Data measurement and control output devices.

These five components can be divided amongst two streams, one stream running to the PC and the other to the final control elements.

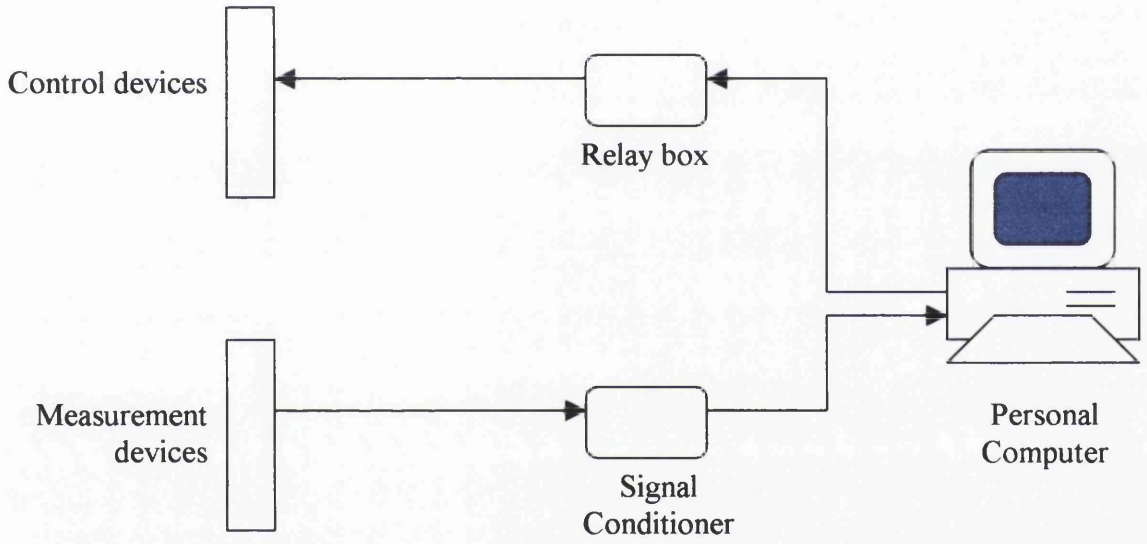

Figure 3-8 Signal flow around control and data logging system

Data acquisition card

Central to the data logging and control system was the data acquisition card. This card, mounted on the motherboard of the PC, enabled the input and output of measurement and control signals. The card, a Blue Chip Technology ADC-44d, was composed of three main functions: an analogue to digital converter, for analogue inputs (e.g. continuous electric signals from measurement devices), a digital to analogue converter and a digital input/output processor. The analogue to digital converter found use in processing signals from the measurement devices (flow rate, temperature and pressure). The digital outputs were used to switch the relays on and

off. This card enabled all facets of the control and data logging system to be easily combined and fed to and from the computer through one connection.

Signal conditioning unit

The signal conditioner was located between the data acquisition card and the measurement devices distributed over the apparatus. This device converted all the signals produced by the temperature sensors, pressure gauges and flow meter to a condition suitable for the inputs on the data acquisition card.

A set of cards, fitted into a case, dealt with each process measurement. There were two cards and therefore two inputs available for flow signal manipulation, the same for pressure and a single card dealt with both temperature signals. Circuit diagrams for all cards are given in Appendix A-6.

As was mentioned earlier connection of the input devices was via DIN or D-type connectors. The conditioned signals were than sent to the data acquisition card through a 15-way D-type connector.

Relay unit

The pump motor and the two solenoid-valves used to control flow of the hot and cold water through the heat exchanger, were 220-240 volt rated. They each required this voltage electricity supply and an appropriate current to be operated. To fulfil this need each unit had a corresponding relay, which acted as remote switch supplying power when it was needed.

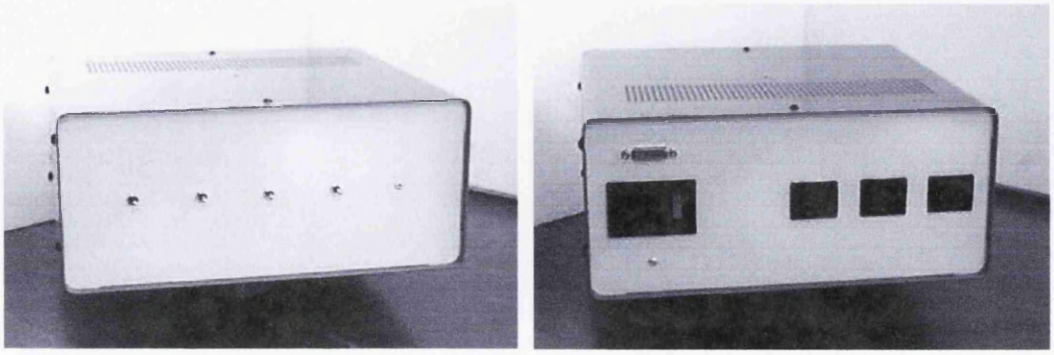

Figure 3-9 Front and rear of the relay unit displaying 3-way switches, 25 pin D-connector for digital output from PC, and 240V output sockets

Each relay in the relay box had a corresponding three-position switch. Each switch had positions that provided an auto mode, an off mode and an override mode. So, for relay-1 that dealt with the switching of the hot water supply to the heat exchanger, the automatic mode relied on the computer for control of the relay whereas the override mode maintained the solenoid valve in the powered up state. The same applied for relays 2 and 3 with only the connected devices differing.

240V mains power was supplied to the unit by means of a switched and fused plug. This was the split and fed in parallel to the three relays in the case. Each relay could then be used to switch power on and off accordingly. Care was taken to ensure that the use of plugs or sockets was appropriate to the direction of flow of electricity.

The switching of each relay in the automatic mode was controlled by the incoming digital signal from the computer. The digital signal from the data card was first translated to a level sufficient to operate the relays.

Control and data logging software

Fundamental to effective system operation was the control software. This piece of PC based programming drew all parts of the control and instrumentation of the apparatus together, facilitating and generating communication. The program was compiled under Qbasic 4.5, which was chosen in preference to Visual Basic due to potential reliability concerns with respect to Windows based applications.

The complete program listing can be found in Appendix A-5, however a general explanation of the program's functions is given below. Segments of the program were apportioned to:

- Conversion of signals to real data values of pressure, temperature and flow rate.
- Logging of all data values with respect to time.
- Control of temperature.
- Switching of pump motor.
- Allowance of different modes of operation.
- Continuous visual display of equipment variables.
- General software operating commands.

The conversion of signals delivered by the signal-conditioning unit, into a form that could be processed by the PC, was a simple procedure. The signal-conditioning unit modified all signals such that they fell within the range of 0-2 V dc. The data acquisition card could be set-up to deal with a number of different input ranges varying from 50 mV to 10 V in either bipolar (±V) or unipolar (0 to +V) modes. In this work the unipolar mode was used exclusively.

The data received at the analogue input port of the card was handled as a "bit reading". The analogue input on the card was 12 bit, thus the data supplied to the PC was provided with a high degree of precision. The signal received by the PC was then equated to a specific value (of temperature, pressure or flow rate) through calibration.

In the case of the flow meter, calibration was conducted using the bucket-and-stop watch technique, the pressure transducers were calibrated against a certified standard gauge. For the Pt_{100} temperature probe however, the corresponding signal conditioning card was adjusted such that the minimum and maximum possible output signals from the probe produced the minimum and maximum input signals required at the card. The response of the probe between these two points is known to be linear and therefore a decimal output of 0 was known to be equal to 0°C and a value of 4095 (corresponding to all bits high in a 12 bit system) equal to 100°C.

For effective data collection all data values were attributed to a specific time, the time value being based on that elapsed since the experiment was commenced. Data values for all devices were stored in a text file every 0.5 minutes. Once the experiment was complete the data file was closed. This file could then be opened in Excel and converted to its own format. Although the program was designed such that data would be sampled every 30 seconds, this was not necessarily always the case as program computations could delay the process (slightly). However data was always recorded with the accurate time value.

Hot and cold heat transfer water was supplied to the shell of the concentric heat exchanger via a manifold and two on/off solenoid valves. The solenoid valves were switched in response to the temperature control part of the computer program. The hot and cold water supplies that provided the heating and cooling were individually

controlled by two proportional-integral control algorithms (PI) using a time frame of 20 seconds.

When work commenced on the development of a control system, it was assumed that one algorithm would be required to control both fluid streams. Each solenoid valve was allotted a 20 second "control cycle". During this cycle the valve could be open for a minimum of 0 seconds and maximum of 20 seconds or any number of seconds in between. The decision as to how long a valve should be open and therefore supplying heating or cooling fluid to the exchanger, was dependent on the time and the extent to which the temperature deviated from the set point temperature and in what "direction". To prevent "integral wind-up" the control output had a maximum (or minimum) value constraint imposed on it such that when a maximum (or minimum) control condition was reached the value could not further increase (or decrease).

With the control software configured such that one PI algorithm controlled the flow of both heat transfer fluids, the controller response was found to be unacceptably slow with steady state only achieved after time periods in excess of 60 minutes. This was put down, in part, to the fact that once the set point temperature was reached and exceeded (in a heating situation) the system had to wait until the controller output for the hot water valve had returned to zero before a signal was produced for the cold water valve. Hence the "overshoot" of the system was excessive. To improve the system two algorithms were used instead of one, one for each fluid. The algorithms were implemented in the software such that they operated independently of each other, this meant that as soon as the set point was exceeded (again in the heating scenario) the cooling water was brought in and thus had immediate effect. This arrangement was found to be adequate.

$$Jn\% = Jo\% + ((Kc! * (En! + ((St\%/TI!) * (SEn! + En!))))/100) \qquad (3.1)$$

Equation (3.1) is the quick basic statement that embodied the control algorithm. It may be seen that this is related to the standard PI control algorithms presented by equation (3.2) (Wardle, 1994).

$$J = J_0 + K_C\left(\varepsilon + \frac{1}{\tau_I}\int_0^t \varepsilon dt\right) \qquad (3.2)$$

The pump was normally under computer control. Its operation was called on during the set-up of operating variables (pressure and flow rate), warm up routines for the process fluid and full filtration experiments. All of these options could be selected through appropriate key presses as indicated by a menu display on the computer screen.

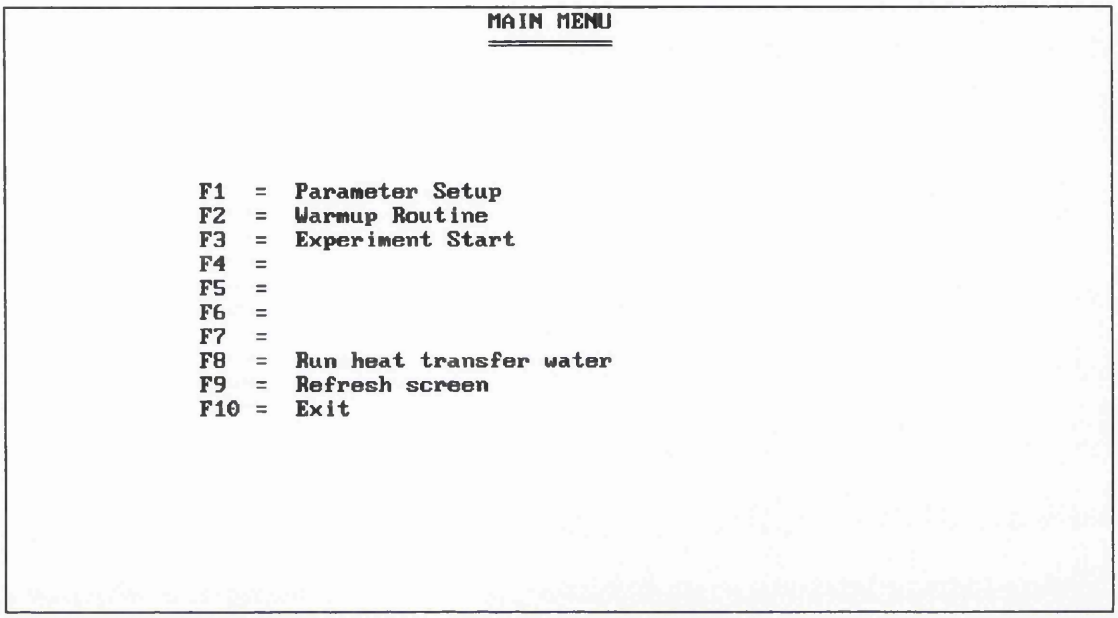

Figure 3-10 the initial start-up display of the computer software. This view indicates the action of each function key that was central to the program.

Figure 3-10 shows the main menu of the control and data-logging program. The main menu provided the user with six options:

- Parameter Setup. When selected this option displayed the operational parameter values on screen. The user could then adjust the pressure control valve (Figure 3-1) and the bypass built into the pump head (Figure 3-5), to manipulate pressure and flow rate across the membrane.
- Warmup Routine. When selected this option gave a full graphical display of the process variables. This option also instigated temperature control with the intention of achieving the appropriate temperature in the feed before starting the experiment.

- Experiment start. This is the core operation of the program. This option was similar to that of the Warmup routine but it added the time and data-logging element of the software. Figure 3-11 is a screenshot of the data element of the command and control software. The grey area contained plots of each data value updated from the right hand side of the area. Each new data value was plotted at time 0 and the old data shifted one time interval to the left. The result was a display of all the operating variables and their behaviour for the last 30 minutes allowing the user to quickly assess the system performance and, most importantly, stability. To the right of the view were six boxes that contained current values for all variables measured. The font colour for the variable names was matched to the colour of the associated variable plots. Along the bottom of the screen was a bar indicating the save status, data was saved to an automatically generated and labelled file every minute.

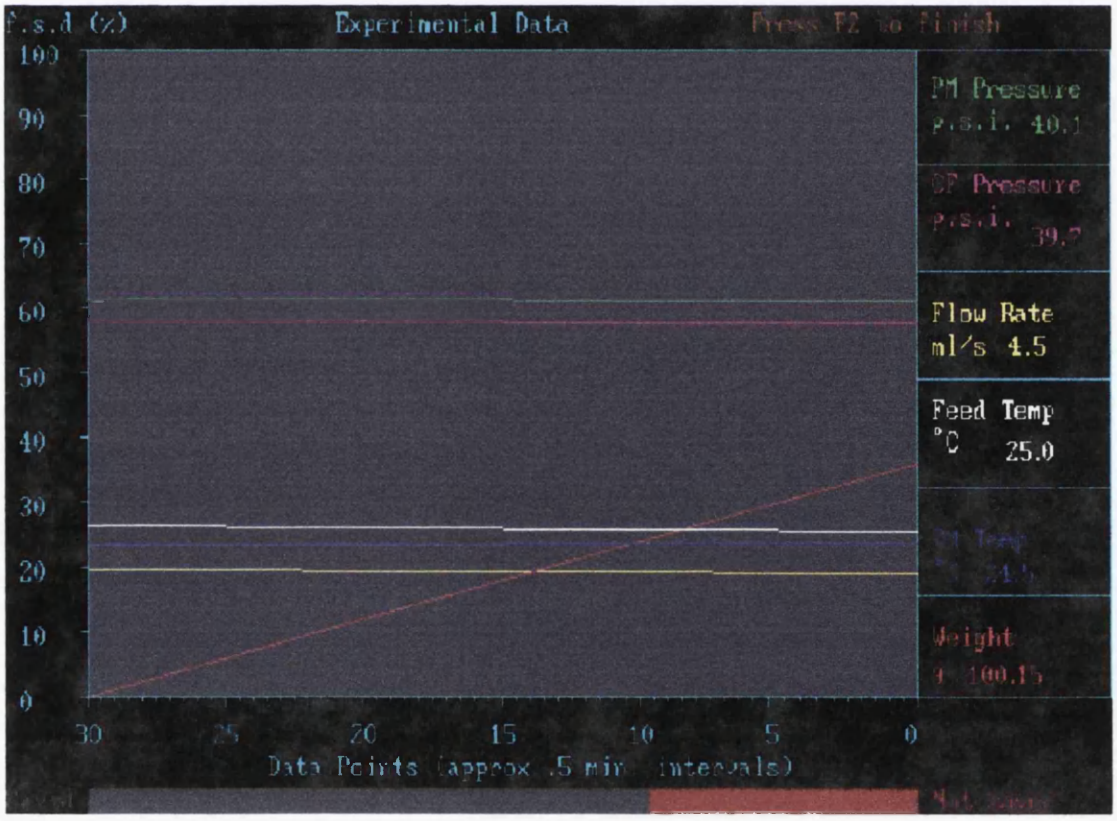

Figure 3-11 Visual output from computer during experiment.

- Run heat transfer water. This opened both hot and cold solenoid valves and allowed water to flow for five minutes. This was necessary, as the water supplies, both hot and cold, may not have been at their desired operating temperature due to residing in their supply lines for a long period of time.
- Refresh screen. When selected this would redraw what was being displayed on the screen. This was useful as artefacts from previous views occasionally carried over.
- Exit. This allowed the user to terminate the programme and exit the software to DOS.

3.3 Experimental procedure

All experimental procedures in this work incorporated methods and techniques that were common to all experiments and could be considered to be "normal" experimental procedure. This section details the techniques that were used in the process of conducting a filtration experiment, from the installation of a new section of membrane in the holder to the cleaning procedures used after the filtration was completed.

The elements of preparation, operation and conclusion that were typical to a filtration or series of filtrations are described as follows:

- Membrane preparation prior to use
- Pre-filtration start-up steps
- Filtration start-up and operating conditions
- Filtration and data collection
- Filtration shut-down
- Apparatus cleaning and preparation of equipment for periods of none use.

3.3.1 Membrane preparation

Membranes were acquired as off-cuts from their respective manufactures. The majority of the membranes obtained for this study were specifically intended for spiral wound applications, but some were designed only for laboratory use. In either

case the membranes would have manufactured in large continuous sheets typically ~100 cm (40") in width and to any length before being shaped according to their end use. Manufacturers were happy to make sections of their membranes available for research purposes. And the author acknowledges the generous donation of membranes from Dow-Filmtec, Sartorious and Osmonics.

Although the membranes had different properties and their active layers were generated from a variety of polymeric compounds, their appearance and mechanical properties were indistinguishable. The membrane sheet had to be cut to the appropriate size for use in the membrane holder. It was essential that the cut membrane should obtain a good fit in order to avoid leaks. To achieve this, a glass disc of the appropriate diameter was drawn around, on the membrane, using a soft pencil and then the membrane cut using scissors. "Leakage", the process of feed passage around the edge of the membrane and into the product stream without filtration, could have been a consequence of either a membrane kinking because it was too large or not a good enough seal with the O-ring (Figure 3-4) due to it being to small.

Once cut to shape the membrane was rinsed before being placed in the holder. Rinsing was conducted with the intention of removing manufacturing residues and preservatives from the surface and pores of the membrane. If the membrane was hydrophobic (e.g Trisep XN45) then the pores had to be opened to allow ingress of water. This was achieved by immersing the membrane in Propan-1-ol followed by immersion in water. This cycle was repeated twice before the membrane was shown to allow normal water flux. Increased washing or immersion time showed no improvement in overall flux.

As indicated previously (Section 3.2.1) the lid was secured to the base of the filter holder by six screws. It was these fixings that provided the compressive force that allowed a seal between the lid and the O-ring and the O-ring and the membrane (supported on the sintered PTFE plate) to be formed. Thus it was imperative that the lid was located correctly with respect to the O-ring and the base. If the six screws were then tightened gradually and care was taken to avoid distorting the load across the membrane surface, it was possible to reliably achieve an effective seal.

Additionally, a good seal was required to impose the flow pattern, provided by the channel in the lid section, on the membrane.

This completed the work required to prepare the membrane itself for use in experiment. All that remained was to reinstall the filter holder in the apparatus, having been removed to facilitate membrane installation.

3.3.2 Pre-filtration

With the membrane ready for use and installed in the filter holder, a number of pre-filtration steps had to be taken before experimental work could be completed. Although already rinsed it was still likely that the membrane contained residues from both manufacture and preparation that may contaminate product solutions. As a consequence, a "running-in" period was instigated on every occasion a fresh piece of membrane was used. This not only ensured that were no contaminants remaining within the membrane but it also acted to compress the membrane. Membrane compressibility is something that is associated with all membranes and although the effect would be negligible on such a small area of membrane, any compression that took place would be completed during the running in. The running in consisted simply of running the membrane at a relatively high pressure for two hours with a feed of deionised water.

The pure water flux of the cleaned membrane was measured as an indication of the quality of the membrane. The behaviour of the water flux with pressure was used a means to verify that a particular membrane was similar to other membranes of the same description and manufacture, that had been used in previous experiments.

3.3.3 Filtration start-up and operating conditions

Experimental work was concerned with membrane performance in terms of operating conditions, solute and solution properties or membrane type. Thus it was essential that membrane operating conditions and feedstock were given due consideration before commencement of a filtration experiment.

To ensure the longevity of the pump and reproducible flow patterns it was necessary to make up an appropriate volume of feed solution. Typically 3 litres was required to eliminate the possibility of air becoming entrained in the feed and drawn into the pump. By starting the filtration with 3 litres it was found that even by the end of an experiment there was enough volume of feed to avoid this eventuality.

It was necessary to be able to produce a consistent solution of known concentration because comparison would later be made of the results of individual experiments. To achieve this the feed was prepared in volumetric flasks and with the use of a high precision electronic balance. Due to the nature of the filtration apparatus a small quantity of fluid would unavoidably remain within the system after it had been "fully" drained. This small quantity of distilled water (less than 20 ml) was considered to be insignificant when compared to the volume of feed solution used. At most it would cause an error of 20 parts in 3000 (<1%) for the feed concentration and it was therefore ignored as a potential source error.

Before feedstock was installed in the system it was necessary to run the filter using RO water. This allowed variables; such as the cross flow flow rate and pre-membrane pressure to be set. As part of the experimental routine the system was run with deionised water for 20 minutes before the experiment was initiated.

With the previous step complete the system was drained and the feed was transferred to the feed tank. Before doing so the isolation valve indicated in Figure 3-1 was closed such that the feed was segregated from the membrane. The warmup routine, detailed in the section on control and data logging software, was then initiated bringing the feed up to operating temperature. Once this condition was reached the warmup routine was stopped, the isolation valve opened and the experiment commenced.

3.3.4 Filtration and data collection

This process was central to the entire procedure and was initiated by a single keystroke on the computer. Before the filtration experiment was started it was important to manually power up the balance. Switching on the balance could not be done from the software and if the computer attempted to read the balance when it was off the programme would freeze.

Due to the nature and design of the system high volumetric flow rates (relative to other experimental techniques) could be achieved at relatively low applied pressures. This meant that multiple samples could be collected as a function of time so that the variation in product concentration could be discussed in relation to the variation of feed concentration. The collection of many samples over the period of each filtration meant that a truly representative value of the rejection could be obtained.

Sample collection was achieved by placing small capped-sample tubes, in a retaining beaker. For most analysis purposes a sample volume of 5 ml was sufficient although on some occasions more than 15 ml was required. The tubes were typically bundled in groups of three to six and stood in the beaker. The number of tubes per beaker depended on the applied pressure (and thus permeate flow rate) and the balance capacity. It was important that the balance was not allowed to exceed capacity as this prevented further data logging. To ensure against this the beaker and sample tubes had to be exchanged, at a known point between sample times, and the balance re-zeroed. The sampling time and the duration of the experiment were both dependant on the operating conditions and the feed composition. Typically the aim was to produce a minimum of 500g of permeate and to sample that product 8-10 times. For example, an experiment operated at 2.75 bar (40 psi) with a trace feed solution might have a permeate flow rate of 5.5 ml/min and therefore would have a duration of 90 minutes and samples would be taken every 10 minutes collecting for one minute at a time.

3.3.5 Termination of experiments and cleaning

The filtration would be concluded when an appropriate mass of permeate had been collected. Such a quantity was decided upon after explorative experiments revealed

that it took 20 – 30 minutes for the filtrate to displace pure water retained downstream of the membrane from the pre-filtration washing period.

The experiment was stopped by pressing the function key F2 as indicated in the top right corner of the screen (Figure 3-11). This action stopped the pump, the data acquisition procedure, saved the data to file for the last time and closed the file. Feed was drained from the tank using the drain valve and unless there were exceptional circumstances this was directly to the laboratory drain.

Typically each membrane was used for 20 experiments before it was replaced. This meant that it was essential to take great care to preserve the membrane and maintain its condition as close to the original condition as possible. To realise this aim the membrane was flushed with ultra pure RO water, for a minimum of twenty minutes, directly after use. The intention of this was to remove residual feed, product and deposits from the membrane surface. Once this phase was complete the clean water was held with the membrane by closing the isolation valve, cross flow valve and sealing the outlet from the filter, thus preventing the membrane from drying out. To assess the effectiveness of this cleaning regime and monitor performance; membrane pure water flux was measured before every experiment.

3.4 Membranes

3.4.1 Selection and acquisition

The membranes that were used throughout this research were obtained from a number of commercial manufacturers. Each membrane was chosen on the basis of information gained from manufacturers' websites and other promotional material.

In the process of choosing appropriate membranes a list of the most desirable filters was formed. Not all were obtainable due either to the inability of manufacturers to supply samples or particular varieties being superseded or discontinued. Table 3-1 lists the membranes that were obtained.

Membrane	Manufacturer	MWCO	Classification
XN-45	Trisep	250	Nanofiltration
NF 90	Filmtec	150-300	Nanofiltration
NF 200	Filmtec	150-300	Nanofiltration
LFC-1	Hydranautics	<50	Reverse osmosis
BW-30	Filmtec	<50	Reverse osmosis
UF 5K	Sartorious	5000	Ultra filtration
RO 3840/30-FF	Filmtec	<50	Reverse osmosis

Table 3-1Membranes and manufacturers

The manufacturers provided the classifications shown in Table 3-1. Membrane classification is an area of membrane technology that is open to interpretation and is discussed in Chapter 1.

3.5 Chemicals

During the course of the study a number of chemicals were chosen for the purpose of: basic filtration studies, explorative work and ultimately detailed investigation. Table 3-2 shows details of all compounds used, their chemical formula, structure, characteristic size and other facts pertaining to their use and properties.

Chemical	Structure	Size – Stokes Radius molar diameter (nm)	Other information
Phenol C_6H_5OH RMM 94.11	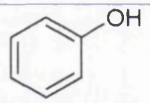	0.24 0.69	Solubility = 8.4/100 parts Analysis = UV spec at 270nm
2,4,6-Trichlorophenol $Cl_3C_6H_2OH$ RMM 197.46	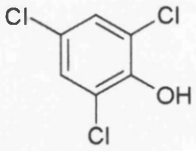	0.19 0.791	Solubility = 0.09/100 parts Analysis = UV spec at 205nm
Benzoic Acid $C_6H_5CO_2H$ RMM 122.12	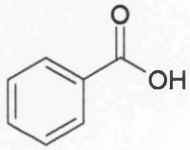	0.35 0.852	Solubility = 0.2/100 parts Analysis = UV spec at 273nm
Sodium benzoate $C_7H_5O_2$. Na RMM 121.12 22.99	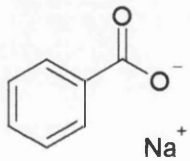	0.35 0.852	Solubility = Analysis = UV spec at 275nm

Chemical	Structure	Size – Stokes Radius molar diameter (nm)	Other information
Phenylalanine $C_9H_{11}NO_2$ RMM 165.19		0.35 0.850	Solubility = Analysis = UV spec at 258nm
Aniline C_6H_7N RMM 93.13	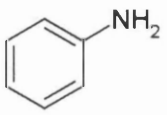	0.25 0.704	Solubility = 3.6/100 parts Analysis = UV spec at 280nm
Benzyl alcohol C_7H_8O RMM 108.14	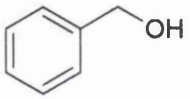	0.27 0.736	Solubility = 4.0/100 parts Analysis = UV spec at 257nm
Glucose $C_5H_{11}O_5CHO$ RMM 180.16	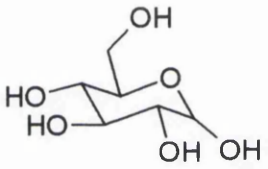	0.32 0.805	Solubility = 82/100 parts Analysis = Phenol-sulphuric acid visible absorption at 480nm
Sucrose $C_{12}H_{22}O_{11}$ RMM 342.30	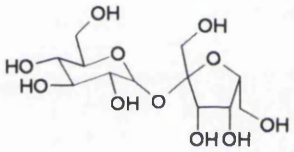	0.47 1.004	Solubility = 179/100 parts Analysis = Phenol-sulphuric acid visible absorption at 480nm
Raffinose $C_{18}H_{32}O_{16}$ RMM 474	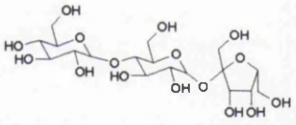	0.59 1.143	Solubility = 14.3/100 parts Analysis = Phenol-sulphuric acid visible absorption at 480nm
Glycerol $C_3H_8O_3$ RMM 92	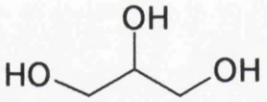	0.23 0.69	Soluble Analysis = Enzyme based kit, absorption at 340nm
Benzylamine C_7H_9N RMM 107.16	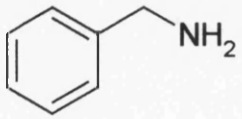	0.28 0.749	Soluble Analysis
Caffeine $C_8H_{10}N_4O_2$ RMM 194	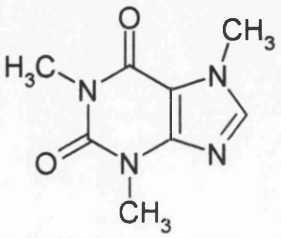	0.34 0.83	21000mg/l water Analysis = UV absorption at 275nm

Table 3-2 The organic solutes used in this investigation

3.5.1 Special properties and handling of compounds used

The majority of the compounds used in this work were specifically selected because of their non-hazardous nature. The concentration selected for each component as a process solute was dictated by either their solubility or the detection limits of the associated measurement technique. 2,4,6-trichlorphenol (TCP) and Benzoic acid proved to be most resistant to dissolution. To encourage the dispersion of TCP into solution a degree of heating was used, solvation of benzoic acid was aided through a prolonged period of agitation.

Aniline, phenol, TCP, benzoic acid and benzyl were classified as toxic chemicals thus it was essential that every reasonable care was taken in their handling and use when in concentrations.

3.6 Chemical analysis

Many membrane studies have focussed on gauging the performance of a membrane or a membrane system by observing solute/solution separation. To gather the information required in order to make these observations it was necessary to measure the concentration of solutes in both the feed and the product and it was beneficial to be able to distinguish between solutes when dealing with multi-component solutions. To help achieve this, techniques of solute concentration measurement were identified or developed for each chemical used.

The Analysis techniques used relied upon typical laboratory equipment and more specialised instruments to perform measurements. Methods used were:

- UV spectrophotometery
- Visible spectrophotometery
- Inductively Coupled Plasma – Optical Emission Spectroscopy
- Conductivity measurement

3.6.1 UV spectrophotometery

This method of chemical analysis found most use in the measurement of compound concentrations containing 6-membered rings (benzene, triazinane). The presence of the benzene ring is important as it absorbs strongly in the UV region. Peak absorbencies for these compounds were found to be at wavelengths between 200 and 280nm. Using 1 cm light path quartz cells, concentrations of between 0.05 and 0.5 g/l were easily detectable, dependant on the solute.

Saccharides were also found to absorb light in the UV region. However, the absorption peak for these compounds existed at around 195 to 200nm, known to be close to the limits of measurement. The lower wavelength limit of the spectrophotometer is 195nm as it is here that air will also begin to absorb UV light thus interfering with the results. Also, when the concentration of saccharides were measured in the presence of salts, these salts were also found to absorb at wavelengths close to that of the sugar hence a more reliable method of analysis was required for the sugars.

Compound	Experimental Concentration (mg/l)	Absorption peak (nm)	Calibration concentrations (mg/l)	Sample measurement requirements
Phenol	1.0	270	0.01, 0.02, 0.05, 0.1, 0.2, 0.5, 1.0, 2.0, 5.0	None
2,4,6-Trichloro-phenol	1.0	205	0.01, 0.02, 0.05, 0.1, 0.2, 0.5, 1.0, 2.0, 5.0	None
Benzoic acid	100	273	100, 200, 300, 400, 500	None
Sodium benzoate	50	275	40, 80, 120, 250, 500, 1000	None
Phenyl-alanine	500	258	100, 200, 500, 1000, 1500	None
Aniline	100	280	10, 20, 50, 100, 150	None
Benzyl alcohol	10	257	10, 20, 50, 100, 200, 500	None
Benzylamine	500	257	100, 200, 500, 1000, 1500	None
Caffeine	500	275	0.5, 1, 2.5, 5, 7.5	100 * dilution

Table 3-3 Bases for calibration and other information regarding the measurement of organic solute with UV spectrophotometery

Solutions that produced acceptable absorption peaks in the UV region did not require any further treatment prior to use. In some cases there was the need for dilution of samples such that saturation was avoided and the resultant measured absorption value fell within the calibrated range.

Calibration was achieved in all cases using accurately produced bulk standard solutions and appropriate dilution thereof. All measurements were performed using 4 cm light-path quartz cuvettes. Table 3-3 outlines the methods of calibration and measurement used for each compound measured in the UV region.

3.6.2 Visible spectrophotometery

To absorb light in the visible part of the radiation spectrum it is necessary for the solution to exhibit some degree of colouration. Unfortunately many aqueous solutions do not produce a measurable colour and none of the compounds used during this work have an associated colour when dissolved in water. Thus to permit the measurement of certain component concentrations, using visible spectrophotometery, they had to be reacted with appropriate reagents to form a colour that was proportional in intensity (and therefore absorption) to the concentration. Two such methods were used, one to measure phenols and the other for saccharide analysis.

Phenol analysis using the 4-aminophenazone test

This technique has a lower detection limit of 1 mg/l of phenol and relied upon the use of two reactants: 4-aminophenazone (conc.) and potassium persulphate (conc). The method used involved the addition of 1ml of each reagent to 6ml of the sample in a capped test tube. The contents of tube were then mixed thoroughly using a test tube agitator (~4s). Each tube was then heated in a 60°C water bath for 20 minutes. The absorption was then measured using a 1cm cuvette at a wavelength of 510 nm. Calibration measurements were made with phenol solutions of 0.001, 0.01, 0.1, 0.5, 1.0, 5.0 mg/l. This technique was superseded by UV measurement.

Saccharide analysis using the phenol-sulphuric acid technique

Phenol in the presence of sulphuric acid can be used for the quantitative colorimetric micro determination of sugars (Dubois et al., 1956). The method has been shown to be simple, rapid and sensitive, and to give reproducible results. The colour produced by this method was permanent and it was unnecessary to pay special attention to the control of temperature. This method was capable of measuring sugar concentrations in the range 0-100 mg/l corresponding to an absorbance range of 0 – 1.2.

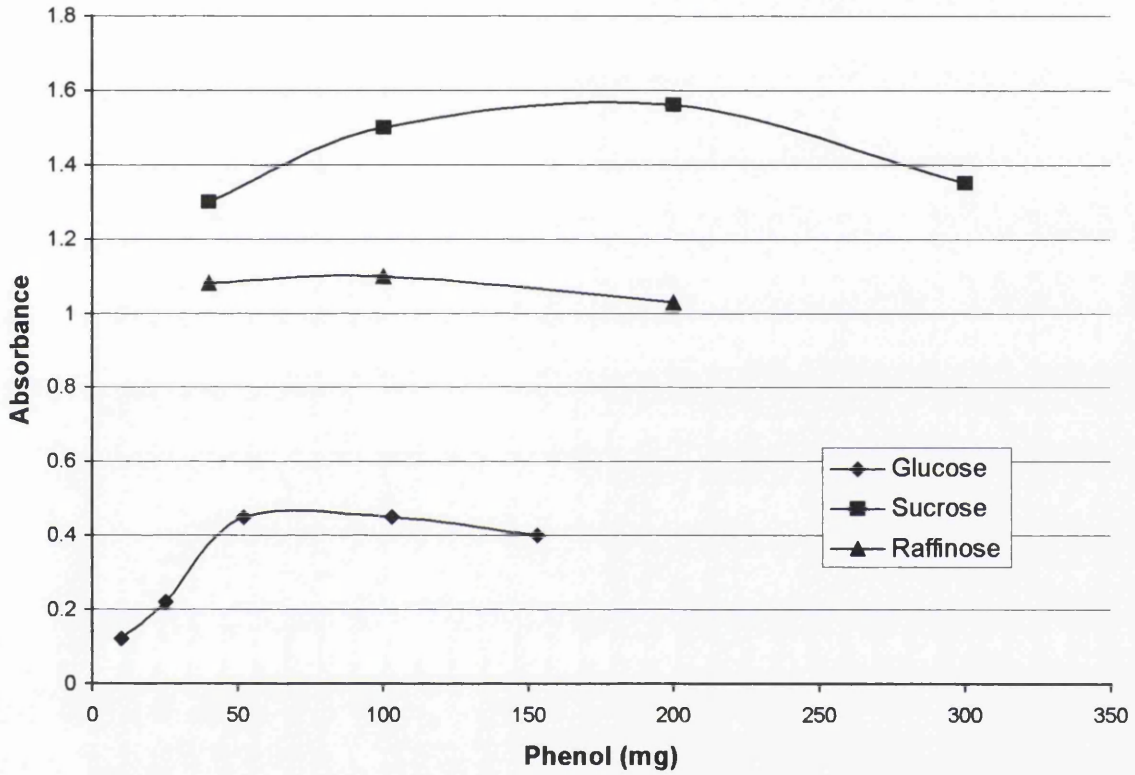

Figure 3-12 Absorbance as function of the absolute mass of phenol present for various sugar solutions. The concentration of glucose was 42mg/l, sucrose was 80mg/l and raffinose was 80mg/l.

Figure 3-12 illustrated the dependence of absorption on the amount of phenol used as the colour-producing reagent. Inspection of this plot indicated that there was an optimum value of phenol used to ensure high sensitivity and stability in the results. This is best demonstrated by the plot for glucose, which exhibits a rapid change in absorbance values between 10 and 50 mg of phenol after which point there is a plateau in the variation. By contrast, sucrose and raffinose display a much gentler variation of absorbance values with respect to phenol concentration. On the basis of

this information a concentration and volume of phenol was selected that would yield good absorption data with high repeatability. The value chosen was 100 mg/L of phenol, as this was considered reasonable for all three saccharides used.

The analytical process for one sample containing a known sugar of unknown concentration was as follows:
1 ml of 0-100 mg/L sugar solution was pipetted into a glass test tube that included a stopper. If the solution was of greater concentration than allowed by the calibration it was diluted appropriately before analysis. 2 ml of 5 wt% phenol solution was then added to the sugar solution. The original method (Dubois et al., 1956) was to micro-pipette 80 wt% phenol solution into the sample, however to reduce the risk associated with this hazardous compound, 2 ml of the lower concentration 5 wt% solution was used. This corresponded to 100 mg of phenol. Inspection of Figure 3-12 reveals that this quantity of phenol coincides with the flatter sections of all three plots. In the next step 5 ml of concentrated sulphuric acid was added to the mix. On doing so, a characteristic orange-yellow colour was produced. Care was taken to avoid adding the acid too quickly and causing the contents of the tube to spit out of the top. After addition of the acid the tube was allowed to stand for ten minutes. Once ten minutes had elapsed after addition of the acid, the tube was capped, the contents thoroughly mixed and then the tube placed in a bath of water at ~ 25°C thus cooling the contents.

The optical density of each test was then taken using a Camspec M302 spectrophotometer set to a wavelength of 490 nm.

The spectrophotometer was zeroed against a reagent blank, made up in the same way but using 1ml of deionised water in place of the sugar solution.

Glycerol analysis using an enzymatic technique

An enzymatic test kit provided by R-Biopharm (Roche) facilitates the measurement of glycerol concentration. The analysis proceeds according to the following principle:
Glycerol is phosphorylated by adenosine-5'-triphosphate (ATP) to L-glycerol3-phosphate in the reaction catalyzed by glycerokinase (GK) (3.3).

$$\text{Glycerol} + \text{ATP} \xrightarrow{\text{GK}} \text{L-glycerol-3-phosphate} + \text{ADP} \qquad (3.3)$$

The adenosine-5'-diphosphate (ADP) formed in the above reaction is reconverted into ATP by phosphenolpyruvate (PEP) with the aid of pyruvate kinase (PK) with the formation of pyruvate (3.4).

$$\text{ADP} + \text{PEP} \xrightarrow{\text{PK}} \text{ATP} + \text{pyruvate} \qquad (3.4)$$

In the presence of the enzyme L-lactate dehydrogenase (L-LDH), pyruvate is reduced to L-lactate by reduced nicotinamide-adenine dinucleotide (NADH) with the oxidation of NADH to NAD (3.5).

$$\text{Pyruvate} + \text{NADH} + \text{H}^+ \xrightarrow{\text{L-LDH}} \text{L-lactate} + \text{NAD}^+ \qquad (3.5)$$

The amount of NADH oxidized in the above reaction is stoichiometric to the amount of glycerol. NADH is determined by means of its light absorption at 340 nm.

Pipette into cuvettes	**Blank**	**Sample**
Solution 1	1.000 ml	1.000 ml
Sample solution	-	0.100 ml
Pure water	2.000 ml	1.900 ml
Suspension 2	0.010 ml	0.010 ml
Mix, by covering tubes with Parafilm and inverting, and wait for reaction completion (5-7min). Read absorption of solution (A_1). Start reaction by addition of:		
Suspension 3	0.010 ml	0.010 ml
Mix as before and wait for reaction to reach completion (5-10min). Read absorbances of blank and sample (A_2).		

Figure 3-13 laboratory procedure for glycerol analysis using enzymatic test kit (procedure taken from instruction provided with the kit)

The test kit was provided containing three bottles (solutions 1-3), each of which contained a mixture of reagents relevant to the analysis. The procedure for the analysis was to dissolve the contents of bottle 1 in 11 ml of redistilled water and then allowing the resultant solution to equilibrate with room temperature. The steps outlined in Table 3-4 were then followed for the rest of the analysis.

Once this work was completed a set of values had been obtained for both the blank and the sample that correspond to absorbances A_1 and A_2 in the following,

$$\Delta A = (A_1 - A_2)_{sample} - (A_1 - A_2)_{blank} \quad (3.6)$$

the corresponding glycerol concentration is then calculated, for this system, using the following relation

$$c[g/L] = \frac{2.781}{\varepsilon} \times \Delta A \quad (3.7)$$

where ε is the extinction coefficient of NADH which at 340 nm is 6.3 L/mmol cm. There is no calibration required with this method.

3.6.3 Inductively Coupled Plasma – Optical Emission Spectroscopy

The inductively coupled plasma – optical emission spectrophotometer (ICP-OES) was used in the course of this study for the measurement of inorganic ion concentrations. The ion concentrations that were assessed with this device were mainly Na^+, SO_4^{2-} and PO_4^{3-}. Chloride ions were also detected and measured. The spectrophotometer only measured the strengths of the detectable elements in each sample (i.e. P, S, Na and Cl), but it was possible to relate these values to their respective ion concentrations.

ICP-OES operation

On collection of samples for ICP-OES analysis it was necessary to ensure that the volume collected was enough for a complete measurement. The spectrophotometer analysed samples on a basis of element counts per second (cps) and as such a finite period of time elapsed during which the sample fluid was drawn into the instrument where it was atomised and then injected into the argon-plasma flame. A typical analysis of one sample (from which three readings were taken) required a minimum volume of 15 ml to complete.

Calibration of the ICP-OES

To enable a quantitative assessment of the samples analysed with the ICP-OES a calibration was required for each element. Calibration through means of a linear regression was achieved by measuring emissions at the following series of concentrations:

1, 2, 5, 10, 20, 50, 100

In the case of the ICP-OES the accompanying software facilitated the procedure. Further information on the overall technique is available in the manufacturer's user handbook (Spectro-Ciros ICP-OES User Manual).

Calibration solutions were produced from specifically manufactured analytical standards obtained from the Fisher Chemical Company. These standards were all provided at 1000ppm concentrations and were diluted accordingly.

3.6.4 Conductivity measurement

Measurement of conductivity is one of the most commonly used tools in the analysis of membrane performance. It was found that a calibration curve could be produced for the meter, relating conductivity readings (S/m) to concentration (mg/l) of a solute (e.g. Magnesium sulphate).

The conductivity meter could not distinguish between solutes so could only be used when solutions contained no more than one solute, for example sodium chloride, magnesium sulphate or sodium sulphate. In these cases it was possible to obtain true values of feed and product concentrations and therefore observed rejection.

The conductivity meter used throughout the course of this work was a Hanna Instruments HI 9635 capable of reading in the range 0 - 12880 μS/cm. Accuracy of this instrument was maintained with regular calibration using three manufactured standards at the concentrations 74, 1440 and 12880 μS/cm.

The only operational requirement of this unit was that enough of a sample was available to ensure the probe could be fully submersed and all air expelled from the concentric sheaf.

4 Membrane selection and characterisation

4.1 Introduction

There exist four widely accepted classes of synthetic membrane, as illustrated by Figure 4-1. Each type of membrane has become predominantly associated with a process or application, for example reverse osmosis membranes are synonymous with sea water desalination (Sourirajan, 1970) (Dresner and Johnson, 1980), ultrafiltration is employed by the dairy industry in whey processing (Eykamp, 1998) and microfiltration, the oldest membrane separation step, is renowned for its ability to remove bacteria and other micro organisms from water streams and thus is sometimes used as a sterilisation process (Eykamp, 1998). However, the limit of application for all types of synthetic membranes, is the tolerance of the membrane fabric to the process stream and its usefulness to the intended process.

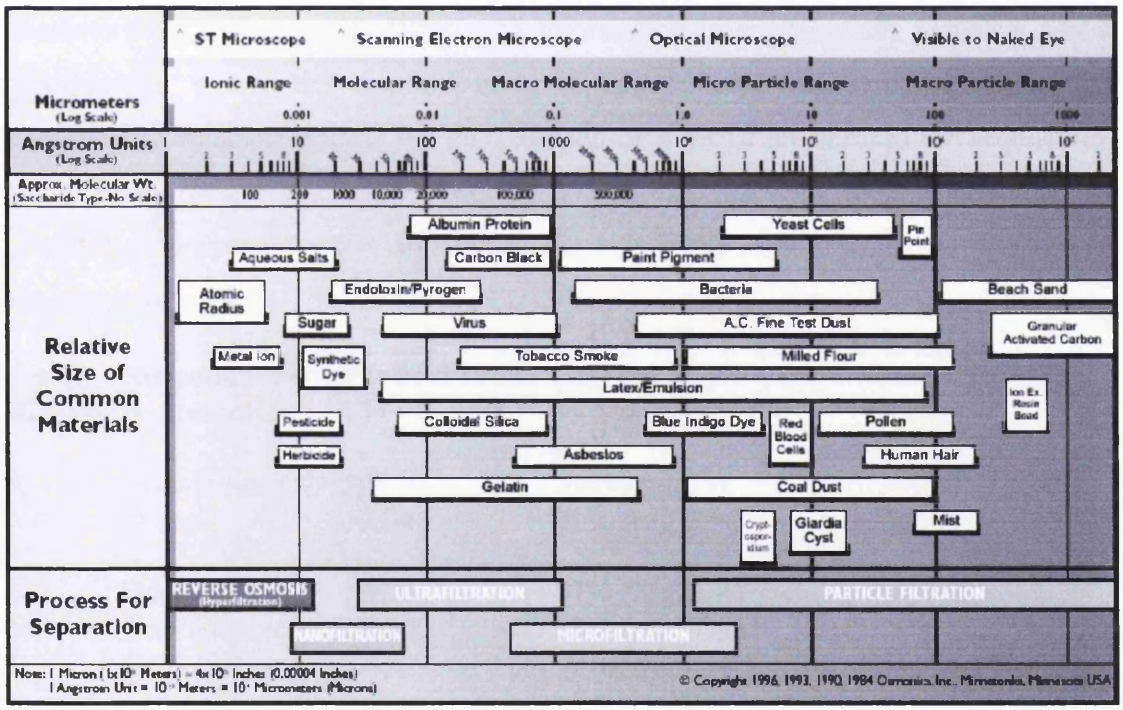

Figure 4-1 The filtration Spectrum (Osmonics 1995) indicating the classes of membrane filtration and size related filterants

The fourth and most recently recognised group of membranes is that which shares its properties with both RO and UF and covers the transition between these two categories. This class is referred to as nanofiltration. The actual difference between

UF and NF remains undecided but it might be proposed that ultrafiltration membranes have discrete pores through which transport occurs, with the remainder of the membrane impermeable to solvent and solute, whereas NF membranes have no visible pores and transport occurs within the polymeric structure. NF membranes might therefore be correctly referred to as "loose" RO.

On the basis of their interesting separation characteristics, nanofiltration membranes present a good case for further theoretical and practical investigation.

4.2 Membrane selection criteria

A wide range of commercial membranes are currently available for exploitation and it might be reasonable to assume that there exists a membrane suitable for each particular application. However, selecting a commercial membrane on the basis of its separation properties is complicated by a lack of data provided by the manufacturers. This may be because the manufacturer has usually completed only the most basic characterisation work, or because such information is commercially sensitive. As a consequence, before the practical body of this research was commenced, it was necessary to establish criteria for the selection of a set of membranes for acquisition. Once these membranes were obtained it was necessary to identify methods of comparison that enabled the isolation of the membrane most suitable for the core of the investigation.

Class	Manufacturer	Product code	Rejection/MWCO	Other remarks
RO	Hydranautics	LFC-1	99.5% (NaCl)	Used in osmometer
RO	Dow Filmtec	BW30	>99% (NaCl)	Loose RO
NF	Trisep	XN-45	92% (MgSO4)	High flux
NF	Dow Filmtec	NF90	97% (MgSO4)	
NF	Dow Filmtec	NF200	95% (MgSO4)	
NF	Osmonics	DK	98% (MgSO4) 150-300 Da	Standard flux
NF	Osmonics	DL	96% (MgSO4) 150-300 Da	High Flux
UF	Osmonics	GE	1000 (PEG)	
UF	Osmonics	GK	3500 (PEG)	
UF	Sartorious	UF 5K	5000	Laboratory membrane

Table 4-1 List of commercial membranes considered for investigation

The Nanofiltration class of membranes were selected because they have molecular weight cut-offs (MWCO) in the range of 150-1000 Da. This group of membranes is "visible" to small organic compounds (uncharged as well as charged) and salts (mono-valent and multi-valent). Reverse osmosis and ultrafiltration membranes were also considered as they provided a "frame" for the results acquired with nanofiltration membranes.

Table 4-1 lists the membranes considered for further investigation, of the ten candidates five are classed as NF. The fourth column in Table 4-1 details the rejection specifications as provided by the manufacturer. One method of performance measurement was to define RO membrane performance through sodium chloride rejection, NF performance through magnesium sulphate rejection and UF membranes on the basis of their MWCO with respect to polyethylene glycol (PEG). All but one of the membranes were commercially available as spiral wound modules, the exception was the Sartorious membrane which was intended purely for laboratory applications.

Manufacturer	**Product code**	**Class**	**Reference**
Dow Filmtec	BW-30	RO	(Adham et al., 1998) (Lee and Lueptow, 2001)
Dow Filmtec	NF-200	NF	(Cho et al., 1998) (Gilron et al., 2001) (Boussahel et al., 2002) (Freger et al., 2000) (Wittmann et al., 1998)
Dow Filmtec	NF-40	NF	(Wang et al., 1997) (Lee et al., 1999) (Schaep et al., 2001)
Dow Filmtec	NF-45	NF	(Cho et al., 1998) (Lee et al., 1999) (Gilron et al., 2001) (Van der Bruggen et al., 1998) (Peeters et al., 1999) (Alkhatim et al., 1998)
Dow Filmtec	NF-70	NF	(Van der Bruggen et al., 2000) (Van der Bruggen et al., 1998) (Van der Bruggen et al., 1999) (Van der Bruggen and Vandecasteele, 2002) (Schaep et al., 1998) (Hofman et al., 1993)
Dow Filmtec	NF-90	NF	(Alkhatim et al., 1998)
Hydranautics	CPA2	RO	(Nemeth, 1998) (Gerard et al., 1998)
Hydranautics	ESNA	NF	(Cho et al., 1998) (van der Meer et al., 1998)
Hydranautics	ESPA	RO	(Nemeth, 1998) (Adham et al., 1998) (Gerard et al., 1998) (van der Meer et al., 1998) (Lee and Lueptow, 2001)
Hydranautics	LFC1,2	RO	(Gerard et al., 1998)

Manufacturer	Product code	Class	Reference
Nitto Denko	ES10	NF	(Magara et al., 1998)
Nitto Denko	ES20		(Ozaki and Li, 2002)
Nitto Denko	NTR-70-SWC	NF	(Magara et al., 1998)
Nitto Denko	NTR-7250	NF	(Nakao and Kimura, 1981) (Kiso et al., 2000) (Kiso et al., 2001) (Berg et al., 1997)
Nitto Denko	NTR-729HF	RO	(Nakao and Kimura, 1981) (Kiso et al., 2000) (Kiso et al., 2001) (Lee and Lueptow, 2001)
Nitto Denko	NTR-7410	NF	(Nakao and Kimura, 1981) (Kiso et al., 2000) (Cho et al., 1998) (Kiso et al., 2001)
Nitto Denko	NTR-7450	NF	(Wang et al., 1997) (Van der Bruggen et al., 2000) (Van der Bruggen et al., 1999) (Schaep et al., 2001) (Van der Bruggen and Vandecasteele, 2002) (Van der Bruggen et al., 1998) (Kiso et al., 2001) (Kiso et al., 2000)
Nitto Denko	NTR-759HR	RO	(Nakao and Kimura, 1981)
Osmonics	DK	NF	(Koyuncu and Topacik, 2002) (Boussahel et al., 2002) (Sojka-Ledakowicz et al., 1998) (Bowen and Welfoot, 2002a) (Bowen and Welfoot, 2002b) (Berg et al., 1997) (Dey et al., 2000) (Bowen et al., 2001b)
Osmonics	DL	NF	(Sojka-Ledakowicz et al., 1998)
Toray	UTC-20	NF	(Van der Bruggen et al., 2000) (Van der Bruggen et al., 1998,Van der Bruggen et al., 1999) (Van der Bruggen and Vandecasteele, 2002) (Schaep et al., 2001) (Schaep et al., 1998)
Toray	UTC-60	NF	(Schaep et al., 1998) (Hofman et al., 1993)
Trisep	ACM4	NF	(Geraldes et al., 2001) (Lee and Lueptow, 2001)
Trisep	X20	RO	(Jenkins and Tanner, 1998)

Table 4-2 A selection of the more important membranes investigated in previous research

Table 4-2 provides a summary of the membranes and their manufacturers most commonly referred to in publications concerning membrane and membrane related research. Table 4-2, when compared with Table 4-1, indicates that the membranes selected for this study coincided with some of those investigated elsewhere.

4.2.1 Membrane performance

Measurement of membrane performance in terms of flux and solute rejections is one method or step towards characterising synthetic membranes. With respect to characterisation techniques it was essential to derive a set of standard procedures. Membrane characterisation is an integral part of membrane research so there is plenty of published material available that allows an overview to be formed of the methods typically employed.

In the first instance membrane performance was discussed on the basis of pure solvent flux. The solvent or pure water flux in this work was measured as a function of the applied pressure, the result was a value of volumetric flow rate per unit membrane area and given pressure. This value was also referred to as hydraulic permeability and once determined for a new membrane it provides a baseline figure to which membrane performance can be compared over the life of the membrane (Geraldes et al., 2001) (Bowen and Mohammed, 1998) (Bowen and Welfoot, 2002).

The second membrane characterisation step was normally a discussion of the salt rejection ability of the membrane or membranes (Bowen and Mukhtar, 1996) (Childress and Deshmukh, 1998). The solutes typically selected for classification purposes were NaCl and $MgSO_4$, where the monovalent sodium salt was commonly used to define the performance of RO membranes, and the divalent magnesium salt rejection was an indicator of NF performance (Jenkins and Tanner, 1998) (Alkhatim et al., 1998). Other solutes used to illustrate the separation abilities of a membrane were uncharged organic compounds such as glucose, sucrose or polyethylene glycol. These solutes were deemed useful as they make it possible to avoid charge effects and discuss separation on the basis of the steric properties alone (Van der Bruggen and Vandecasteele, 2002) (Kim et al., 2001). Ultimately the "pore size" and respective size distribution was evaluated by an investigation of the rejections for a size range of organic solutes. Molecular weight cut-off was also determined by this means and was defined as the molecular weight at which 95% rejection is exhibited.

Other methods of characterisation exist that could be referred to as direct techniques. These methods such as Atomic Force Microscopy (AFM) (Bowen and Doneva, 2000),

Scanning Electron Microscopy (SEM) (Kim et al., 2001), streaming potential analysis (Peeters et al., 1999) and membrane charge density measurements (titrimetric) (Schaep and Vandecasteele, 2001) provide a greater insight into the physical properties of the membranes. The information provided through such methods has allowed more informed speculation about the controlling factors in membrane transport and separations. In this study, streaming potential analysis was used, in conjunction with conventional techniques, to provide further insight into the nature of the membranes investigated.

Hydraulic permeability

Hydraulic permeability was measured for all of the membranes used in this study and, where available, was compared with data provided by the manufacturers.

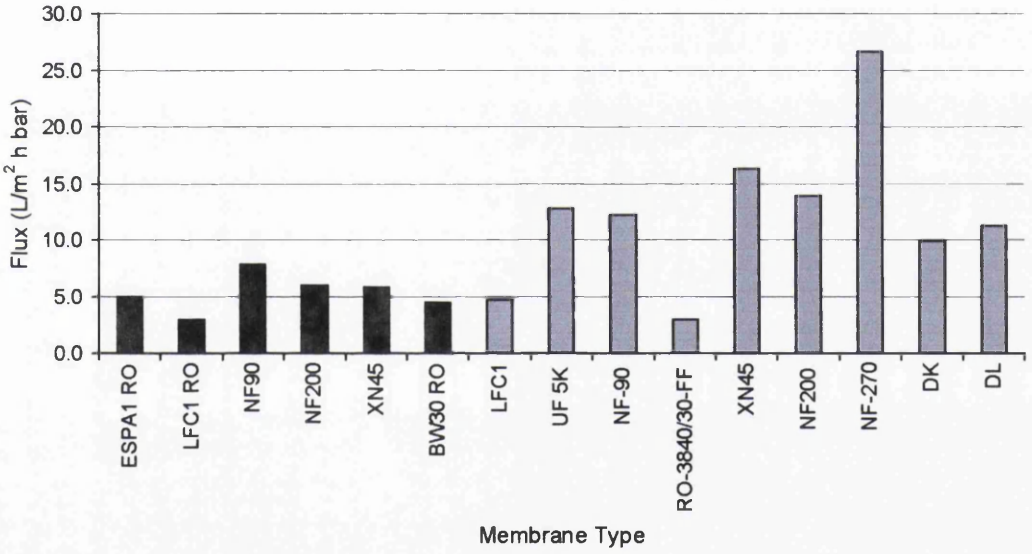

Figure 4-2 Pure solvent flux (L/m^2 h bar) of a range of commercially available membranes (black bars represent manufacturers data, grey bars represent experimental data) (key to membrane manufacturers: Hydranautics (LFC1 and ESPA1); Trisep (XN45); Dow filmtec (NF90, NF200, NF270 and RO-3840/30-FF); Osmonics (DK and DL); Sartorious (UF5K).)

Manufacturers' pure water flux values were typically quoted to be in the region of 2.5-7.5 L/m^2 h bar (LMHB) for both RO and NF membranes. By contrast the experimental flux results ranged from 2.5 to 27 L/m^2 h bar. This discrepancy might have been due to one, or a combination, of two factors. Firstly the flux values may have been dependant on membrane orientation. In a flat sheet arrangement, the

pressure the membrane was exposed to might have differed significantly from that for SPW modules even though the apparent operating pressures appeared to be the same. Secondly, membranes, as supplied in commercial modules, are pre-treated and standardised before they are supplied to the end user but flat sheet samples are often supplied dry and without quality control. This might have been enough to result in differences in the nature of the membrane surface and therefore its transport properties.

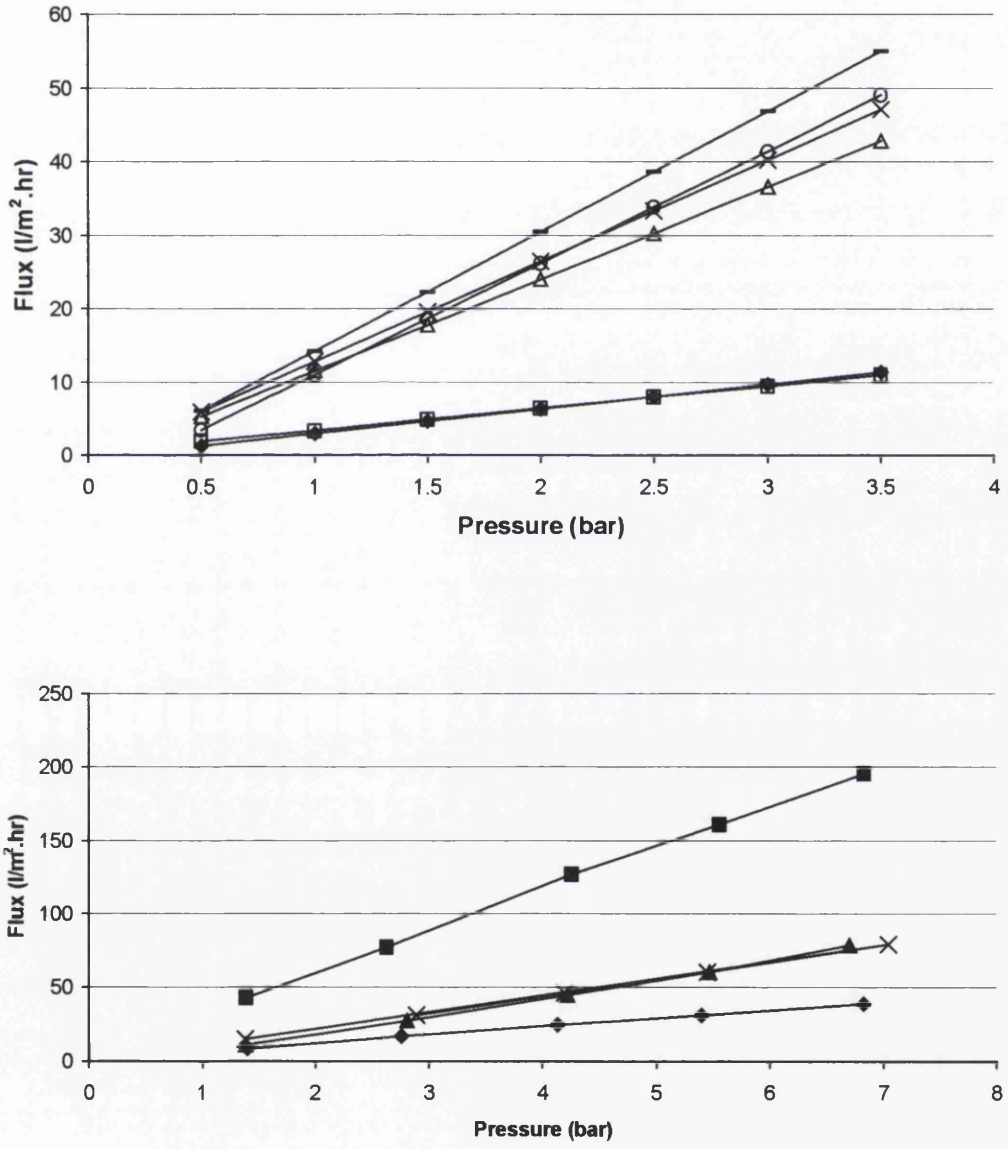

Figure 4-3a) and b) the linear relation between flux and pressure for a range of commercial membranes. Key to membranes: (a) BW30 (diamonds), LFC1 (squares), NF90 (triangles), NF200 (crosses), XN45 (dashes), UF5K (circles), (b) NF270 (squares), NTR7450 (diamonds), DK (triangles), DL (crosses).

In all of the cases investigated the relation between applied pressure and flux was linear for 0-7 bar. This relationship is illustrated by Figure 4-3a) and b).

Salt rejection

Monovalent and divalent salt rejection is used for specifying the rejection capabilities of reverse osmosis and nanofiltration membranes respectively. Salt rejection can also be measured over ultrafiltration membranes and the result is useful as it clearly demonstrates the effect of charge on rejection where steric effects are negligible.

Class	Brand	Product code	Salt	Rejection (1)	(2)	Literature values
RO	Hydranautics	LFC-1	Na_2SO_4 (10 mg/L) *	98.9		
RO	Dow Filmtec	BW30	Na_2SO_4 (10 mg/L) *	92.4	90.7	(Lee et al., 1999)
			NaCl		87.0	(Lee et al., 1999)
NF	Trisep	XN-45	NaCl (750 mg/L)	9.40		
			NaCl (2000 mg/L)	11.3		
NF	Dow Filmtec	NF90	$MgSO_4$	89.0	94.0	(Alkhatim et al., 1998)
			NaCl (2000 mg/L)	45.6	60.0	(Alkhatim et al., 1998)
			KCl		65.0	(Alkhatim et al., 1998)
NF	Dow Filmtec	NF200	$MgSO_4$	88.7		
			Na_2SO_4	88.4		
			KCl (2000 mg/L)	49.1		
			NaCl		68.0	(Gilron et al., 2001)
NF	Osmonics	DK	NaCl (2000 mg/L)	28.8	79.0	(Koyuncu and
					75.0	Topacik, 2002)
					51.5	(Bowen and Welfoot, 2002)
						(Dey et al., 2000)
NF	Osmonics	DL	KCl (2000 mg/L)	19.5		
NF	Nitto Denko	NTR7450	KCl (2000 mg/L)	32.5		
			NaCl		41.0	(Schaep et al., 2001)
					51.0	(Kiso et al., 2001)
			$MgSO_4$		53.0	(Schaep et al., 2001)
UF	Sartorious	UF 5K	$MgSO_4$	37.9		

Table 4-3 Salt rejection values obtained during the course of this study (1) and sourced from literature (2) (* concentration of sodium ions)

Salt rejection is discussed when evaluating membranes as it provides a general indication of their separation performance. It might be reasonable to suppose that the values obtained with mono- and divalent salts represent the membrane properties in terms of both steric exclusion and charge effects. On this basis the salt rejection is found to be a simple and yet powerful performance evaluation tool.

In this work salt rejections at single salt concentrations were evaluated for the membranes available. This provided a means of rapidly comparing the rejection performances of the membranes and enabled an investigation of the reproducibility of the results produced by the equipment used in this study.

A measurement of the repeatability was achieved using a feed comprising Benzyl alcohol and four measurements of rejection at a pressure of 40 psi. This demonstrated that the rejection, an average of 7.2%, could be achieved with a relative error margin of ± 2.2% (an absolute error of 0.16% rejection). This value represents a high level of reproducibility.

Table 4-3 provides a comparison of the salt rejections achieved by the membranes in this study and data obtained from literature. Where comparison can be made the rejection of divalent salts was found to be roughly twice that of monovalent salts. Monovalent and divalent salts that differed only in their cation, exhibited similar rejections. Where there were data available, values obtained experimentally compared favourably with literature values, those values that did not were attributed to the pressure and concentration dependencies of observed rejection in membrane transport processes. The plot shown in Figure 4-4 demonstrates the concentration dependence of rejection.

For reverse osmosis membranes rejections of monovalent salts are quoted in excess of 98% in the marketing literature. It is therefore surprising to find that divalent salts exhibit rejections in the region of 90% both in this work and other studies. Arguably therefore, RO membrane salt rejection is in the range of 85-100%.

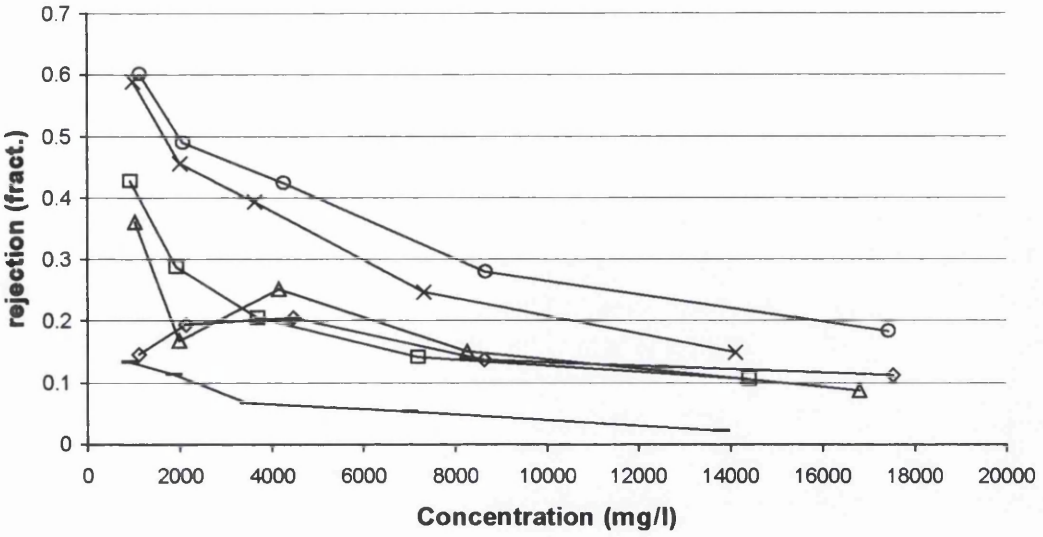

Figure 4-4 salt rejection as a function of concentration. (key to data series: Osmonics DL (diamonds), Osmonics DK (squares), Trisep XN45 (dashes), Nitto Denko NTR7450 (triangles), Dow filmtec NF90 (crosses), Dow filmtec NF200 (circles)

For nanofiltration membranes the rejection of divalent salts is normally quoted by manufacturers as being 96-100% and ~50% for monovalent salts. Again, values obtained in the course this investigation and the work of other authors provides measurements that differ from these values to a significant extent. Therefore, divalent salt rejection by NF membranes is considered to be in the range 85-95% and monovalent rejection in the range 0-50%.

Membrane Charge

Membrane charge is an important factor in membrane separations and when considered in conjunction with properties such as molecular weight cut-off and hydraulic permeability it becomes possible to make, in some cases, quantitative predictions of membrane separation operations. As a consequence surface charge measurements were made on the membranes considered in this work, the results of which are presented here.

Zeta Potential was evaluated from streaming potential measurements and was known to be influenced by the electrolyte concentration, used to create the streaming potential, and the pH. For the results shown here the electrolyte was a solution of 0.001M NaCl. The effective concentration range for streaming potential

measurements was 0.001M to 0.025M for the equipment used (Anton Paar Electrokinetic Analyser). Above and below this range the accuracy of measurement was known to be poor. The lowest concentration in this range was used for all measurements as it provided the most sensitivity to the charge present on the membrane surface.

Membrane charge can be measured and plotted as a function of both pH or electrolyte concentration. The result is a charge variation profile that provides a clear impression of the properties of the membrane in this respect, and also enables comparison between membranes to be made easily.

The plots shown in Figures 4-5 and 4-6 show the zeta-potential variation, according to pH, for the following six membranes: Osmonics DL and DK, Dow Filmtec NF90 and NF200, Nitto Denko 7450 and Trisep XN45. All four plots are typical of measurements of this type. The main characteristics of the graphs are the charge variation with pH across a significant proportion of the pH range and the change in charge sign at a low pH value (~ pH 4.5), see Table 4-4. The point at which the plot of zeta potential versus pH passes through zero is known as the isoelectric point.

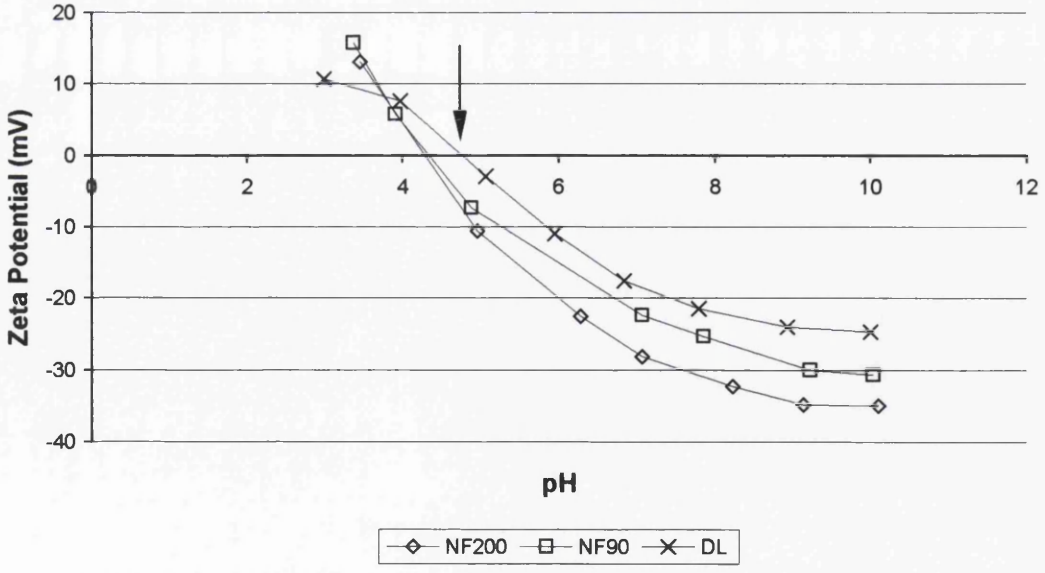

Figure 4-5 Dow Filmtec NF90, Dow Filmtec NF200 and Osmonics DL membrane surface charge variation with pH

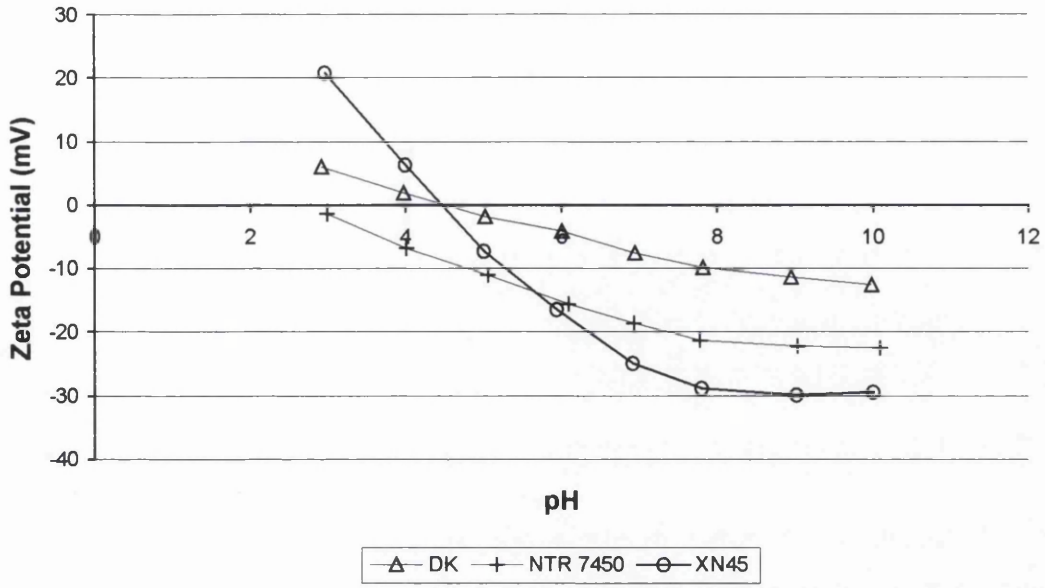

Figure 4-6 Osmonics DK, Nitto Denko NTR7450 and Trisep XN45 membrane surface charge variation with pH

An arrow, in Figure 4-5, indicates the isoelectric point for the Osmonics DL membrane. All six membranes retain a negative charge for most of the pH range investigated. This is normal for nanofiltration membranes that are polyamide based. The variation in charge magnitude exhibited by the membranes is a property of the differing functional groups on the polymer backbone, and their respective dissociation constants. The Osmonics DK and DL membranes are deemed to be very similar in nature and they exhibit only a slight difference between their surface charges. The Nitto Denko NTR7450 membrane has a charge that is intermediate within the six membranes and the Trisep XN45 membrane has the largest charge variation. As with the Osmonics membranes the Dow-Filmtec membranes present very similar potential curves to one another suggesting that they share similar surface chemistries.

Membrane	Zeta potential at pH 7	PH at isoelectric point
DK	-7.650	4.5
DL	-18.15	4.8
NF90	-21.82	4.3
NF200	-27.60	4.3
NTR7450	-18.82	2.7
XN45	-25.26	4.5

Table 4-4 Membrane charge at neutral pH and the pH value of the isoelectric point of each membrane

4.3 Trisep XN45

One of the aims of this stage of the experimental work was to select one membrane that was to be used in all of the practical investigations that followed. The Trisep XN45 membrane was chosen as it displayed a relatively high flux, low salt rejection and high charge. Flux or hydraulic permeability is an important consideration in membrane processes as it ultimately relates to the economics of the process and high flux is preferable as it equates to a higher permeate rate for a lower energy input. The high charge on the membrane surface makes it a distinctive membrane and it was thought that this property might aid qualitative discussions and conclusions on certain aspects of the results.

4.3.1 Trisep XN45 – theoretical characterisation

Membrane characterisation can be conducted in two parts, the first a direct measurement of properties such as permeate fluxes and charge and the second a theoretical discussion of measured data. This theoretical examination typically involves fitting phenomenological models to experimental data by variable adjustment. These variables represent key features of the system and once fitted they provide new insight into the properties of the membrane.

The two main mathematical theories have already been discussed extensively in Chapter 3 and they are that derived from irreversible thermodynamics (Spiegler and Kedem) and the extended Nernst Planck based model (Donnan-Steric Partitioning Pore Model, DSPM). Both theories, with some modification, have been related to specific tangible properties of the membranes. What follows is a discussion of these models in conjunction with actual experimental data acquired from the Trisep XN45 membrane

Rejection of uncharged molecules – the Van der Bruggen method

Spiegler and Kedem (S-K) proposed a transport model, based upon the thermodynamics of irreversible processes, which presented a "black-box" description of the solute flux through a membrane. This model was composed of a diffusion term and a convection term, with the convection term controlled by the solvent flux, J_v.

In the context of this work this theory has two uses; the first is to provide a means of predicting the rejection of uncharged solutes, with no salt present, and the second is to allow determination of several important membrane properties. To evaluate coefficients that represented key properties of the membrane such as solute permeability, pore size distribution and molecular weight cut-off it was necessary to fit the relevant models to data obtained by experiment.

Theoretical Background

Spiegler and Kedem (S-K) derived a transport model that consisted of two components: a diffusion component and a convection component (Van der Bruggen and Vandecasteele, 2002). This was reflected by the following transport equation:

$$j_s = -P_s \Delta x \frac{dc_s}{dx} + (1-\sigma) j_v c_s \tag{4.1}$$

Where P_s was the solute permeability, x a distance perpendicular to the surface of the membrane, σ was the reflection coefficient and c_s was the solute concentration at the membrane.

On the basis of Hagen-Poiseuille's law solvent flux, j_v, was represented by:

$$j_v = \frac{A_k r}{8\eta\tau} \frac{\Delta P}{\Delta x} \tag{4.2}$$

Where A_k represents the porosity, r the pore radius, η the viscosity, τ the tortuosity ΔP the trans-membrane pressure and Δx the membrane thickness.

At non-infinite pressures equation (4.1) can be solved to define rejection in terms of reflection coefficient and solute permeability, hence

$$R = \frac{(1-F)\sigma}{1-\sigma F} \tag{4.3}$$

where

$$F = \exp\left(-\frac{1-\sigma}{P_s} J_v\right) \tag{4.4}$$

Historically these two equations, (4.3) and (4.4), were fitted to experimental data to obtain values for the solute permeability, P_s, and the reflection coefficient, σ. However, several workers made efforts to provide theoretical descriptions of these coefficients.

Van der Bruggen and co-workers proposed an array of models that provided a theoretical description of the "black-box" parameters used in the S-K model, namely the reflection coefficient and the solute permeability. Of the approximations discussed the reflection coefficient was found to be best represented by a log-normal function. This log-normal model considered the reflection coefficient to be controlled by a logarithmic function of the pore radius and standard deviation, and the size of the solute molecules. To aid simplicity the size of solutes and pores were not described in terms of a radial dimension but these size characteristics were represented by molecular weight (MW) and molecular weight cut-off respectively ($\overline{MW}$). The resulting model was written as follows:

$$\sigma(MW_s) = \int_0^{MW_s} \frac{1}{s_{MW}\sqrt{2\pi}} \frac{1}{MW} \exp\left(-\frac{\left(\ln(MW) - \ln(\overline{MW}) + 0.56 s_{MW}\right)^2}{2 s_{MW}^{\ 2}} \right) dMW \tag{4.5}$$

Where the parameter s_{MW} related to the standard deviation of the pore size distribution, and $\sigma(MW_s)$ was the reflection coefficient of a solute molecular weight MW_s.

The pressure dependency of the retention, implicated through inclusion of the solvent flux in the transport model (equation (4.4)), was evaluated through experiment and denoted as a coefficient of water permeability, K. Although equation (4.2) indicates that water permeability is a function of the membrane porosity, pore radius, and tortuosity as well as the membrane thickness and the solution viscosity, this coefficient was determined from an experimental investigation of the variation of pure solvent flux with trans-membrane pressure and is given as a flux per unit applied pressure.

Application of the theory

A mathematical description of this type has little value unless it can be applied in a practical way. Models can be used in two ways, the first as a method of predicting the performance of the system that is the subject of the model and the second as a discussion tool for use with experimental data produced by the system. Van der Bruggen demonstrated that the effect of pressure on the retention of a compound, and the relation between molecular size and retention could be discussed using these models (Van der Bruggen and Vandecasteele, 2002).

The reflection coefficient represents a maximal condition of the membrane system: the rejection at infinite pressure. However, infinite pressure is an idealised condition and as such is impossible to achieve. Collection of a data set such as that illustrated in Figure 4-7, which was produced when the retention of maltose was measured as a function of pressure, allowed equations (4.3) and (4.4) to be fitted to the data and therefore enable computation of the reflection coefficient (Van der Bruggen and Vandecasteele, 2002). Although the quality of the fit between the model and the data is poor, suggesting a weakness in the model, the parameters may still retain a significant relevance.

When investigating uncharged compound rejections, one of the key governing factors for rejection is the solute size. A number of authors have shown that there is a strong relation between retention and molecular size and this relation is strongest for uncharged solutes (Ozaki and Li, 2002) such as sugars (Nakao and Kimura, 1981) (Wang et al., 2002). It has been shown that if a set of data were available, which provided retention values as a function of molecular size then it was possible to fit a model that related molecular size to rejection. Such a model is provided by equations (4.3), (4.4) and (4.5).

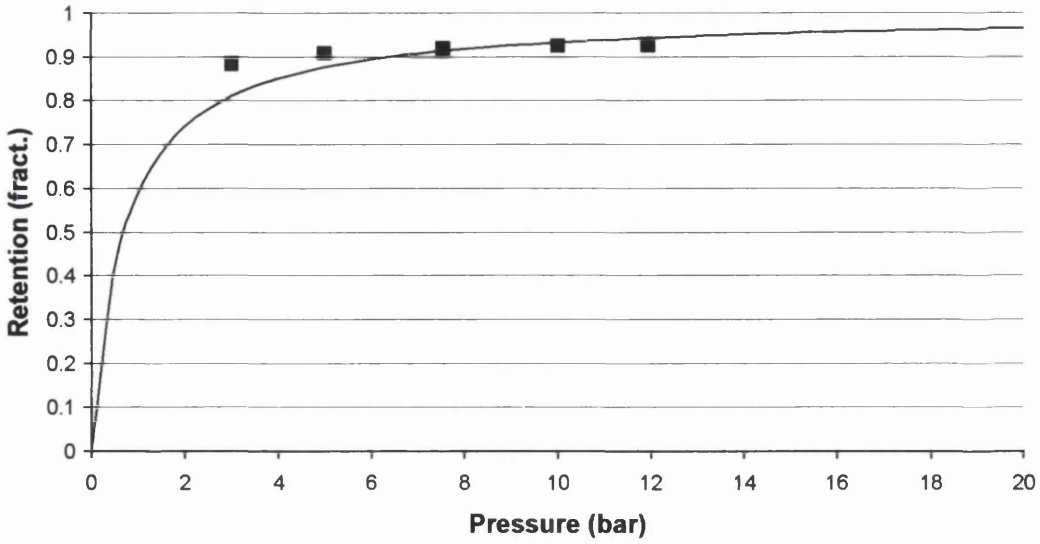

Figure 4-7 The retention of maltose as a function of pressure, the solid line represents fitted data (Van der Bruggen and Vandecasteele, 2002)

The results of the curve fitting procedure are given in Figure 4-8. The values for the molecular weight cut-off, pore size distribution and a coefficient referred to as the membrane specific diffusion parameter, ρ, that dictate the form of the curve, were evaluated using the Solver function within Microsoft Excel 2000 and Mathcad 2000 Professional (Mathsoft applications). Mathcad was used to provide a numerical solution to the differential equation, equation (4.5) and was used here as a tool for the execution of a fourth-order Runge-Kutta numerical technique. The solver function in Excel was used to optimise the value of ρ, the diffusion parameter. The diffusion parameter described a general property of the membrane and allowed prediction of the solute permeability on the basis of solute size, hence equation (4.6).

$$P_s = \frac{\rho}{d_s} \tag{4.6}$$

In the tuning of the model parameters ($\overline{MW}$, S_{MW} and ρ) an observation of the influence and therefore importance that each parameter had within the model was made. Molecular weight cut-off corresponded to the molecular weight of molecules whose rejection was greater than 90%; this value therefore dictated the location of the curve in relation to the x-axis. The standard deviation of molecular weight retention (S_{MW}) affects the slope of the main (central) part of the curve.

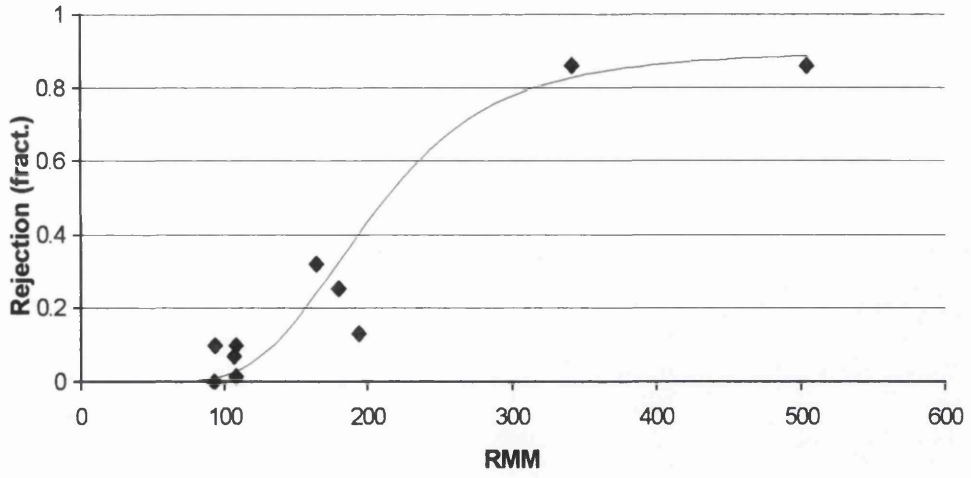

Figure 4-8 Plot showing the relation between molecular weight (RMM) and rejection, incorporating the curve that represents the fitted Van der Bruggen/Speigler-Kedem model (solid line).

Solute	Molecular weight	Rejection
Aniline	93	0
Phenol	94	0.1
Glycerol	107	0.07
Benzyl alcohol	108	0.015
Benzyl amine	108	0.1
Phenylalanine	165	0.32
Glucose	180	0.253
Caffeine	194	0.13
Sucrose	342	0.86
Raffinose	504	0.86

Table 4-5 The series of organic compounds chosen to indicate the relation between molecular size and the rejection. Note that Phenol, Phenylalanine and Benzylamine are partially ionised and therefore carry a charge. Since the larger ions are negatively charged their rejections would be expected to be increased. Caffeine is deemed to be anomalous

A smaller gradient in the central section suggested a broad spread in the pore size distribution, whereas a steeper slope was indicative of a narrower deviation or sharper cut-off. The membrane permeability coefficient (ρ) has most influence upon the high-rejection high-molecular weight end of the curve increasing or decreasing the

rejection accordingly. This suggests that solute permeability has a marked influence only when molecules are equivalent to or larger than the MWCO.

Although Van der Bruggen noted that the permeability coefficient can be determined, for any membrane, from the rejection of just one compound at a range of pressures, it should be noted that the results of the majority of their work relied upon measurements of retention that simulate the reflection coefficient. To produce values of retention that represent reflection requires filtration at high pressure. The type of pressures required to emulate maximal retention were not achievable by the experimental apparatus used in this study. This was not an issue with respect to determination of MWCO and S_{MW} since both were independent of pressure, even though retention is not. As a consequence of equipment limitations, the permeability coefficient also had to be evaluated as part of the fitting exercise.

Additional parameters and initial values

Additional to the parameters discussed previously the solvent permeability of the membrane was determined. This was evaluated by measuring water flux as a function of pressure, the final value being reduced to a flux per unit pressure. For the Trisep XN-45 membrane solvent permeability was found to be 7.63×10^{-6} m^3/m^2 s bar.

Before commencing the iterative procedure that deduced the values of $\overline{MW}$, S_{MW} and ρ it was beneficial to enter initial values that would closely resemble the final optima. Molecular weight cut-off and standard deviation were estimated through inspection of the points illustrate in Figure 4-8. Values published for other membranes were also useful as a guide and were wholly relied on for a starting value for the solute permeability coefficient.

4.4 Results

Membrane	Solvent permeability, K (m^3/m^2s bar)	Diffusion parameter, ρ (m^2/s)	Molecular weight cut-off, $\overline{\overline{MW}}$	Standard deviation of molecular weight retention, S_{MW}
NF 70	3.06×10^{-6}	7.15×10^{-15}	90	1.233
UTC-20	5.28×10^{-6}	3.06×10^{-15}	146	0.388
NTR 7450	4.72×10^{-6}	2.07×10^{-15}	595	1.187
XN 45	7.63×10^{-6}	14.0×10^{-15}	255	0.350

Table 4-6 Model parameters for four commercial membranes. Data for the NF70, UTC-20 and NTR 7450 membranes were acquired from literature. Data for the XN45 were determined in this study.

The plot shown in Figure 4-8 illustrates that the data obtained for the Trisep XN45 membrane of rejection with molecular size, provides a curve that is close to that predicted by the VDB/S-K combination model. A well shaped curve was expected as the rejection data was for uncharged species whose rejection was dependent almost entirely on the steric factors of pore size, pore size deviation and molecular size. The plot has both the typical sigmoidal shape that was expected and the curve for the fitted model. On inspection the curve fit appears reasonable, although the experimental data shows some degree of scatter around the line. Scatter is to be expected, as the compound molecules do not necessarily resemble the perfectly uncharged and symmetrical species of the type upon which the model is reliant.

The parameters printed in Table 4-6 for the Trisep membrane were derived through fitting the model to the data points shown Figure 4-8 and Table 4-5. The molecular weight cut-off for the membrane was found to be 255 Da, this value compares favourably with values normally expected for commercial nanofiltration membranes that typically have MWCOs of 150-300 Da. The manufacturer's literature states that $MgSO_4$ (120 Da) and Sucrose (342 Da) both have rejections of 92%, a range within which the MWCO value calculated here falls comfortably.

The solvent permeability was, in all cases, determined from experimental water flux measurements and was deemed to be a reliable value. In the case of the XN45 membrane, the flux was exceptionally high even when compared with the NTR 7450 membrane with its large MWCO. This might be related to the membrane's high relative magnitude of charge.

It was expected that the solute permeability coefficient might be related to the solvent permeability. In the case of the membranes reviewed in the literature, high solute permeability coincided with lower values of solvent flux. However the XN45 membrane had both a high flux and a high permeability coefficient relative to the other membranes. This might have indicated that either the XN45 possessed some exceptional properties, or as was more likely, the sample of membranes studied here is to small to allow these observations to be made.

4.4.1 Trisep XN45 membrane experimental data

As found in Section 4.3 the Trisep XN45 membrane presented the most interesting choice for use in the majority of the experimental investigations conducted within this study. The aim of the experimental work undertaken with this membrane, was to assess the properties of combined uncharged organic / charged inorganic feed systems. The hypothesis was that the interactions between each solute species or the solute species and the membrane might be more complex than had previously been acknowledged or observed.

4.4.2 Three ion solution systems

Three ion systems are comprised of a solution containing two coions with a common counter ion: for example (where the membrane is negatively charged) sodium chloride and sodium sulphate. One of the features of a three-ion system is their ability to negatively reject one of the coions. This behaviour was explained by the Donnan exclusion theory.

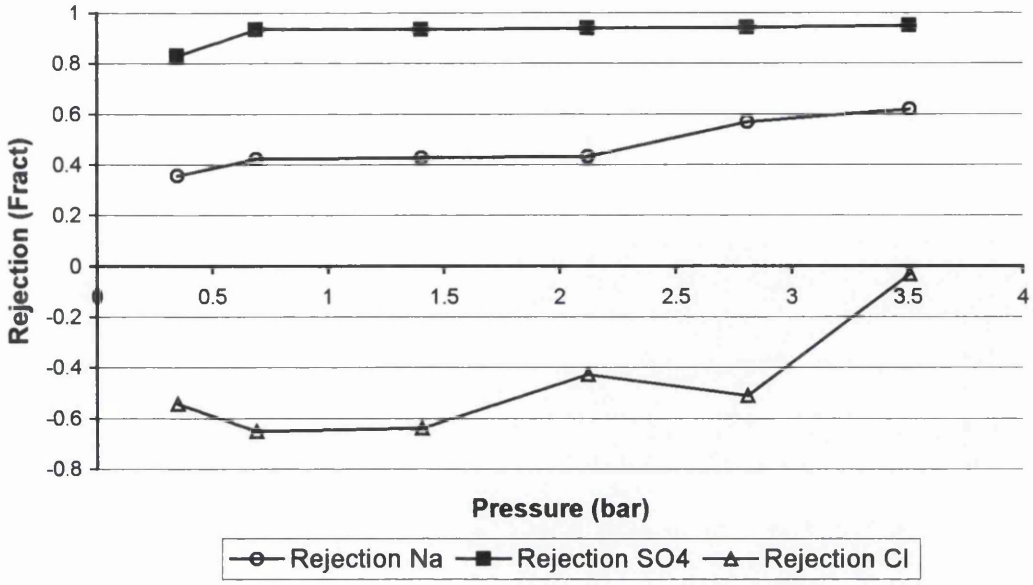

Figure 4-9 Individual ion rejections in a three-ion system as a function of pressure for sodium chloride and sodium sulphate.

Since the membrane was negatively charged at the pH of the system, the counter (sodium) ions were attracted to the surface of the membrane. from there they were drawn, by the convective flow of water, through the membrane. Conversely the coions (sulphate and chloride) were repelled by the surface charge of the membrane. Hence, in a theoretical dynamic-stage, there existed a charge imbalance on either side of the membrane. In an attempt to regain this balance the chloride ion concentration increased on the permeate side of the membrane such that it became higher than that on the feed side. It is chloride ions and not sulphate ions that undergo this process on account of the higher valence and greater size of sulphate ions.

Figure 4-9 provides practical evidence of the phenomena of negative chloride rejection. Inspection of the plot shows that the highest rejection (up to 95%) was achieved by the sulphate ions. Sodium ions show a rejection value in the region of 40 to 50% and chloride ion exhibit a rejection of up to -50%. What this plot demonstrated was that the sulphate was very nearly totally rejected thus supporting the argument that increased valence results in increased rejection. With half of the total present sodium permeated to the product side of the membrane, the result was a

chloride concentration in the product that was twice that in the feed, hence negative rejection was achieved.

4.4.3 Organic compound rejection and pH

The charge properties of a solution/membrane system and pH are known to be strongly related, a fact that has been demonstrated by the results of the electrokinetic analysis work shown in Section 4.2.1. Consequently, the investigation of system pH and its influence on the rejection of a variety of organic compounds by nanofiltration, provided an important starting point for the study of organic interactions.

Compound	Molecular mass	Dissociation constant (if applicable)
Aniline	93	
Benzoic acid	122	4.20
Benzylamine	107	
Glucose	180	
Phenylalanine	165	
Sodium benzoate	121	

Table 4-7 Organic compounds whose rejection was investigated as a function of pH

Seven compounds were selected for this investigation and they are detailed, with other relevant information, in Table 4-7. They are both charged and uncharged, are similar in size and share similarities in their molecular structures (Table 3-2).

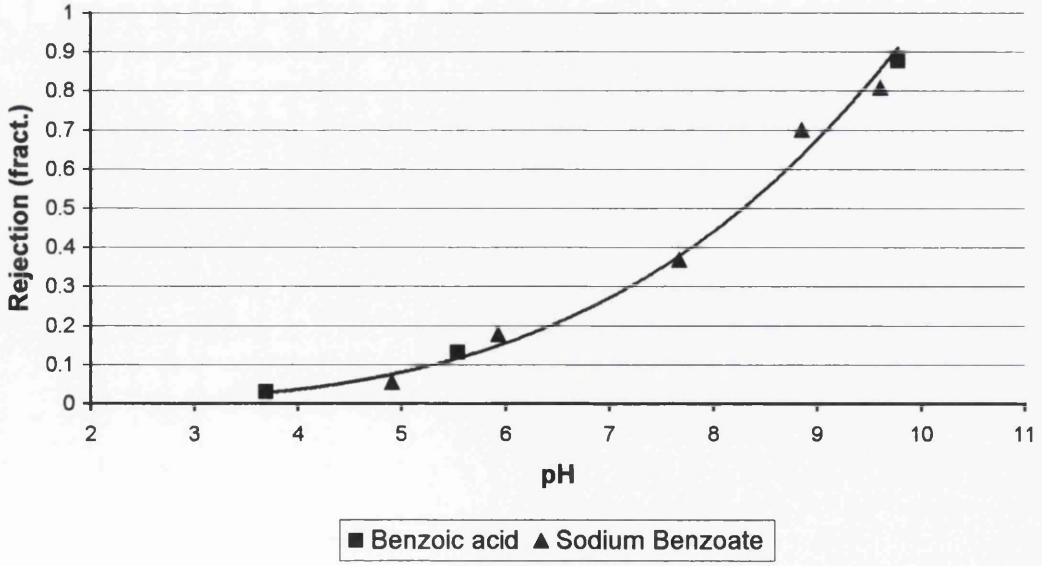

Figure 4-10 pH affect on rejection of ionised organic compounds (the trendline created using a power-law regression is for illustration purposes only)

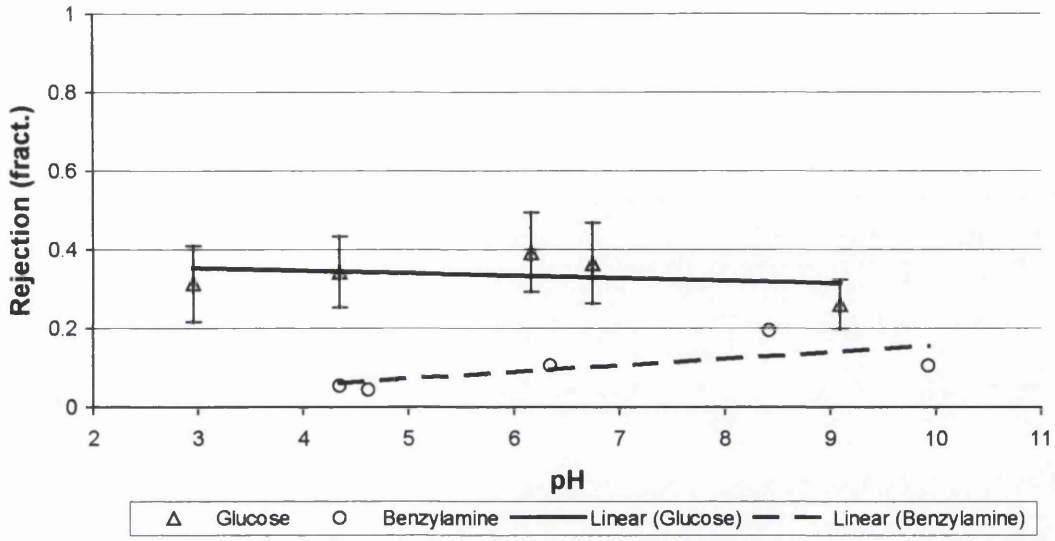

Figure 4-11 pH affect on "uncharged" organic compounds

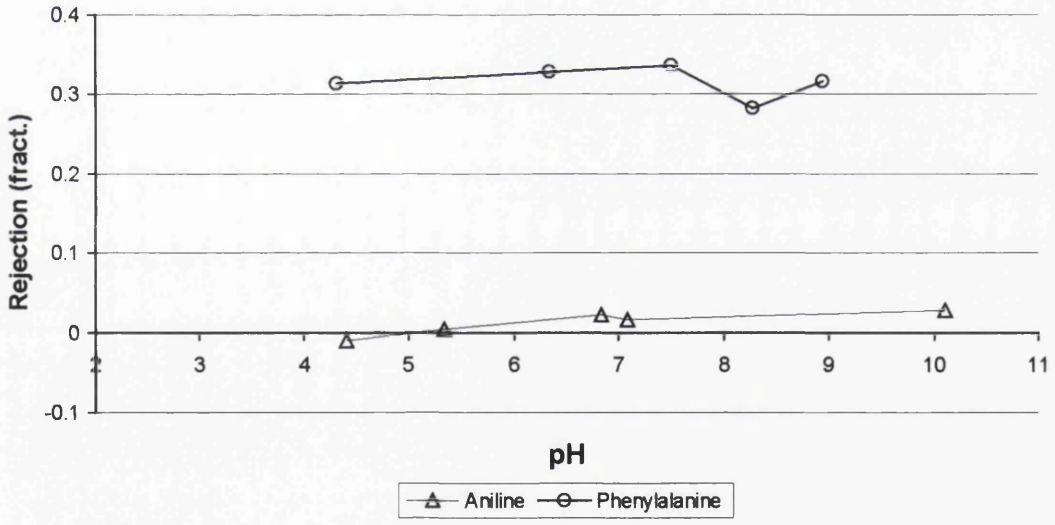

Figure 4-12 pH affect on the rejection of Aniline and Phenylalanine (uncharged)

Figures 4-10 to 4-12 present plots of organic compound rejections and their response to pH variation. Figure 4-10 displays the response of charged (ionised) compounds and can be contrasted with Figures 4-11 and 4-12, which demonstrate the behaviour of neutral (non-dissociated) compounds. These plots clearly illustrate that pH has a significant influence over rejection. For the solutes in Figure 4-10 the rejections are

shown to increase, markedly, with an increase in pH value. The rejection of benzoic acid and its sodium salt sodium benzoate, display a strong dependence on pH, the relation is a curve of moderately increasing gradient. Since these compounds are acids it would probably be neutral or positively charged in an acidic solution and hence the low rejection exhibited at low pH. In a basic system the compound would become more negatively charged and would show increased rejection by a negatively charged membrane.

4.4.4 The influence of salt concentration on uncharged organic solute rejection

Salts in this context conform to the standard definition. Three salts were chosen, they were: sodium chloride (NaCl), sodium sulphate (Na_2SO_4) and disodium hydrogen orthophosphate (Na_2HPO_4). These were selected because they retained common cations, and had anions of increasing valence and molecular weight. The basic assumption was that inorganic salts influence the rejection of uncharged compounds through a distribution of salt ions in the membrane system.

Monovalent salt

It was considered important to study monovalent salt (sodium chloride) addition in complex feed systems. Sodium chloride is commonly used in investigations of membrane rejections and could not be ignored in this work.

For this study, the rejections of two organic compounds with respect to prevailing salt concentration were investigated. The two compounds were glucose and sodium benzoate. They were selected, as both compounds are roughly of similar size and are respectively undissociated and dissociated when in solution.

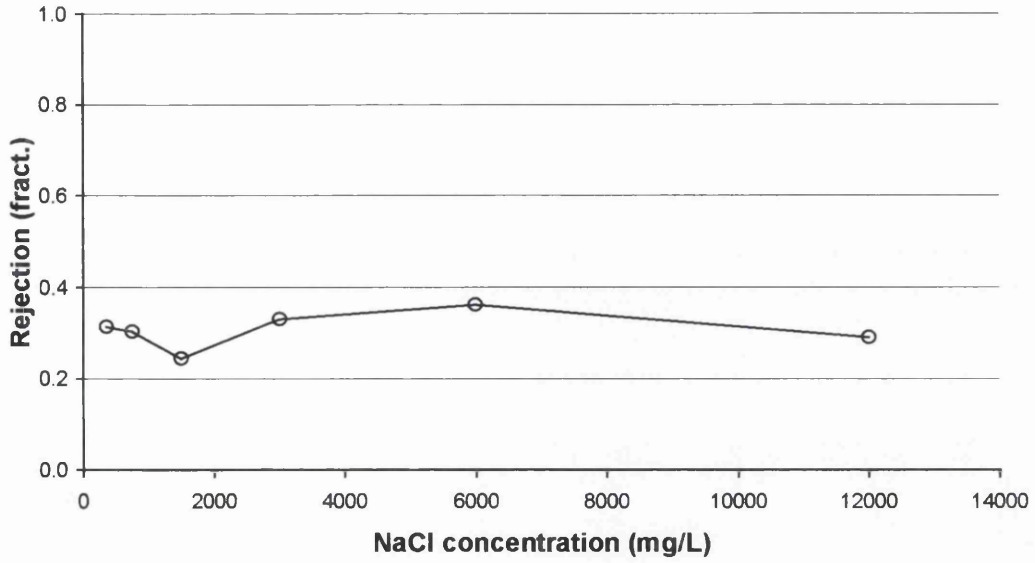

Figure 4-13 The influence of NaCl concentration on glucose rejection

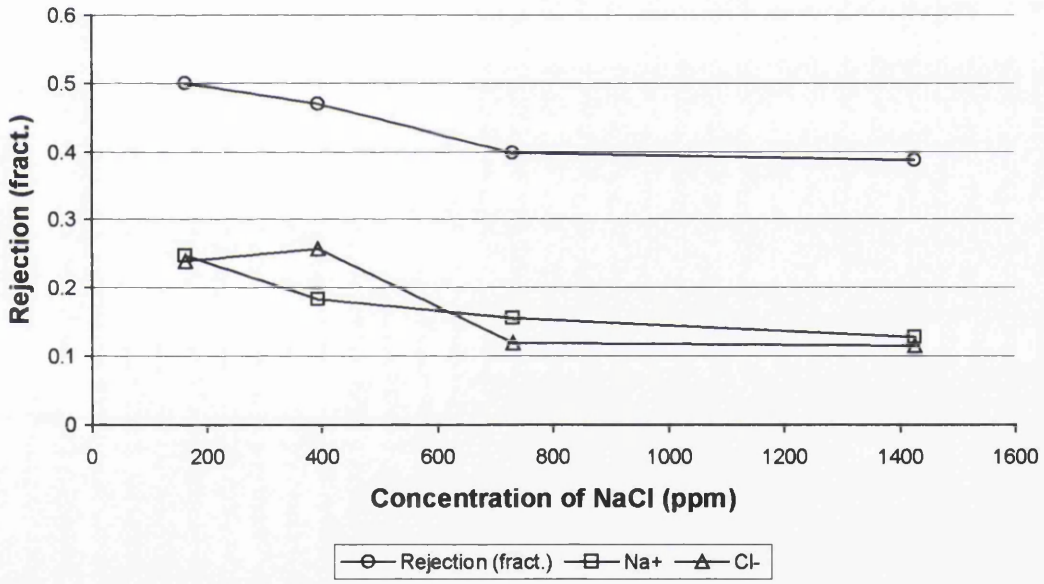

Figure 4-14 The influence of NaCl concentration on sodium benzoate rejection

The graph in Figure 4-13 shows the results of an increase of NaCl concentration on Glucose rejection. There was not a clear pattern to the fluctuation in glucose rejection, the data points varied around an average value of 30.7%. This variation may not be random but could be attributed to an interaction between NaCl and the material of the membrane. The plot in Figure 4-14 presents a consideration of the effect of NaCl concentration on Sodium Benzoate rejection. Again there was little to suggest that

sodium chloride influences the rejection. Sodium benzoate was assumed to be a strong candidate for exhibiting Donnan behaviour in the presence of salt. However, as can be seen in the plot in Figure 4-14, there were no distinctive features to the plotted data for the rejection of either sodium benzoate or the salt ions.

From this data it was concluded that a monovalent salt such as sodium chloride does not strongly influence the rejection of organic compounds charged or uncharged in the nanofilter used in this investigation. As such no further experiments involving NaCl and uncharged molecular species were carried out.

Divalent Salt

Following on from NaCl, use of the divalent salt Sodium Sulphate advanced the investigation. This electrolyte contained the bivalent anion (SO_4^{2-}), which was known to be repelled more strongly by the membrane; this in turn meant that a greater charge differential across the membrane was possible. Additionally the anion was physically large relative to the corresponding chloride ion.

Seven organic compound rejections were measured as a function of the sodium sulphate concentration. These organic solutes were both ionic and non-ionic. The results of this work are presented in plots shown in Figures 4-15 to 4-20.

Figure 4-15 gives the rejection curves for the organic solute and inorganic ions in the sodium benzoate/sulphate system. In contrast to the results for the sodium chloride system, the plot in Figure 4-15 implies that there was a strong charge effect associated with Na_2SO_4. The change in sodium benzoate rejection with sodium sulphate concentration was apparently linear with increasing salt concentration, and rapidly decreases to show negative rejection. The final rejection achieved in this experiment series was –51% at a salt concentration of 3.2g/L. In the same plot, the rejection of the salt ions was shown to tend to a constant value of 95% and the ratio of sodium and sulphate ions in the product remained close to stoichiometric ratios.

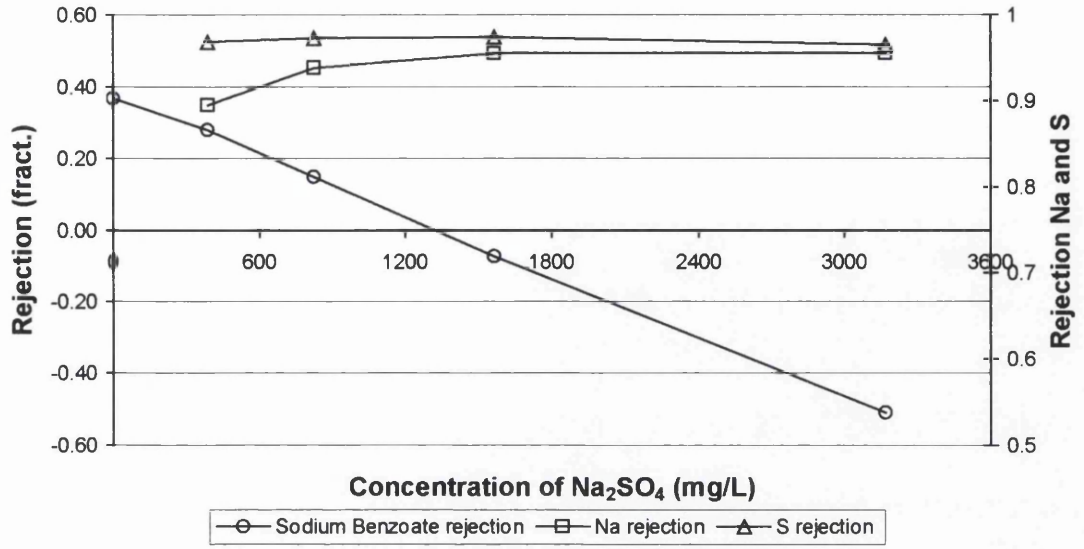

Figure 4-15 Sodium benzoate rejection according to Na_2SO_4 concentration

Figure 4-16 details the rejection behaviour of glucose in the presence of sodium sulphate. As in the case of sodium benzoate, the rejection of glucose also exhibited a marked fall with increasing salt concentration but this action diminished at higher salt levels. The salt ion rejections were shown to initially increase and then decrease with increasing concentration.

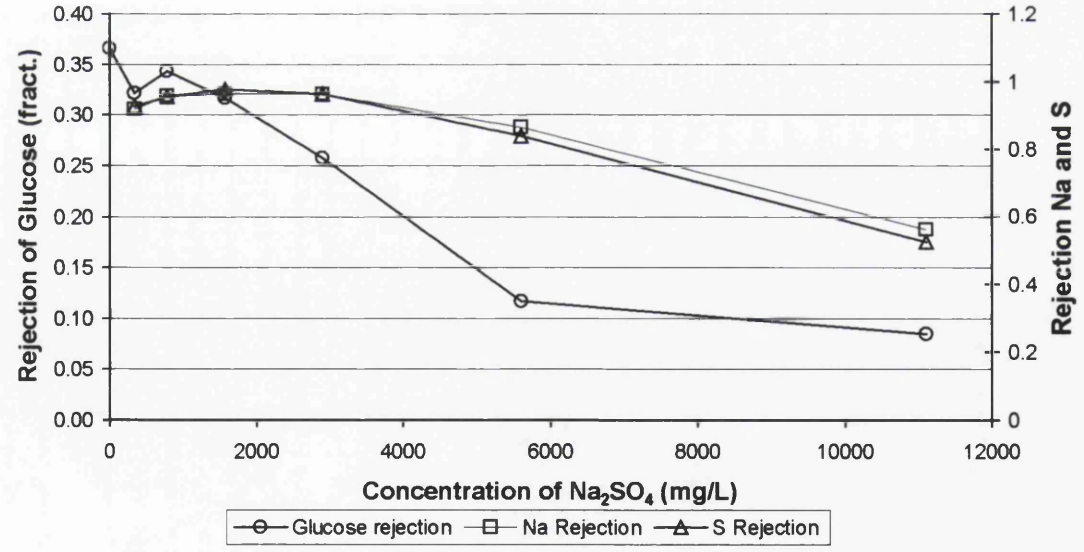

Figure 4-16 Glucose rejection according to Na_2SO_4 concentration

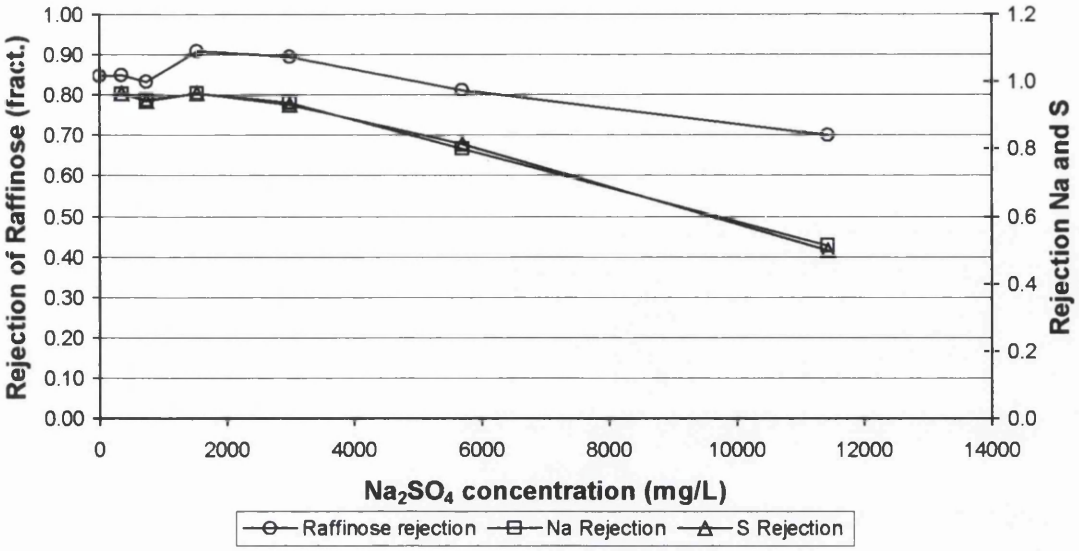

Figure 4-17 Raffinose rejection according to Na_2SO_4 concentration

Figures 4-17, 4-18, 4-19 and 4-20 present the results of the same experimental procedure as that used for sodium benzoate and glucose filtration, applied to raffinose, glycerol, caffeine and benzyl alcohol respectively. Similar observations can be made regarding the rejection of salt ions and for these four compounds as were made for glucose. The solute rejections decrease with salt concentration, the rate of decrease diminishing at higher salt concentrations. Most pertinently glycerol, caffeine and benzyl alcohol all show negative final rejection values.

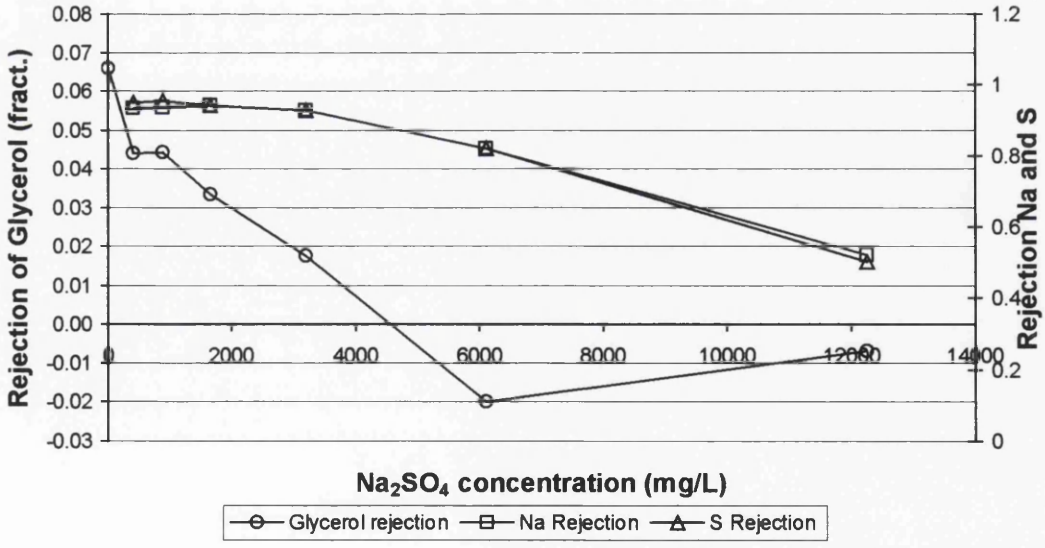

Figure 4-18 Glycerol rejection according to Na_2SO_4 concentration

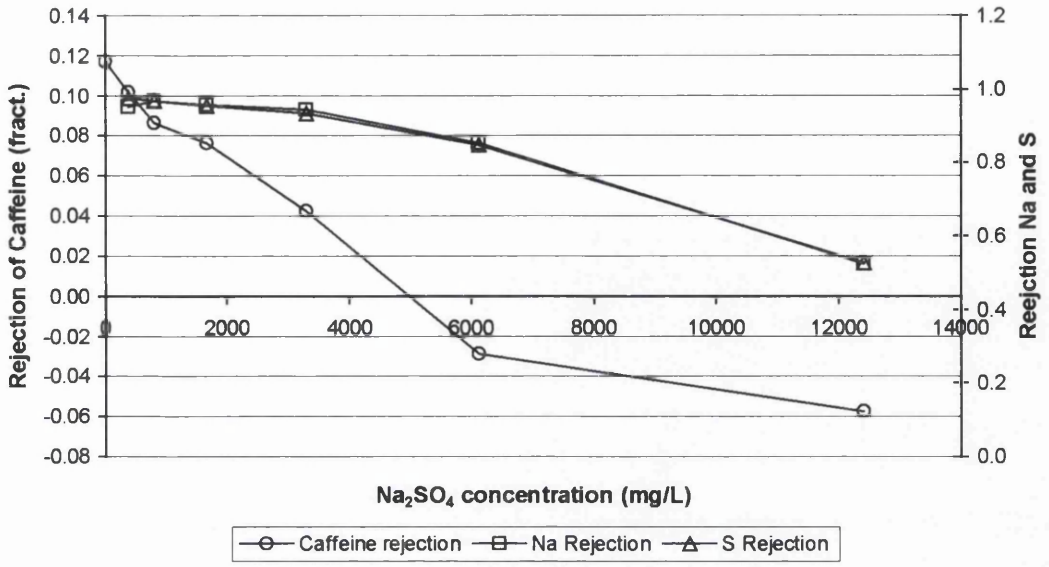

Figure 4-19 Caffeine rejection according to Na_2SO_4 concentration

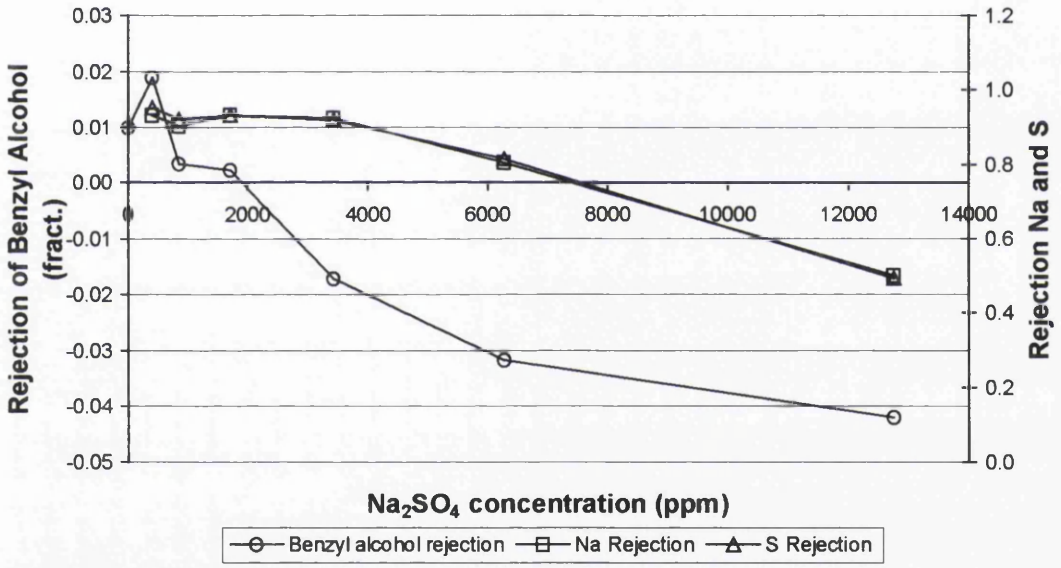

Figure 4-20 Benzyl Alcohol rejection according to Na_2SO_4 concentration

Multi valent salt

The inclusion of the multi-valent salt: disodium hydrogen orthophosphate provided the next, and in this study, final investigation. The phosphate salt contained an anion that has a higher valence than the sulphate ion examined previously. The presence of a higher valence salt ion increased the probability of co-solute transport being influenced by charge potential in the membrane system.

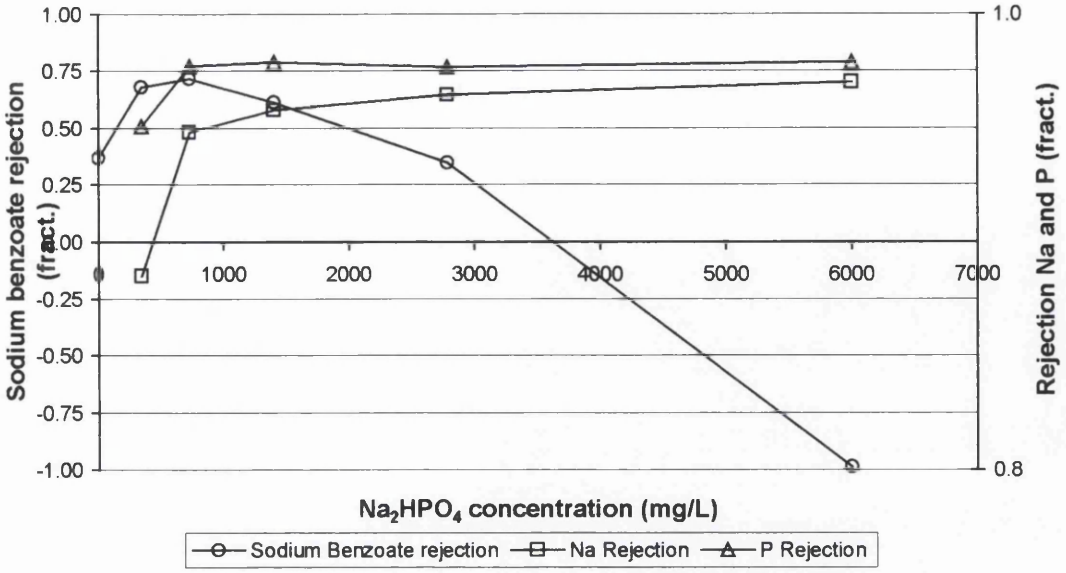

Figure 4-21 Sodium benzoate rejection according to Na_2HPO_4 concentration

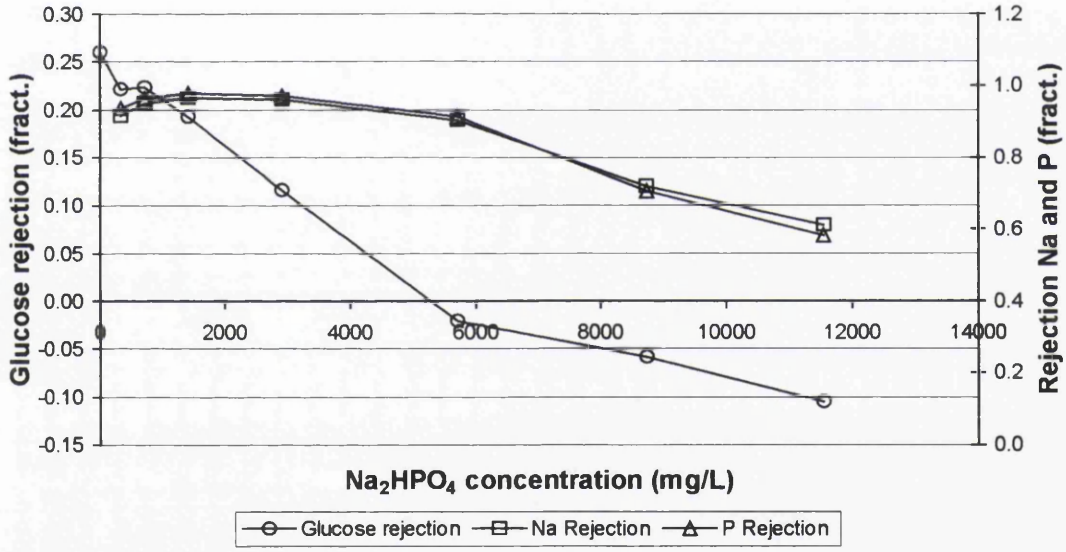

Figure 4-22 Glucose rejection according to Na_2HPO_4 concentration

The effect of the multivalent salt concentration on the rejection of organic compounds was measured in the same manner as for Na_2SO_4. The same six compounds were used and the results are presented in Figures 4-21 to 4-26.

Figure 4-21 shows the rejection profile for sodium benzoate in the presence of Na_2HPO_4. The shape of the curve projected by the data points is quite different to that for sodium benzoate with Na_2SO_4. With sodium sulphate there is a distinct linear

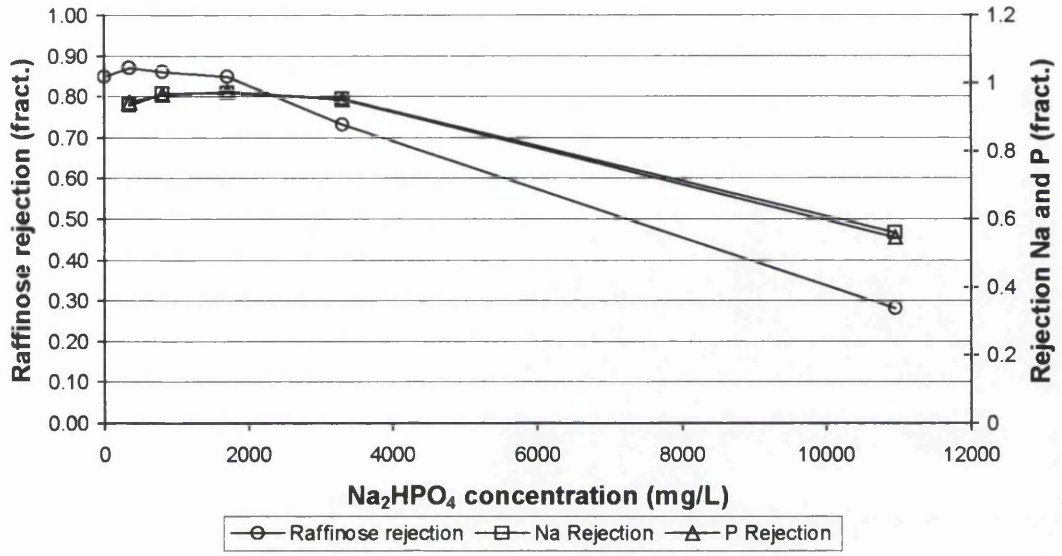

Figure 4-23 Raffinose rejection according to Na_2HPO_4 concentration

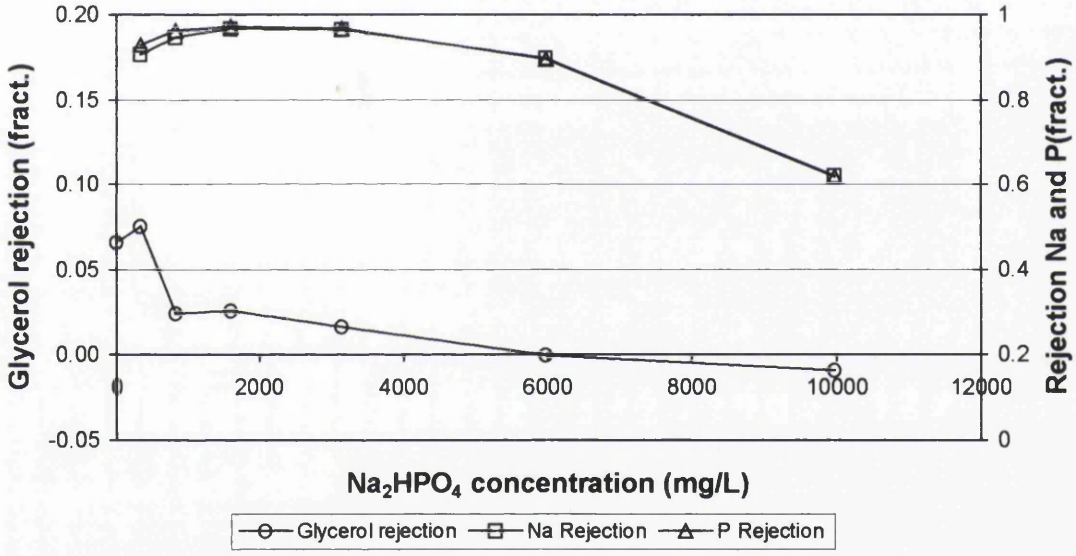

Figure 4-24 Glycerol rejection according to Na_2HPO_4 concentration

behaviour to the change in rejection whereas for the phosphate salt a pronounced curve is produced where at first the rejection increases with salt concentration before it decreases rapidly and eventually becoming negative for phosphate concentrations above 3600 mg/L.

Figure 4-22 details the results of the same scenario applied to glucose. The pattern of behaviour is similar to that seen for the sulphate system but with a difference in the

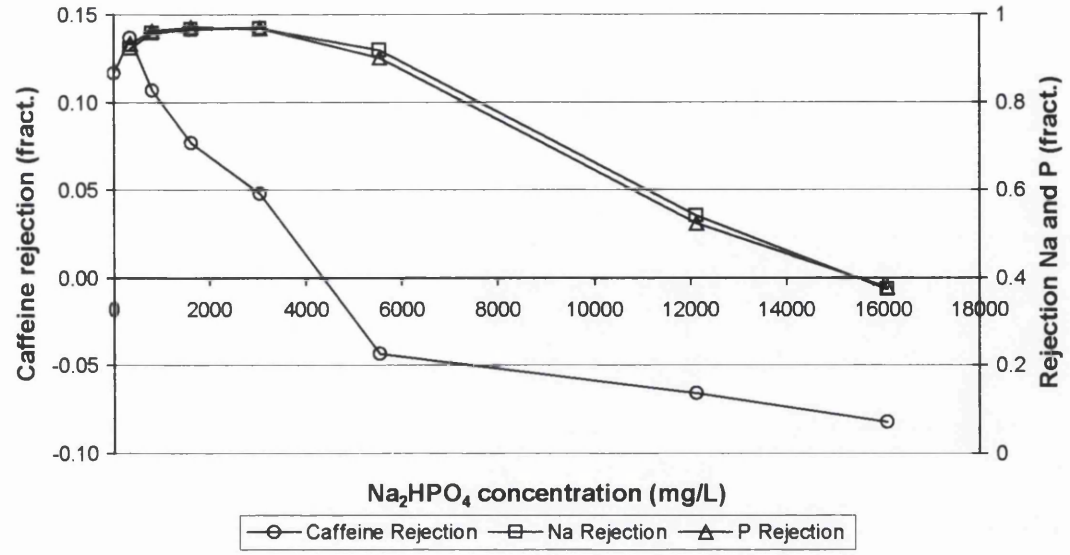

Figure 4-25 Caffeine rejection according to Na_2HPO_4 concentration

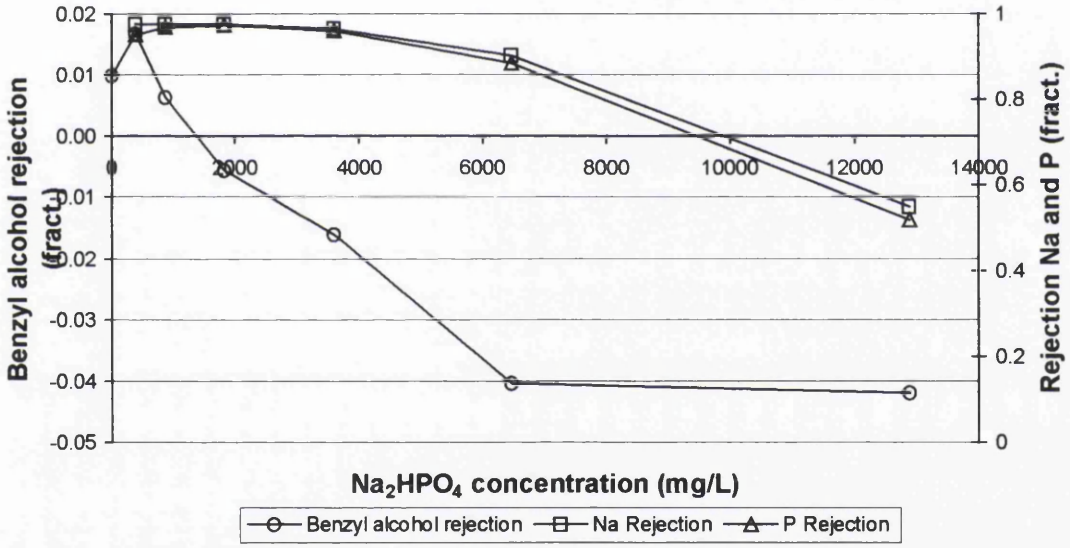

Figure 4-26 Benzyl alcohol rejection according to Na_2HPO_4 concentration

magnitude of the final rejection values. It was noted that the final rejection values for glucose are negative. The same observations apply to glycerol, caffeine and benzyl alcohol (Figures 4-23, 4-25 and 4-26) with the rejection patterns being similar but the rate of change in rejection values being increased in the presence of phosphate. Raffinose provides an exception but this is attributable to its relatively large molecular size.

An unusual feature of the plots shown in Figures 4-16 to 4-20, 4-22, 4-24 and 4-25 is a sometimes prominent kink at the beginning of the plot, coinciding with a

concentration ~350 mg/L. No matter what the controlling behaviour, it is unsurprising that the introduction of salt in to the solution modifies the system significantly enough to effect the organic species rejection. However, it is unusual that the rejection of organic solute passes through a maximum with respect to salt concentration. If an explanation were determined for this response it might provide more insight into the interactions between salts and undissociated organic solutes.

4.4.5 Salt rejection

The rejection of the disodium hydrogen orthophosphate was monitored for each solute system (shown in the secondary plots in Figures 4-21 to 4-26). A seventh experiment was conducted where only Na_2HPO_4 was present and the phosphate rejection was investigated as a function of its own concentration. All seven data sets were then combined into one plot allowing observation of whether the organic solute had any influence on the salt rejection. Figure 4-27 shows the result of this work. The rejection pattern produced is consistent and the values for all systems compare well with the results obtained for solitary phosphate rejection.

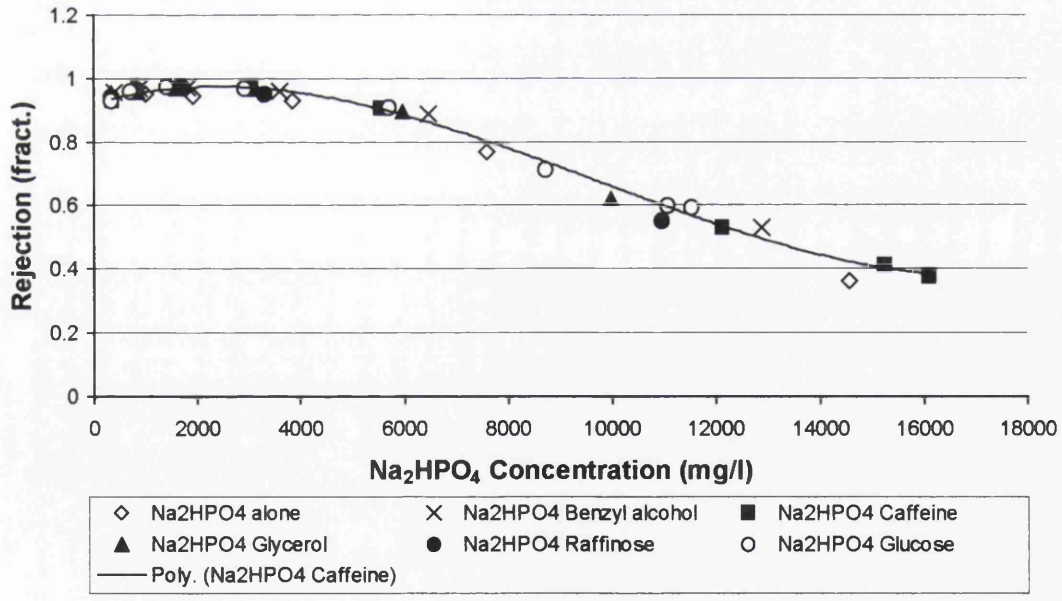

Figure 4-27 rejection of disodium orthophosphate with respect to solute type (the curve is a fitted using a polynomial for illustrative purposes only)

The same comparison was conducted for the sodium sulphate rejection observed in the divalent salt experiments. This also demonstrated a distinct pattern to the salt rejection behaviour where the organic solute was uncharged (Figure 4-28).

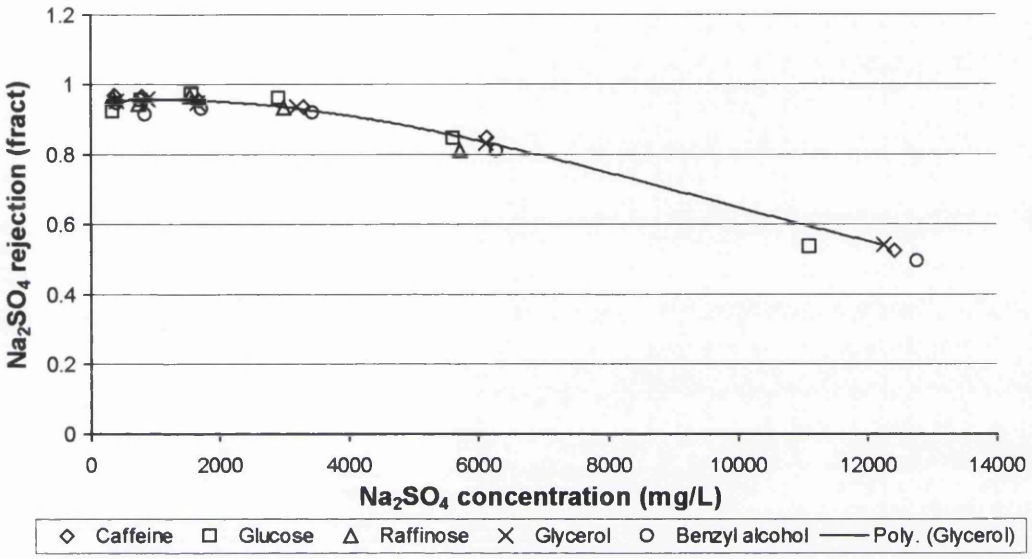

Figure 4-28 rejection of sodium sulphate with respect to solute type (the curve is a fitted using a polynomial for illustrative purposes only)

4.5 Conclusions

Before commencing a series of membrane based filtration investigations, it was useful to identify one membrane that could be used throughout the work. Membrane selection was based on certain performance characteristics, such as hydraulic permeability and salt rejection, as well as membrane properties such as zeta potential. The Trisep XN45 membrane was chosen because the permeate flux was generally high as was the magnitude of charge across the pH range, and the rejection properties were found to be high to intermediate for Nanofiltration membranes (250 Da) where MWCOs range from 150 – 1000 Da.

To further quantify the membrane selected for this study a theoretical model was fitted to an experimental data set, thus yielding a set of parameters that provide further insight into the properties of the membrane. The Spiegler and Kedem model was used by incorporation of the Van der Bruggen modification (Van der Bruggen and

Vandecasteele, 2002). The results of this work indicated a molecular weight cut-off of 255 Da and a corresponding standard deviation of molecular weight retention of 0.35. This second value indicates the sharpness of the cut-off, the low value indicating a cleanly defined MWCO. The third value obtained through this theoretical analysis was the diffusion parameter and the Trisep membrane was found to have a value of 14.0×10^{-15} m^2/s.

Several sets of experiments were carried out and the results of these have been presented in this chapter. The first set of results was for the three-ion filtration system, which promotes negative rejection of chloride ions and is a replication of experimental results seen elsewhere (Bowen and Mukhtar, 1996). Following this an investigation was made of the influence of pH, on the rejection of a variety of organic compounds. As expected, only charged compounds were found to be strongly influenced by a pH variation. As a final step, a comprehensive investigation of the effect of salt concentration on the rejection of charged and uncharged organic solutes was made. Salts of increasing valence were used and negative rejection was unexpectedly observed for a number of uncharged organic solutes at higher salt concentrations.

5 The negative rejection phenomenon

5.1 Introduction

Negative rejection is a phenomenon that has already been observed in membrane separation processes. Normally, negative rejection is a product of a charge imbalance across the membrane that is brought about by the distribution of ions between the feed and permeate. In the case of this study however, negative rejection of uncharged species has been witnessed. These systems have combined a salt with an uncharged solute and it has been found that the salt influences the rejection and consequently negative rejection of the organic solute. This occurrence has been seen for several organic solutes with both divalent and multivalent salts.

Before any speculation was made with respect to what might cause this behaviour there remained the need to verify the eligibility of the data. It had to be made certain that the results presented in Chapter 4 indicate an actual property of membrane-solution systems and was not simply an artefact and erroneous experimental technique or equipment. To achieve this, mathematical and theoretical discussions were made with regard to the data. The first such discussion was an error analysis. Since the negative rejection values rarely proceeded beyond a value of –10% it was conceivable that the negative rejection was brought about by experimental errors. Thus this possibility had to be ruled out through conventional evaluation of the magnitude of error. Following the error analysis the theoretical concept of Real Rejection was introduced enabling an effective discussion to be made in regard to the nature of the negative rejection system. A quantitative interpretation of the data was also possible using the real rejection theory. Real rejection theory is discussed in some detail in this chapter as it forms an important part of the overall discussion.

5.2 Error

5.2.1 Glucose

Glucose concentration was measured according to the analysis technique described in Chapter 3. There are two ways in which to evaluate the error related to the

determination of glucose concentration using the phenol-sulphuric acid method. The first is to consider the accumulated error related to the preparation of a sample for measurement in the spectrophotometer and the second is to assess the statistical error by determining the deviation in repeated analyses of the same sample or to consider the deviation of data points from the curve or straight line fitted to the calibration data.

Accumulated error

Several steps are involved in the phenol-sulphuric acid analysis of saccharide, one is a dilution, two are reagent additions and the final step is an absorption measurement in a spectrophotometer. All stages have an error associated with them, these errors are summarised in Table 5-1.

Source of error	Maximum condition	Absolute error ±	Units
Variable pipette	1	0.006	ml
Volumetric flask	10	0.025	ml
Variable pipette	5	0.030	ml
Spectrophotometer	2.000	0.005	Absorbance (dimensionless)

Table 5-1 Error sources and magnitudes for saccharide analysis using the phenol-sulphuric acid method

The error accumulated during sample preparation was found to be negligible, as was that associated with the spectrophotometer measurements (Appendix A-1).

Statistical error

There are two ways in which the statistical error can be evaluated. The first is a study of the standard deviation in a set of repeated measurements (collected for absorption calibration purposes) and the second is a study of the standard deviation in the same set of repeated measurements but using a "midpoint" value obtained from a fitted linear equation rather than a statistical mean. Appendix A-1 presents the determination of both values for glucose analysis. The greatest error, of 4.3%, was found for the latter "best-fit" analysis. This value was chosen as the measurement of error for this work as it represents a worst case in that it is several orders of magnitude higher than the calculated accumulated error.

From the absorbance error discussed in the last paragraph it was possible to evaluate how this value equated to an error on the calculated rejection. Paying particular consideration to negative rejection cases it was found that for a rejection of –10% there was an actual error of ±0.6%. The error bars were determined for all data points and the plot in Figure 4-22 was modified to give the plot in Figure 5-1:

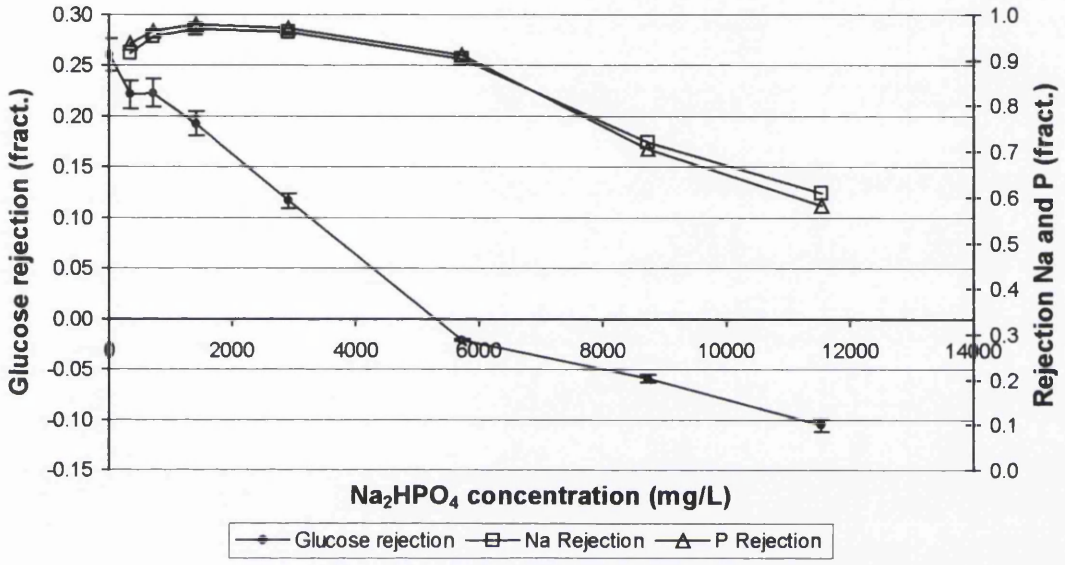

Figure 5-1Glucose rejection as a function of Na_2HPO_4 concentration including error bars

5.2.2 Caffeine and Benzyl Alcohol

The same error analysis as conducted for the glucose experiment was carried out for caffeine and benzyl alcohol rejection investigations. Error analysis was particularly relevant to the data from experiments with these three compounds as they exhibited the negative rejection that is central to this discussion. The results of this work are presented in two plots, Figures 5-2 and 5-3.

5.2.3 Glycerol

Glycerol concentration was ascertained using an enzymatic technique as described in Section 3.6.2 *Glycerol analysis using an enzymatic technique*. This method relied on the production of oxidised nicotinamide-adenine dinucleotide (NADH) in stoichiometric proportions to the glycerol. The absorbencies measured for both the

blank and the sample produced by this method, are directly related to glycerol concentration and a calibration curve is not required. The literature provided with the test kit included information on the precision of the method and this information was used for the error analysis.

In a worst case scenario the concentration value may deviate ±0.01g/L, which equates to a relative error value of 2%, for a concentration of 0.5 g/L. This error margin was then plotted as error bars on the glycerol rejection plot, Figure 5-4.

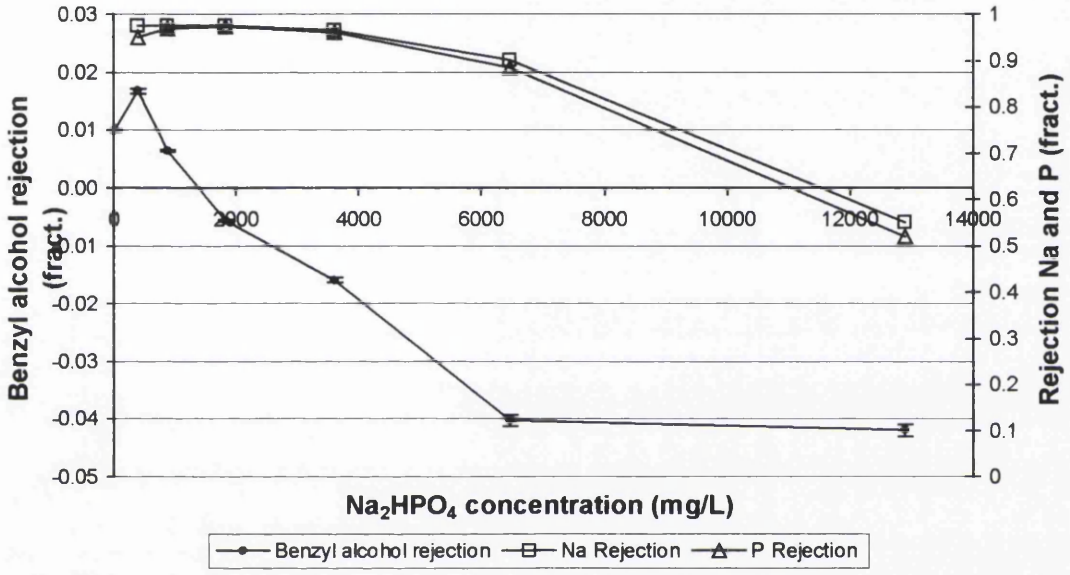

Figure 5-2 benzyl alcohol rejection as a function of Na_2HPO_4 concentration including error bars

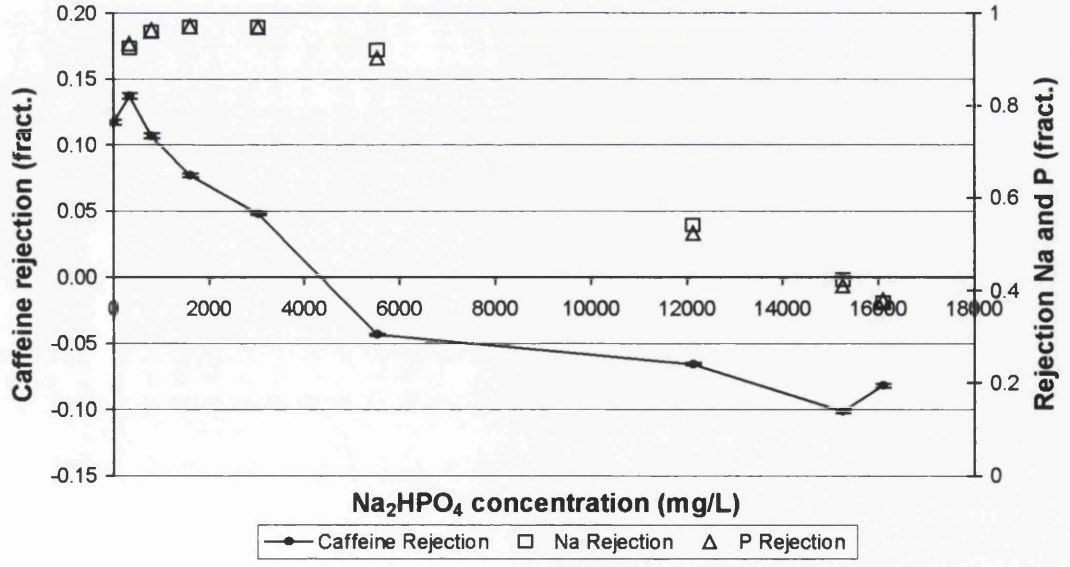

Figure 5-3 Caffeine rejection as a function of Na_2HPO_4 concentration including error bars

It may be seen from the error bars shown in the plots, Figures 5-1 to 5-4, that the error on the rejection of the uncharged compounds is insignificant and therefore does not provide an explanation for the negative values achieved at high salt concentrations. On the basis of this discussion it is possible to conclude that the phenomenon is a real observation and not just an artefact of measurement or experimental error.

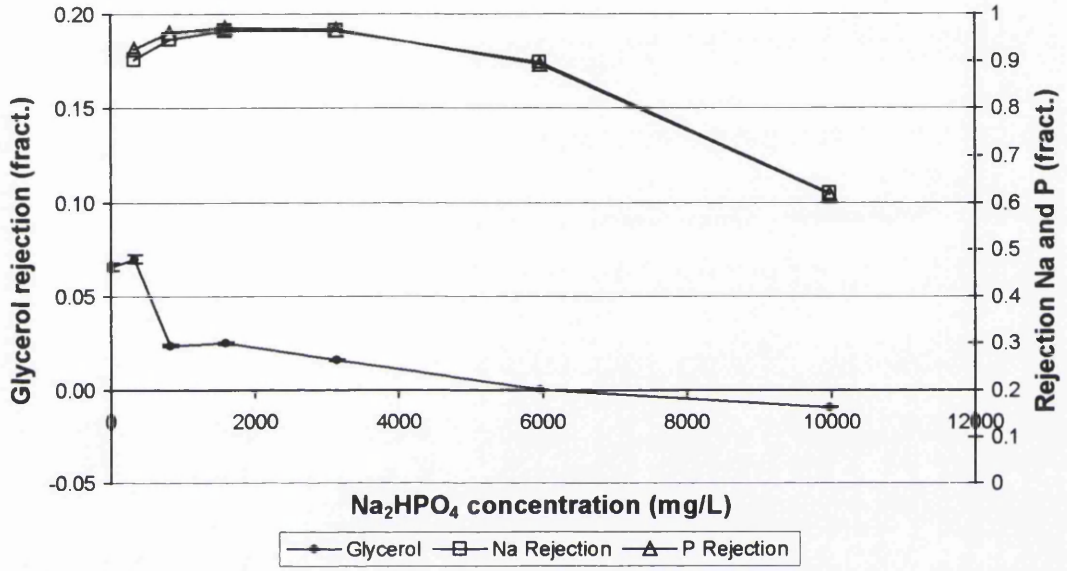

Figure 5-4 Glycerol rejection as a function of Na_2HPO_4 concentration including error bars

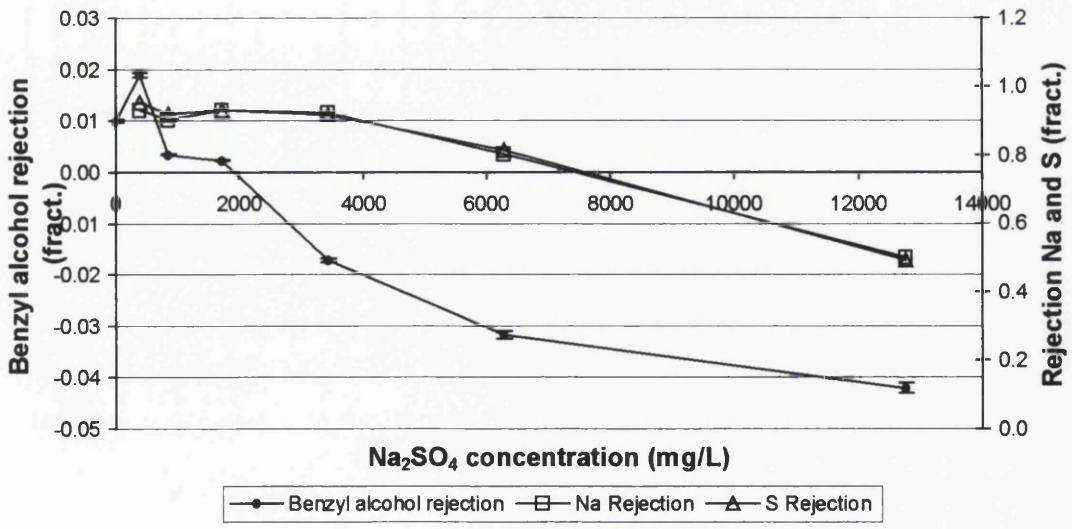

Figure 5-5 Benzyl alcohol rejection as a function of Na_2SO_4 concentration including error bars

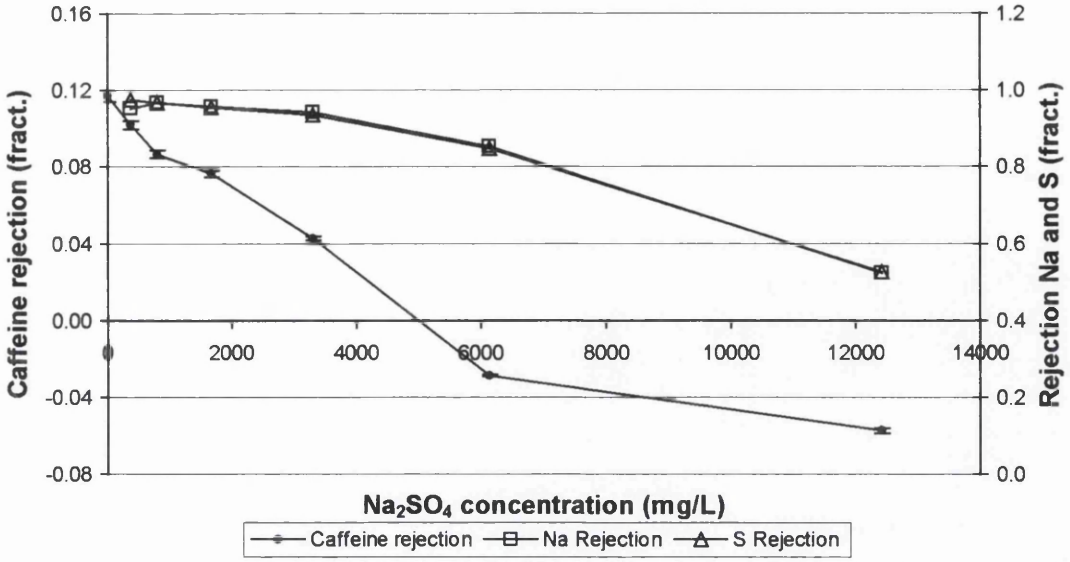

Figure 5-6 Caffeine rejection as a function of Na_2SO_4 concentration including error bars

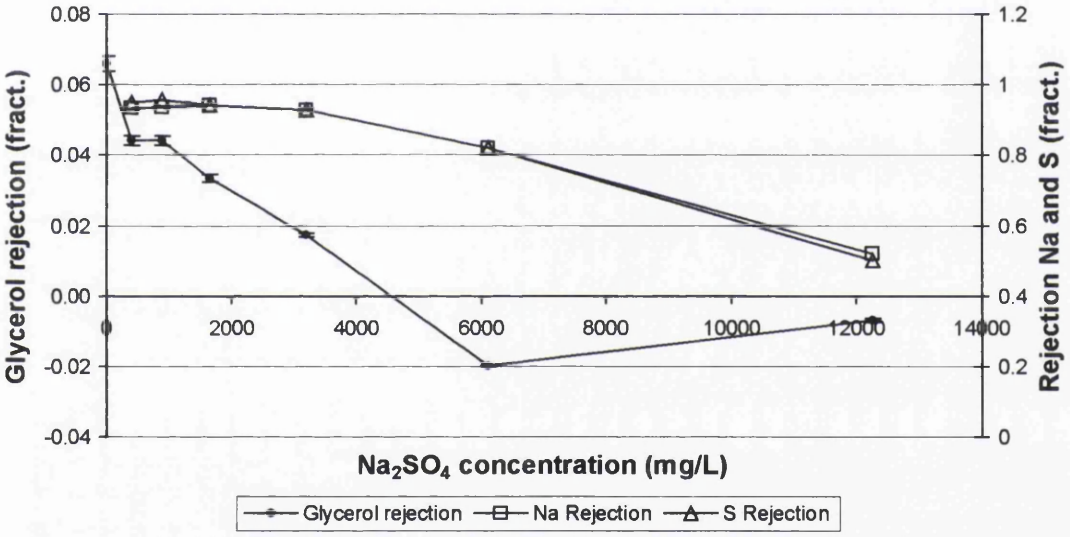

Figure 5-7 Glycerol rejection as a function of Na_2SO_4 concentration including error bars

An error analysis, similar in manner to that carried out for the Na_2HPO_4 data, was completed for the Sodium sulphate data, Figures 5-5 to 5-7. As for the disodium hydrogen orthophosphate results the error estimate is not great enough to provide an explanation for the negative rejection values achieved. Hence the negative rejection observed is again found to be evidence of a genuine phenomenon.

5.3 Real rejection

When discussing membrane separation performance the accepted approach was to determine a value defined as rejection. Rejection, of a particular solute, was calculated as the ratio of feed concentration to product concentration, as indicated by

$$\boldsymbol{R} = \frac{C_f - C_p}{C_f} \tag{5.1}$$

or,

$$R = 1 - \left(\frac{C_p}{C_f}\right) \tag{5.2}$$

This relation was originally defined as the sieve constant (Ferry, 1936), but has since been generally named rejection, as sieving only applies to membrane processes where steric factors alone contribute to separation. The rejection was a useful way of defining system performance as it was dimensionless and can therefore be used for direct comparison between different systems and the effect of variable adjustment on them.

The definition of rejection provided by equations (5.1) and (5.2) was convenient as both the bulk feed, C_f, and permeate, C_p, concentrations can easily be measured. However, this method was considered to be unsound, as the calculated rejection values do not provide a true representation of the separation performance of the membrane. This was because of a phenomenon known as concentration polarisation. Concentration polarisation is process of solute build up at a membrane surface that is a direct effect of the rejection and fluid flow in relation to the membrane surface. The qualitative concept of concentration polarisation is presented in Figure 5-8.

Figure 5-8(a) illustrates the typical concentration profile for a positive rejection system. In all theoretical situations the concentration of solute in the permeate is a function of that "seen" by the membrane on the feed side. Since the concentration at the membrane surface is not equal to the bulk concentration, the permeate concentration is not directly related to that of the feed. The zero rejection case (Figure

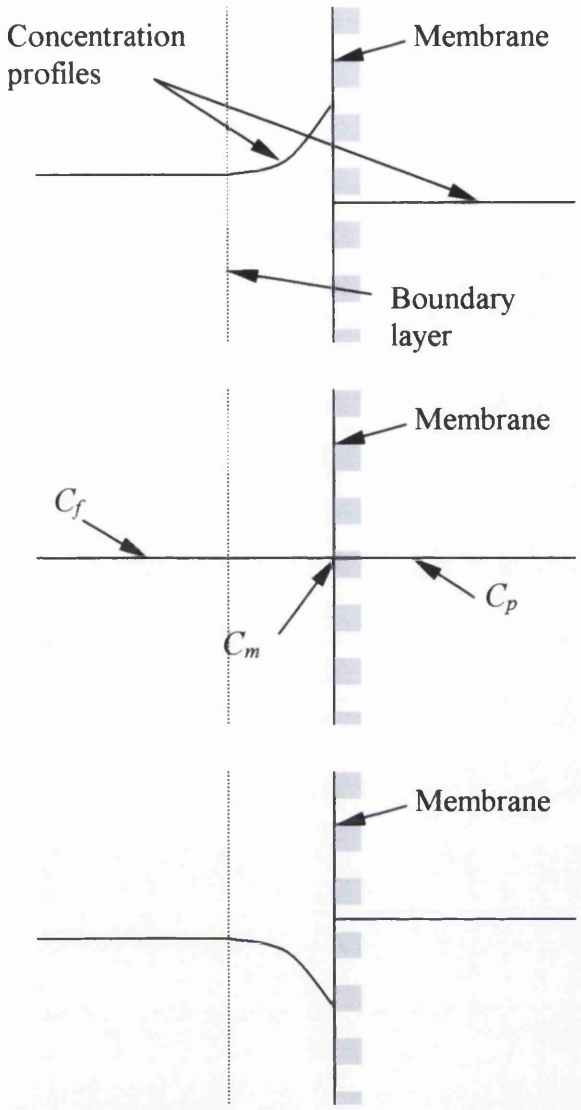

(a) Positive rejection. Concentration of the solute increases towards the membrane surface within the boundary layer.

(b) Zero rejection. The membrane retains none of the solute, therefore there is no retention at the membrane and as such there is no concentration profile.

(c) Negative rejection. Transport of solute through the membrane is such that the ratio of solute to solvent is higher than in the feed. Hence the concentration of solute in the boundary layer decreases or *solvent concentration* increases.

Figure 5-8 (a) Positive rejection, (b) Zero rejection and (c) Negative rejection concentration profiles.

5-8(b)) is the only situation where the rejection equation (5.1) represents the true performance. The third scenario, provided by Figure 5-8(c), is that of negative rejection. In this circumstance the permeate has a higher concentration than the feed and this results from a higher relative flux of solute than solvent through the membrane.

As a result of the concentration polarisation phenomenon an alternative definition of rejection referred to as the *real rejection* has been provided. Retrospectively, the original definition of rejection was referred to as the observed rejection; hence the following was derived,

$$\mathscr{R} = \frac{C_m - C_p}{C_m} = 1 - \frac{C_p}{C_m} \tag{5.3}$$

where $\mathscr{R}$ was the real rejection and equation (5.2) becomes

$$R_{obs} = 1 - \frac{C_p}{C_f} \tag{5.4}$$

where R_{obs} was the observed rejection.

Although the real rejection provides a definition of performance that was correct relative to the observed rejection, the membrane surface concentration, C_m, could not be measured directly and consequently a method was required that allowed a theoretical evaluation of this value.

5.3.1 Theoretical evaluation of real rejection

Perhaps the most commonly used technique for real rejection evaluation was the velocity variation method but there are also alternative techniques that rely on flux variation, maximum rejection and, most recently, flux change due a stepped increase in salinity (Sutzkover et al., 2000). The two methods of concentration polarisation evaluation discussed here are both reliant on experimental measurements. The main purpose of the experimental work was to determine a mass transfer coefficient (k_m) such that this value could be inserted in the following equation,

$$CP = \frac{C_m - C_p}{C_b - C_p} = \exp\left(\frac{J_v}{k_m}\right) \tag{5.5}$$

Where equation (5.5) was derived from the simple film model,

$$j_s = C_p J_v - D_\infty \frac{dC}{dy} \tag{5.6}$$

Here D_∞ was the salt diffusion coefficient and $k_m = D_\infty / \delta$, where δ was the thickness of the boundary layer on the membrane surface. Using equation (5.5) and a value for

k_m it was possible to determine c_m, the concentration at the membrane surface and thus $\mathscr{R}$ as defined by equation (5.3).

Velocity variation method

The correlation between the mass transfer coefficient and the fluid velocity was defined by the Sherwood number,

$$Sh = \frac{k_m d}{D_\infty} = a_m \left(\frac{du}{\upsilon}\right)^f \left(\frac{\upsilon}{D_\infty}\right)^g = a_m \cdot \mathrm{Re}^f \cdot Sc^g \tag{5.7}$$

Where d was hydraulic diameter of the flow passage, a_m a dimensionless numerical constant, v the kinematic viscosity and u the flow velocity through the membrane passage. Re and Sc are the Reynolds and Schmidt numbers respectively. Consequently the relationship between k_m and the velocity was known to be,

$$k_m = \frac{u^{a_m}}{b} \tag{5.8}$$

where b was a constant.

On this basis the following expression was derived from the solution-diffusion/film model (Nakao and Kimura, 1981),

$$\ln\left(\frac{1-R_{obs}}{R_{obs}}\right) = \ln\left(\frac{1-\mathscr{R}}{\mathscr{R}}\right) + b\left(\frac{J_v}{u^{a_m}}\right) \tag{5.9}$$

This relation predicted a linear dependency between the velocity across the membrane, u^{a_m}, and $\ln\left(\frac{1-R_{obs}}{R_{obs}}\right)$. The technique used in the velocity variation method was to complete a series of filtration experiments where only the cross flow velocity was altered (hence "velocity variation") and all other variables were held constant. The aim was to produce a data set for rejection as a function of velocity and plot it

according to equation (5.9). The intercept, on the x-axis, of the resultant straight line equates to $\ln\left(\frac{1-\mathscr{R}}{\mathscr{R}}\right)$.

A sequence of velocity variation experiments were completed on the filtration equipment used for the majority of this study. Glucose rejection at 0.0028 M (0.5g/L) concentration and 2.75 bar (40psi) was measured. A plot of this data is shown in Figure 5-9.

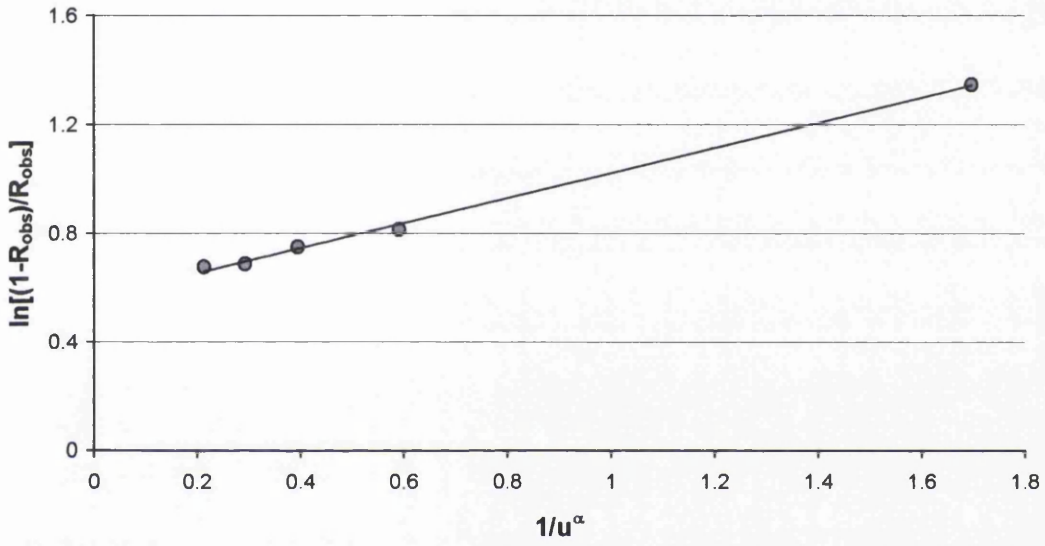

Figure 5-9 Velocity variation plot for glucose 0.0028M

The gradient of the line plotted in Figure 5-9 equates to the value of b in equation (5.9) and was thus used to determine k_m from equation (5.8). This technique had a number of failings when used in this study; firstly, the line was a fit of equation (5.9) and was achieved through optimisation of a_m and b. The former, a_m, is defined as a numerical constant that relates to the geometry of the flow channel but this is unknown for the filter arrangement used in this work and there is no definition of how this is evaluated. The second failing of this method was that it relied upon the real rejection being held constant while the change in observed rejection is measured as a function of cross flow velocity at constant flux. However flux was noted to vary by 100% over the range of cross flow rates studied. In addition, an inspection of the plot shown in Figure 5-9 indicated a bunching of the data even though cross-flow velocity values were chosen with an even spacing, this again indicated a difficulty with applying this technique to the apparatus used here. As a result of these observations

the velocity variation technique was deemed unreliable for the filtration equipment used in this study. Consequently an alternative method was sought.

Salinity induced flux decrease method

An addition of salt to a pure water stream was known to modify the osmotic pressure of the solution. In a constant pressure membrane filtration system this resulted in a decrease in flux. The basis of the Sutzkover (Sutzkover et al., 2000) method was to equate this change in flux to the mass transfer coefficient of the membrane transport system under evaluation.

Flux in pure water systems and salt water systems was defined as,

$$(J_v)_{H_2O} = L_P \cdot \Delta P \tag{5.10}$$

and,

$$(J_v)_{salt} = L_P\left[\Delta P - (\pi_m - \pi_p)\right] \tag{5.11}$$

Where L_p was the hydraulic permeability, π_m and π_p were the osmotic pressures of solution at the membrane and in the permeate respectively. Through combination of equations (5.10) and (5.11) on the basis of the membrane permeability being a constant, the trans membrane osmotic pressure differential was defined by the flux of pure solvent and solution.

$$\pi_m - \pi_p = \Delta P\left[1 - \frac{(J_v)_{salt}}{(J_v)_{H_2O}}\right] \tag{5.12}$$

With this and through consideration of equation (5.5) the mass transfer coefficient was found to be,

$$k_m = \frac{(J_v)_{salt}}{\ln\left\{\frac{\Delta P}{\pi_f - \pi_p} \cdot \left[1 - \frac{(J_v)_{salt}}{(J_v)_{H_2O}}\right]\right\}} \tag{5.13}$$

5.3.2 Method application

The Sutzkover method of mass transfer coefficient evaluation was advantageous when compared to conventional methods, as there was no requirement for additional experimental work. Since the majority of experiments completed in this investigation were carried out at one constant pressure value and pure solvent and solute fluxes were well recorded, most of the data was already available for calculation purposes with the exception of solution osmotic pressure data. Osmotic pressure is discussed and evaluated in Section 5.4.

5.3.3 Results

The purpose of evaluating the real rejection was to deduce whether the negative rejections observed for uncharged organic compounds in the presence of Phosphate were not simply a result of concentration polarisation. Although this was improbable it was important to provide practical and theoretical argument in support of this conclusion.

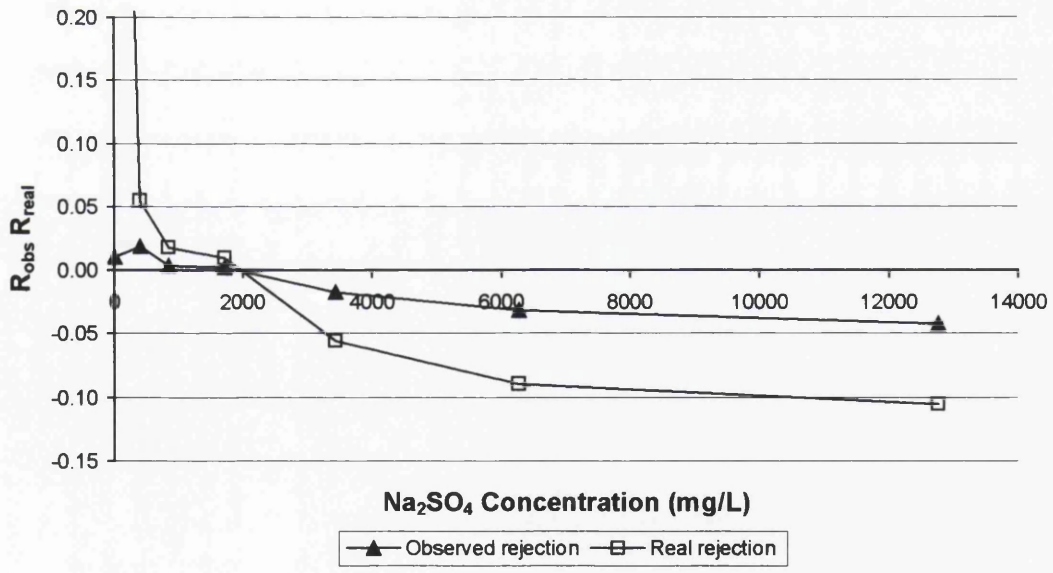

Figure 5-10 The observed rejection (triangles) and real rejection (squares) of Benzyl alcohol 0.0046M (0.5 g/L) in the presence of increasing concentrations of sodium sulphate (for clarity, some data points have been omitted in this and other plots)

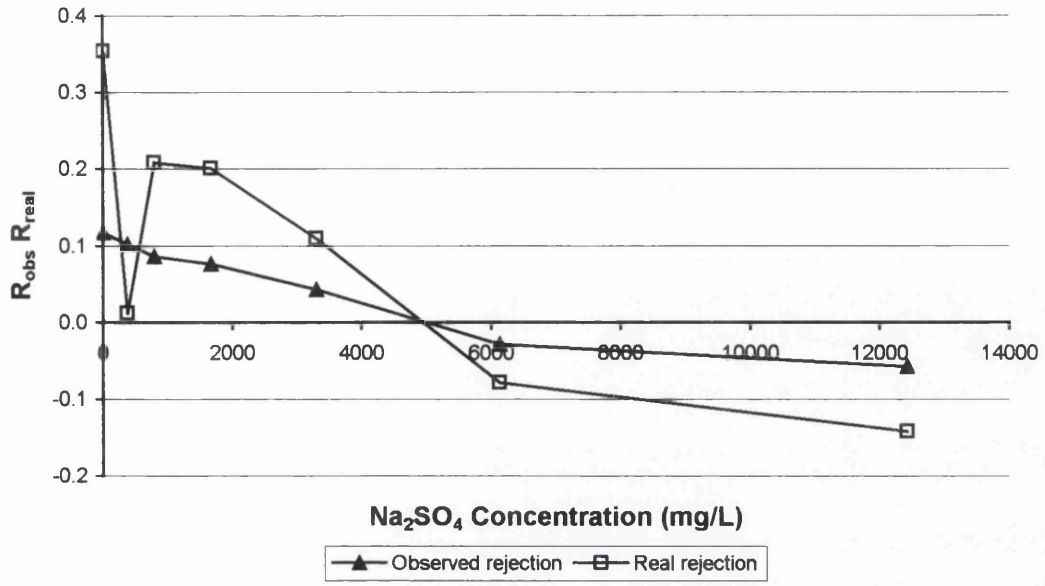

Figure 5-11 The observed rejection (triangles) and real rejection (squares) of Caffeine 0.0026M (0.5 g/L) in the presence of increasing concentrations of sodium sulphate

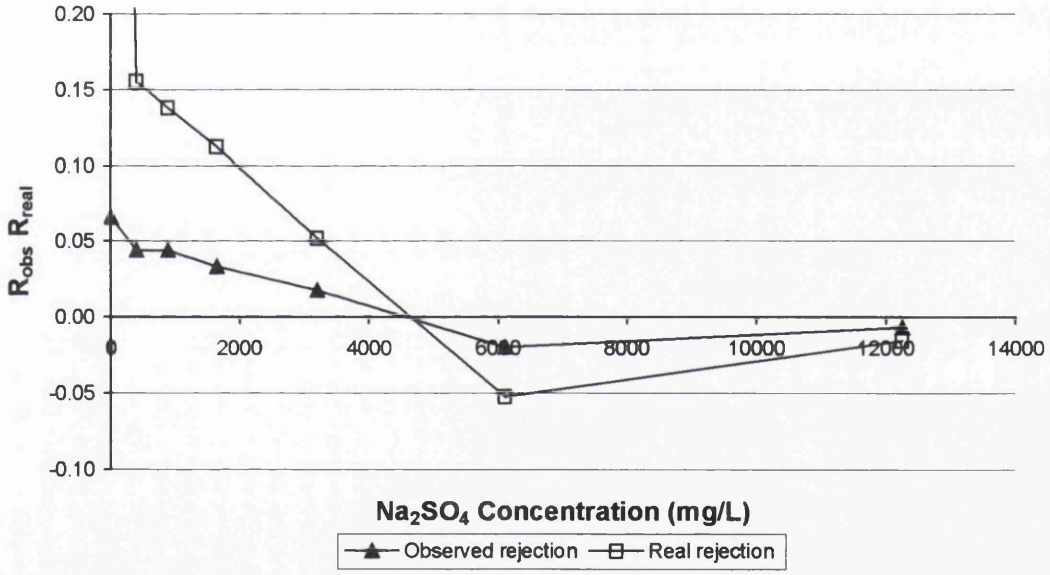

Figure 5-12 The observed rejection (triangles) and real rejection (squares) of Glycerol 0.0028M (0.5 g/L) in the presence of increasing concentrations of sodium phosphate (value for real rejection of glycerol at 0 mg/L salt concentration is 0.87)

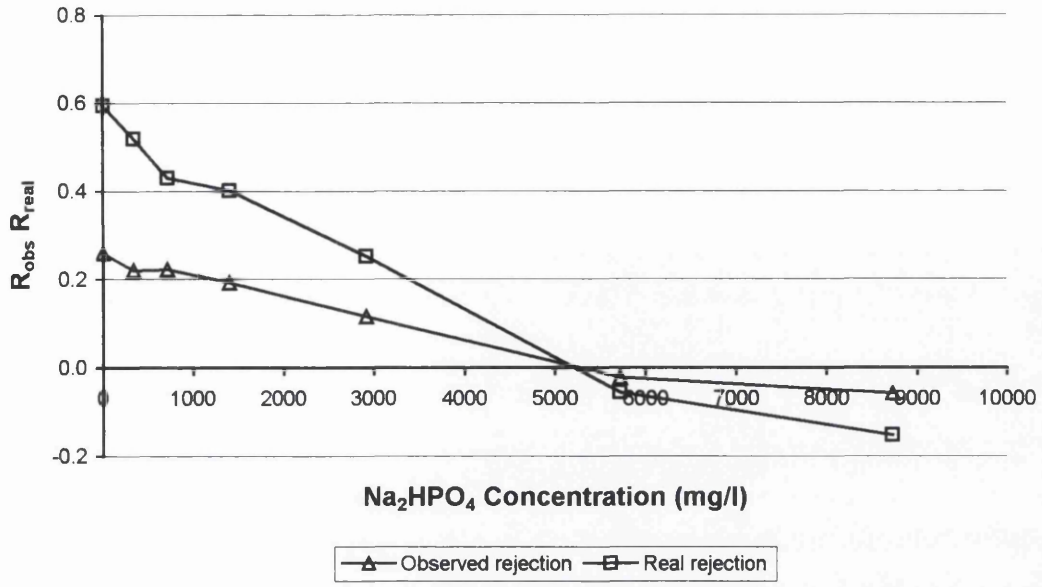

Figure 5-13 The observed rejection (triangles) and real rejection (squares) of Glucose 0.0028M (0.5 g/L) in the presence of increasing concentrations of sodium phosphate

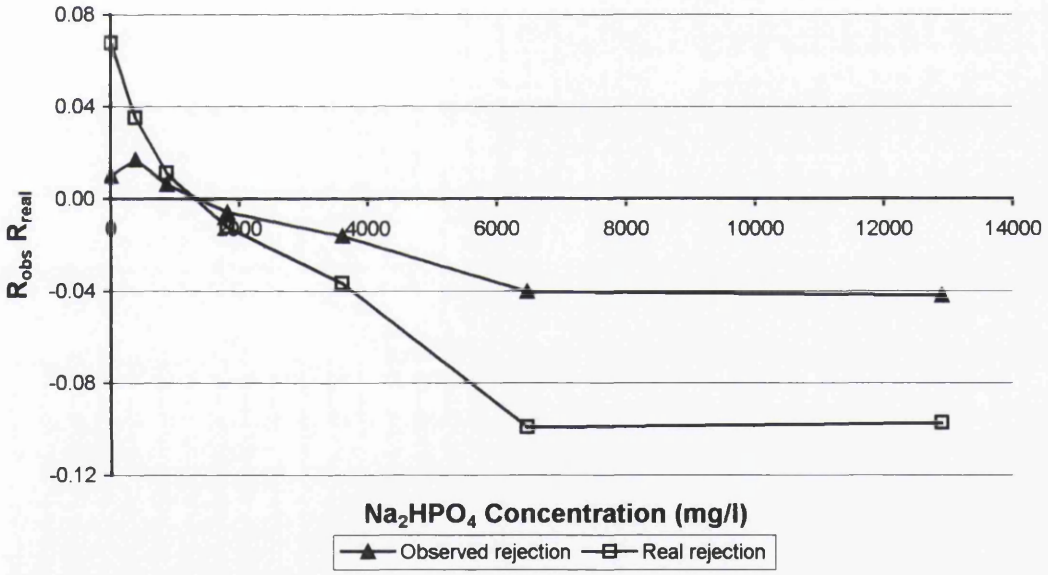

Figure 5-14 The observed rejection (triangles) and real rejection (squares) of Benzyl Alcohol 0.0046M (0.5 g/L) in the presence of increasing concentrations of sodium phosphate

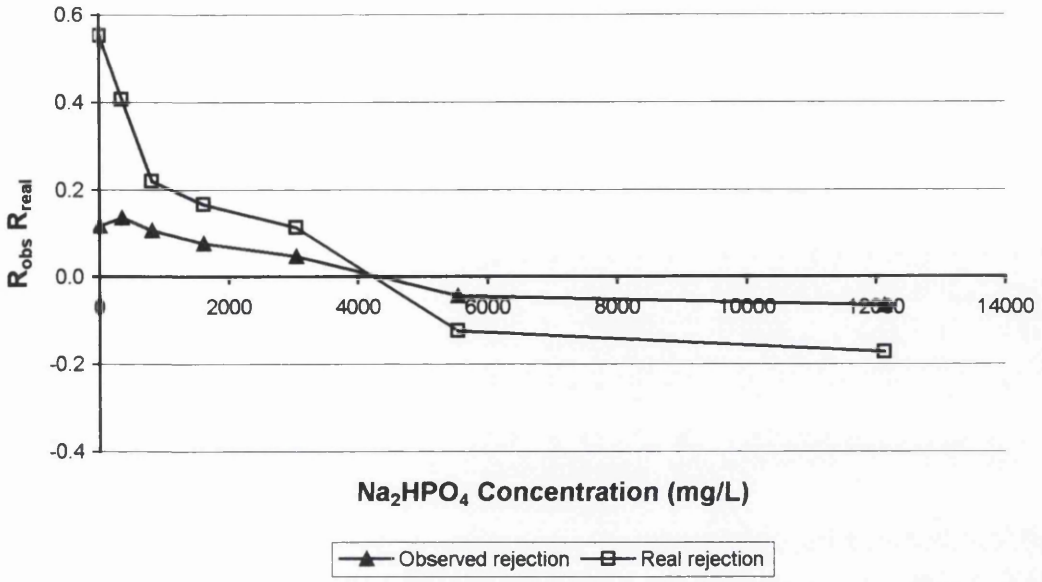

Figure 5-15 The observed rejection (triangles) and real rejection (squares) of caffeine 0.0026M (0.5 g/L) in the presence of increasing concentrations of sodium phosphate

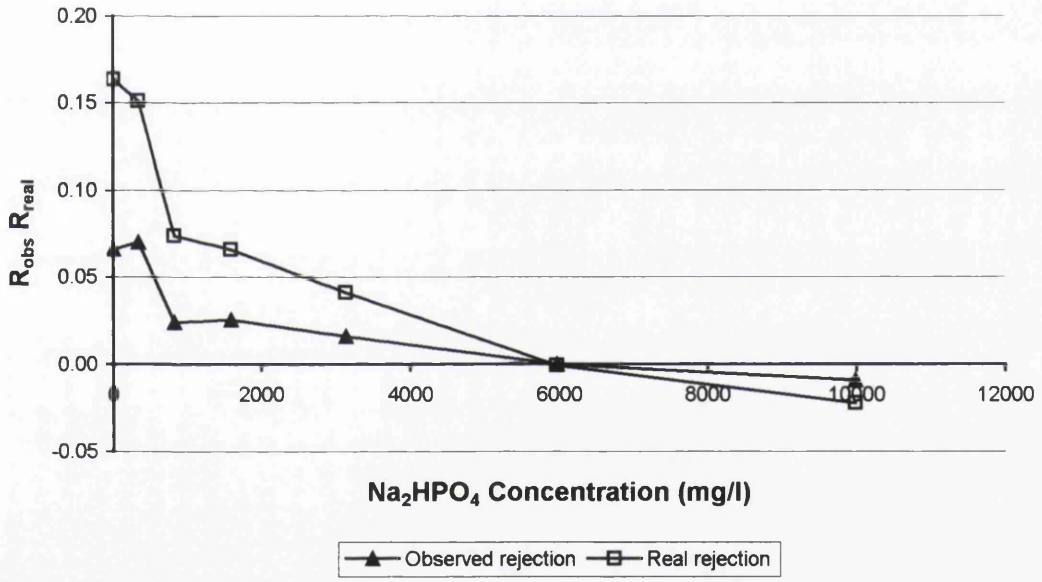

Figure 5-16 The observed rejection (triangles) and real rejection (squares) of glycerol 0.0054M (0.5 g/L) in the presence of increasing concentrations of sodium phosphate

The mass transfer coefficient approximated by equation (5.13) was a function of the operating pressure, the flux of pure solvent and solution and the osmotic pressure differential across the membrane. This dependency implied that the mass transfer coefficient differed for all solutions investigated and was not a characteristic of the membrane alone.

Figures 5-10 to 5-16 show plots of both the observed rejection data and real rejection values for glucose, benzyl alcohol, caffeine and glycerol in the presence of increasing concentrations of sodium sulphate and disodium hydrogen orthophosphate. For both positive and negative rejection the real rejection values are of a greater magnitude than the observed data. In the case of positive rejection this was normal and inspection of Figure 5-8(a) shows that this was expected as the concentration at the membrane, upon which real rejection was based, was higher than in the bulk solution, the basis of observed rejection. The results for negative rejection were also well supported by the theoretical discussion represented by Figure 5-8(c) with concentration at the membrane surface much lower than in the bulk solution hence the greater negative values for real rejection.

Both the determination of real rejection and the theoretical discussions with respect to observed rejection indicate that negative rejection was a genuine observation and thus a phenomenon that was real. Negative rejection was therefore not an artefact of some transport process that generates misleading results, but was a property of membrane filtration.

5.4 Osmotic pressure – measurement and theoretical assessment

5.4.1 The importance of osmotic pressure

Osmotic pressure is a solution property that is central to membrane filtration problems. It has been defined as the pressure differential that results when two chambers, separated by a semi permeable membrane and containing two solutions distinguished by the presence in one of a membrane impermeable substance, are allowed to equilibrate (Levine, 1988). Traditionally the apparatus used for this experiment was very simple in arrangement, with the pressure difference measured according the change of liquid level in each chamber.

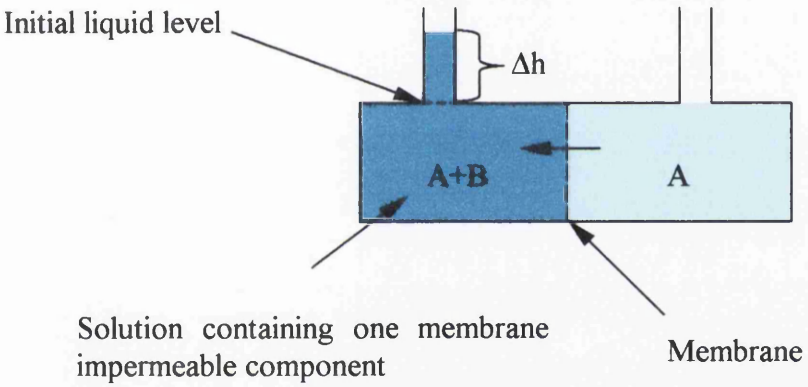

Figure 5-17 A traditional arrangement for the measurement of osmotic pressure. Arrow shows the direction of flux for the membrane permeable solute.

Figure 5-17 not only presents a practical technique for the evaluation of the osmotic pressure of a solution but is also a general illustration of the fundamentals of osmotic pressure as a phenomenon. Osmosis, a process relied upon by biological systems, was defined as the flow of a solution from a low concentration zone to one of high concentration. Driven by the concentration differential, this process endeavours to dilute the high concentration zone such that it becomes equivalent in composition to the low concentration side (Sourirajan, 1970).

Reverse osmosis represents, although not precisely, a reversal of the osmosis process. The intention of developing artificial reverse osmosis was to make use of the separating properties of the semi permeable membrane. This has been achieved by applying a positive pressure to the high concentration side of the membrane. As a result the osmotic pressure became a factor in this process as it equated to the minimum pressure needed to prevent (normal) osmosis and to achieve a flux in a direction opposing that dictated by the concentration driving force.

Osmotic pressure is very influential in membrane transport processes and as such must be included as a parameter in any related modelling. Within this study the value of the osmotic pressure exerted by a solution was required for rejection modelling and for consideration of concentration polarisation and the associated theoretical concept of real rejection. The evaluation of real rejection was, for the experimental equipment used in this study, dependent on a realistic osmotic pressure value being available for the solutions investigated. For this purpose a study was made of the methods available for determination of this value.

5.4.2 Evaluation of Osmotic Pressure

Three methods were assessed as a means of identifying the osmotic pressure. These methods comprised an experimental measurement and two computational determinations.

Experimental assessment

There are a number of different experimental techniques used in the measurement of osmotic pressure but they are all based on the same fundamental arrangement as indicated by Figure 5-17. The simplest arrangement was that illustrated, with a system that is allowed to come to steady state and the pressure differential between the system at time zero and at equilibrium (measured as a height of solution), equal to the osmotic pressure.

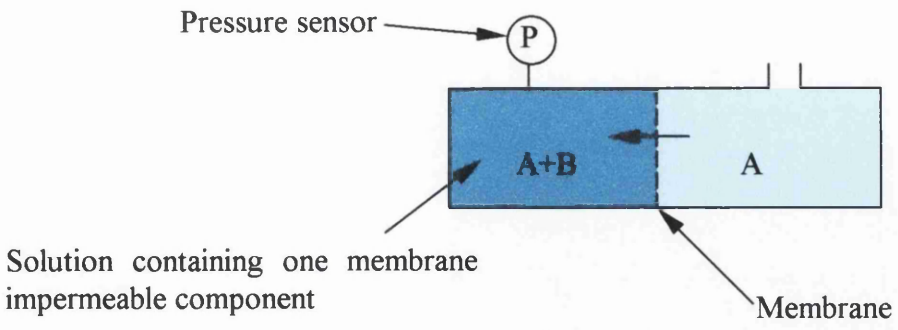

Figure 5-18 The second type of experimental osmometer with the enclosed solution chamber and pressure gauge

This basic system was limited because the lack precision attributed to the type of pressure measurement used. This precision can be improved significantly by closing the high concentration side to atmosphere and fitting an appropriate pressure gauge. It was a device of this type, shown in Figure 5-18 that was used in this work.

A third type of conventional membrane osmometer, shown in Figure 5-19, relies on a negative pressure to develop in the solvent chamber that is equal to the osmotic pressure of the solution. In this arrangement the pressure is measured in the enclosed solvent chamber and the solution is continuously replaced in order to avoid any dilution that would affect the final reading. It has been stated that this system is only suitable for weak solutions as it is dependent on the negative pressure capabilities of the gauge used which are often limited.

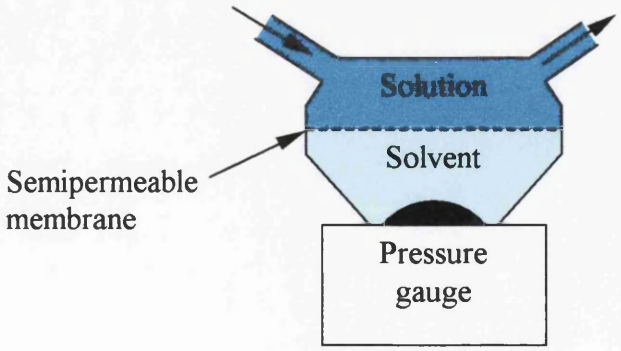

Figure 5-19 The third type of osmometer relies upon the measurement of negative pressures and continuously replenished solution.

All three of the conventional methods used for the determination of osmotic pressure are disadvantaged by the long time they require to achieve steady state. A minimum of 5 to 6 hours was required for the second osmometer illustrated. Faster results have been achieved through the use of extrapolation (Nabetani et al., 1992). The basis of this technique relies on the fact that if the permeate flux through a membrane was measured and then studied with respect to pressure, the resultant plot would provide a linear relation between both values and could be extrapolated to provide a value of (osmotic) pressure that equates to zero flux.

To exploit the extrapolation method required a different equipment arrangement to that previously discussed. The main differences were due to the need for a pressure driving force, a means of measuring flux and the facility for eliminating concentration polarisation triggered by mass flow through the membrane. An example of the type of unit required for these measurements has been developed and discussed (Nabetani et al., 1992).

Membrane osmometer

Although the basic principles of the osmometer used in this work are outlined in Figure 5-18 a more detailed diagram of the equipment used to measure osmotic pressures in this work is shown in Figure 5-20.

The body of the osmometer was constructed from two halves of machined acrylic polymer ("Perspex"), between which a pressure resistant seal was created using butyl O-rings and the compressive force provided by six bolts that held both halves of the unit together. The seal that was created between the membrane surface and the "high-pressure" O-ring was critical to the success of the device since a leak here resulted in a false reading. The membrane, located centrally in the unit, was supported by a disc of sintered stainless steel and acted as the division between the two compartments. Each side was then loaded with pure solvent or solution through the port or valve provided on top of the unit. The valve (a ball valve) enabled the corresponding cell to be sealed off to atmosphere without generating a contribution to pressure within the cell. The low-pressure side remained entirely open to atmosphere to prevent a vacuum affect hindering the diffusion of solvent into the high-pressure cell.

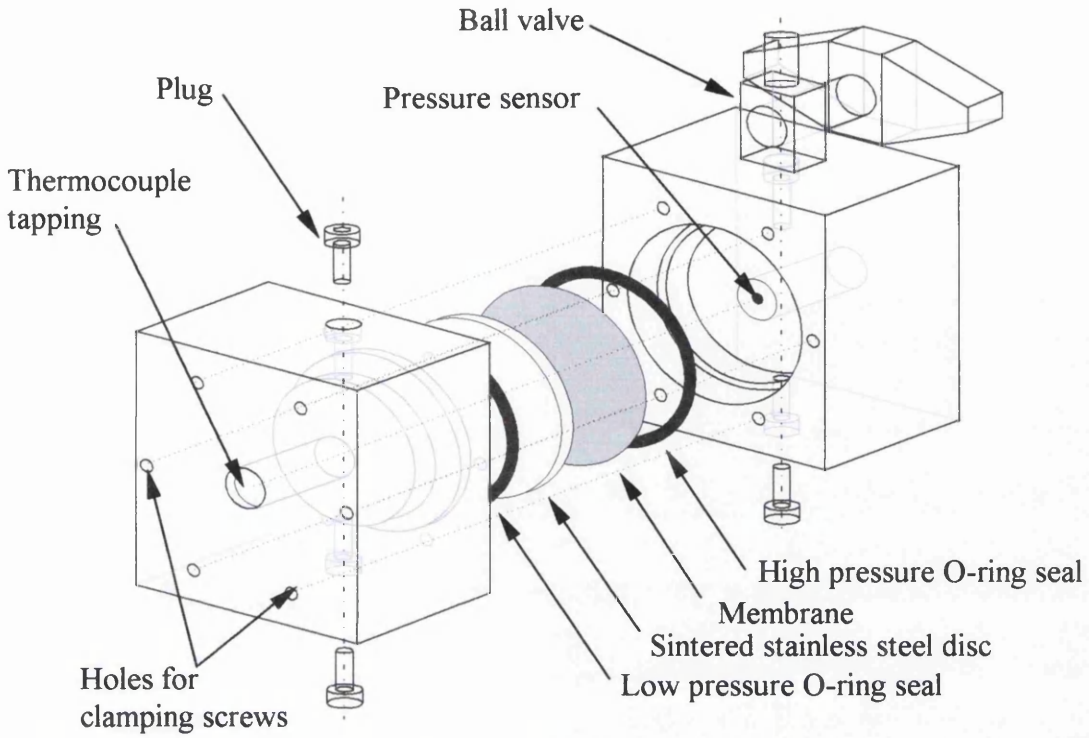

Figure 5-20 Three-dimensional partially exploded view of the osmometer used for osmotic pressure measurement.

The procedure for completing a measurement of osmotic pressure was to firstly fill the low-pressure cell (no valve) with solvent followed by the high-pressure cell with the solution. The solution was delivered using a large syringe (50 ml) and needle in order to ensure the chamber was filled rapidly and without the generation of air bubbles that would affect the final reading. The sample volume required was 12.25 cm^3 equivalent to the volume of the cell. Once the cell was full the valve could be closed and pressure monitoring commenced.

The pressure was monitored using a digital pressure gauge (Druck DPG 270) and a pressure transducer (Druck PDCR 910). The pressure gauge was capable of being interrogated by a computer using an RS-232 connection and as a result a computer program was used to read and log the pressure value every 0.5 to 2 minutes (dependent on the stage in the equilibration process).

Membrane Selection

Osmotic pressure measurement with a membrane osmometer is dependent on the existence of an ideal semi-permeable membrane. Historically, it was the paucity of such membranes that prevented this technique being widely used. More recently, membrane development has proceeded to the extent that a wide variety of membranes have become available from which to select candidates for this purpose.

One method for membrane selection was to compare an array of membranes through investigation of the maximum osmotic pressure achieved with a solution of NaCl. Salt presents a useful tool for investigating the suitability of a membrane, as it is one of the smallest solutes available in terms of its molecular/ionic dimensions. As such it should magnify the variations in maximum pressure exhibited by each membrane, where maximum pressure is the value reached in an equilibrated osmometer.

Nabetani (Nabetani et al., 1992) compared a range of membranes with respect to their maximum pressures, P_{max}, and the time taken to reach those values, t_{max}. The results of this work are shown in Table 5-2.

Membrane	Manufacturer	P_{max} (kPa)	t_{max} (h)
NTR-7199	Nitto Denko	320	50
NTR-7250	Nitto Denko	37	7
NTR-729HF	Nitto Denko	0	-
HR-99	DDS	99	4
HR-98	DDS	199	3
CA-960PP	DDS	0	-
DRS-92	Daicel	10	12
LFC-1	*Dow Filmtec*	*30.60*	*20*

Table 5-2 Maximum pressure values for 0.1 M NaCl solution achieved with a range of membranes. The final italicised entry is from this work.

Using this data, Nabetani selected a membrane (DDS HR-98) that exhibited a good combination of properties (P_{max} and T_{max}) and could be used to assess the performance of the new type of osmometer through measurement of glucose and sucrose osmotic pressures. A 0.1 M solution of NaCl at 20°C was known to have an osmotic pressure of 470 kPa (Sourirajan, 1970), but it was interesting to note that none of the membranes listed achieved this pressure with the closest only reaching 68% of this value (Nitto Denko NTR-7199). This result was surprising since all the membranes listed were classified as reverse osmosis with salt rejections typically in the region of 99%.

The final membrane listed in Table 5-2 (italicised) was obtained and characterised for this study. Again there was a considerable difference in the value obtained for osmotic pressure of salt with this membrane and that provided by the literature. However, the discrepancies apparent in all these values could be overlooked since the solutes intended for investigation were all uncharged organic compounds that would certainly be excluded by RO membranes.

Results acquired using a conventional osmometer

The osmometer used in this study was proven to reliably provide values of osmotic pressure (Cao, 1994). In that study it was used to measure the osmotic pressure of Bovine Serum Albumin suspensions, which contain particles of high molecular weights. As a result no great care was required over the selection of the membrane and an ultrafiltration membrane was found to be acceptable. By the same token a reverse osmosis membrane, as employed in this study, was assumed to be suitable for the osmotic pressure measurement of solutions of small (~ 200Da MW) organic compounds.

The process of osmosis was monitored to ensure that the equilibrium condition was reached. Figures 5-21 and 5-22 show the typical profile of the curves generated whilst monitoring the dynamic progress of an osmotic pressure measurement. The osmotic pressure of the solution was determined as the maximum value of pressure achieved. These two plots clearly display the timescale of the process with steady state only attained after a minimum of 4 hours had elapsed.

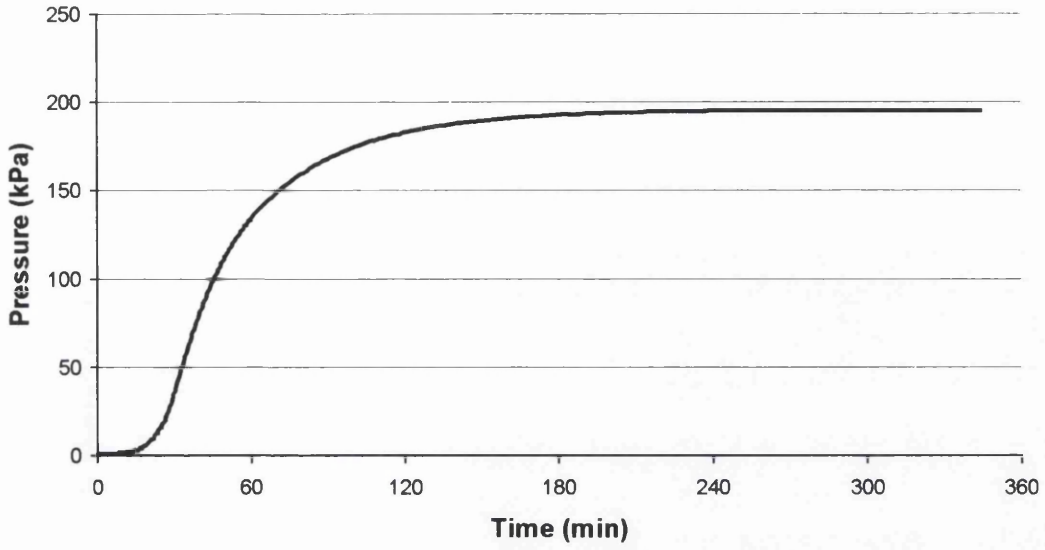

Figure 5-21 Dynamic osmotic pressure measurement curve for a 0.0026M Caffeine/0.042M Na_2HPO_4 solution (the "lag-phase", occurring within the first 20 minutes of the experiment, is most probably due to the wetting of the membrane and the consequential opening of "pores", it did not appear to influence the final result).

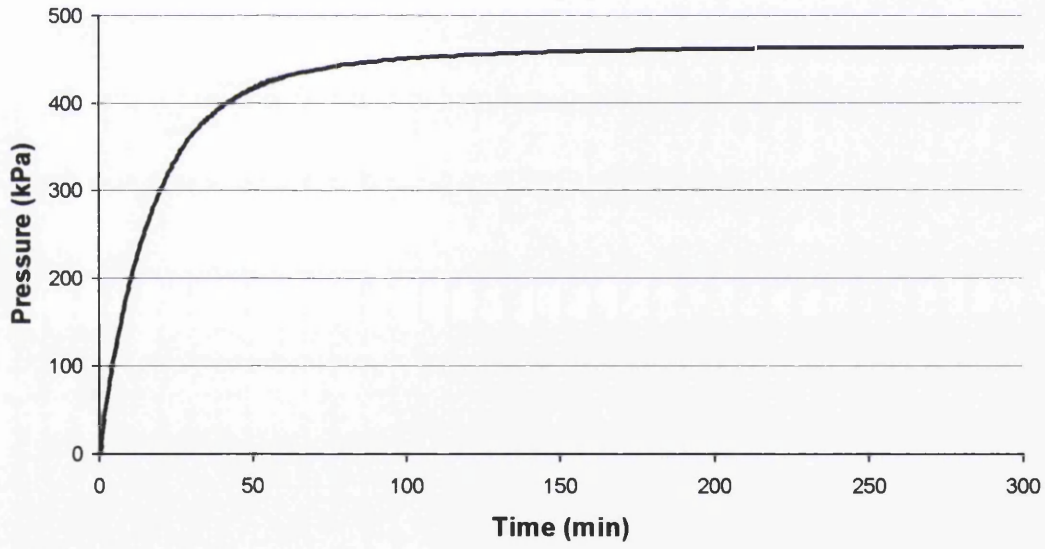

Figure 5-22 Dynamic osmotic pressure measurement curve for 0.22M glucose solution

To enable comparison with osmotic pressure correlations from other data sources (International Critical Tables, 1929), (Sourirajan, 1970), a series of osmotic pressure values were measured for several solute concentrations. The device used in this study was limited in operation due to the material of construction and the pressure transducer having a maximum range of 0 to 7 bar. As a consequence only a small part of the range, typically presented in the literature, could be measured. This meant that

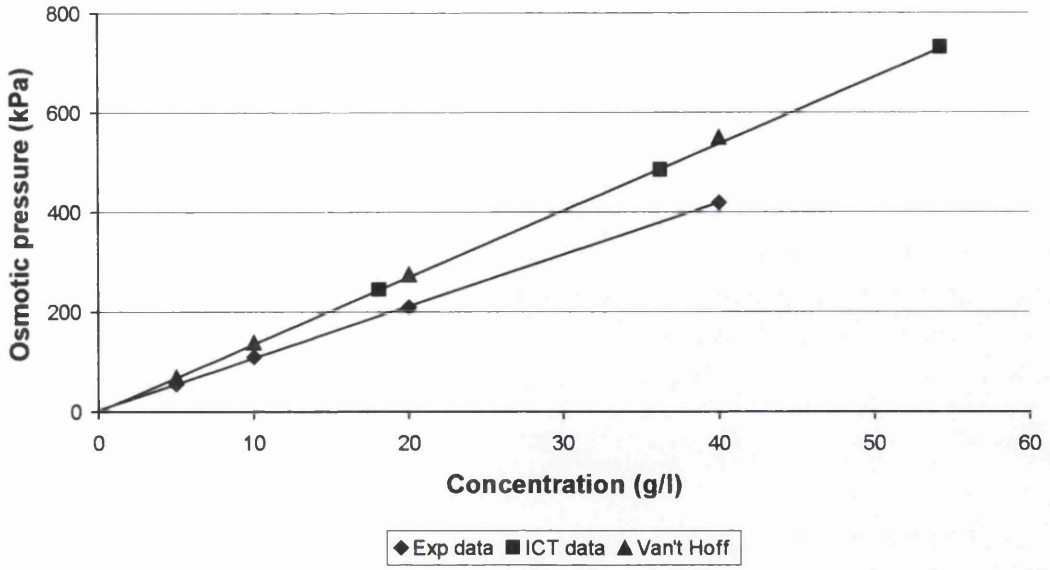

Figure 5-23 Osmotic pressure of glucose measured by experiment, determined using the Van't Hoff approximation and obtained from the International Critical Tables

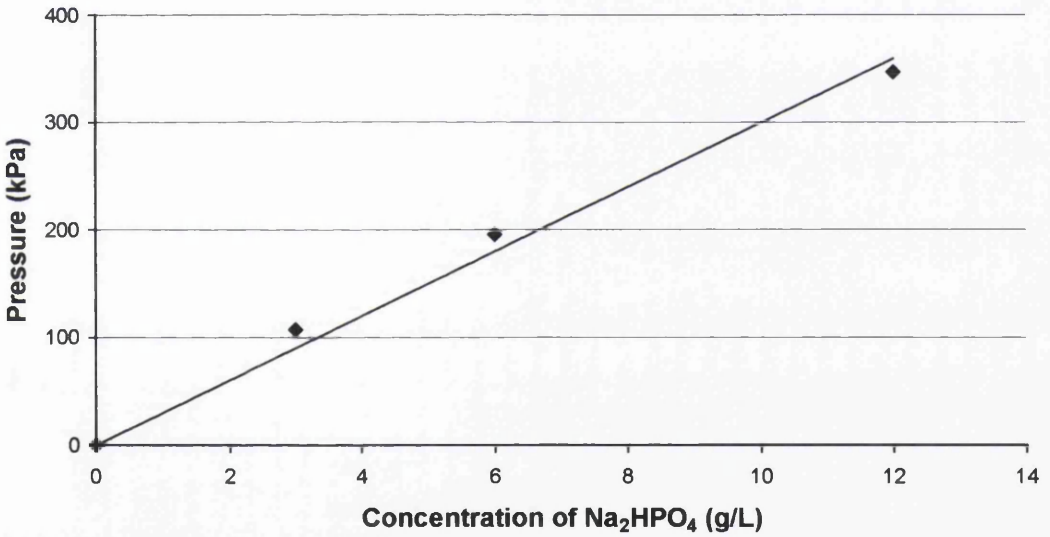

Figure 5-24 Osmotic pressure of Sodium Phosphate (in the presence of Caffeine 0.0026M) measured by experiment

some of the more distinctive features of the osmotic pressure curve were not observed. However, this was unimportant as the osmometer was still suitable for measurements in the range of relevance to the solutions concentrations used predominantly in this work. Figures 5-23 and 5-24 show the resulting correlation between concentration and osmotic pressure for Glucose and di-Sodium orthophosphate (in the presence of caffeine (0.0026M). The relationship was notably straight in this part of the concentration range.

Figure 5-23 also includes correlations obtained from the International Critical Tables and the Van't Hoff approximation. The Van't Hoff approximation provides a theoretical description of osmotic pressure and was defined as,

$$\pi = cRT \tag{5.14}$$

This simplified form was derived from the thermodynamic description of osmotic pressure (Sourirajan, 1970), which stated

$$\pi = -\frac{RT}{V_w}\ln a_s \tag{5.15}$$

Where a_s was the activity coefficient and V_w the partial molar volume of water. The values a_s and V_w were known to be very difficult to evaluate, hence the simplification presented by equation (5.14).

Equation (5.14) has also been modified for the osmotic pressure difference across a membrane (Mohammed and Takriff, 2003),

$$\Delta\pi = RT\left(\Sigma C_f - \Sigma C_p\right) \tag{5.16}$$

5.4.3 Osmotic pressure - theoretical evaluation, practical measurement or use of literature values

It has been seen that there are number of means available for ascertaining the osmotic pressure of a solution. It was therefore necessary to identify one of the three methods detailed (practical measurement, literature values or theoretical prediction) as being the most suitable for application.

The most reliable and perhaps justifiable approach to obtaining osmotic pressure was to use data from literature sources such as the International Critical Tables. However, the data available is often limited to a narrow spectrum of solutes and certainly does not consider solutions of multiple components.

With data sources inappropriate due their limitations, the most effective way of evaluating osmotic pressure, of more complex solutions, was through the use of an osmometer. An osmometer was considered more convenient as it would allow the assessment of an unlimited number of solutes. However, the results showed that at low solute concentrations the relationship between osmotic pressure and concentration was linear and the theoretical approximation propounded by Van't Hoff closely matched experimental data values and literature values (Figure 5-23 and Figure 5-24). Since the concentration values used in this work are low it was concluded that osmotic pressure values could be predicted using the Van't Hoff approximation and hence real rejection was evaluated using the Sutskover method.

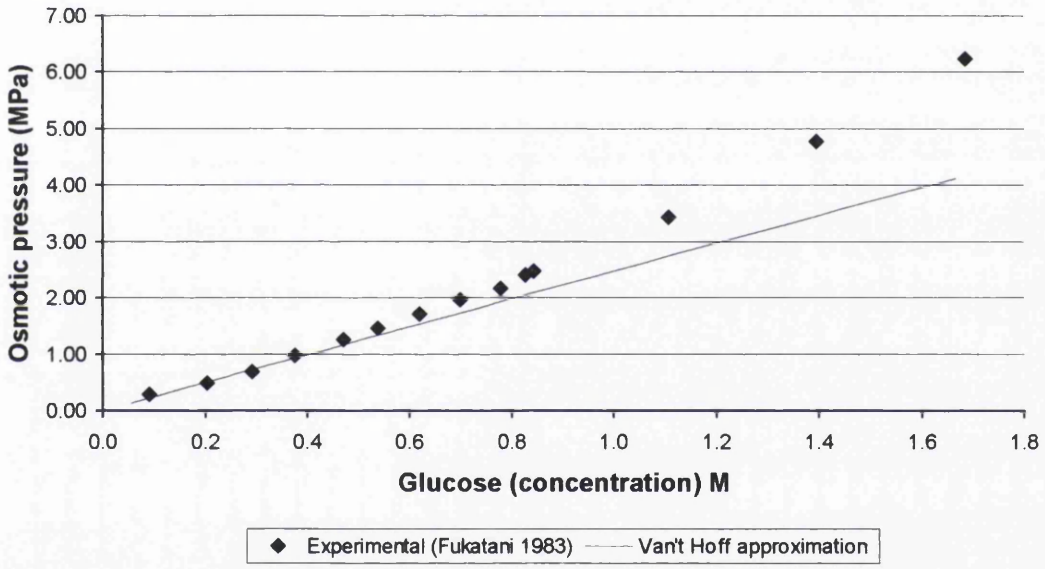

Figure 5-25 A comparison between measured and theoretically predicted osmotic pressure of glucose

5.5 Conclusion

In the first instance an effort was made to ensure that experimental error was not responsible for the observed behaviour. A discussion of the error was completed, that concluded in an evaluation of the error bars most pertinent to the raw data. Error was deduced on a cumulative basis and through consideration of the various sources of deviation in both accuracy and precision during the calculation of observed rejection. The error was also determined from a statistical assessment of the calibration data for analysis of solute concentrations. This statistical discussion provided error values that were derived from the standard deviation of the measured calibration data from a fitted curve or line of best fit. It was found that this deviation was several magnitudes greater than that predicted by cumulative error discussions, consequently the standard deviation based error was used in the work. The error was found to be insignificant for all organic component rejections, in the case of glucose a typical rejection value and associated error was found to be -10 ±0.6%

To further establish the veracity of the observed phenomenon a theoretical analysis of the situation was required that incorporated a quantitative computation of the raw rejection data. This theoretical discussion was constructed around the condition known as concentration polarisation. It was believed that this process might provide an explanation for the negative rejection behaviour observed in presence of "high" salt concentrations. However, it soon became apparent on a qualitative basis, that the rejection could not be a consequence of increased solute concentration at the membrane surface. This was confirmed through calculation of the real rejection for all situations where negative rejection was observed. It was found that the magnitude of the real rejection was always greater than the observed value. This was true for both positive and negative values.

As part of the analysis of concentration polarisation, a value was required for the osmotic pressures of all the solution systems discussed. A consideration of several osmotic pressure evaluation techniques ensued with both physical and theoretical methods assessed. In conclusion it was decided that the optimal approach was to use the theoretical approximation of Van't Hoff. This was found to provide a reliable

prediction of the osmotic pressure as it compared well with data from the literature, but only for low concentration systems similar to those presented in this study.

6 Negative rejection theory

6.1 Introduction

The manner in which contemporary modelling theories provide support or otherwise for the phenomena of negative rejection is important to this discussion. In the first instance it is necessary to consider the models that most closely represent this behaviour, and discuss how relevant each model is in terms of its component parameters.

The connection between the rejections of the salt and the neutral solute is central to the behaviour observed in this study. It is the presence of the salt that brings about the negative rejection and as such there must be some type of interaction occurring between the two compounds present. To facilitate the deduction of what this interaction is, a discussion of the behaviour of the solutes, in relation to one another, is provided.

Ultimately, where mathematical theories successfully and correctly represent physical processes, it is possible to use models to synthesise and predict the behaviour of hypothetical systems. However, when deriving models for any physical process a number of approximations may be arrived at, as in the case of membrane transport, none of which may be entirely correct. Although this may be the case, these models are still valuable as they can provide a greater understanding of a system and its governing processes. On this basis a model has been selected and "modified" accordingly. The modification and the quality of the fit to experimental data are given in this chapter. In addition there is discussion of the assumptions that had to be made and whether they were reasonable.

In this chapter there is a consideration of how well the model behaves when used to predict the outcome of a known solvent-solute system. In this case the model parameters are drawn from previous fitting exercises and applied as is appropriate. The value of this work is that it provides an assessment of the worth of the parameters already deduced.

6.2 Negative rejection models

Models based on irreversible thermodynamics that account for the negative rejection of ions are few and those that cover negative rejection of uncharged solutes do not exist. Presented here are the three models that account for negative rejection in ionic systems. Three theoretical discussions are presented as proposed by Perry and Linder (Perry and Linder, 1989), Dey and co-workers (Dey et al., 2000) and Schirg and Widmer (Schirg and Widmer, 1992).

6.2.1 Perry and Linder

Perry and Linder considered the situation where large charged organic compounds are concentrated in the presence of salts. In this scenario high negative rejection values of one of the ionic species present are often observed. The theoretical work outlined here follows that of Spiegler and Kedem, negative salt rejection is analysed in terms of reflection coefficient, solute and hydraulic permeabilties and the valence and concentration of the retained organic ion (Spiegler and Kedem, 1966).

Rejection of a single electrolyte

In a single salt situation the salt can be treated as an electroneutral species. Spiegler and Kedem defined the solute and total volume flux as follows

$$J_s = -\bar{P}\frac{dc_s}{dx} + (1-\sigma)c_s J_v \tag{6.1}$$

$$J_v = -\mathscr{P}_1\left(\frac{dp}{dx} - \sigma\frac{d\pi}{dx}\right) \tag{6.2}$$

Where $\bar{P}$ was the local solute permeability, c_s the solute concentration, x the distance perpendicular to the surface of the membrane and σ the reflection coefficient. The total flux was given as a function of the specific hydraulic permeability, $\mathscr{P}_1$, the applied pressure and the osmotic pressure. The rejection was defined as,

$$R = \frac{(1-F)\sigma}{1-\sigma F} \tag{6.3}$$

where,

$$F = \exp\left(-J_v \frac{1-\sigma}{P_s}\right) \tag{6.4}$$

Where P_s was overall salt permeability.

In the absence of a Donnan contribution to salt passage, the limit of the rejection, R, is the reflection coefficient, σ. However in a mixture of electrolytes, due to the variation in ion permeabilties and the generation of an electric field, the behaviour becomes more complex.

3-ion systems containing a large impermeable organic ion

In a system where two anions share a common cation (Na^+) and one of the anions is an impermeable organic ion (Figure 6-1) three flows were considered J_1, J_2 and J_w along with three conjugated electrochemical potential driving forces $\Delta\bar{\mu}_1$, $\Delta\bar{\mu}_2$ and $\Delta\mu_w$.

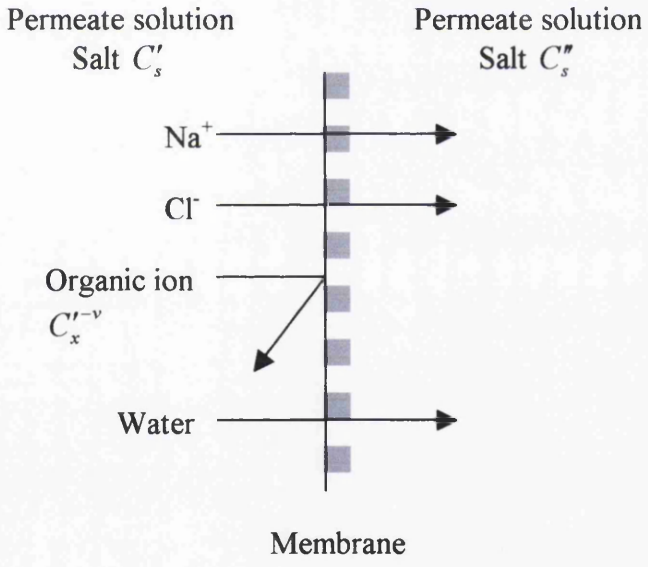

Figure 6-1 Solute distribution across the membrane (Perry and Linder, 1989)

The electrochemical potential of the mono-monovalent salt in each aqueous solution can be described in terms of electrochemical potentials of the permeable ions Na^+ and Cl^-.

$$\bar{\mu}_1' = \mu_1^{0'} + RT\ln a_1' + zF\Psi'$$
$$\bar{\mu}_2' = \mu_2^{0'} + RT\ln a_2' + zF\Psi' \quad (6.5)$$
$$\mu_s' = \bar{\mu}_1' + \bar{\mu}_2' = \mu_s^{0'} + RT\ln a_1' a_2'$$
$$\mu_s'' = \bar{\mu}_1'' + \bar{\mu}_2'' = \mu_s^{0''} + RT\ln a_1'' a_2'' \quad (6.6)$$

Where (′) indicates the feed side of the membrane and (″) the permeate side. Equations (6.5) and (6.6) describe the electrochemical potentials of the permeable ions in the feed and the permeate. The electrochemical potentials ($\bar{\mu}$) of ions 1 and 2 (Na^+ and Cl^-) are given as the sum of their respective standard chemical potentials (μ^0), their ion activities (a) and their electrical potential (Ψ). The electrochemical potential of the salt is therefore the sum of that of the two ions hence the third equation (6.5) and the corresponding equation (6.6)

The driving force for salt across the membrane is therefore given by the potential difference:

$$\Delta\mu_s = RT\ln\left(\frac{a_1' a_2'}{a_1'' a_2''}\right) \quad (6.7)$$

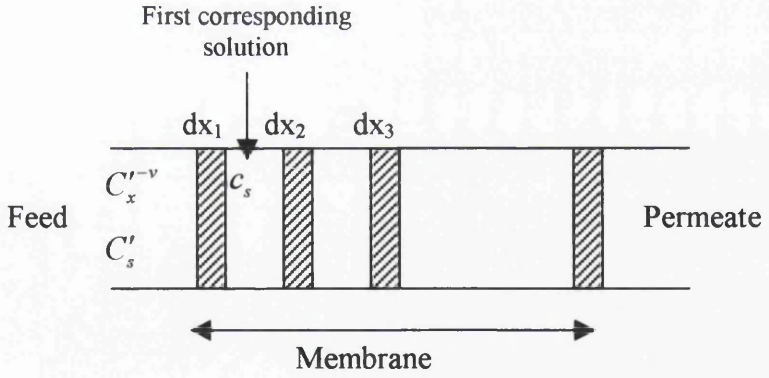

Figure 6-2 Theoretical interpretation of the membrane transport system (Perry and Linder, 1989)

If the membrane is considered to be composed of thin differential elements (dx_n) separated by aqueous layers that are in equilibrium with the adjacent membrane slices (Figure 6-2) then the concentrations of the salt at the membrane feed interface can be calculated from equation (6.8) where $\bar{a}_1$ and $\bar{a}_2$ are the activities of the two ions in the first corresponding solution (Figure 6-2).

$$a_1' a_2' = \bar{a}_1 \bar{a}_2 \tag{6.8}$$

Figure 6-2 illustrates the elemental interpretation of the active membrane layer. This analysis creates a theoretical "new" feed side designated as the *first corresponding solution*; c_s denotes the concentration of salt just inside the membrane surface. It is here that the concentration of the non-permeable solute (C_x) is zero. v in the superscript for the non-permeable solute concentration designates the number of charged groups on the impermeable organic ion.

The activity coefficients were equated to concentrations and the concentration of the various ions in the feed and within the membrane were described as follows,

$$\left[\mathrm{Cl}^-\right]' = C_s'$$
$$\left[\mathrm{X}^-\right]' = C_x' \tag{6.9}$$
$$\left[\mathrm{Na}^+\right]' = C_s' + vC_x'$$

$$\left[\overline{\mathrm{Cl}^-}\right] = \left[\overline{\mathrm{Na}^+}\right] = c_s \tag{6.10}$$

where X^- was the large, impermeable, organic ion. Through substitution into equation (6.8) the following expression iwas reached

$$c_s = C_s'\left(1 + \frac{vC_x'}{C_s'}\right)^{0.5} \tag{6.11}$$

Spiegler and Kedem integrated equation (6.2) over x with the following condition

$$C_s'' = \frac{j_s}{J_v} \tag{6.12}$$

and thus derived,

$$\frac{J_v(1-\sigma)\Delta x}{\bar{P}} = \ln\frac{C_s''\sigma}{C_s'' - C_s''(1-\sigma)} \tag{6.13}$$

(Spiegler and Kedem, 1966).

The boundary condition expressed by equation (6.11) was observed in the derivation of equation (6.13), so

$$\frac{J_v(1-\sigma)\Delta x}{\bar{P}} = \ln\frac{C_s''\sigma}{C_s''-c_s(1-\sigma)} \tag{6.14}$$

and using the definitions of $\boldsymbol{F}$ and P of equation (6.4), the following was obtained

$$F = \frac{C_s - c_s(1-\sigma)}{C_s''\sigma} \tag{6.15}$$

Dividing this through by C_s' and observing that $\frac{C_s''}{C_s'} = 1-R_s$, the salt rejection in the presence of a large impermeable organic ion was thus defined by the following expression

$$R_s = \frac{(1-\sigma\boldsymbol{F}) - (1-\sigma)\left(1+\frac{\nu C_x'}{C_s'}\right)^{0.5}}{1-\sigma\boldsymbol{F}} \tag{6.16}$$

Equation (6.16) was simplified by defining

$$\left(1+\frac{\nu C_x'}{C_s'}\right)^{0.5} = B \tag{6.17}$$

thus

$$R_s = 1-\frac{(1-\sigma)B}{1-\sigma\boldsymbol{F}} \tag{6.18}$$

In the situation where only salt is present, i.e. $C_x' = 0$, then $B = 1$ and equation (6.18) becomes identical to equation (6.3).

Overview of Perry and Linder modification

Perry and Linder considered the scenario where two anions share a common cation and one of the anions was wholly retained by the membrane (Perry and Linder, 1989). This retention provides a Donnan contribution to the passage of the salt and it was this that was accommodated by their modification of the Spiegler and Kedem model. Perry and Linder treated the membrane as a body comprising a series of differential elements with each element divided by a thin slice of solution. They considered the

first element and corresponding solution to be representative of the conditions found just within the membrane surface, where none of the impermeable ion is present. On the basis of these theoretical considerations, the authors derived an expression for salt rejection that was obviously related to that derived by Spiegler and Kedem, but now accommodated the presence of an impermeable ion.

This theory was considered appropriate for application to the data obtained in this study. Similarities were found to exist between the two circumstances. The first being the presence of an "impermeable ion". In the case of Perry and Linder this was a large organic anion, in this work the impermeable component was the larger of the two ions that constituted the salt; the ion retained by the membrane was the sulphate group in sodium sulphate or the phosphate ion in sodium dihydogen orthophosphate. The second similarity was the presence of a component that was influenced by a Donnan effect. In the theory described above, this was the chloride ion, when the model was applied to the solutions used in this work, the chloride ion was replaced by the uncharged organic compounds that exhibited negative rejection in Chapter 4. The final similarity was that both scenarios share the same permeable cation of sodium.

6.2.2 Dey, Ramachandhran and Misra

Dey and co-workers arrived at the same conclusion as Perry and Linder through consideration of a binary system comprised of NaCl and Na_2SO_4 (Dey et al., 2000). However, rather than considering the membrane as a series of thin elements, the model was developed according to Donnan equilibrium theory and the requirement of charge neutrality in both feed and permeate solutions. Hence, assuming the sulphate ion was completely retained by the membrane

$$C'_{Na^+} = C'_{Cl^-} + 2C'_{SO_4^{2-}} \tag{6.19}$$

and

$$C''_{Na^+} = C''_{Cl^-} \tag{6.20}$$

The mean thermodynamic activity of the membrane permeable salt can be given by

$$a_{NaCl} = \sqrt{\left(a_{Na^+}\right)\left(a_{Cl^-}\right)} \tag{6.21}$$

Assuming activities are approximated by concentration then

$$C'_{Cl^-} = \sqrt{\left(C'_{Na^+} C'_{Cl^-}\right)} = \sqrt{\left(C'_{Cl^-} + 2C'_{SO_4^{2-}}\right) C'_{Cl^-}} \tag{6.22}$$

and for the permeate solution

$$C''_{Cl^-} = \sqrt{\left(C''_{Na^+} C''_{Cl^-}\right)} \tag{6.23}$$

Taking into account these considerations the following expression for rejection was arrived at

$$R_{Cl^-} = 1 - \frac{\frac{2\omega'}{J_v}\sqrt{\left(1 + 2C'_{SO_4^{2-}}/C'_{Cl^-}\right)} + (1-\sigma)}{\frac{2\omega'}{J_v} + (1+\sigma)} \tag{6.24}$$

where,

$$\omega' = \omega i R T \tag{6.25}$$

ω and ω' were the solute permeability and solute permeability coefficient respectively. Since equation (6.24) equates to (6.16), then the work of Dey and co-workers does not provide a significantly useful development for it to be considered further. However, that work does provide another demonstration of the applicability of this modelling approach to a number of negative rejection systems.

The modification of the Spiegler and Kedem model as proposed by Perry and Linder, was the more accessible of the two derivations shown above, as it incorporated a term for the valence of the retained ion. As such this model was selected for application to the data produced here.

6.2.3 Schirg and Widmer

Schirg and Widmer considered the situation where a salt is separated from a dye (Schirg and Widmer, 1992). The dye molecule, presented as R-salt, was large and thus had a very high retention (>99%). R-salt represented a "large" organic ion (302 Da),

with two associated sodium ions. Due to its size and charged nature the organic ion was highly rejected by the membrane creating a Donnan contribution to the passage of salt as discussed by Dey and co-authors. The Donnan effect was advantageous in this case as it enhanced the separation of salt and dye, and improved recovery of the dye.

For the concentration dependence of single salt solution rejections the authors introduced an exponential function defining the salt permeability, P, used in equation (6.4) as

$$P_s = \alpha c_m^{\beta} \tag{6.26}$$

Where c_m was the concentration of salt at the membrane surface. Thus salt permeability, P, is a function of concentration and is not simply a constant as has been previously assumed. Thus the Spiegler and Kedem rejection model becomes

$$R = 1 - \frac{1-\sigma}{1-\sigma \exp\left(\frac{(\sigma-1)J_v}{\alpha c_m^{\beta}}\right)} \tag{6.27}$$

for single salt solutions. To predict the rejection of mixed salt solutions the Donnan effect has to be accounted for hence Schirg and Widmer used the model proposed by Perry and Linder (6.16) combined with (6.26) and arrived at

$$R_{\mathrm{NaCl}} = 1 - \frac{(1-\sigma_{\mathrm{NaCl}})\left(1+\frac{\nu^{-} M_{W\,\mathrm{NaCl}} c_{m\text{R-salt}}}{M_{W\,\text{R-salt}} c_{m\mathrm{NaCl}}}\right)^{0.5}}{1-\sigma_{\mathrm{NaCl}} \exp\left(\frac{(\sigma_{\mathrm{NaCl}}-1)J_v}{\alpha_{\mathrm{NaCl}} c_{m\mathrm{NaCl}}^{\beta_{\mathrm{NaCl}}}}\right)} \tag{6.28}$$

Where α and β were coefficients for salt permeability and the concentration dependence of salt permeability respectively, ν^{-} the number of free negative charge groups and M_w was the molecular weight of the respective salt. Schirg and Widmer also observed that there is an opposite Donnan effect with a large concentration of NaCl being capable of driving a small quantity of the R-salt through the membrane. Thus an equation analogous to equation (6.28) can be assumed:

$$R_{\text{R-salt}} = 1 - \frac{(1-\sigma_{\text{R-salt}})\left(1+\dfrac{M_{W\,\text{R-salt}}c_{m\text{NaCl}}}{\nu^{-}M_{W\,\text{NaCl}}c_{m\text{R-salt}}}\right)^{0.5}}{1-\sigma_{\text{R-salt}}\exp\left(\dfrac{(\sigma_{\text{R-salt}}-1)J_v}{\alpha_{\text{R-salt}}c_{m\text{R-salt}}^{\beta_{\text{R-salt}}}}\right)} \tag{6.29}$$

6.2.4 Extended Nernst Planck models

An assessment of models suitable for describing negative rejection systems, would not be complete without discussion of those theoretical approximations based on the extended Nernst-Planck equation. The most recent derivation was termed the Donnan-Steric Partitioning Model (DSPM) and was proposed by Bowen and co-workers (Bowen et al., 1997). This model assumed a porous membrane structure and that ion transport was described by the extended Nernst-Planck equation modified to include hindered transport:

$$j_i = -D_{i,p}\frac{dc_i}{dx} - \frac{z_i c_i D_{i,p}}{RT}F\frac{d\psi}{dx} + K_{i,c}c_i V \tag{6.30}$$

Where $D_{i,p}$ was the hindered diffusion coefficient of ion i in the pore, z_i and c_i the valance and concentration respectively of the ion, ψ the electric potential and $K_{i,c}$ and V were the hindrance factor for convection and the solute velocity. The equilibrium partitioning of ions at the pore inlet and outlet was assumed to be due to a combination of electrical (Donnan) and sieving (steric) mechanisms, giving

$$\frac{c_i}{C_i} = \Phi_i \exp\left(-\frac{z_i F}{RT}\Delta\psi_D\right) \tag{6.31}$$

Where the steric partitioning coefficient, was defined by Deen as

$$\Phi = (1-\lambda)^2 \tag{6.32}$$

and λ was the relative size of solute to pore radius (r_s/r_o) (Deen, 1987).

Manipulation of equation (6.30) together with consideration of pore electroneutrality gave the following expressions for pore potential and concentration gradient for a system of n ions,

$$\frac{d\psi}{dx} = \frac{\sum_{i=1}^{n} \frac{z_i V}{D_{i,p}} \left(K_{i,c} c_i - C_{i,p} \right)}{\frac{F}{RT} \sum_{i=1}^{n} \left(z_i^2 c_i \right)} \tag{6.33}$$

$$\frac{dc_i}{dx} = \frac{V}{D_{i,p}} \left(K_{i,c} c_i - C_{i,p} \right) - \frac{z_i c_i}{RT} F \frac{d\psi}{dx} \tag{6.34}$$

Equations (6.33) and (6.34) are solved using the following boundary conditions

$$x = 0,\ C_i = C_{i,f} \text{ and } x = \Delta x,\ C_i = C_{i,p} \tag{6.35}$$

where $C_{i,f}$ and $C_{i,p}$ were the concentrations of the ion i at the feed side of the membrane and permeate side of the membrane, respectively. The real rejection of the ion was given by R = 1- $C_{i,p}$/ $C_{i,f}$ and the equations were solved numerically using the Runge-Kutta-Gill method.

The proposed DSPM can be used for membrane characterisation. This was achieved by fitting the model to data for rejection as a function of flux. A fit of the model was achieved by adjustment of three parameters that represent physical properties of the membrane. These parameters were the pore radius, r_p, the ratio of membrane thickness to porosity $\Delta x/A_k$, and the membrane charge density, X_d. Once these parameters were obtained it was then possible to use the model for predictive purposes.

The performance of this model when applied to systems of multivalent cations, was deemed to be poor relative to the quality of agreement seen for simple systems of single organic solutes or univalent salts (Schaep et al., 2001). The deficiency of the DSPM was due to the fact that the three model parameters (r_p, $\Delta x/A_k$, and X_d) are in many ways fitting parameters and only have limited correspondence to the structural and electrical properties of the membrane.

Due to the shortcomings of the 3-parameter model outlined above, Welfoot derived a new version of the model, incorporating a term that accounted for electrochemical potential (Welfoot, 2001). The result was shown by the following two equations

$$\frac{dc_i}{dx} = \frac{V}{D_{i,p}}\left[\left\{K_{i,c} - Y_i\right\}c_i - C_{i,p}\right] - \frac{z_i c_i}{RT} F \frac{d\psi}{dx} \tag{6.36}$$

and

$$\frac{d\psi}{dx} = \frac{\sum_{i=1}^{n} \frac{z_i V}{D_{i,p}}\left[\left\{K_{i,c} - Y_i\right\}c_i - C_{i,p}\right]}{\frac{F}{RT}\sum_{i=1}^{n}\left(z_i^2 c_i\right)} \tag{6.37}$$

Where,

$$Y = \frac{D_p}{RT} V_s \frac{8\eta}{r_p^2} \tag{6.38}$$

and,

$$\frac{c_i}{C_i} = \Phi_i \exp\left(-\frac{z_i F}{RT}\Delta\psi_D\right)\exp\left(-\frac{\Delta W_i}{kT}\right) \tag{6.39}$$

Equation (6.39) accounts for the relation between bulk solution concentrations, C_i, and the pore concentration, c_i, which is governed by the steric and Donnan (electrostatic) partitioning effect and the solvation energy barrier (ΔW_i).

This system of transport equations was again solved using a fourth order Runge-Kutta numerical method.

With this two-parameter model and the models based upon irreversible thermodynamics, there were essentially two theories in existence that provide a means of describing negative rejection systems. The next step was to decide on how these mathematical descriptions relate to and can be adapted for the system under scrutiny here.

6.3 Patterns of salt rejection

As was observed in Section 4.4.5 and is re-plotted in Figures 6.3 and 6.4, salt rejection for both Na_2SO_4 and Na_2HPO_4 conformed to a distinct pattern that repeated independently of the secondary (organic) solute that was present. This was expected, as the secondary compound was non-dissociated and was considered to have zero concentration in a model describing salt rejection.

At this stage in the work there remained two issues that required resolution. The first was the identification of the factors that influence the behaviour of salt transport and the second was to consider how this then relates to a change in the rejection of uncharged organic compounds and most significantly their negative rejection. To achieve this the first step was to see whether the models outlined above would fit the rejection curves obtained for the two salts (Figures 6-3 and 6-4). For comparison the rejection pattern with concentration shown on Figure 6-5 was observed for Na_2SO_4 rejection over a PES5 membrane (Hoescht Separation Products, Germany), (Bowen and Mukhtar, 1996).

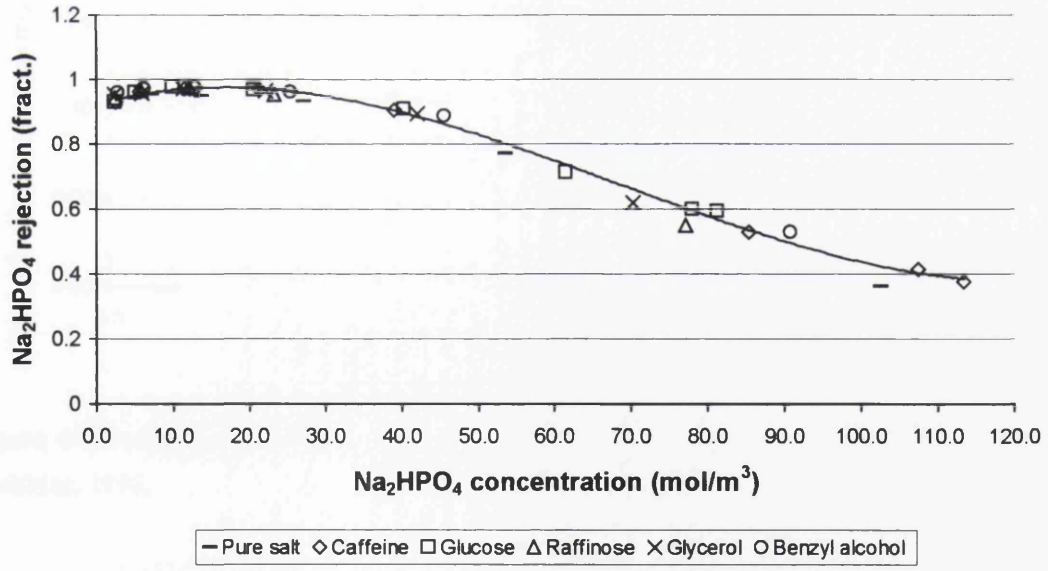

Figure 6-3 Rejection of Na_2HPO_4 with respect to secondary solute type (the curve is provided by a third order polynomial)

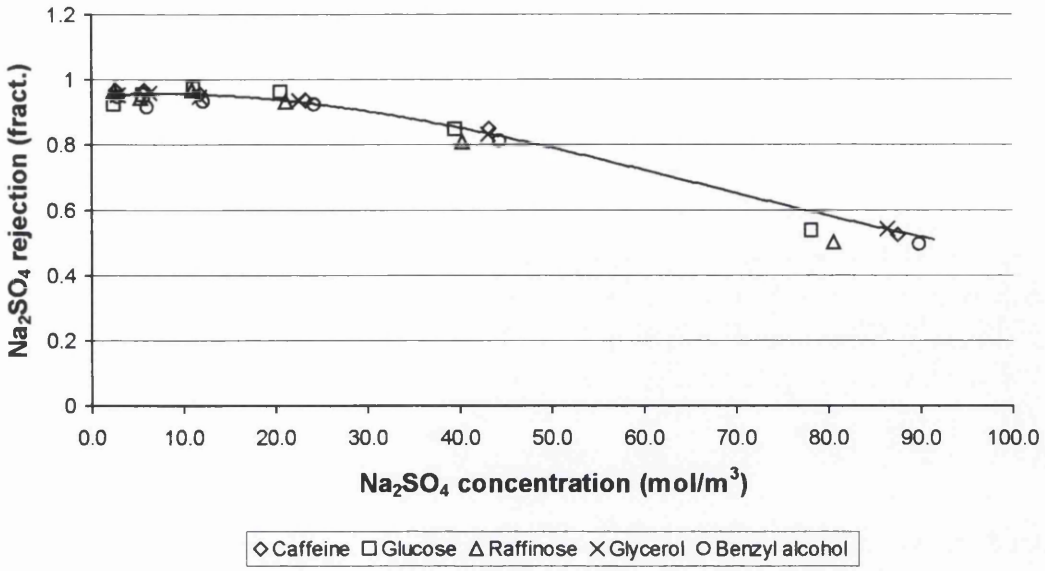

Figure 6-4 Rejection of sodium sulphate with respect to secondary solute type (the curve is provided by a third order polynomial)

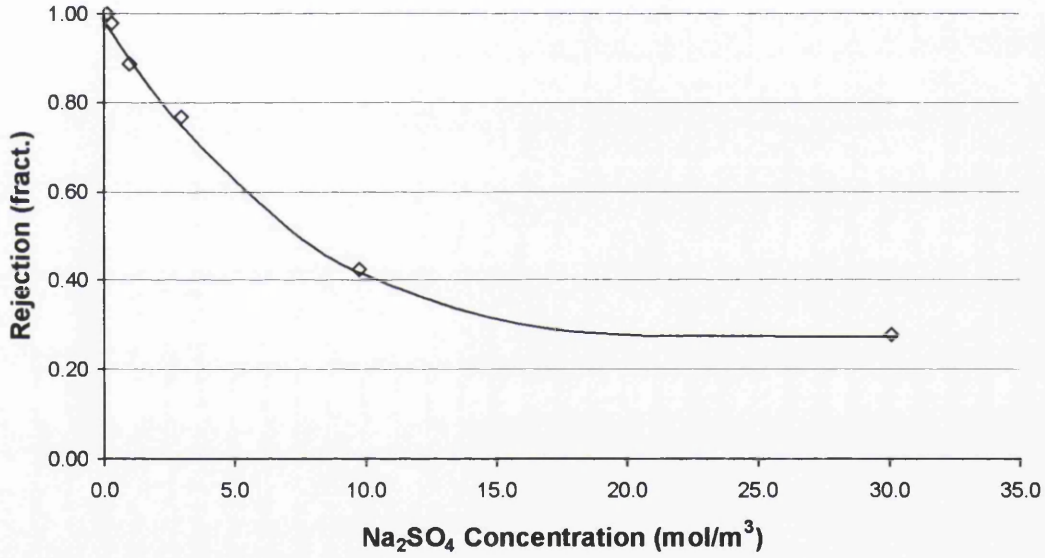

Figure 6-5 Sodium sulphate rejection as a function of concentration, recorded by Bowen and Mukhtar, 1996.

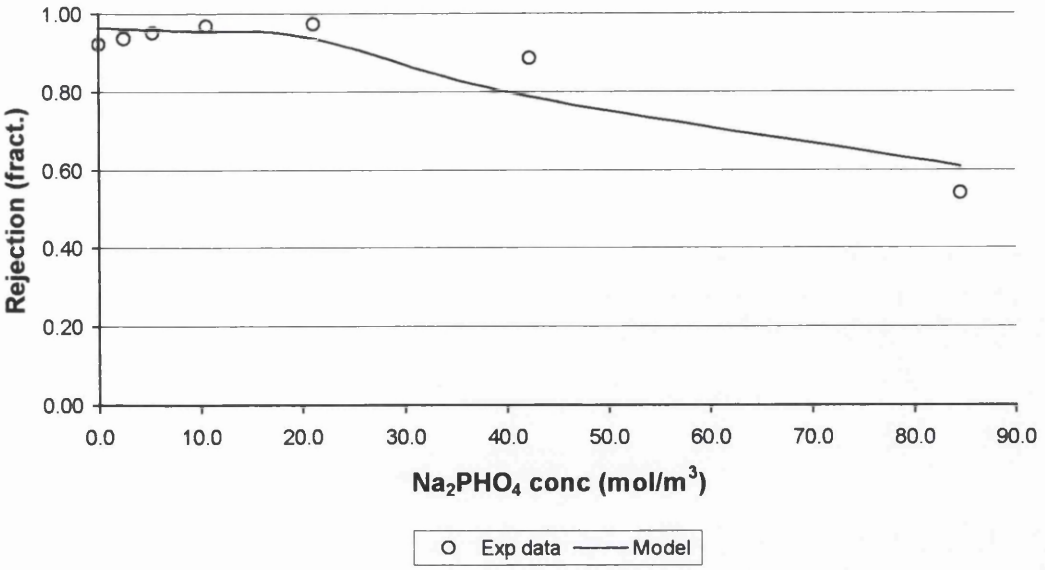

Figure 6-6 Fit of Spiegler and Kedem model to data for Na_2HPO_4 rejection (data points averaged from data shown in Figure 6-3).

Perry and Linder

The Perry and Linder model was a derivation of the theory developed by Spiegler and Kedem. When there is no secondary solute present then $C_x' = 0,$ and $\beta = 0$ (equation (6.17)) and equation (6.18) equates to the description of rejection originally provided by Spiegler and Kedem (equation (6.3)).

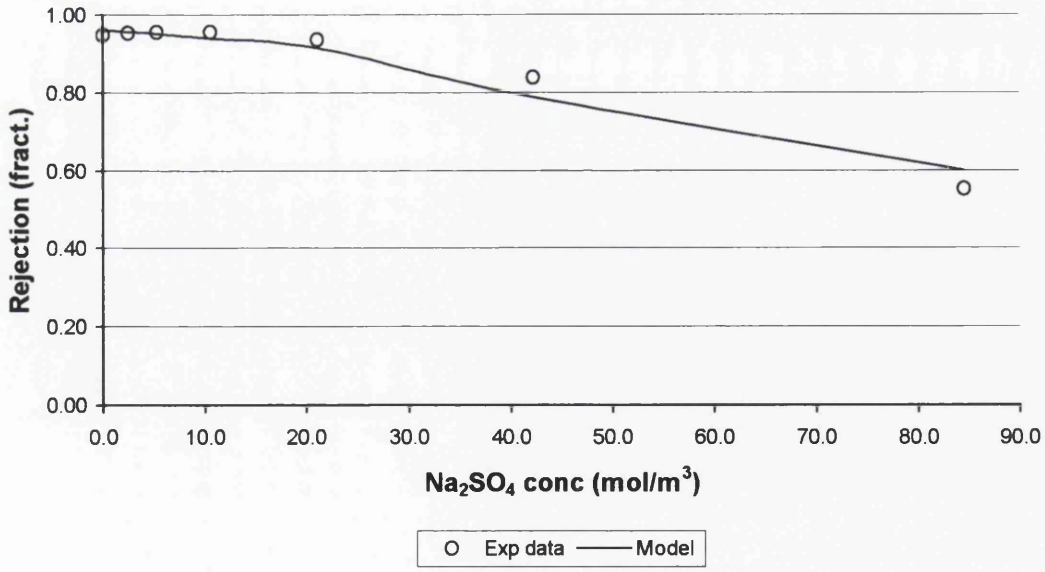

Figure 6-7 Fit of Spiegler and Kedem model to data for Na_2SO_4 rejection (data points averaged from data shown in Figure 6-3).

It was thus possible to use the modelling described in Section 6.2.1 of this chapter to attempt to describe the patterns of salt rejection observed in Figures 6-3 and 6-4.

The two graphs in Figures 6-6 and 6-7 show a reasonable quality of fit between the model and the experimental data. However one of the more distinctive features of the data was not represented well and that was the tendency of both data sets to pass through a maxima at a salt concentration of between 10 and 30 mol/L (dependent on the salt). Additionally, an inspection of the values derived for the reflection coefficient, σ, and solute permeability, P, (see equations (6.3) and (6.4)) revealed an ambiguousness in the meaning or worth of these values, since the reflection coefficient tends to the maximum of unity unless it was constrained within the *solver* function of Excel that was used to fit the model. The solute permeability for the sulphate salt was 4.85×10^{-5} cm/s and 3.67×10^{-5} cm/s for the phosphate. At the pressure of operation the hydraulic permeability was 1.22×10^{-3} cm/s, observing that the salts are highly rejected then their permeabilties must be far lower than that of the solvent hence these values are reasonable.

Extended Nernst Planck model - use and application

As suggested in Section 6.2.4 the Donnan-Steric Partitioning Model (DSPM) and the refinements provided by Bowen and Welfoot present the most recent development in membrane transport theory based on the extended Nernst Planck equation (Bowen and Welfoot, 2002).

As with the Spiegler and Kedem modelling an attempt was made to approximate the salt rejection data illustrated in Figures 6-3 and 6-4 using the two-parameter model. The two-parameter model is suitable for modelling electrolyte rejection and was found to be reliable for two ion solutions. The model has also been used on three and four ion systems with varying degrees of success, for example the model was used to successfully replicate the 3-ion system (Na^+, SO_4^{2-} and Cl^-) as presented in Figure 4-9 in Chapter 4.

Figure 6-8 shows the standard of fit achieved between the 2-parameter model and experimental data obtained from the filtration of an equimolar $NaCl:Na_2SO_4$ solution using the Trisep XN45 membrane. On this occasion the two parameters central to the

model, namely the pore radius, r_p, and the membrane charge density, X_d, had values of 0.38 nm and 0 mol/m^3 respectively. The pore radius value is reasonable, considering that the radius of pores in nanofiltration membranes is assumed to be in the region of 0.5 to 2 nm. In contrast, the charge density does not compare favourably with what might be expected for a strongly negatively charged membrane.

As one of the two parameters in the model, r_p has a particular influence on properties such as the viscosity effect in small pores, the determination of hindrance factors that are dependent on the ratio of pore radius to solute ion radius and the calculation of dielectric constants.

The model has been implemented using a program written in Fortran (Welfoot, 2001). The program used an iterative technique to arrive at a solution to the model that provides rejection as a function of pressure for a certain membrane and a specific solute concentration.

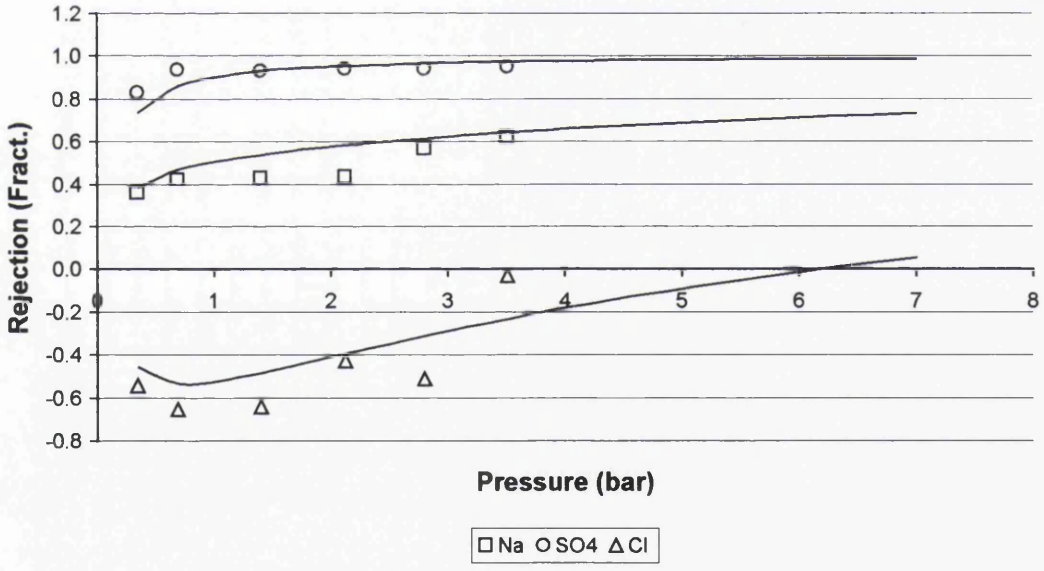

Figure 6-8 Plot of rejection data for a three-ion system including modelled rejection curves

For the purposes of this work, the appropriate programs were modified where necessary and prepared to model the variation of salt rejection with concentration. To reach a successful approximation of the experimental data using the program, a set of constants, specific to the membrane and solute, were required. The solute was characterised by four properties, these were the diffusivity, radii, valence and bulk

concentration of each ion. Table 6-1 provides a summary of the values required for the ions studied here and other ion values for comparison.

Ion	Salt	Bulk diffusivity (10^{-9} m^2/s)	Radii (nm)	Valence
	NaCl			1
Na	Na_2SO_4	1.33	0.18	1
	Na_2HPO_4			1
Cl	NaCl	2.03	0.12	-1
SO_4	Na_2SO_4	1.06	0.23	-2
PO_4	Na_2HPO_4	-	-	-3
HPO_4	Na_2HPO_4	-	-	-2

Table 6-1 Solute data required by the modified DSPM transport model

The model, implemented in Fortran, used the data presented in Table 6-1 to determine solute rejection in membrane transport systems. These values have been obtained from Atkins (Atkins, 1990).

Since the Fortran programs were devised such that rejection was modelled according to applied pressure, then to obtain a set of data for rejection as a function of concentration demanded repeated adjustment of the concentration value and execution of the program. The sequence of concentrations used for calculation was the same as those used in the experimental investigations (i.e. 0, 2.5, 5.3, 10.6, 21.1, 42.3, and 84.5 mol/m^3). Limiting the calculation to a few concentrations values reduced the computational load of the exercise and allowed direct comparison between the model and the experimental data.

Due to a failing in the Fortran implementation of the 2-parameter model it was not possible to solve the model for the conditions described. The program was unable to run with concentrations less than 84.5 mol/m^3 and in order to calculate at this concentration it required values for charged density, X_d, and pore radius, r_p, that did not concur with those expected. The implementation was very complex and time precluded debugging.

6.4 Modelling the negative rejection phenomena

Having considered how the available theories handled the basic, better-known aspects of filtration behaviour, it was useful to follow this with a discussion of the phenomena of negative neutral solute rejection witnessed in this work. For this purpose the same models as discussed above were used, incorporating any adjustments necessary to account for the unusual behaviour.

The benefit of theoretical analyses of this type was that they provide added insight into properties of the system that influence transport behaviour. For example, the modelling based on irreversible thermodynamics relies on a value known as the reflection coefficient. The reflection coefficient is the maximal rejection of a solute for a membrane and as such the value varies with respect to the solute but is a constant of the membrane. Similarly the solute permeability, P, is also dependent on the relation between the membrane and the solute and varies for each solute considered. In contrast the DSPM based 2-parameter model enabled quantification of the pore radius r_p, which is a specific membrane property as is membrane charge X_d, the other "fitting" parameter used in this model.

Although the extended Nernst-Planck equation based models have proven to be very capable, the debate about whether pores exist and thus whether pore radius is an appropriate measure of steric hindrance in membrane transport, remains to be resolved. The presence of membrane pores in Nanofiltration membranes has been reported (Bowen and Doneva, 2000), but is yet to be supported convincingly by the findings of other workers. It was therefore concluded that a model which treats the membrane as a black-box or semi black-box might be a more justifiable solution to the problem. Hence only the Perry and Linder model was used to fit the experimental data considered here.

6.4.1 Model application – general method

Perry and Linder

The equations presented in Section 6.2.1 of this Chapter were central to the evaluation of the experimental data. They enabled application of the Spiegler and Kedem theory

to a negative rejection system. However, the discussion does not clearly illustrate the practical means by which the equations have been applied to the data. This information is provided below.

For the condition where the rejection of a solute of constant concentration was observed as a function of complimentary salt concentration, the following approach to modelling was required.

i) The concentration of salt at the membrane surface, c'_{xm}, was determined from the theory for concentration polarisation as demonstrated in Section 5.3. It was important to consider the surface concentration rather than that of the bulk solution, as it was the value at the membrane surface that related directly to the concentration of the filterable solute. Membrane concentration values for the retained salt were derived from the sequence of bulk solution concentrations commonly used in the experiments (Table 6-2).

Figure 6-9 shows the plot of real rejection and observed rejection for Na_2HPO_4 with concentration. As was previously noted (Section 5.3.3) the real rejection values were greater than the observed rejection. Consequently the concentration of salt at the membrane was higher than that of the bulk solution.

Bulk solution Concentration	**Observed rejection**	**Real rejection**	c'_{xm}	c'_{xp}
mg/L			mg/L	mg/L
1	0.922	1	395.2	2.78
350	0.937	0.986	1664.7	11.7
750	0.951	0.984	1973.4	13.8
1500	0.969	0.987	3836.6	27.0
3000	0.973	0.988	7673.1	54.0
6000	0.885	0.963	13904.4	97.9
12000	0.541	0.725	20779.8	146.3

Table 6-2 Typical observed and real rejection data for Na_2HPO_4 (where c'_{xm} and c'_{xm} are the concentrations of salt at the membrane surface and in the permeate respectively)

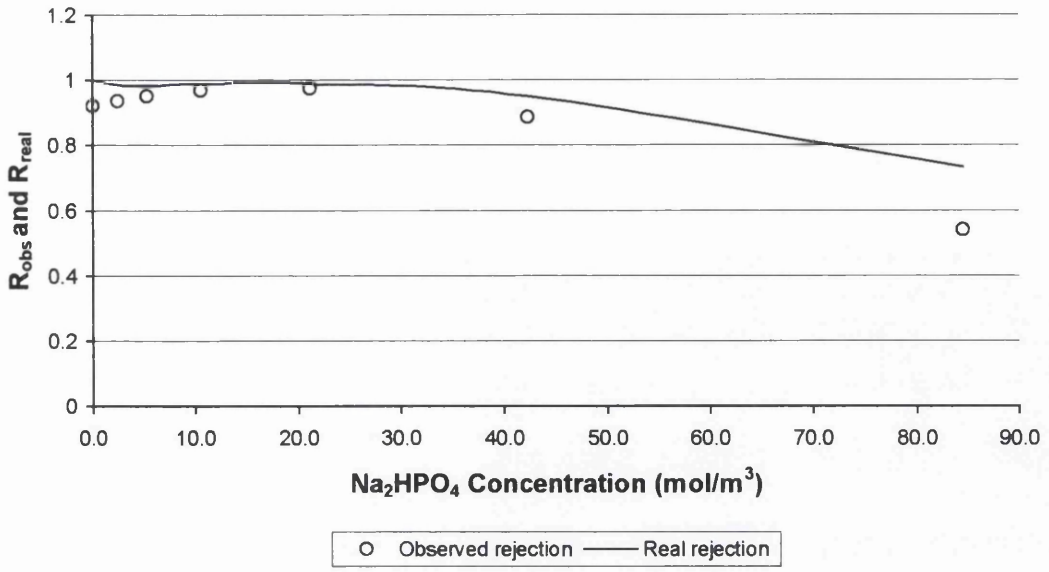

Figure 6-9 Comparison of observed rejection with real rejection for Na_2HPO_4

ii) The osmotic pressure effect of the salt in solution at the membrane surface was determined using the Van't Hoff approximation discussed in Chapter 4. This value was then inserted into equation (6.40) to obtain the total volume flux in a single salt system.

$$J_v = L_p\left(\Delta P - \sigma\Delta\pi\right) \tag{6.40}$$

Equation (6.40) is the same as equation (6.2) except for the use of global coefficients rather than the local approximations. The hydraulic permeability, L_p (cm/s.atm), was a property of the membrane and was determined from water flux experiments carried out on the membranes. The same applies to the reflection coefficient, σ, which was determined for the XN45 membrane from a model fitting exercise (the results of which are presented in Chapter 4).

iii) The rejection of the organic solute was then determined using equations (6.4), (6.17) and (6.18). The organic solute permeability, P_s, and reflection coefficient, σ, were evaluated by fitting the model to the data and by inspection respectively. The valence value was normally a constant and was usually discerned from the molecular formula of the retained ion. However, although the salt (Na_2HPO_4) provides the retained ion and therefore should have a known valence at the conditions of the system, in this case the value v

was used to approximate the possible charge interactions that occur between the salt ion and the "neutral" organic solute, which cannot be evaluated by inspection.

6.4.2 The valence assumption

In the original derivation the ion that provides the Donnan contribution to salt passage was a large organic ion with a known valence, v and this value related directly to the to the salt concentration just within the membrane (equation (6.11)). If this methodology were applied directly to the current situation then the value for valence would be taken from that for the phosphate ion at the prevailing pH of the system. However, in the original work the permeable ions were univalent and therefore no extra representation was required for these species in the model. In this case the compound with a high permeability was a neutral molecule, so charge interactions between this and the retained ion were to be accounted for in another way.

The main assumption was that the neutral solute had a charge effect associated with it (e.g. polarity) that made it susceptible to a charge imbalance across the membrane. To accommodate this interaction between the salt ion and the organic solute, the valence value was retained but this time it was used as a variable rather than a constant, to fit the model to the experimental data.

6.4.3 Model parameters

To model the rejection behaviour of each solute required three values for the model parameters, these are: the reflection coefficient, σ, the solute permeability, P, and the "valance", v.

For glucose (Figure 6-10) these three values were 0.27, 4.7×10^{-6} cm/s and 0.025 respectively. The relative molecular mass of glucose is 180 g/mol which when compared with the plot in Figure 4-6 coincided with a rejection of ~0.3. Thus a reflection coefficient close to 0.3 (0.27), used to produce the curve in Figure 6-10, was considered reasonable. In contrast, the magnitude of solute permeability was several orders lower than the hydraulic permeability at the pressure of operation.

When compared with salt permeabilties obtained for the rejection curves in Figures 6-6 and 6-7, it was clear that these values were not appropriate, as the permeability of glucose, with its low rejection relative to salt, should have had a higher permeability value than the salt.

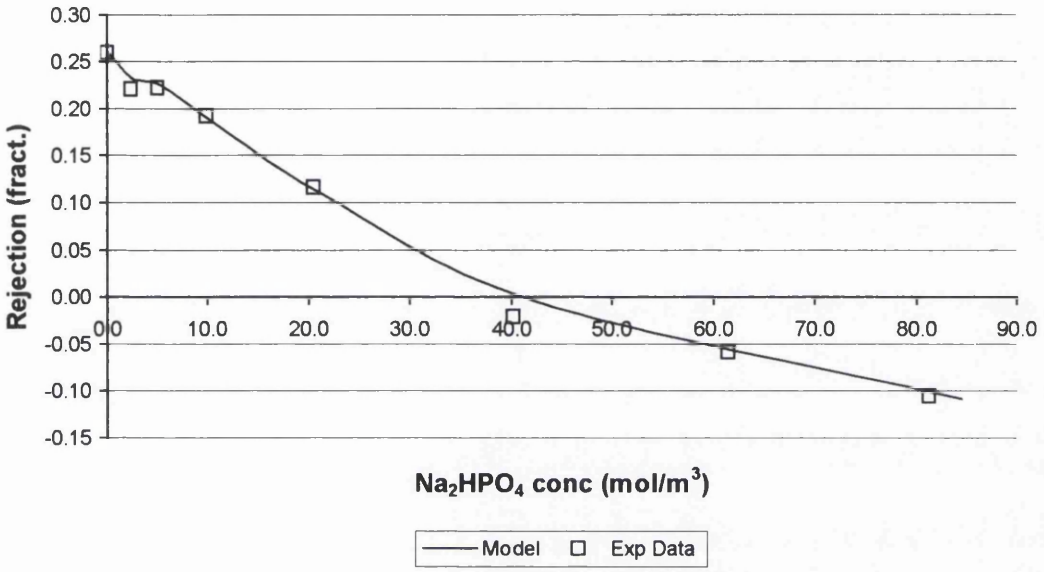

Figure 6-10 Rejection of glucose, experimental data and fitted model

The final fitting parameter was the "valance" which in this case represented the charge interaction between the retained phosphate ions and the organic solute glucose. Relative to the normal valence of 1 for a univalent salt this value was very small. This fits well with the concept of a small charge property of the organic molecule.

6.4.4 Charge properties of neutral molecules

Although neutral molecules (in this context) do not have corresponding dissociated ions when in solution it is normal that there would be some charge properties associated with the molecule. These may either come about from the distribution of electrons in the molecule (polarisation) or a result of attraction forces such as Van der Waals. The possible sources of molecular interaction are discussed below and compared with the behaviour observed to see if they could provide an adequate explanation.

Polarisability

Although molecules of a compound might have no permanent dipoles, the substance can be polarised by an applied electric field (Hendrickson et al., 1970). In the case of the membrane system an electric field is provided by the charge of the membrane, which in the case Trisep XN45 was strongly negative (relative to other membranes, see Table 4-4). When a molecule becomes polarised the average electron distribution is changed in comparison with that of an identical molecule not subjected to an externally applied field.

With respect to polarisation of molecules, the charge distribution of unsaturated and aromatic molecules, is much more easily deformed than saturated systems. This might explain the more pronounced negative rejection of caffeine and benzyl alcohol.

It is known that Refractive index (RI) is a physical measure that is directly related to the polarisability of a molecule (Hendrickson et al., 1970). Benzyl alcohol, benzylamine and glycerol have a RI of 1.5399, 1.5440 and 1.4729 respectively, these values fall centrally for those exhibited by organic compounds whose refractive indices range from 1.3330 for water to >1.7000 for naphtholic compounds and indicate that they are subject to polarisation. (NB RI data are only available for pure compounds that are liquids at standard temperature and pressure).

Hydrogen bonding

Glucose, raffinose, glycerol and benzyl alcohol all retain oxygen-hydrogen bonds. It is possible that a Donnan contribution provided by an imbalance of ions across the membrane, could present a charge system that in turn might promote transport of compounds containing hydrogen bonds. Indeed, in the case of glucose and glycerol the molecule is *covered* in hydrogen bond sites. However, an examination of the structural chemistry of these two compounds indicates that the positive end of the dipole created by the hydrogen-oxygen bond is on the outside of the molecule. This suggests that the molecules retain a positively charged appearance, which does fit in with the assumption of negative rejection induced by a Donnan effect. Permanent dipoles, such as hydrogen bonds, have been used by Van der Bruggen and co-workers to explain non-conformity of organic molecules to theories of solute rejection (Van der Bruggen et al, 1999).

6.5 Model Performance

The model, now modified to accommodate a parameter that represents the "charge" of organic solutes was tested for all negatively rejected solutes, where negative rejection was observed for solutions incorporating sulphate and phosphate sodium salts. The results of this modelling are shown here. The Quality of agreement between the model and the experimental data was assessed according to the shape of the resultant curve in comparison with the experimental data and the actual magnitudes of the values calculated, with particular reference to the start and finish values.

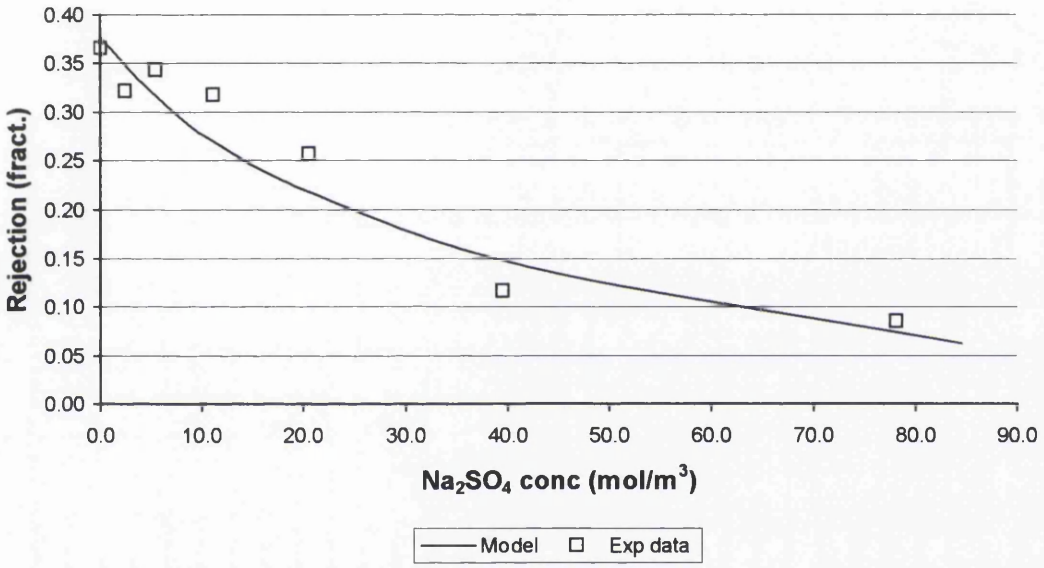

Figure 6-11 Rejection of glucose as a function of Na_2SO_4 concentration, experimental data and fitted model

The graph shown in Figure 6-11 indicates the rejection of glucose as a function of sodium sulphate concentration. It should be noted that this plot provides an exception to the series presented here (Figures 6-11 to 6-17), as all values of glucose rejection are positive. Even so, the model provides a reasonable approximation of the curve presented by the individual data points. This suggests that the same hypothetical charge effects that promote negative rejection, also govern the observed change in solute rejection in the positive rejection range. This contrasted with suggested theories (Freger et al., 2000) that attempted to explain the fall off in rejection already observed in systems of this type. In these theories pore dilation related to shrinkage of the active layer or charge masking was proposed to occur in the presence of increasing

electrolyte concentrations. This was due to the presence of charged groups on the membrane and how an electrolyte modifies their influence on the membrane structure.

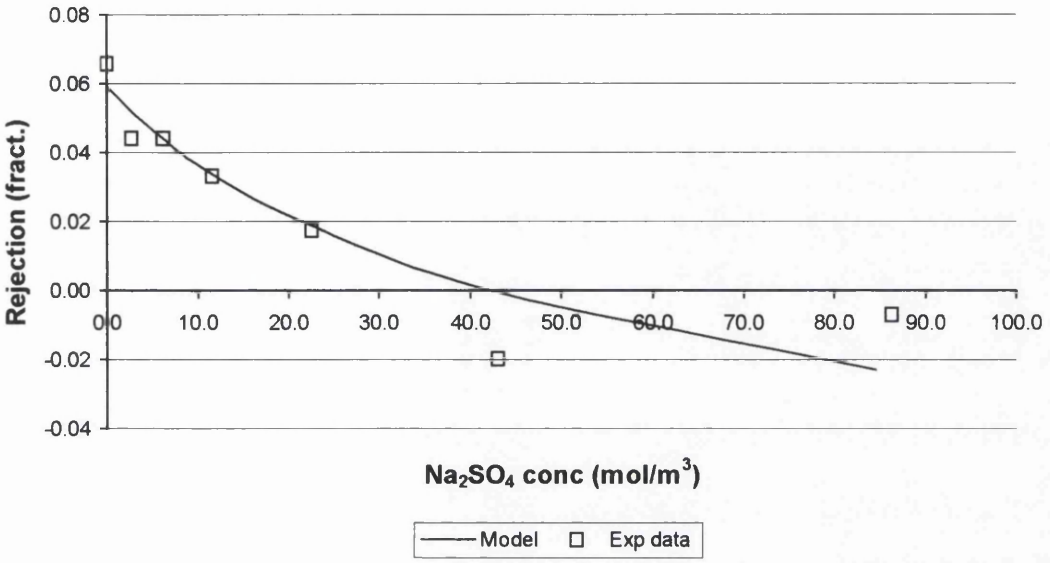

Figure 6-12 Rejection of glycerol as a function of Na_2SO_4 concentration, experimental data and model

Figures 6-12, 6-13 and 6-14 all demonstrate negative rejections in the presence of sodium sulphate for glycerol, caffeine and benzyl alcohol respectively. In all three cases the quality of fit was good with a good approximation of the trends apparent in the data. Indeed a poor quality of fit was attributed to scatter in the experimental data rather than deficiencies in the model theory.

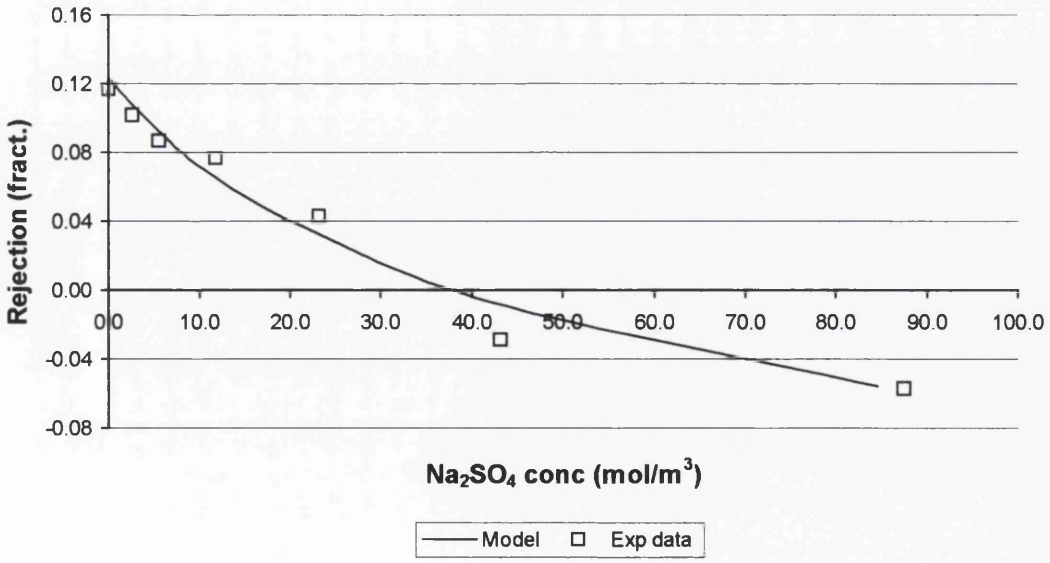

Figure 6-13 Rejection of Caffeine as a function of Na_2SO_4 concentration, experimental data and fitted model

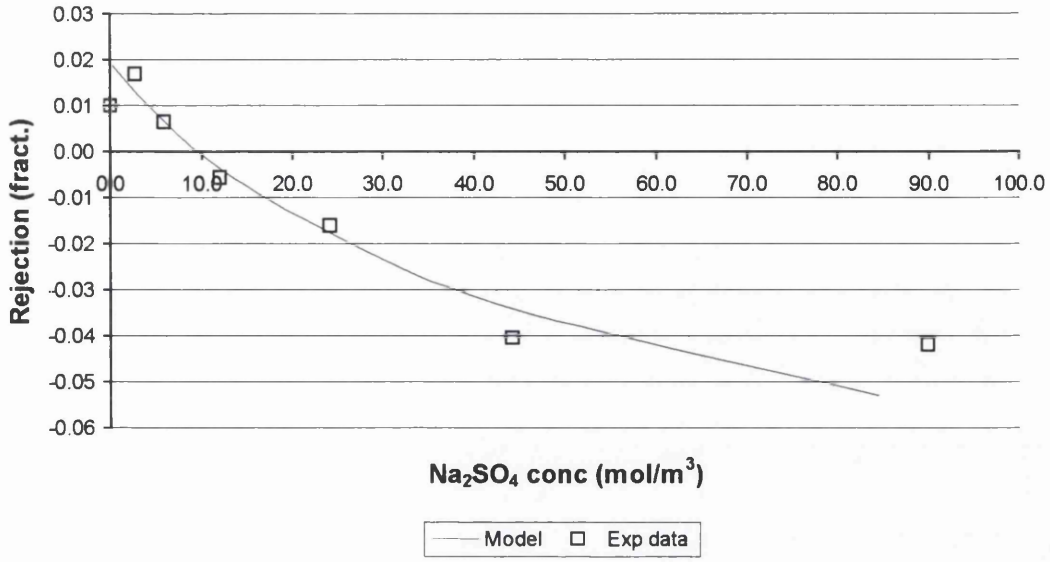

Figure 6-14 Rejection of Benzyl alcohol as a function of Na_2SO_4 concentration, experimental data and fitted model

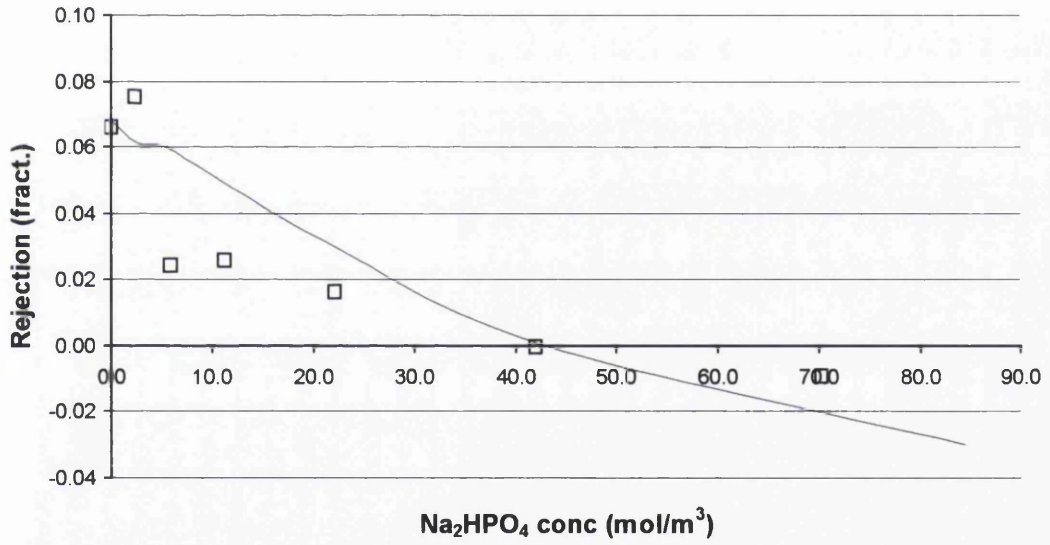

Figure 6-15 Rejection of Glycerol as a function of Na_2HPO_4 concentration, experimental data and fitted model

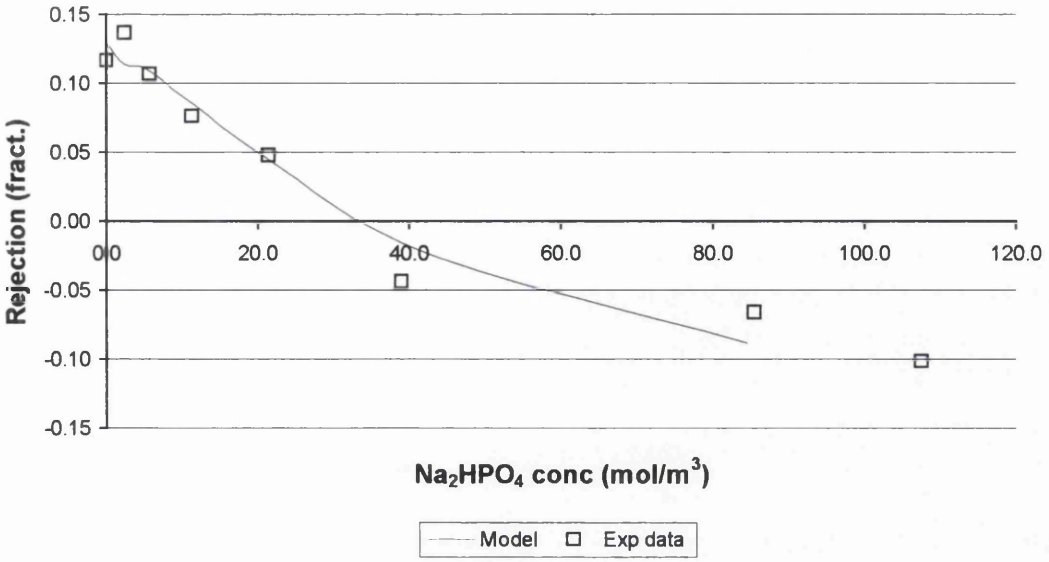

Figure 6-16 Rejection of Caffeine as a function of Na_2HPO_4 concentration, experimental data and fitted model

Figures 6-10 and 6-15 to 6-17 demonstrate the negative rejections observed for glucose, glycerol, caffeine and benzyl alcohol respectively in the presence of increasing concentrations sodium phosphate. As with the plots for sodium sulphate the trend for the rejection behaviour was well represented by the model. The best standard of fit can be observed for glucose and the poorest for glycerol, but again this was attributed to a high degree of scatter in the experimental data.

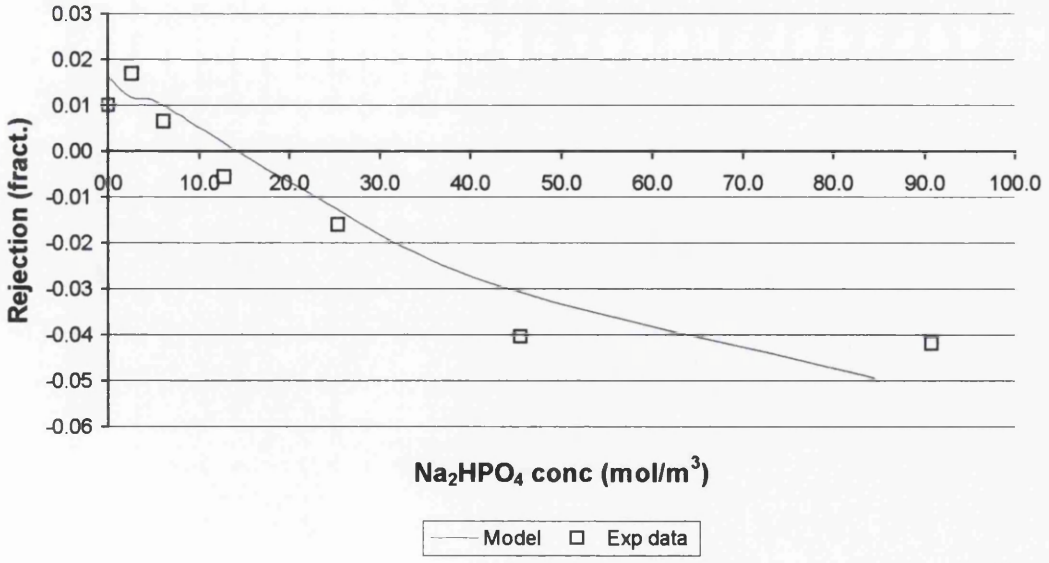

Figure 6-17 Rejection of Benzyl alcohol as a function of Na_2HPO_4 concentration, experimental data and model

6.5.1 Model parameters and data trends

The key model parameters used to fit the model to the experimental data were the reflection coefficient, σ, the solute permeability, P, and the "valence", v. "Valence" was the term ascribed to the charge interaction between the neutral organic molecules and the salt ions, consequently this varied for each salt/solute system evaluated as is shown in Table 6-3.

Salt	Solute	Reflection coefficient	Solute permeability (cm/s)	Valence
Na_2SO_4	Glucose	0.38	4.70E-06	0.025
	Glycerol	0.06	7.79E-06	0.007
	Caffeine	0.14	2.69E-05	0.008
	Benzyl alcohol	0.02	2.69E-05	0.005
Na_2HPO_4	Glucose	0.27	4.70E-06	0.025
	Glycerol	0.07	7.79E-06	0.0085
	Caffeine	0.15	2.69E-05	0.01
	Benzyl alcohol	0.0175	2.69E-05	0.0045

Table 6-3 Model parameters obtained by fitting to the experimental data for each salt/solute system

Values for the three model parameters are shown in Table 6-3. The reflection coefficient remains constant in the majority of cases for each solute with the exception of glucose. The values used here for reflection coefficient were based upon the initial rejection - the rejection at zero salt concentration. It was apparent that in this modelling the reflection coefficient essentially controls the value of the intercept on the rejection axis. This value does not adhere to the true definition of reflection coefficient, which was stated as being the maximal rejection observed at infinite pressure for a single compound. However, the value used here was the maximal rejection observed at the pressure of operation and therefore conforms with the alternative definition provided in Section 4.3.1.

The other values for solute permeability and valence are largely constant with only small variations observed in the valence. It was possible to conclude that the closeness of values, particularly for the valence, supported the assumption that there are small charge effects influencing the rejection, as only small variations might be expected between the two salts used.

It was observed (Chapter 5) that the trend shown by the solute rejection appeared to relate to the pattern of rejection exhibited by the salt. Figures 6-3 and 6-4 show that for both Na_2SO_4 and Na_2HPO_4 the salt rejection was high at first (>0.8) and then fell rapidly beyond a salt concentration of ~ 6 g/L (40 mol/m^3). For the region of high salt retention the corresponding organic solute rejection fell almost linearly and passed through zero to become negative. When the salt rejection dropped, at bulk feed concentrations greater than 6 g/L, the rate of decline of the solute rejection slowed and the value tended toward a constant value that was no lower than –0.1 in all cases. If the salt rejection remained high, it is theoretically possible that the solute rejection might maintain a rate of descent similar to that exhibited in the early part of the curve (salt concentration 0 - 40 mol/m^3) and even greater magnitudes of negative rejection might be achieved.

The effect of the salt rejection pattern was superimposed onto the model by inserting experimental data into the calculations. This was facilitated by the fact that the pattern of salt rejection behaviour was constant and independent of the co-solute. As demonstrated in Section 6.3 it was possible to model the salt rejection with concentration and therefore it might be feasible to model the rejection of solute on a basis of simple solute and membranes properties.

6.6 *Importance of the phenomena*

Negative rejection has already been considered as a means of enhancing separations. Salt/dye systems have been found to be particularly receptive to exploitation of the Donnan effect. In one case (Levenstein et al., 1995), the dye Procion Red was desalted using a nanofiltration membrane, a salt rejection of –68% was achieved with the addition of an ionised polyelectrolyte (sodium salt of poly acrylic acid). The concentration of acid in the feed was more than three and half times the maximum concentration of salt used here. Therefore, it is feasible that the selection of a suitable electrolyte might promote the flux of uncharged solutes through a membrane and thus increase the degree of separation achievable. Indeed, as a recommendation for further work, it would be desirable to pinpoint an electrolyte, possibly one similar to that used by Levenstein and co-workers to see if lower values of negative rejection were achieved for non-ionised organic molecules.

6.7 Conclusions

To improve understanding of the negative rejection phenomena, experimental data were discussed in relation to current rejection modelling theories. Two main modelling methodologies exist: those based on irreversible thermodynamics (Spiegler and Kedem) and those derived from the extended Nernst Planck equation. The two iterations of these theories that are most appropriate for application to the current scenario are the Perry and Linder modification of the Spiegler and Kedem model and the 2-parameter derivation of the extended Nernst-Planck proposed by Bowen and Welfoot. An apparent weakness in the Fortran implementation of the 2-parameter model prevented further consideration of this theory. Therefore discussion was centred on the Perry and Linder model alone. This was considered acceptable as the Spiegler and Kedem model is semi black box and as such made a more general discussion of the data possible.

The observation that the patterns of salt rejection (for both Na_2SO_4 and Na_2HPO_4) with concentration remain the same for all uncharged solutes, was reiterated. As the salt rejection behaviour was assumed to be central to the rejection of the co-solute an attempt was made to fit the Spiegler and Kedem model for single salt rejection to the data. A reasonable standard of fit was achieved with the trend in the experimental data being well approximated by the model. However, a deficiency in the model meant that the reflection coefficient parameter would have exceeded unity if left unchecked.

To model the negative rejection of uncharged solutes using contemporary modelling techniques, capable of simulating negative rejections, an assumption regarding the charge properties of the solute was necessary. In the current modelling, the ion valence accommodates the Donnan contribution to the membrane transport of the permeable species. However, in this work the permeable species was non-ionic and consequently the interaction between the salt ions and the solute was assumed to be a result of temporary polarisation or the presence of a permanent dipole. In the organic molecule, polarity is induced by the presence of an electric field. In the case of membrane separations the electric field was suggested to be provided by the surface charge of the membrane. In the current theory this polarity parameter occupies the same position as the valence but is a real number rather than an integer.

The Perry and Linder model, modified such that the *valence* became a non-integer parameter, was fitted to the experimental data for neutral solute rejections. The quality of fit was found to be good with the properties of the experimental data plot approximated well by the model. Due to the inclusion of a term for solute charge the model also successfully accommodated the negative rejection behaviour of the data.

The membrane transport phenomenon observed in this work was compared to the negative rejection that has already been exploited in ionic systems. If greater magnitudes of negative rejection could be achieved using polyelectrolytes then the possibilities for exploitation of this behaviour are limited only by feed and permeate requirements.

7 Conclusions and Recommendations

Membrane technology and membrane research has undergone a state of continuous progress since the early part of the last century and the basic principles of filtration have seen documented anthropological use since the existence of the Roman Empire. With respect to developments in synthetic membrane technology, nanofiltration represents the most recent advance and consequently is subject to much scrutiny. Nanofiltration is also of significant interest to the membrane researcher since its characteristics fall between those of reverse osmosis and ultrafiltration membranes and the molecular weight cut-offs fall in a range where molecular interactions become important.

On a basis of the work completed and published with regard to both theoretical and practical investigation of solute/membrane systems, it was decided that the aim of this thesis was to investigate interactions in charged/uncharged solute combination separations. The importance of such work was apparent when the complexity of multi-solute solutions, which are very often processed via synthetic membranes, was considered. Thus the interactions that might be observed and evaluated through this work may be of significant importance for future theoretical or commercial exploitaton.

7.1 Conclusions

The present state of research with respect to pressure driven membrane separation processes was investigated on a basis of the nature and aim of the experimental investigation undertaken. It was concluded that although there are numerous reasons for conducting membrane research those of genuine academic merit are limited to investigations of the processes governing membrane separations. These processes have been investigated through the development of theoretical models containing parameter definitions of governing properties. In most cases the theories are discussed in parallel with experimental data for simple process systems comprised of single, binary or tertiary solutions. The area of membrane research least investigated was found to be transport of multi-solute systems with particular reference to combinations of charged and uncharged species.

The zeta potentials of six commercially available nanofiltration membranes were measured at different pH values. One membrane (Trisep XN45) was shown to exhibit a negative charge of greater or equivalent magnitude than the other membranes considered. This membrane was chosen for use in further investigations. The membrane was further theoretically quantified and a value for MWCO at the pressure of operation was found to be 255 Da, which was close to the molecular weight of small organic compounds and multi-valent salts. This property of the membrane qualified it for use in membrane transport investigations since it was the membrane most likely to emphasise interactions between the solutes.

A series of experiments investigating the effect of the presence of salt and the variation of salt concentration and valence on the transport of non-dissociated organic compounds, was conducted. High valency salts are capable of inducing negative rejections of uncharged compounds whose molecular weight was comparable or low with respect to the MWCO of the membrane. This was considered unusual and worthy of further discussion since such behaviour had not been observed previously.

To ensure that the phenomenon observed in the experimental data was true, the error associated with results was analysed to assess whether the results could be attributed to more than just experimental error. At a negative rejection value of –10% an associated error value of 0.6% was evaluated thus the observed negative rejection was not attributed to random experimental error.

To further ensure the veracity of the observed phenomena it was discussed in conjunction with concentration polarisation effects that were thought to present a possible explanation of the outcome. However, concentration polarisation was not found to provide an explanation and once accounted for, amplified the results.

When the results of the experimental investigation were discussed in relation to current transport theories it was shown that with little modification the trends observed in the experimental data could be reasonably approximated by the theory proposed by Spiegler and Kedem.

To project curves, produced algebraically, onto data for negatively rejected uncharged solutes it was necessary to use the modification of the S-K model proposed by Perry and Linder. This version of the theory was for use with tertiary systems of charged solutes but was found to be applicable to a solution of uncharged/charged species by changing the valence term to a variable charge term. It was assumed that the non-ionic organic compounds retained a charged that was the result of either a permanent dipole or induced by the electric field created by the salt-membrane arrangement. Evidence of charge in "neutral" solutes and its influence on rejection, was well supported by the literature.

7.2 Recommendations

Future work related to the content of this thesis should be concerned with assessing the extent of the measured phenomena. To achieve this a series of compounds needs to be identified that are non-ionic, have equivalent molecular sizes and structures but sequential variation in permanent dipole Debye lengths and/or polarisability. Such work should be extended to the correlation between solute properties and membrane charge, valence and size of the membrane impermeable co-ion (e.g. organic polyelectrolytes).

Ultimately a modification or addition would be made to contemporary transport theories that would successfully account for the behaviour of such systems and would, in the long term, furnish the process engineer with a means of predicting separation performance of complex solutions at the surface of a known membrane. In part this might involve extending the program developed by Welfoot such that it would successfully accommodate the solute systems discussed in this work.

As observed in Section 4.4.4 in the presence of divalent and multi-valent salts there is a distinct kink in the data at a concentration of 350 mg/L salt. It is unclear what might induce the kink, but further investigation and discussion should be undertaken to evaluate its cause.

Nomenclature

A	Pore cross-sectional area	[m^2]
a	Constant derived from Stokes-Einstein Equation	[$m^3\ s^{-1}$]
a_i	Activity of i^{th} ion	[-]
a_m	Numerical constant of dimensionless mass transfer coefficient	[-]
A_k	Fraction of membrane area occupied by pores	[-]
A_m	Membrane area	[m^2]
a_s	Solute activity	[mol m^{-3}]
b	Constant in velocity variation eq. 5.8	[m s^{-1}]
C	Concentration in external solution	[mol m^{-3}]
C_f	Concentration of solute in feed	[mol m^{-3}]
$\langle c_i \rangle$	Molar concentration of solute averaged over pore cross section	[mol m^{-3}]
c_i	Concentration of ion in membrane	[mol m^{-3}]
$C_{i,p}$	Permeate concentration of ion	[mol m^{-3}]
C_m	Concentration of fixed membrane charges	[mol m^{-3}]
c_m	Concentration of solute at the membrane surface	[mol m^{-3}]
C_p	Concentration of solute in permeate	[mol m^{-3}]
c_s	Concentration of solute in feed	[mol m^{-3}]
CP	Concentration polarisation modulus	[-]
D_∞	Bulk diffusivity	[$m^2\ s^{-1}$]
$D_{i,\infty}$	Bulk diffusion coefficient of ion *i*	[$m^2\ s^{-1}$]
$D_{i,p}$	Pore diffusion coefficient of ion *i*	[$m^2\ s^{-1}$]
d	Hydraulic diameter of membrane flow passage	[m]
d_p	Pore diameter effective in filtration	[m]
D_p	Pore diffusion coefficient of solute	[m s^{-2}]
$\langle D \rangle$	Average effective diffusivity of solute in pore	[$m^2\ s^{-1}$]
d_s	Solute diameter	[m]

e	Electronic charge (1.602177×10^{-19})	[C]
F	Faraday constant, 96487	[C mol^{-1}]
$\boldsymbol{F}$	Flow parameter defined by equation 2.13	[m^2 s^{-1}]
f	Reynolds number exponent eq. 5.7	[-]
g	Schmidt number exponent eq. 5.7	[-]
G	Lag coefficient	[-]
J_i	Total flux of ion i	[mol m^{-2} s^{-1}]
j_i	Flux of ion i (pore area basis)	[mol m^{-2} s^{-1}]
j_s	Solute flux (pore area basis)	[mol m^{-2} s^{-1}]
J_v	Total volume flux	[m^3 m^{-2} s^{-1}]
j_v	Volume flux (pore are basis)	[mol m^{-2} s^{-1}]
$\langle j_i \rangle$	Molecular flux averaged over pore cross section	[mol m^{-2} s^{-1}]
K	Enhanced drag coefficient	[-]
k	Boltzmann constant, 1.38066×10^{-23}	[J K^{-1}]
K_c	Coefficient defined by eq. 2.42	[-]
K_c	Hindrance factor for convection eq. 2.47	[-]
K_d	Coefficient defined by eq. 2.41	[-]
K_d	Hindrance factor for diffusion eq. 2.46	[-]
K_i', K_i''	Integrals defined by eq. 2.34	
$K_{i,d}$	Hindrance factor for diffusion of ion i	[-]
k_w'	Permeability coefficient of water	[-]
K_s	Membrane solution distribution coefficient	[-]
L_p	Filtration coefficient/solvent permeability	[-]
M_i	Molecular weight of the solute	[m^3 mol^{-1}]
M_w	Molecular weight of the solvent	[Da]
MW_s or MW_i	Molecular weight of uncharged or charged solute	[Da]
$\overline{MW}$	Molecular weight cut-off	[Da]
N_s^i	Number of moles of solute permeate	[mols]
P_e	Dimensionless parameter (Peclet number)	[-]
P_m	Hydrodynamic permeability of the membrane	[m^3 s^{-1} N^{-1}]

P_s	Global solute permeability	[m s^{-1}]
$\mathscr{P}_I$	Specific hydraulic permeability	[m^3 s^{-1} N^{-1}]
$\overline{P}$	Local solute permeability (S-K)	[m^2 s^{-1}]
$\boldsymbol{R}$	Rejection coefficient	[-]
$\mathscr{R}$	Real rejection	[-]
R_{obs}	Observed rejection	[-]
Re	Reynolds number	[-]
r	Pore radius	[m]
r^*	Mean pore radius	[m]
$\overline{r}$	Dimensionless radial coordinate	[-]
r_p	Effective pore radius	[m]
r_s	Radius of solute molecule	[m]
S_c	Steric hindrance factor for convection	[-]
Sc	Schmidt number	[-]
S_d	Steric hindrance factor for diffusion	[-]
S_p	Pore size standard deviation	[m]
S_{MW}	Standard deviation of molecular weight	[Da]
Sh	Sherwood number	[-]
t	Time	[s]
T	Temperature	[K]
t_n	Transport number	[-]
u	Flow velocity thorugh the membrane passage	[m s^{-1}]
v	Number of free, charged groups	[-]
V	Solvent velocity eq. 2.58	[m s^{-1}]
$\langle V \rangle$	Solvent velocity average of pore cross section	[m s^{-1}]
V_i	Partial molar volume of the solute	[m^3 mol^{-1}]
v_i	Specific volume	[m^3 mol^{-1}]
V_p	Volume permeated	[m^3]
V_s	Uncharged solute partial molar volume	[m^3 mol^{-1}]
V_w	Partial molar volume of the solvent	[m^3 mol^{-1}]
x	Distance co-ordinate perpendicular to the membrane	[m^2 s^{-1}]

x	Axial position in the pore	[m]
X_d	Membrane charge density	[mol m^{-3}]
X_d	Charge density	[mol m^{-3}]
Y_i	Dimensionless group eq. 2.57	[-]
z_i	Valence of ion *i*	[-]

Greek Symbols

β	Convective coupling coefficient	[-]
γ_i^0	Bulk activity coefficient of ion *I*	[-]
γ_i	Activity coefficient of ion *I* in the pore	[-]
Δc	Concentration gradient across the membrane	[mol m^{-3}]
$\Delta\pi$	Osmotic pressure difference	[N m-^{2}]
ΔP_e	Effective pressure driving force	[N m^{-2}]
ΔW_i	Born solvation energy barrier	[J]
Δx	Membrane thickness	[m]
Δp	Hydrostatic pressure difference	[N m^{-2}]
δ	Thickness of membrane surface boundary layer	[m]
ε_b	Bulk dielectric constant	[-]
ε_p	Pore dielectric constant	[-]
ε_0	Permitivity of free space (8.85419 x 10-12)	[C^2 m^{-1}]
η	Solvent viscosity within pores	[N s m^{-2}]
Λ	Ionic equivalent conductivity	[m^2 Ωeq]
λ	Solute-pore size ratio	[-]
μ_i	Electrochemical potential of i^{th} ion	[J mol^{-1}]
ν	Kinematic viscosity	[m^2 s^{-1}]
π	Solution osmotic pressure	[N m^{-2}]
π_c	Osmotic coefficient	[-]
ρ	Diffusion parameter	[m^2 s^{-1}]
ρ_{el}	Electrical space charge per unit volume of pore medium	[C m^{-3}]

σ	Reflection coefficient	[-]
τ	Tortuosity factor	[-]
Φ	Steric partition coefficient	[-]
φ	Sieve constant (Ferry, 1936)	
$\overline{\varphi}$	Electric potential of the membrane	[V]
$\overline{\phi_i}$	Dimensionless potential	[-]
ϕ_w	Water content of the membrane	[m^{-3}] or [-]
$\overline{\psi}$	Dimensionless radial potential	[-]
ψ	Electrical potential within pore	[V]
ψ	Interaction energy between solute and pore wall	[-]
ψ'	Electric potential	[V]
ω	Mobility	[m s^{-1} N^{-1}]
ω	Solute mobility	[mol s^{-1} N^{-1}]
ω_I	Molar mobility	[mol m^{-2} J^{-1} s^{-1}]

Subscripts

w	Solvent
s	Solute
-	Anion
+	Cation
I	Impermeable ion
p	In membrane/pore condition
f	Feed
p	Permeate
m	Membrane surface
1	Permeable ion 1
2	Permeable ion 2

Superscripts

'	Feed side of the membrane
"	Permeate side of the membrane
o	Free solution

Bibliography

Adham, S., Gagliardo, P., Smith, D., Ross, D., Gramith, K. and Trussell, R.: Monitoring the integrity of reverse osmosis membranes. *Desalination* **119**, 143 (1998).

Ahn, K.-H., Cha, H.-Y., Yeom, I.-T. and Song, K.-G.: Application of nanofiltration for recycling of paper regeneration waste water and characterisation of filtration resistance. *Desalination* **119**, 169 (1998).

Alkhatim, H. S., Alcaina, M. I., Soriano, E., Iborra, M. I., Lora, J. and Arnal, J.: Treatment of whey effluents from dairy industries by nanofiltration membranes. *Desalination* **119**, 177 (1998).

Atkins, P.: *Physical chemistry* (Oxford University Press, Oxford, 1990).

Baig, M. B. and Al Kutbi, A. A.: Design features of a 20 migd SWRO desalination plant, Al Jubail, Saudi Arabia. *Desalination* **118**, 5 (1998).

Bandini, S. and Vezzani, D.: Nanofiltration modeling: The role of dielectric exclusion in membrane characterisation. *Chemical Engineering Science* **58**, 3303 (2003).

Berg, P., Hagmeyer, G. and Gimbel, R.: Removal of pesticides and other micropollutants by nanofiltration. *Desalination* **113**, 205 (1997).

Boussahel, R., Montiel, A. and Baudu, M.: Effects of organic and inorganic matter on pestcide rejection by nanofiltration. *Desalination* **145**, 109 (2002).

Bowen, W. R. and Mukhtar, H.: Characterisation and prediction of separation performance of nanofiltration membranes. *Journal of Membrane Science* **112**, 263 (1996).

Bowen, W. R.: in *Particle technology & separation processes* (eds. Richardson, J. and Peacock, D.) 868 (Butterworth and Heinemann, 1997).

Bowen, W. R., Mohammed, A. W. and Hilal, N.: Characterisation of nanofiltration membranes for predictive purposes - use of salts, uncharged solutes and atomic force microscopy. *Journal of Membrane Science* **126**, 91 (1997).

Bowen, W. R. and Mohammed, A. W.: Diafiltration by nanofiltration: Prediction and optimisation. *AIChE Journal* **44**, 1799 (1998).

Bowen, W. R. and Doneva, T. A.: Atomic force microscopy studies of nanofiltration membranes: Surface morphology, pore size distribution and adhesion. *Desalination* **129**, 163 (2000).

Bowen, W. R., Jones, M. G., Welfoot, J. S. and Yousef, H. N. S.: Predicting salt rejections at nanofiltration membrane using artificial neural networks. *Desalination* **129**, 147 (2000).

Bowen, W. R., Doneva, T. A. and Stoton, J. A. G.: The use of atomic force microscopy to quantify membrane surface electrical properties. *Colloids and Surfaces A* **201**, 73 (2001a).

Bowen, W. R., Doneva, T. A. and Yin, H. B.: Polysulfone - sulfonated poly(ether ether) ketone blend membranes: Systematic synthesis and characterisation. *Journal of Membrane Science* **181**, 253 (2001b).

Bowen, W. R. and Welfoot, J. S.: Modelling the performance of membrane nanofiltration - critical assessment and model development. *Chemical Engineering Science* **57**, 1121 (2002a).

Bowen, W. R. and Welfoot, J. S.: Modelling of membrane nanofiltration - pores size distribution effects. *Chemical Engineering Science* **57**, 1393 (2002b).

Cao, X.: in Colloid and interface aspects of ultrafiltration. *PhD Thesis* (University of Wales Swansea, 1994)

Childress, A. E. and Deshmukh, S. S.: Effect of humic substances and anionic surfactants and the surface charge and performance of RO membranes. *Desalination* **118**, 167 (1998).

Cho, J., Amy, G., Pellegrino, J. and Yoon, Y.: Characterisation of clean and natural organic matter (NOM) fouled NF and UF membranes, and foulants characterisation. *Desalination* **118**, 101 (1998).

Deen, W. M., Satvat, B. and Jamieson, J. M.: Theoretical model for glomerular filtration of charged solutes. *American Physiological Society (Renal Fluid Electrolyte Physiology)* **238**, F126 (1980).

Deen, W. M.: Hindered transport of large molecules in liquid filled pores. *AIChE Journal* **33** (1987).

Dey, T., Ramachandhran, V. and Misra, B.: Selectivity of anionic species in binary mixed electrolyte systems for nanofiltration membranes. *Desalination* **127**, 165 (2000).

Donnan, F. G.: Theory of membrane equlibria and membrane potentials in the presence of non-dialysing electrolytes. A contribution to physical-chemcial physiology. *Journal of Membrane Science* **100**, 45 (1995).

Dow-Filmtec. Seawater sulphate removal with filmtec SR90 nanofiltration membranes (Company Brochure, 1999).

Dresner, L.: Some remarks on the integration of the extended Nernst-Planck equations in the hyperfiltration of multicomponent solutions. *Desalination* **10**, 27 (1972).

Dresner, L. and Johnson, J. S.: in *Principles of desalination* (eds. Spiegler, K. S. and Laird, A. D. K.) 401 (Academic Press, 1980).

Dubois, M., Gilles, K., Hamilton, J., Rebers, P. and Smith, F.: Colourimetric method for determination of sugars and related substances. *Analytical Chemistry* **28**, 350 (1956).

Eriksson, P.: Nanofiltration extends the range of membrane filtration. *Environmental Progress* **7** (1988).

Eykamp, W.: in *Perry's chemical engineers' handbook* (ed. Henry, J. D.) 22 (McGraw-Hill, 1998).

Ferry, J. D.: Statistical evaluation of sieve constants in ultrafiltration. *Journal of General Physiology* **20**, 95 (1936).

Freger, V., Arnot, T. and Howell, J.: Separation of concentrated organic/inorganic salt mixtures by nanofiltration. *Journal of Membrane Science* **178**, 185 (2000).

Geraldes, V., Semiao, V. and Pinho, M. N. D.: Flow and mass transfer modelling of nanofiltration. *Journal of Membrane Science* **191**, 109 (2001).

Gerard, R., Hachisuka, H. and Hirose, M.: New membrane developments expanding the horizon for the application of reverse osmosis technology. *Desalination* **119**, 47 (1998).

Gilron, J., Gara, N. and Kedem, O.: Experimental analysis of negative salt rejection in nanofiltration membranes. *Journal of Membrane Science* **185**, 223 (2001).

Glueckstern, P. and Priel, M.: Advanced concept of large seawater desalination systems for Israel. *Desalination* **119**, 33 (1998).

Goosen, M. F., Sablani, S. S., Al-Maskari, S. S., Al-Belushi, R. H. and Wilf, M.: Effect of feed temperature on permeate flux and mass transfer. *Desalination* **144**, 267 (2002).

Goubert, J.-P.: *The conquest of water* (Polity Press, 1986).

Hendrickson, J. B., Cram, D. J. and Hammond, G. S.: *Organic chemistry* (McGraw-Hill Kogakusha, Tokyo, 1970).

Hodge, A. T.: *Roman aqueducts and water supply* (Duckworth, London, 1992).

Hoffer, E. and Kedem, O.: Hyperfiltration in charged membranes: The fixed charge model. *Desalination* **2** (1967).

Hofman, J. A. M. H., Noij, T. and Schippers, J.: Removal of pesticides and other organic micropollutants with membrane filtration. *Water Supply* **11**, 129 (1993).

Hofman, J. A. M. H., Beerendonk, E. F., Folmer, H. C. and Kruithof, J. C.: Removal of pesticides and other micropollutants with cellulose-acetate, polyamide and ultra-low pressure reverse osmosis membranes. *Desalination* **113**, 209 (1997).

Holden, P.: Anglian water membrane hybrid system for the soft drinks industry. *Desalination* **118**, 267 (1998).

International critical tables 429 (McGraw-Hill N.Y., 1929).

Jenkins, M. and Tanner, M. B.: Operational experience with new fouling resistant reverse osmosis membrane. *Desalination* **119**, 243 (1998).

Jitsuhara, I. and Kimura, S.: Structure and properties of charged ultrafiltration membranes made of sulphonated polysulphone. *Journal of Chemical Engineering of Japan* **16**, 389 (1983a).

Jitsuhara, I. and Kimura, S.: Rejection of inorganic salts by charged ultrafiltration membranes made of sulphonated polysulphone. *Journal of Chemical Engineering of Japan* **16**, 394 (1983b).

Kedem, O. and Katchalsky, A.: Thermodynamic analysis of the permeability of biological membranes to non-electrolytes. *Biochimica et Biophysica acta* **27**, 229 (1958).

Kiely, G.: *Environmental engineering* (McGraw-Hill, 1997).

Kim, I.-C., Lee, K.-h. and Tak, T.-M.: Preparation and characterisation of integrally skinned uncharged polyetherimide asymmetric nanofiltration membrane. *Journal of Membrane Science* **183**, 235 (2001).

Kiso, Y., Kitao, T., Jinno, K. and Miyagi, M.: The effects of molecular width on permeation of organic solute through cellulose acetate reverse osmosis membranes. *Journal of Membrane Science* **74**, 95 (1992).

Kiso, Y., Nishimura, Y., Kitao, T. and Nishimura, K.: Rejection properties of non-phenylic pesticides with nanofiltration membranes. *Journal of Membrane Science* **171**, 229 (2000).

Kiso, Y., Kon, T., Kitao, T. and Nishimura, K.: Rejection properties of alkyl phthalates with nanofiltration membranes. *Journal of Membrane Science* **182**, 205 (2001).

Koenders, M. A., Reymann, S. and Wakeman, R. J.: The intermediate stage of the dead-end filtration process. *Chemical Engineering Science* **55**, 3715 (2000).

Koyuncu, I. and Topacik, D.: Effect of organic and inorganic matter on pesticide rejection by nanofiltration. *Journal of Membrane Science* **195**, 247 (2002).

Laros, T.: in *Perry's chemical engineers handbook* (eds. Perry, R. H. and Green, D. W.) 18 (McGraw-Hill, New York, 1999).

Lee, S., Kim, J. and Lee, C.-H.: Analysis of $CaSO_4$ scale formation mechanism in various nanofiltration modules. *Journal of Membrane Science* **163**, 63 (1999).

Lee, S. and Lueptow, R. M.: Reverse osmosis filtration for space mission wastewater: Membrane properties and operating conditions. *Journal of Membrane Science* **182**, 77 (2001).

Levenstein, R., Hasson, D. and Semiat, R.: Utilisation of the Donnan effect for improving electrolyte separation with nanofiltration membranes. *Journal of Membrane Science* **116**, 77 (1995).

Levine.: Physical chemistry., (1988).

Linder, C. and Kedem, O.: Asymmetric ion exchange mosaic membranes with unique selectivity. *Journal of Membrane Science* **181**, 39 (2000).

Lonsdale, H. K., Pusch, W. and Walch, A.: Donnan-membrane effects in hyperfiltration of ternary systems. *Journal of the Chemistry Society Faraday Transcipts 1* **71**, 501 (1974).

Lonsdale, H. K.: The evolution of ultrathin synthetic membranes. *Journal of Membrane Science* **33**, 121 (1987).

Magara, Y., Tabata, A., Kohki, M., Kawasaki, M. and Hirose, M.: Development of a boron reduction system for seawater desalination. *Desalination* **118**, 25 (1998).

Marsh, N., Howard, J., Rybar, S., Finlayson, F. and Linstrum, A.: The largest seawater plant in Great Britain. *Desalination* **118**, 53 (1998).

Matsuura, T.: Progress in membrane science and technology for seawater desalination - a review. *Desalination* **134**, 47 (2001).

Mohammed, A. W. and Takriff, M.: Prediciting flux and rejection of multicomponent salt mixtures in nanofiltration. *Desalination* **157**, 105 (2003).

Murrer, J. and Rosberg, R.: Desalting of seawater using UF and RO - results of a pilot study. *Desalination* **118**, 1 (1998).

Nabetani, H., Nakajima, M. and Watanabe, A.: Development of a new type of membrane osmometer. *Journal of Chemical Engineering of Japan* **25**, 269 (1992).

Nakao, S.-I. and Kimura, S.: Analysis of solutes rejection in ultrafiltration. *Journal of Chemical Engineering of Japan* **14**, 32 (1981).

Nakao, S.-I. and Kimura, S.: Models of membrane transport phenomena and their applications for ultrafiltration data. *Journal of Chemical Engineering of Japan* **15**, 200 (1982).

Nemeth, J. E.: Innovative system designs to optimise performance of ultra-low pressure reverse osmosis membranes. *Desalination* **118**, 63 (1998).

Ozaki, H. and Li, H.: Rejection of organic compounds by ultra-low pressure reverse osmosis membrane. *Water Research* **36**, 123 (2002).

Peeters, J. M. M., Mulder, M. H. V. and Strathmann, H.: Streaming potential measurements as a characterisation method for nanofiltration membranes. *Colloids and Surfaces A* **150**, 247 (1999).

Pentz, M. and Shott, M.: *Handling experimental data* (ed. Aprahamian) (Open University Press, Milton Keynes, 1988).

Perry, M. and Linder, C.: Intermediate reverse osmosis ultrafiltration (RO UF) membranes for concentration and desalting of low molecular weight organic solutes. *Desalination* **71**, 233 (1989).

Peters, T. A.: Purification of landfill leachate with reverse osmosis and nanofiltration. *Desalination* **119**, 289 (1998).

Pontalier, P.-Y., Ismail, A. and Ghoul, M.: Specific model for nanofiltration. *Journal of Food Engineering* **40**, 145 (1999).

Probstein, R. F., Sonin, A. A., Yung, D. and Jacazio, G.: Electrokinetic salt rejection in hyperfiltration through porous materials. Theory and experiment. *The Journal of Physical Chemistry* **76**, 4015 (1972).

Probstein, R. F., Sonin, A. A. and Yung, D.: Brakish water salt rejection by porous hyperfiltration membranes. *Desalination* **13**, 306 (1973).

Raman, L. P., Cheryan, M. and Rajagopalan, N.: Consider nanofiltration for membrane separations. *Chemical Engineering Progress* **90**, 68 (1994).

Schaep, J., Van der Bruggen, B., Uytterhoeven, S., Croux, R., Vandecasteele, C., Wilms, D., Van Houtte, E. and Vanlerberghe, F.: Removal of hardness from groundwater by nanofiltration. *Desalination* **119**, 295 (1998).

Schaep, J. and Vandecasteele, C.: Evaluating the charge of nanofiltration membranes. *Journal of Membrane Science* **188**, 129 (2001).

Schaep, J., Vandecasteele, C., Mohammed, A. W. and Bowen, W. R.: Modelling the retention of ionic components for different nanofiltration membranes. *Separation and Purification Technology* **22-23**, 169 (2001).

Schirg, P. and Widmer, F.: Characterisation of nanofiltration membranes for the separation of aqueous dye-salt solutions. *Desalination* **89**, 89 (1992).

Schlogl, R.: Membrane permeation in systems far from equilibrium. *Berichte der Bunsengesellschaft* **70**, 400 (1966).

Sinnot, R.: *Chemical engineering design* (eds. Coulson, J. and Richardson, J.) (Butterworth-Heinmann Ltd, Oxford, 1993).

Sojka-Ledakowicz, J., Koprowski, T., Machnowski, W. and Knudsen, H. H.: Membrane filtration of textile dyehouse wastewater for technological water reuse. *Desalination* **119**, 1 (1998).

Soltanieh, M. and Sahebdelfar, S.: Interaction effects in mulicomponent separation by reverse osmosis. *Journal of Membrane Science* **183**, 15 (2001).

Sourirajan, S.: *Reverse osmosis* (Academic Press, New York, 1970).

Spiegler, K. S. and Kedem, O.: Thermodynamics of hyperfiltration (reverse osmosis): Criteria for efficient membranes. *Desalination* **1**, 311 (1966).

Sutzkover, I., Hasson, D. and Semiat, R.: Simple technique for measuring the concentration polarisation level in a reverse osmosis system. *Desalination* **131**, 117 (2000).

Tsuru, T., Nakao, S.-I. and Kimura, S.: Effective charge density and pore structure of charged ultrafiltration membranes. *Journal of Chemical Engineering of Japan* **23**, 604 (1990).

Tsuru, T., Nakao, S.-I. and Kimura, S.: Calculation of ion rejection by extended Nernst-Planck equation with charged reverse osmosis membranes for single and mixed electrolyte solutions. *Journal of Chemical Engineering of Japan* **24**, 511 (1991).

Tu, S.-C., Ravindran, V., Den, W. and Pirbazari, M.: Predictive membrane transport model for nanofiltration processes in water treatment. *AIChE Journal* **47**, 1346 (2001).

Van der Bruggen, B., Schaep, J., Maes, W., Wilms, D. and Vandercasteele, C.: Nanofiltration as a treatment method for the removal of pesticides from ground waters. *Desalination* **117**, 139 (1998).

Van der Bruggen, B., Schaep, J., Wilms, D. and Vandecasteele, C.: Influence of molecular size, polarity and charge on the retention of organic molecules by nanofiltration. *Journal of Membrane Science* **156**, 29 (1999).

Van der Bruggen, B., Schaep, J., Wilms, D. and Vandercasteele, C.: A comparison of models to describe the maximal retention of organic molecules in nanofiltration. *Separation Science and Technology* **35**, 169 (2000).

Van der Bruggen, B. and Vandecasteele, C.: Modelling of the retention of uncharged molecules with nanofiltration. *Water Research* **36**, 1360 (2002).

van der Meer, W. G. J., Riemersma, M. and van Dijk, J. C.: Only two membrane modules per pressure vessel? Hydraulic optimisation of spiral-wound membrane filtration plants. *Desalination* **119**, 57 (1998).

Vellenga, E. and Tragardh, G.: Nanofiltraion of combined salt and sugar solutions: Coupling between retentions. *Desalination* **120**, 211 (1998).

Ventresque, C., Gisclon, V., Bablon, G. and Chagneau, G.: An outstanding feat of modern technology: The mery-sur-oise nanofiltration treatment plant (340,000 m^3/d). *Desalination* **131**, 1 (2000).

Vrouwenvelder, H. S., van Paassen, J. A. M., Folmer, H. C., Hofman, J. A. M. H., Nederlof, M. M. and van der Kooij, D.: Biofouling of membranes for drinking water production. *Desalination* **118**, 157 (1998).

Wang, X.-L., Tsuru, T., Nakao, S.-I. and Kimura, S.: The electrostatic and steric-hindrance model for the transport of charged solutes through nanofiltration membranes. *Journal of Membrane Science* **135**, 19 (1997).

Wang, X.-L., Zhang, C. and Ouyang, P.: The possibility of separating saccharides from a NaCl solution by using nanofiltration in diafiltration mode. *Journal of Membrane Science* **204**, 271 (2002).

Wardle, A.: in *Chemical & biochemical reactors & process control* (eds. Richardson, J. and Peacock, D.) (Pergamon, 1994).

Weißbrodt, J., Manthey, M., Ditgens, B., Laufenberg, G. and Kunz, B.: Separation of aqueous organic multicomponent solutions by reverse osmosis - development of a mass transfer model. *Desalination* **133**, 65 (2001).

Welfoot, J. S.: in Predictive modelling of membrane nanofiltration. *PhD Thesis* (University of Wales Swansea, 2001)

Wittmann, E., Cote, P., Medici, C., Leech, J. and Turner, A. G.: Treatment of hard borehole water containing low levels of pesticide by nanofiltration. *Desalination* **119**, 347 (1998).

Yaroshchuk, A. E.: Rejection of single salts versus transmembrane volume flow in RO/NF: Thermodynamic properties, model of constant coefficients, and its modification. *Journal of Membrane Science* **198**, 285 (2002).

Yeom, C. K., Lee, S. H. and Lee, J. M.: Effect of ionic characteristics of charged membranes on the permeation of anionic solutes in reverse osmosis. *Journal of Membrane Science* **169**, 237 (2000).

Zander, A. K. and Curry, N. K.: Membrane and solution effects on solute rejection and productivity. *Water Research* **35**, 4426 (2001).

Appendix

A.1 Error in glucose analysis

A.1.1 Accumulated error

Table A.1-1 contains error margins attributed to the equipment used for the phenol-sulphuric acid method for saccharide analysis.

Source of error	Maximum condition	Actual error	Units
Variable pipette	1	0.006	ml
Volumetric flask	10	0.025	ml
Variable pipette	5	0.030	ml
Spectrophotometer	2.000	0.005	Absorbance (arbitrary)

Table A.1-1Error sources and magnitudes for saccharide analysis using the phenol-sulphuric acid method

Experimental samples typically contained 0.5 g/L of glucose therefore this will be used as a basis for an example of the error calculation.

i) 1ml of sample is diluted in 10 ml of pure water to present it to the reagents as a 50 mg/L solution. Standard error equations have been presented by Pentz and Shott (Pentz and Shott, 1988)

If either of the following are true

$$X = AB \text{ or } kAB$$
$$X = A/B \text{ or } kA/B \tag{1.1}$$

then,

$$\frac{\Delta X}{X} = \sqrt{\left(\frac{\Delta A}{A}\right)^2 + \left(\frac{\Delta B}{B}\right)^2} \tag{1.2}$$

and if

$$X = kA \tag{1.3}$$

where k is constant, with no associated error, then

$$\Delta X = k\Delta A \tag{1.4}$$

So the dilution step can be represented by the following mathematics

$$\frac{0.5g/L \times 1ml}{10ml} = \frac{0.5g/L \times 0.001L}{0.01L} = 0.05g/L \text{ or } 50mg/L \qquad (1.5)$$

the error associated with this step is then determined according to equation (1.2) where ΔA and ΔB are the error margins for the 1 ml pipette and 10ml volumetric flask.

Use of equation (1.2) establishes an error value of $3.25*10^{-7}$ g/L.

The addition of reagents to 1 ml of sample containing 50 mg/L of glucose equates to another dilution step, ignoring the dilution effect as the colour formed at this stage is related directly to the 50 mg/L concentration, the error accumulated here can still be evaluated and found to be $2.34*10^{-5}$ g/L.

The final step that contributes error is the colour measurement in the spectrophotometer. The calibration curve presented in Appendix A-3 yields the following relationship between concentration and absorbance.

$$Abs = C \times 0.0118 \qquad (1.6)$$

the spectrophotometer reading error of ±0.005 equates to concentration error of ±0.000059 mg/L ($5.9*10^{-8}$ g/L) which equates 0.25% of the error accumulated during sample preparation. Taking this latter accumulated error value it is found to be 0.05% of the value it is associated and is therefore negligible.

A.1.2 Statistical error analysis

The three data sets used for the absorption calibration is shown in the following table (Table A.1-2). The final two columns in Table A.1-2 present, respectively, the average absorbance for each concentration and the absorbance values determined from the best-fit line of the average data points. A statistical calculation of the error

based on the mean absorbance values is given in Table A.1-3 and Table A.1-4 presents the results of the same error calculations based on the best-fit values.

	Absorption				
Conc. (mg/L)	**Data set 1**	**Data set 2**	**Data set 3**	**Mean**	**Best-fit**
10	0.099	0.095	0.096	0.097	0.093
30	0.273	0.225	0.287	0.262	0.279
50	0.456	0.459	0.42	0.445	0.465
70	0.661	0.603	0.723	0.662	0.651
100	0.95	0.927	0.923	0.933	0.930

Table A.1-2 Glucose absorption calibration data

Concentration	**Standard deviation**	**% Standard deviation**	**Standard error on the mean**	**% Standard error on the mean**
10	0.002	1.758	0.0012	1.243
30	0.027	10.15	0.0188	7.175
50	0.018	3.982	0.0125	2.816
70	0.049	7.398	0.0347	5.231
100	0.012	1.275	0.0084	0.901

Table A.1-3 Statistical error evaluation based on the mean

Concentration	**Standard deviation**	**% Standard deviation**	**Standard error on the mean**	**% Standard error on the mean**
10	0.004	4.346	0.0029	3.073
30	0.032	11.37	0.0224	8.036
50	0.027	5.746	0.0189	4.063
70	0.050	7.725	0.0356	5.463
100	0.012	1.329	0.0087	0.939

Table A.1-4 Statistical error evaluation based on the best-fit value

The standard error on the mean is defined as,

$$S_m = \frac{s}{\sqrt{n-1}} \tag{1.7}$$

where s is the standard deviation and n is the number of absorbance measurements. Therefore the average error is 3.5% if taken from the deviation from the mean or 4.3% when based on the deviation from the best-fit values.

Since rejection is determined from concentration according the relation,

$$R = 1 - \frac{c_p}{c_f} \tag{1.8}$$

then according to equation (1.4) and (1.6) the error associated with a –10% rejection is as follows. For rejection of –10% the feed and product concentrations can be assumed to be 50 and 55 mg/L respectively.

Feed

A 4.3% error on the absorbance measurement for the feed equates directly to an error of ±2.15 mg/L.

Product

A 4.3% error on the absorbance measurement for the product equates directly to an error of ±2.365 mg/L.

Thus the error on the rejection is found to be,

$$\Delta X = -0.1 \times \sqrt{\left[\left(\frac{2.365}{55}\right)^2 + \left(\frac{2.15}{50}\right)^2\right]} \tag{1.9}$$

$$\Delta X = -0.006$$

Therefore the error margin is ~0.6%.

A.2 Instrument Calibration curves

A.2.1 Pressure transducers

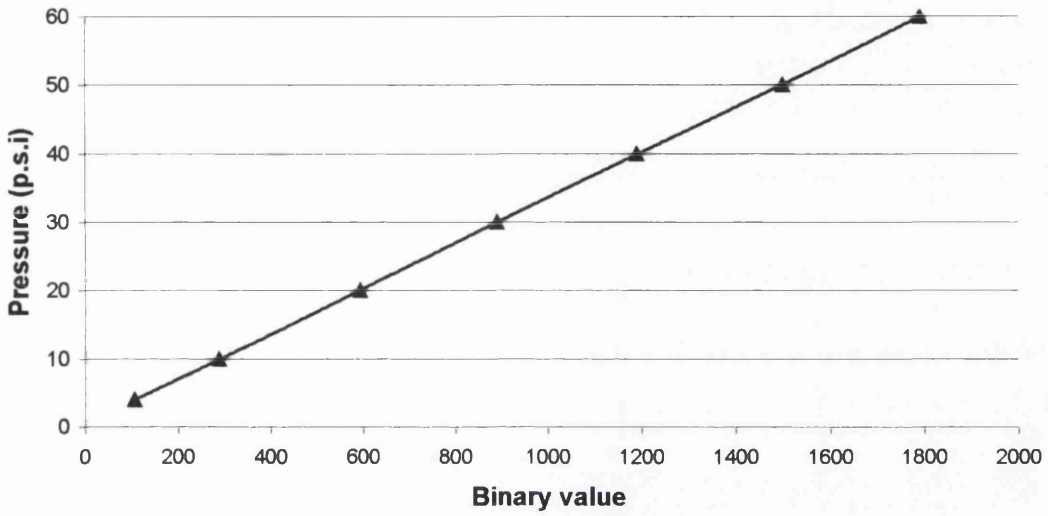

Figure A.2-1 Calibration curve for Sensym pressure sensor P2

Figures A.2-1 provides one of the calibration curves for the pressure transducers used on the experimental filtration equipment. The data points, manually measured in conjunction with a conventional bourdon pressure gauge, were fitted with a fourth order polynomial equation. The respective equations were used in the control and data-logging program to convert the bit readings to temperature values in °C.

P1: $y = 7.803E\text{-}10x^4 - 7.988E\text{-}07x^3 + 2.768E\text{-}04x^2 + 8.272E\text{-}02x + 6.257E+00$

P2: $y = 1.375E\text{-}12x^4 - 5.310E\text{-}09x^3 + 6.835E\text{-}06x^2 + 2.991E\text{-}02x + 8.475E\text{-}01$

A.2.2 Temperature measurement

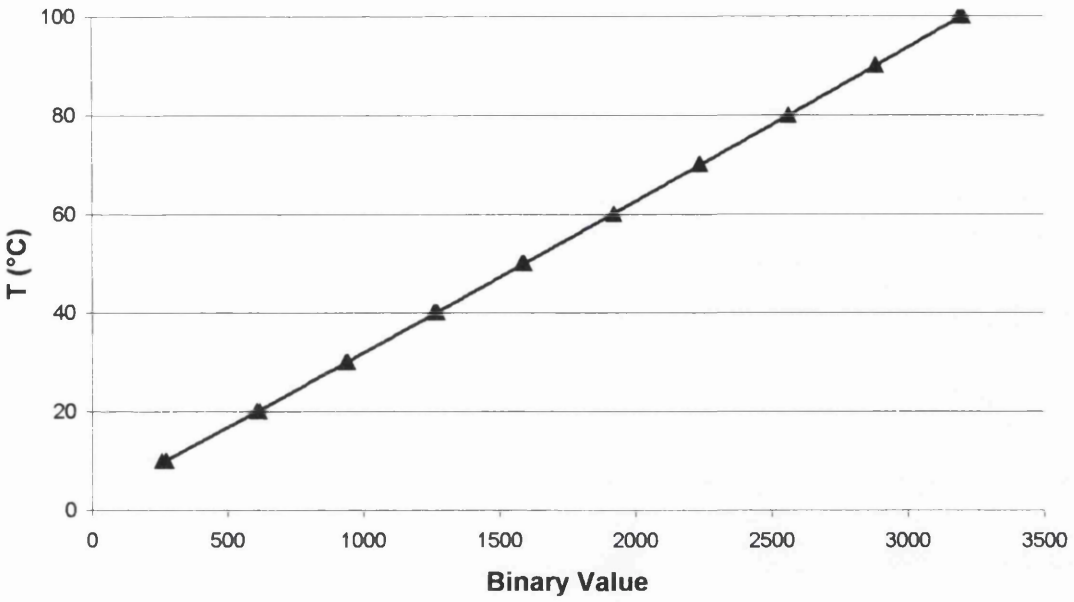

Figure A.2-2 Calibration curve for platinum resistance (Pt 100) thermometer T1

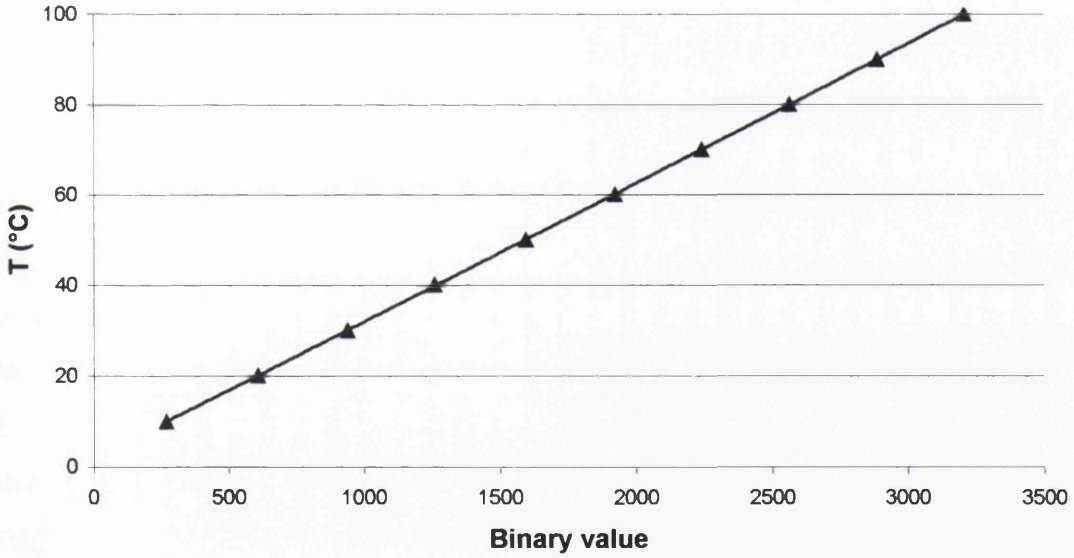

Figure A.2-3 Calibration curve for platinum resistance (Pt 100) thermometer T2

Figures A.2-2 and A.2-3 show the calibration curves for the Pt-100 platinum resistance thermometers. The voltage signal read received by the signal conditioning unit is generated using a Platinum resistance thermometer replicator, which is made possible due to the standard behaviour of Pt-100 thermometers. The fourth order polynomials used in the data logging and control software to convert from bit signals to real temperature values are presented below.

T1: $y = 8.085E\text{-}14x^4 - 6.090E\text{-}10x^3 + 1.815E\text{-}06x^2 + 2.835E\text{-}02x + 2.213E+00$

T2: $y = 3.410E\text{-}14x^4 - 2.623E\text{-}10x^3 + 9.180E\text{-}07x^2 + 2.918E\text{-}02x + 2.060E+00$

A.2.3 Flow Measurement

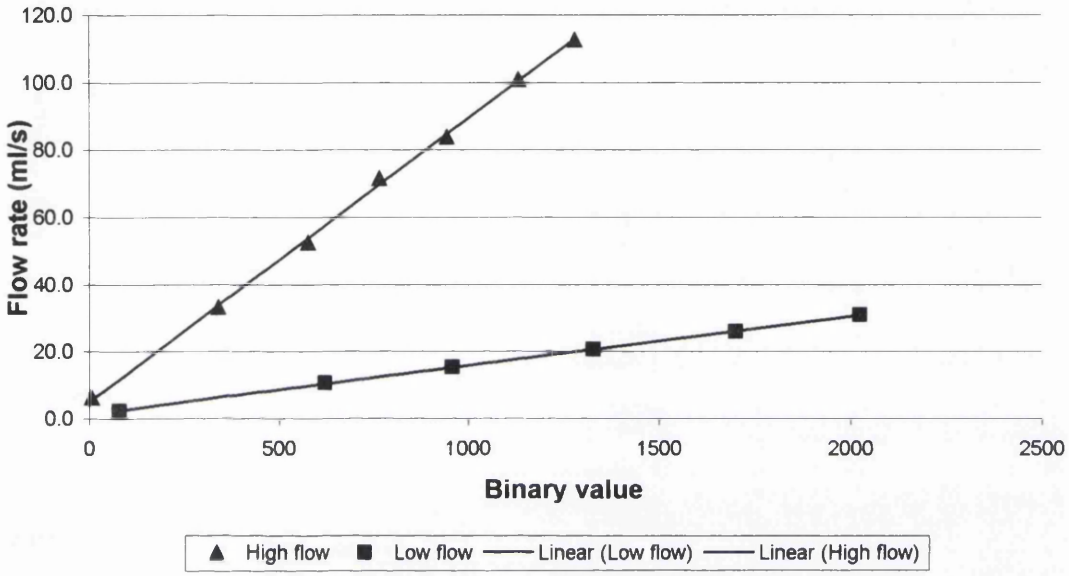

Figure A.2-4 Calibration plot for Hall effect flow meter F1

The flow meter has two modes of operation as illustrated by the two data sets on Figure A.2-4. The low-flow mode was achieved by introducing a grommet into the flow line that reduced the area for flow and increased the velocity of fluid entering the paddle wheel chamber. The main advantage of this mode of operation was an increased sensitivity and accuracy for the measurement of low flows. The low-flow arrangement was employed in this work and the equation used in the control and data-logging program to convert from a binary signal to volumetric flowrate (ml/s) is shown below.

F1: $y = 0.0146x + 1.288$

A.3 Chemical analysis calibration curves

A.3.1 Saccharides

Glucose

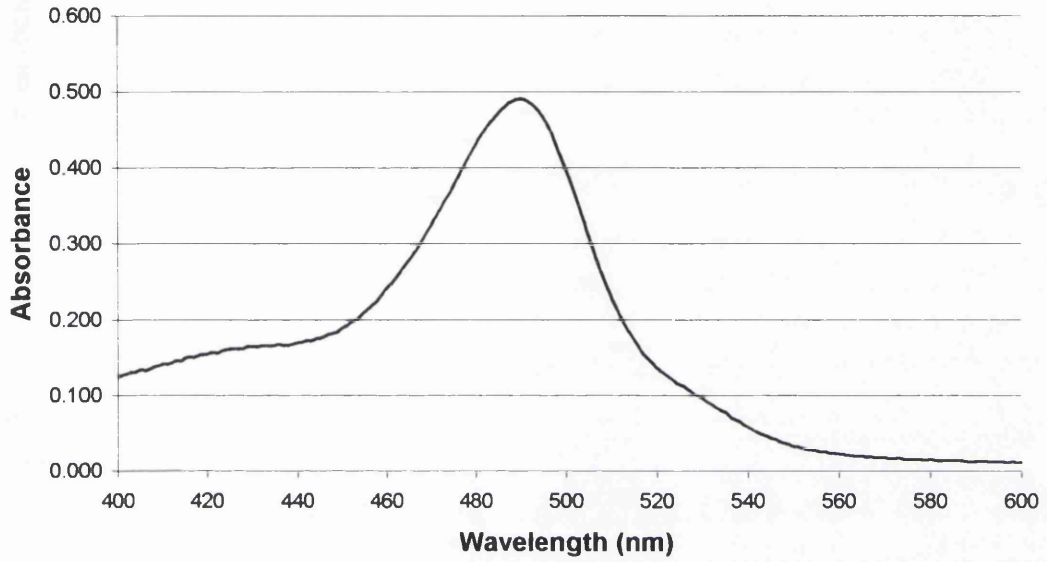

Figure A.3-1 Absorption scan peak for glucose prepared using the phenol-sulphuric acid method

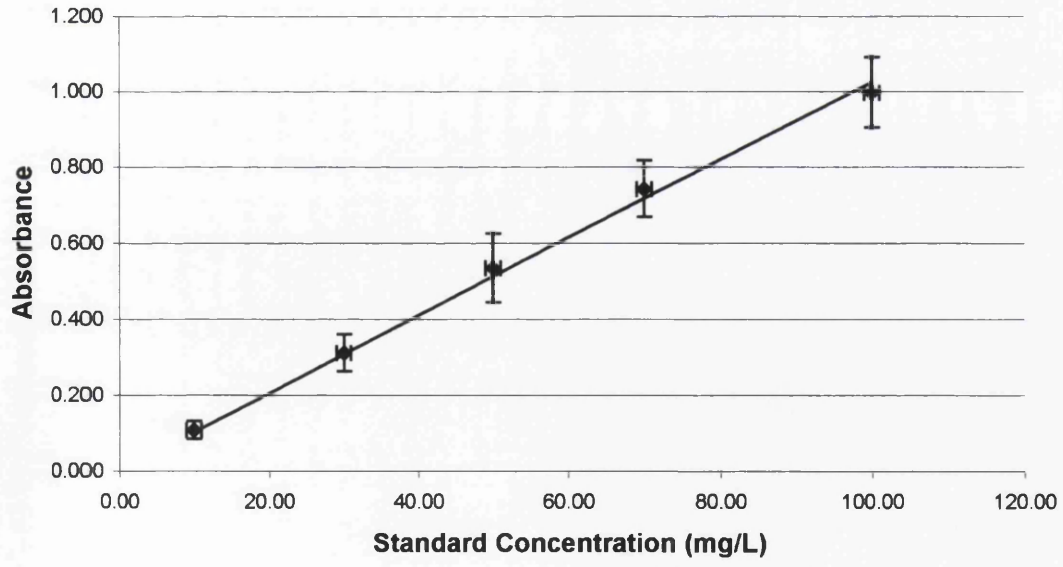

Figure A.3-2 Calibration plot for glucose prepared using the phenol-sulphuric acid analysis technique

Raffinose

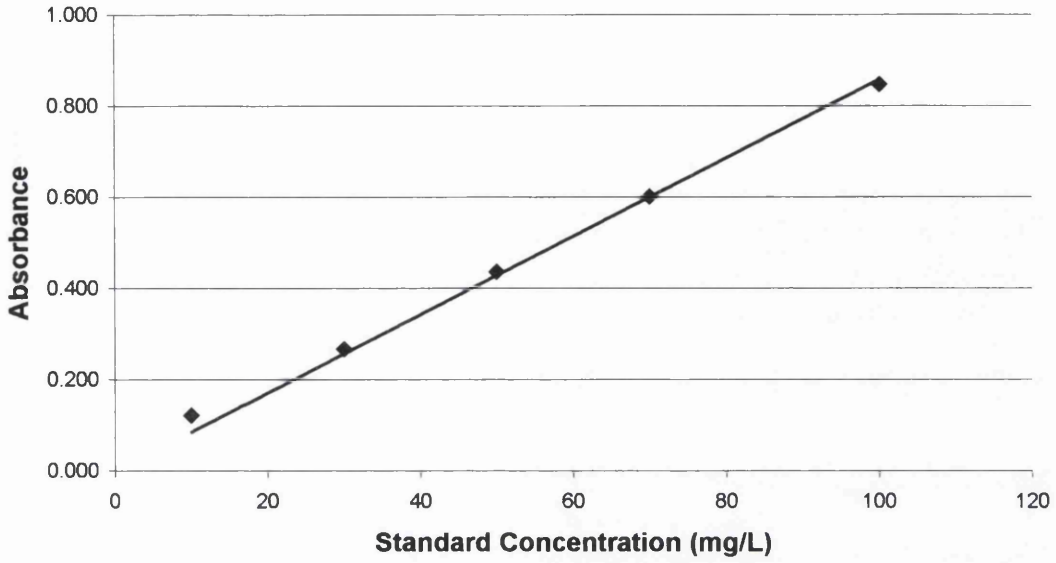

Figure A.3-3 Calibration plot for Raffinose prepared using the phenol-sulphuric acid analysis technique

A.3.2 Substances with absorptions in the UV region

Phenol

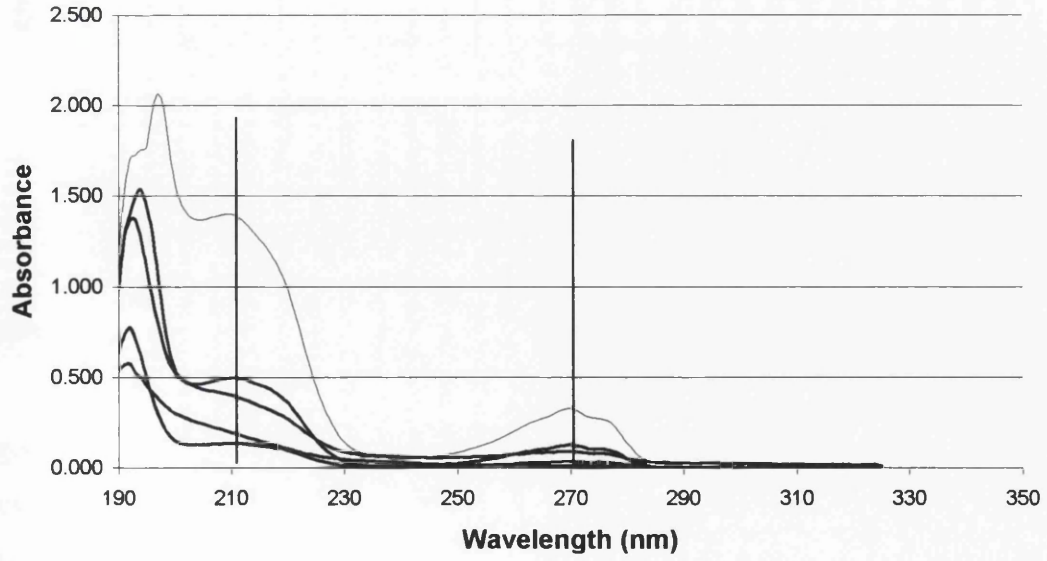

Figure A.3-4 UV-Absorption scans showing multiple peaks for Phenol

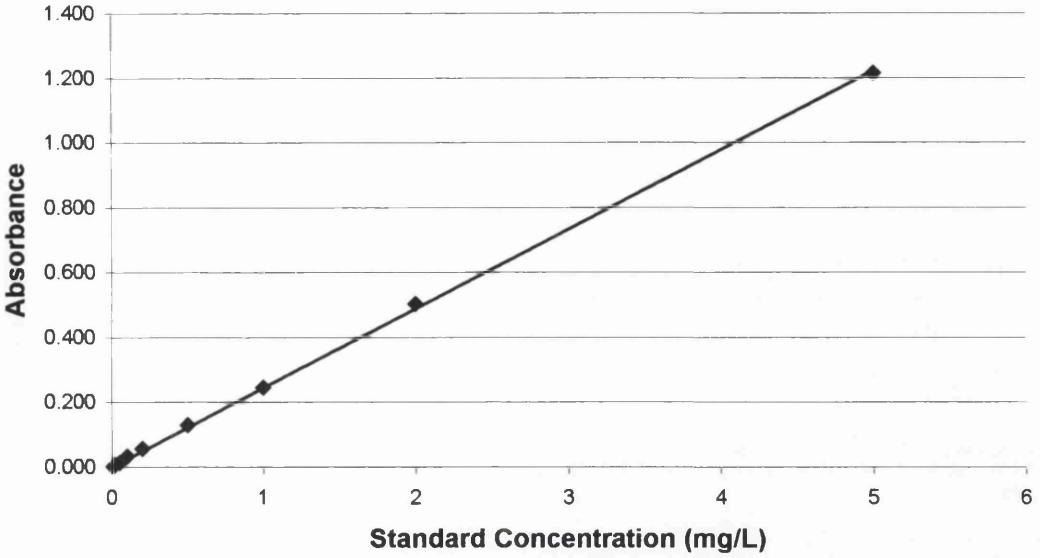

Figure A.3-5 Calibration plot for Phenol using UV-absorbance at 210nm

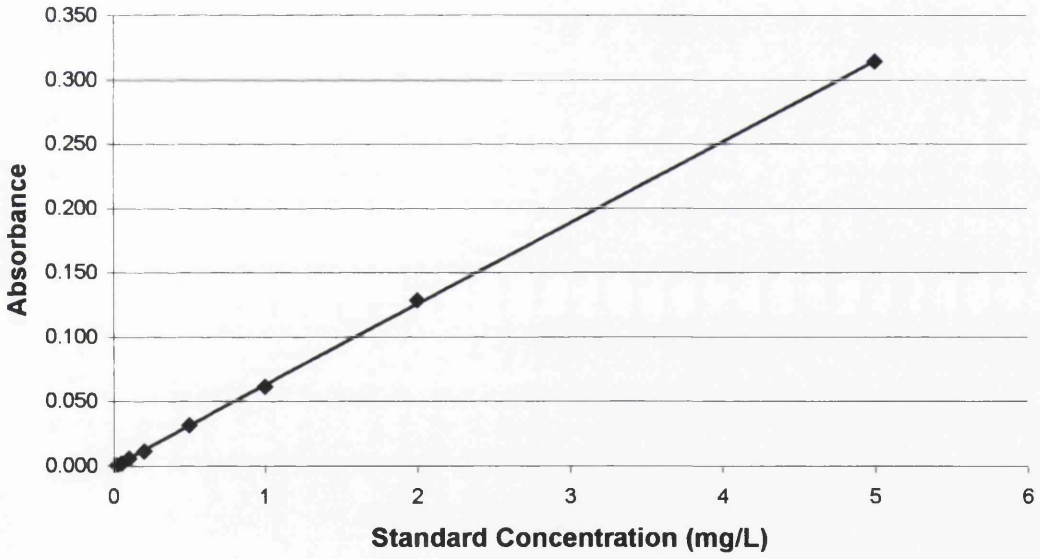

Figure A.3-6 Calibration plot for Phenol using UV-absorbance at 270nm

Figures A.3-5 & A.3-6 show the two possible calibration curves for phenol due to the presence of two peaks in the UV absorption scan. Deviation from the line of best fit is least for the calibration at 270nm so this was used for experimental phenol concentration analysis.

2,4,6-trichlorophenol

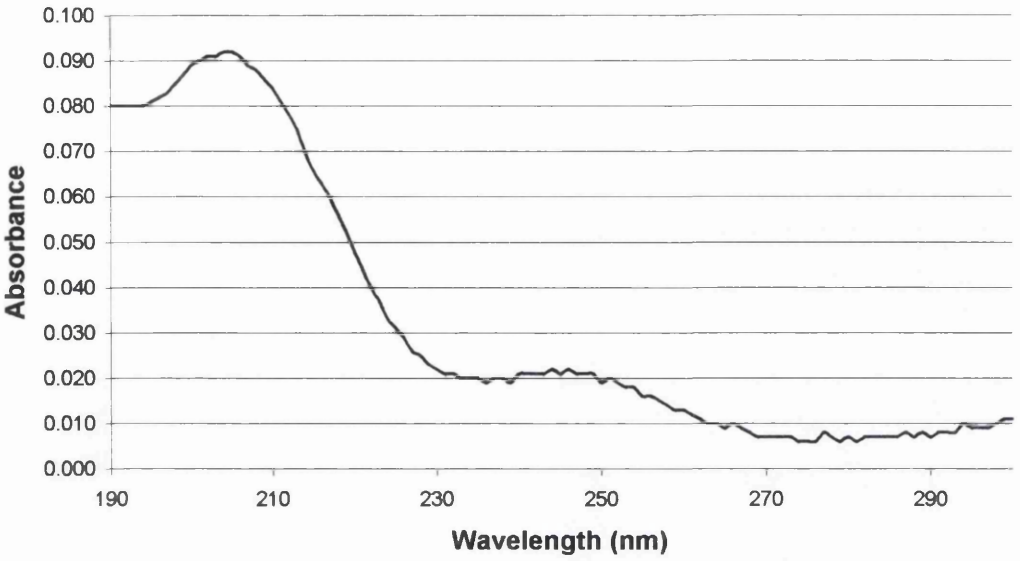

Figure A.3-7 UV-Absorption scans showing multiple peaks for 2,4,6-trichlorophenol

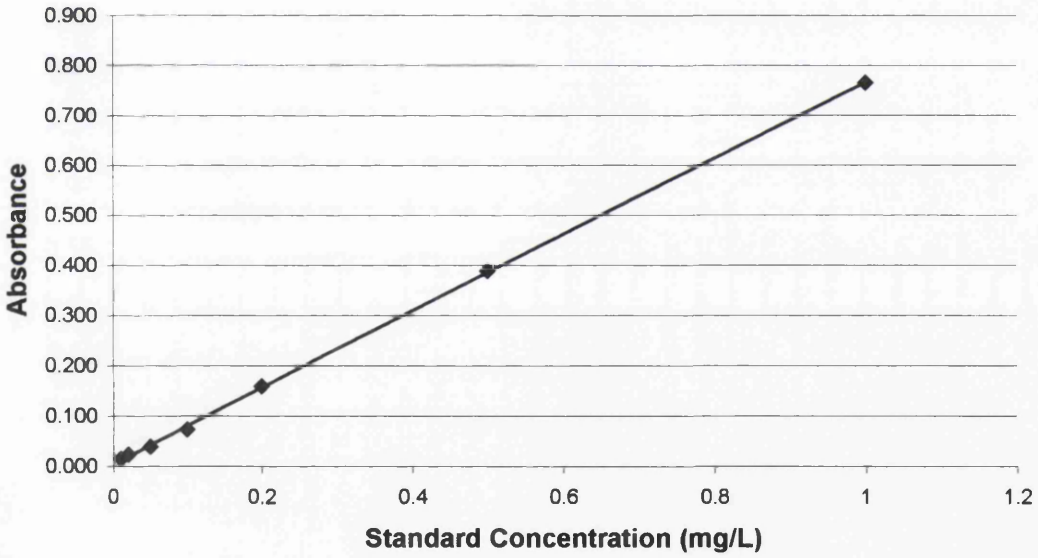

Figure A.3-8 Calibration plot for 2,4,6-trichlorophenol using UV-absorbance at 202nm

Benzoic Acid

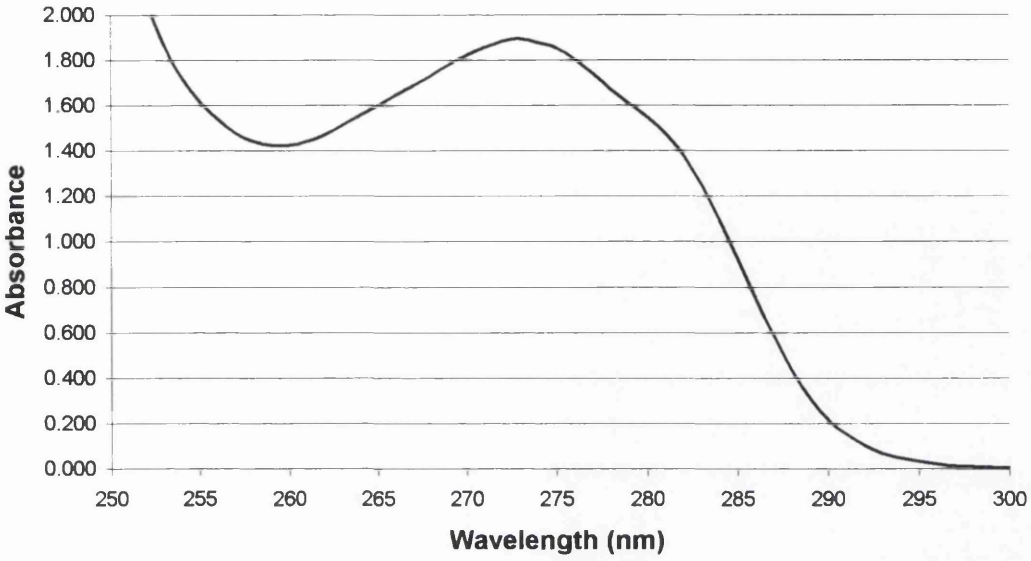

Figure A.3-9 UV-Absorption scans showing peak for Benzoic acid

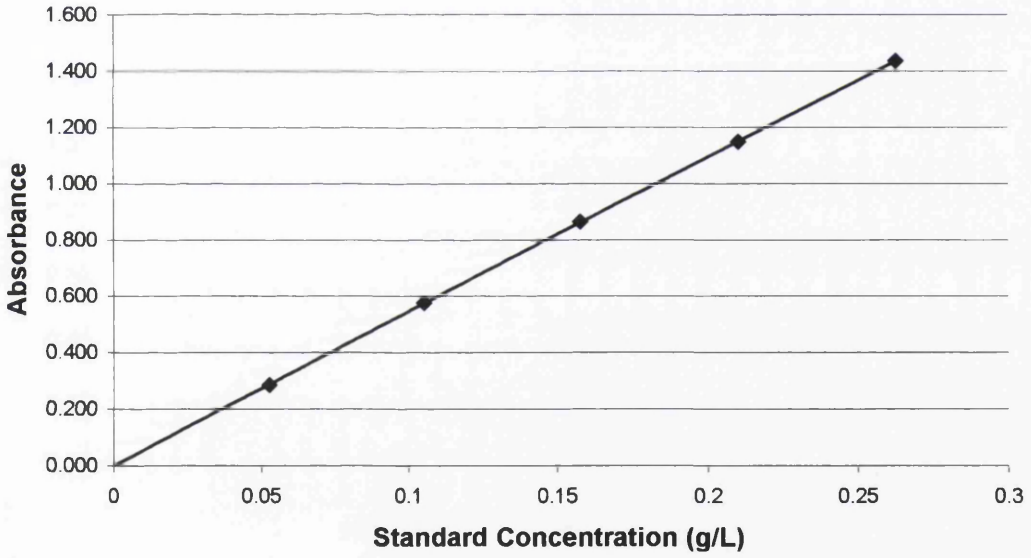

Figure A.3-10 Calibration plot for Benzoic acid using UV-absorbance at 273nm

Phenylalanine

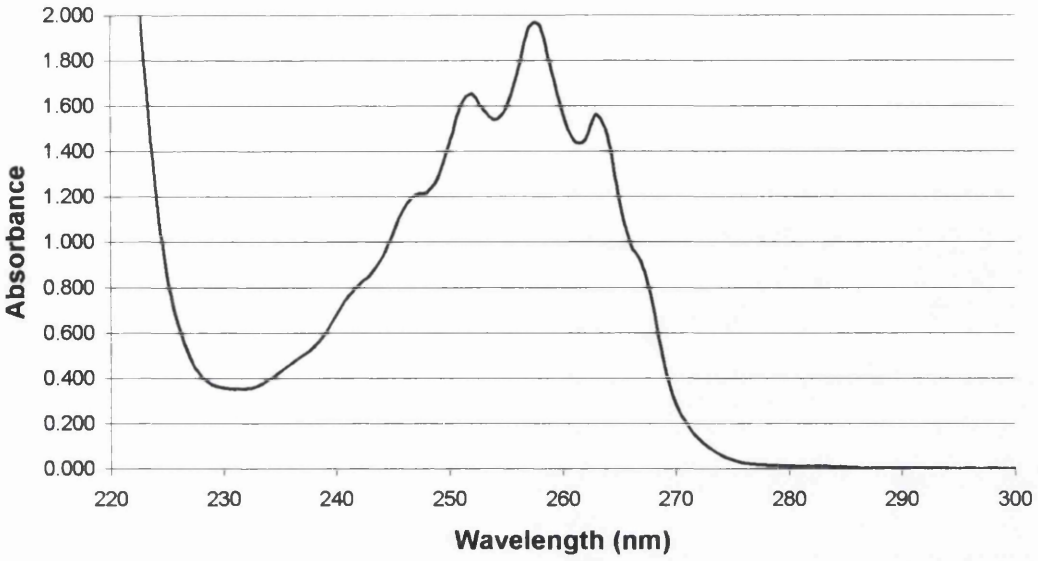

Figure A.3-11 UV-Absorption scans showing multiple peaks for Phenylalanine

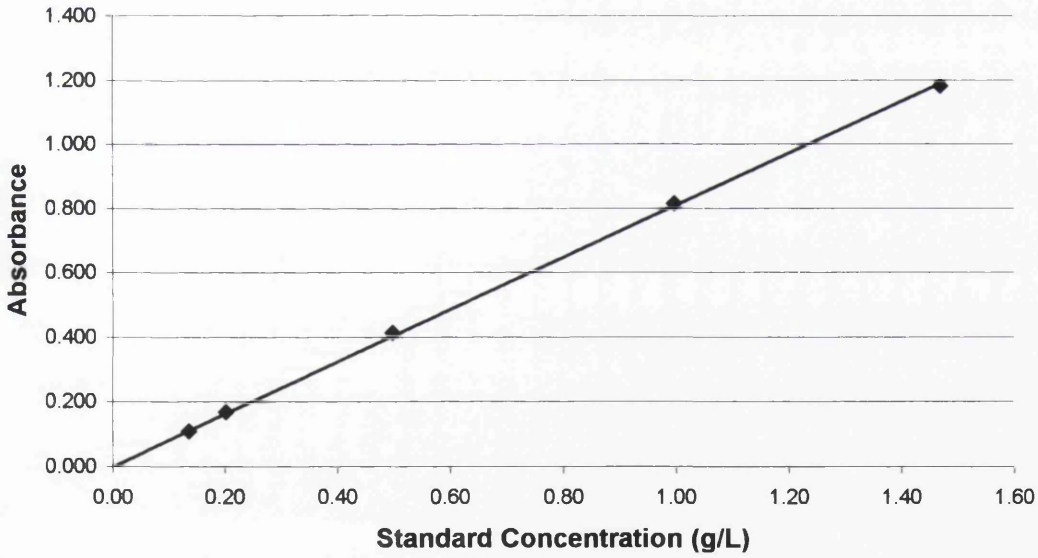

Figure A.3-12 Calibration plot for Phenylalanine using UV-absorbance at 258nm

Aniline

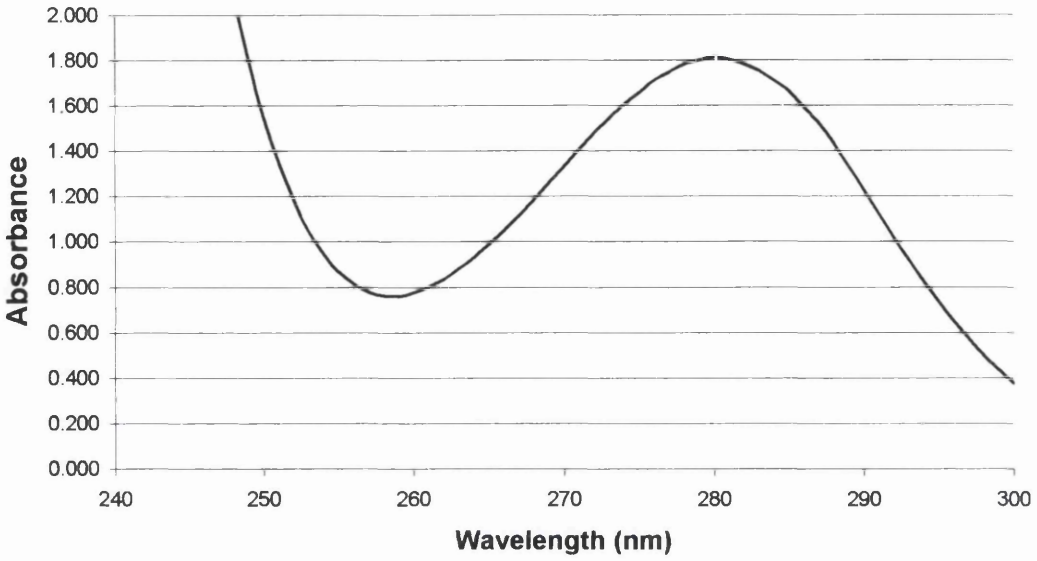

Figure A.3-13 UV-Absorption scans showing peak for Aniline

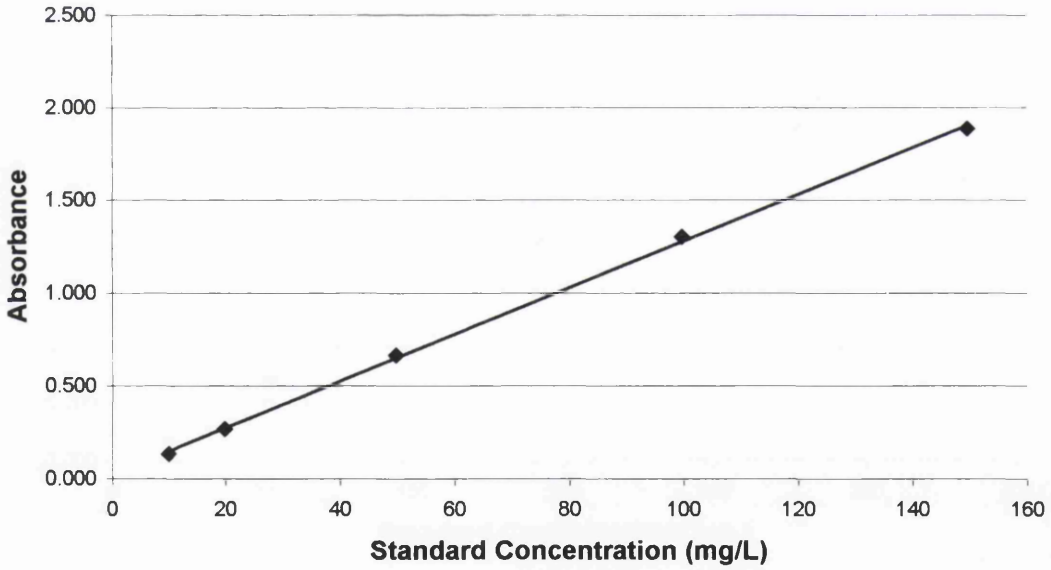

Figure A.3-14 Calibration plot for Aniline using UV-absorbance at 281nm

Benzyl alcohol

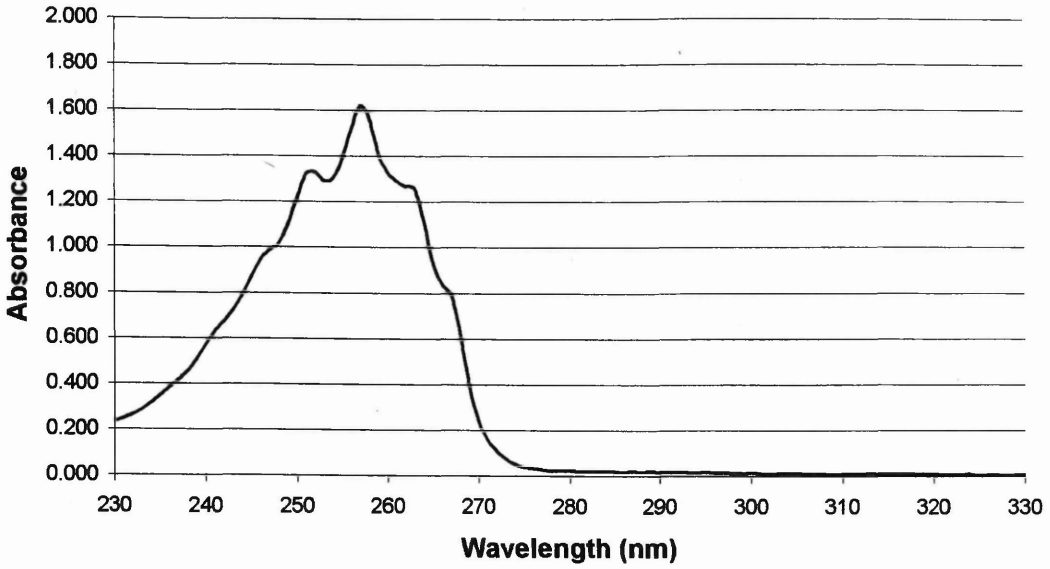

Figure A.3-15 UV-Absorption scans showing multiple peaks for Benzyl alcohol

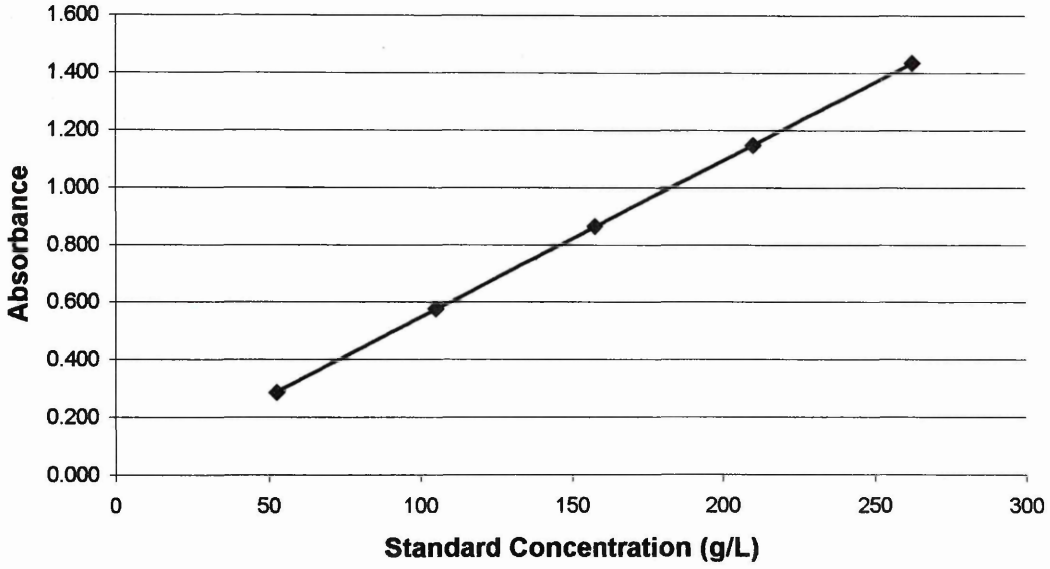

Figure A.3-16 Calibration plot for Benzyl alcohol using UV-absorbance at 257nm

Benzylamine

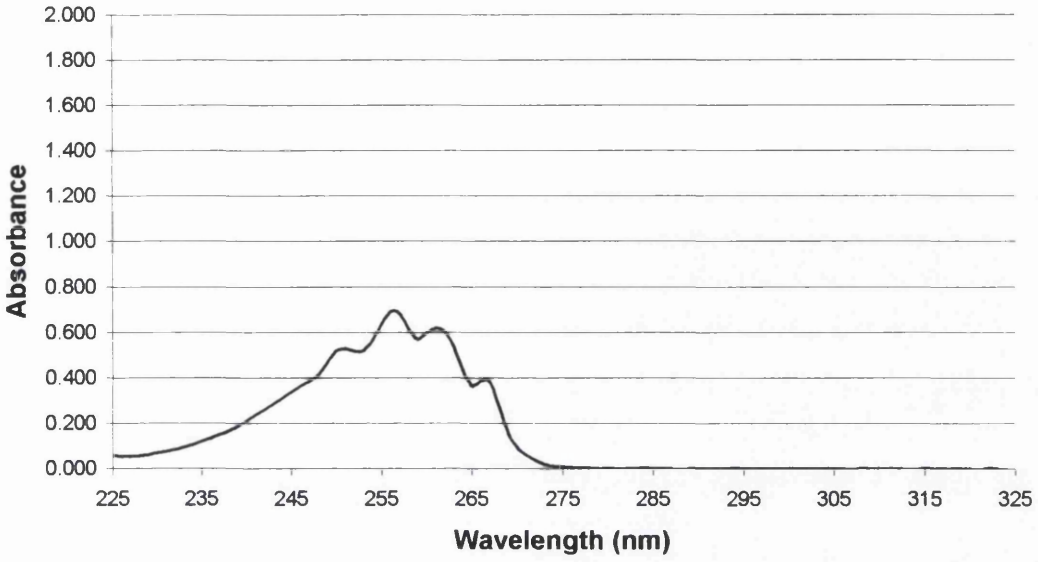

Figure A.3-17 UV-Absorption scans showing multiple peaks for Benzylamine

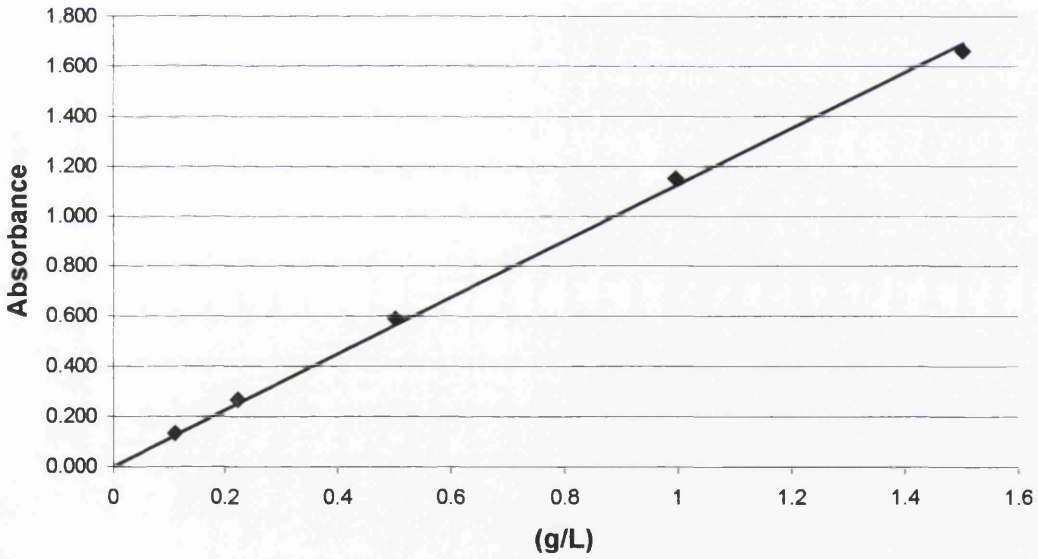

Figure A.3-18 Calibration plot for Benzylamine using UV-absorbance at 256nm

Caffeine

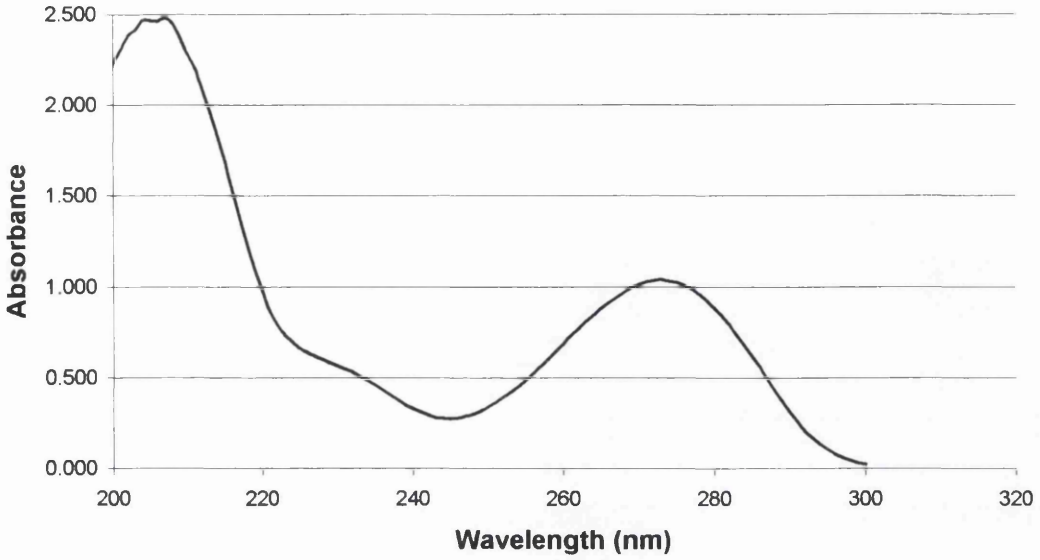

Figure A.3-19 UV-Absorption scans showing multiple peaks for Caffeine

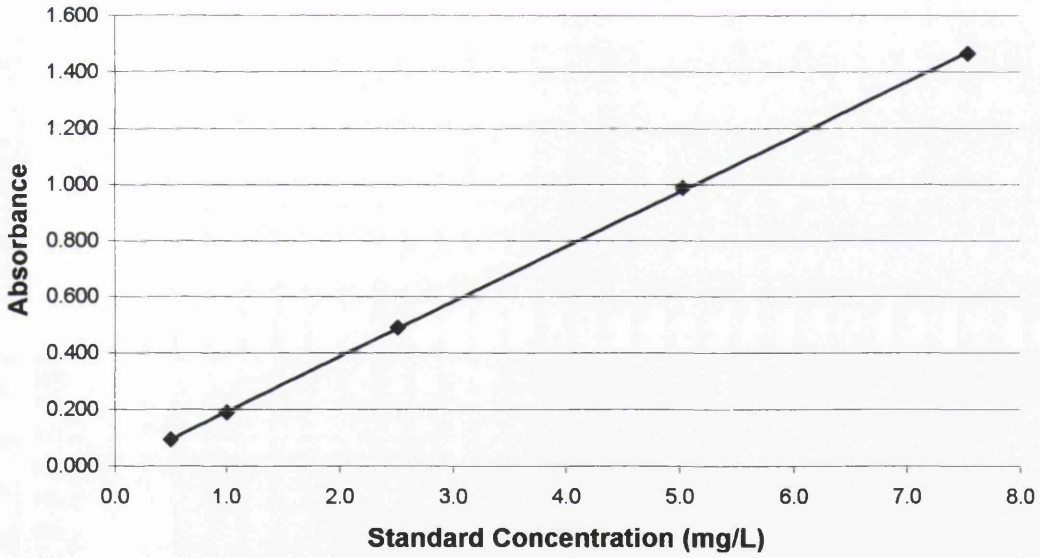

Figure A.3-20 Calibration plot for Caffeine using UV-absorbance at 275nm

A.4 Pump performance curves

A.4.1 Rotaflow pump

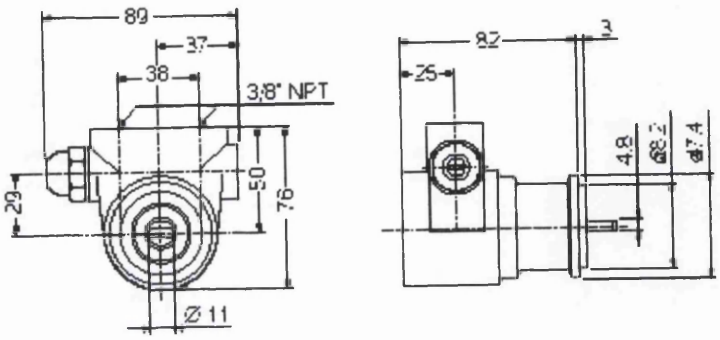

Figure A.4-1 Pump head dimensions (Fluidotech Rotaflow PO311)

MODEL PO/PA	0710	0711	0711F	110	111	111F	1510	1511	1511F	210	211	211F
Flow (l/h) at 2 BAR		100			150			190			236	
Flow (l/h) at 7 BAR		89			139			179			225	
Flow (l/h) at 14 BAR		70			120			160			206	
Figure		A-A			B-B			C-C			D-D	
Mount	Clamp		Flange	Clamp		Flange	Clamp		Flange	Clamp		Flange
By-Pass	NO	YES		NO	YES		NO	YES		NO	YES	
MODEL PO/PA	2510	2511	2511F	310	311	311F	3510	3511	3511F	410	411	411F
Flow (l/h) at 2 BAR		295			345			390			445	
Flow (l/h) at 7 BAR		284			334			379			434	
Flow (l/h) at 14 BAR		265			315			360			415	
Figure		E-E			F-F			G-G			H-H	

Table A.4-1Pump performance data and key for Figure A4-3 (Fluid-o-tech) technical literature

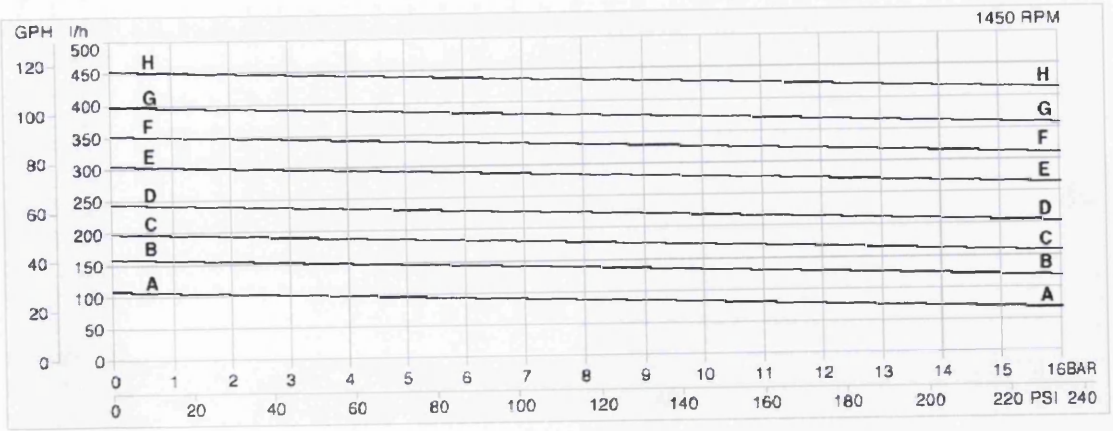

Figure A.4-2 Pump performance curves (Fluid-o-tech technical literature)

A.5 Control and data logging program

A.5.1 Qbasic 4.5

```
'        ********  Filtration Control and Data Logging  ********
'        ********          by Stephen Mandale           ********

DECLARE SUB Communication ()
DECLARE SUB Control ()
DECLARE SUB ControlCold ()
DECLARE SUB DataReadings ()
DECLARE SUB DataSave (Num, T())
DECLARE SUB Equipment (Jn%)
DECLARE SUB EquipmentCold (jcn%)
DECLARE SUB Footnote ()
DECLARE SUB FootNote1 ()
DECLARE SUB Footnote2 ()
DECLARE SUB GraphDataSave (T())
DECLARE SUB GraphDraw (a(), ReadUnit!(), C%(), fsd!(), T0!, T!())
DECLARE SUB GraphFrameSU (C%(), period%)
DECLARE SUB KeyOff ()
DECLARE SUB KeyDefine ()
DECLARE SUB KeyDefineOff ()
DECLARE SUB KeyDefineETS ()
DECLARE SUB KeyDefineEndEx ()
DECLARE SUB KeyDefineEx ()
DECLARE SUB KeyDefineTS ()
DECLARE SUB KeyDefineWW ()
DECLARE SUB KeyOn ()
DECLARE SUB KeyOnEndEx ()
DECLARE SUB KeyOnETS ()
DECLARE SUB KeyOnEx ()
DECLARE SUB KeyOnTS ()
DECLARE SUB KeyOnWW ()
DECLARE SUB KeyWait ()
DECLARE SUB Menu ()
DECLARE SUB PumpOff ()
DECLARE SUB PumpOn ()
DECLARE SUB SafeState ()
DECLARE SUB ScaleSelect2 (Scale$)
DECLARE SUB Valve1On ()
DECLARE SUB Valve1Off ()
DECLARE SUB Variprint ()
DECLARE SUB Warning ()
DECLARE SUB WaterWarm ()
DECLARE SUB WaterWarmOff ()

CONST BASEADD = &H300                  'Base address of card
CONST Datada = 0                       'Port definitions
CONST Mrset = 0
CONST Dactrl = 1
CONST Darset = 1
CONST Stdarq = 2
CONST Dataad = 3
CONST Adctrl = 4
CONST Adrset = 4
CONST Stad = 5
CONST Mux = 6
```

```
CONST Status = 6
CONST PIOA = 8
CONST Piob = 9
CONST Pioc = 10
CONST Pioctrl = 11
CONST TI0 = 12
CONST TI1 = 13
CONST TI2 = 14
CONST Tctrl = 15
CONST adscale = 2.5 / 4095

COMMON SHARED a%, dig%, En!, Er!, exp$, Jn%, jcn%, Num, nt%, period%,
P$
COMMON SHARED reset$, SEn!, SEr!, st%, State$, sp!, T$, tim$, T0, w$,
y%

DIM SHARED a(7, 62), AvChan(6)
DIM SHARED chan(6, 10), C%(7), fsd(6), Reading(6)
DIM SHARED ReadUnit!(6, 60), SAVChan(6), T(60), V$(60), w(62)

P$ = "P"
T$ = "T"

dummy = INP(BASEADD + Mrset)          'Resets DAQ card

OUT BASEADD + Pioctrl, &H80           'Configures digital ports

OUT BASEADD + Adctrl, 1               'Sets a gain of *2 on Analogue
                                      inputs

'ON ERROR GOTO Safemode               'prevents a program from
                                      crashing
                                      'if an error code is generated
st% = 1                               'Sampling interval of one second
C%(1) = 12
C%(2) = 10
C%(3) = 13
C%(4) = 14
C%(5) = 15
C%(6) = 9
C%(7) = 8
fsd(1) = 410
fsd(2) = 100
fsd(3) = 100
fsd(4) = 36.25
fsd(5) = 50
fsd(6) = 50
period% = 30
sp! = 25

ON TIMER(st%) GOSUB Update            'Obtains data at sampling period

GOSUB Start                           'Produces main menu and
                                      configures keyboard

WHILE end$ <> "end"                   'Main program loop
WEND

END                                   'End of main program
```

```
'**** Gosub Routines ****
Dumb:                                   'Ignores incorrect key press
RETURN

EndExperiment:
CLS
CALL KeyOff
CALL KeyOn
CALL KeyDefine
CALL Menu
RETURN

EndTempSetup:
CLS
CALL KeyOff
CALL KeyOn
CALL KeyDefine
CALL Menu
State$ = ""
RETURN

Experiment:
CLS
CALL KeyOff
exp$ = "exp"
a% = 59
Num = 0
OPEN "COM1:2400,N,7,2,CS,DS,OP0" FOR RANDOM AS #4 PRINT #4, T$

FOR i% = 1 TO 10
   CALL DataReadings
   Countdown% = 11 - i%
   LOCATE 12, 38: PRINT Countdown%
   SLEEP 1
NEXT i%
w(62) = w(a% + 1)
FOR j% = 2 TO 6
   a(j%, 62) = AvChan(j%)
NEXT j%

CALL GraphFrameSU(C%(), period%)
y% = period%
CALL KeyDefineEx
CALL KeyOnEx
CALL PumpOn
State$ = "Control"
'reset$ = "reset"
T0 = TIMER
TIMER ON
RETURN

Finish:
SCREEN 9, , 0, 0: CLS 0
SCREEN 9, , 1, 1: CLS 0
end$ = "end"
LOCATE 3, 10: COLOR 10
PRINT "Please turn off equipment before pressing any key to
continue."
RETURN

Refresh:
```

```
CALL Menu
RETURN

Safemode:
CALL SafeState
RETURN

Screenhold:
TIMER OFF
VIEW: WINDOW
CLS
CALL PumpOff
CALL WaterWarmOff
CALL Footnote2
CALL KeyOff
CALL KeyDefineETS
CALL KeyOnETS
warmup$ = ""
ERASE a
RETURN

ScreenHold2:
TIMER OFF
VIEW: WINDOW
CLS
CLOSE #4
State$ = "ExpEnd"
exp$ = ""
CALL DataSave(Num, T())
ERASE a
State$ = ""
reset$ = "reset"

CALL PumpOff
CALL WaterWarmOff
CALL Footnote2
CALL KeyOff
CALL KeyDefineEndEx
CALL KeyOnEndEx
RETURN

Start:
CALL KeyDefine
CALL KeyOn
CALL Menu
RETURN

StartSetParam:                    'This Gosub-routine redefines
CLS                               'keyboard function, starts timer
State$ = "paramadj"
CALL KeyOff                       'and after a pause engages the
                                  pump
CALL Footnot                      'When the timer is the program
CALL KeyDefineOff                 'calls the update gosub every
                                  second

CALL KeyOn
T0 = TIMER
TIMER ON
SLEEP 1
CALL PumpOn
RETURN
```

```
StopSetParam:                          'stops parameter setup brings
TIMER OFF
State$ = ""                            'back original settings and menu
SLEEP 3
CALL PumpOff
CLS
CALL KeyOff
CALL KeyOn
CALL KeyDefine
CALL Menu
RETURN

Tare:
OPEN "COM1:2400,N,7,2,CS,DS,OP0" FOR RANDOM AS #3
PRINT #3, T$
CLOSE #3
RETURN

TempSetup:
CLS
CALL KeyOff
CALL GraphFrameSU(C%(), period%)
y% = period%
a% = 59
CALL DataReadings
CALL KeyDefineTS
CALL KeyOnTS
reset$ = "reset"
State$ = "Control"
warmup$ = "warmup"
CALL Control
CALL ControlCold
T0 = TIMER
TIMER ON
CALL PumpOn
RETURN

Update:
IF State$ <> "Runthro" THEN
  CALL DataReadings
END IF

'IF ReadUnit!(2, a%) > 60 THEN
' CALL PumpOff
' CALL Warning
'END IF

IF a% = 60 THEN a% = 0
T(a% + 1) = (TIMER - T0) / 60

IF warmup$ = "warmup" THEN
  CALL Variprint
    IF y% = period% THEN
      CALL GraphDraw(a(), ReadUnit!(), C%(), fsd(), T0, T())
      CALL GraphDataSave(T())
      y% = 0
    END IF
  y% = y% + 1
END IF
```

```
IF State$ = "Control" THEN
  CALL Control
  CALL ControlCold
END IF
reset$ = ""

IF exp$ = "exp" THEN
  CALL Variprint
    IF y% = period% THEN
      CALL GraphDraw(a(), ReadUnit!(), C%(), fsd(), T0, T())
      CALL GraphDataSave(T())
      y% = 0
    END IF
  y% = y% + 1
  'CALL Communication
  'w(a%) = VAL(w$)
  IF a% = 60 THEN
    CALL DataSave(Num, T())
    a% = 0
  END IF
END IF

IF State$ = "Runthro" THEN
  IF nt% < 300 THEN
    LOCATE 11, 10: PRINT USING "###"; nt%
  END IF

  IF nt% >= 300 THEN
    GOSUB WaterWarmEnd
  END IF
END IF
nt% = nt% + st%
RETURN

WaterWarm:
nt% = 0
CALL WaterWarm
CLS
LOCATE 10, 10: PRINT "Water Run through"
State$ = "Runthro"
T0 = TIMER
TIMER ON
CALL KeyOff
CALL KeyDefineWW
CALL KeyOnWW
RETURN

WaterWarmEnd:
TIMER OFF
CALL WaterWarmOff
State$ = ""
CALL Menu
CALL KeyOff
CALL KeyOn
CALL KeyDefine
RETURN


'*****Sub Routines*****
```

```
SUB Communication

PRINT #4, P$
INPUT #4, w$

END SUB

SUB Control

'STATIC SEn!, En!                       'Ensures that values are
                                        remembered in this sub-routine.

'IF TIMER - T0 < 10 THEN
'En! = 0
'SEn! = 0
'Jn% = 0
'END IF

IF reset$ = "reset" THEN
En! = 0
SEn! = 0
Jn% = 0
END IF

Kc! = 30                                'Prop. gain
TI! = 15                                'Integral time
Jo% = 0

Ste! = ((Kc! * (En! + ((st% / TI!) * (SEn! + En!)))) / 100)
IF Ste! > 20 THEN En! = 0
SEn! = SEn! + En!                       'Sum of all previous errors
En! = sp! - AvChan(5) 'ReadUnit!(5, A%)
                                        'Error


Jn% = Jo% + ((Kc! * (En! + ((st% / TI!) * (SEn! + En!)))) / 100)


IF Jn% > 20 THEN
Jn% = 20                                'Effectively prevents integ.
                                        windup
END IF

IF SEn! < 0 THEN
SEn! = 0
END IF

IF Jn% < 0 THEN
Jn% = 0
END IF

                                        'Control command
LOCATE 5, 50
PRINT USING "       ##"; Jn%
LOCATE 6, 50
PRINT USING "##########"; SEn!
LOCATE 7, 50
PRINT USING "##########"; En!
```

```
CALL Equipment(Jn%)

END SUB

SUB ControlCold

'STATIC SEr!, Er!                       'Ensures that values are
                                        remembered in this sub-routine.

'IF TIMER - T0 < 10 THEN
'Er! = 0
'SEr! = 0
'jcn% = 0
'END IF

IF reset$ = "reset" THEN
Er! = 0
SEr! = 0
jcn% = 0
END IF

Kcc! = 30                               'Prop. gain
TIc! = 15                               'Integral time
Jco% = 0

Stec! = ((Kcc! * (Er! + ((st% / TIc!) * (SEr! + Er!)))) / 100)
IF Stec! < -20 THEN Er! = 0
SEr! = SEr! + Er!                       'Sum of all previous errors
Er! = sp! - AvChan(5) 'ReadUnit!(5, A%)
                                        'Error


jcn% = Jco% + ((Kcc! * (Er! + ((st% / TIc!) * (SEr! + Er!)))) / 100)

IF jcn% < -20 THEN
jcn% = -20
END IF

IF SEr! > 0 THEN
SEr! = 0
END IF

IF jcn% > 0 THEN
jcn% = 0
END IF


                                        'Control command
LOCATE 5, 40
PRINT USING "       ##"; jcn%
LOCATE 6, 40
PRINT USING "#########"; SEr!
LOCATE 7, 40
PRINT USING "#########"; Er!

CALL EquipmentCold(jcn%)

END SUB
```

```
SUB DataReadings

FOR N% = 2 TO 6
  OUT BASEADD + Mux, (N% - 1) * 16  'Reads each channel in isolation.

  OUT BASEADD + Stad, 0             'Converts signal from
                                    'voltage to a binary signal

    WHILE INP(BASEADD + Status) AND 1
                                          'Waits until conversion is
                                          complete.
    WEND

  lowval = INP(BASEADD + Dataad)          'The port is read in two
  hival = INP(BASEADD + Dataad)           'sections this section
  Reading(N%) = hival * 256 + lowval      'converts it to one No.

'IF N% = 1 THEN
'ReadUnit!(N%, a%) = 0                    'Converts from bin to units

IF N% = 2 THEN
ReadUnit!(N%, a%) = (.00000000000137# * Reading(N%) ^ 4) + (-
.00000000530977# * Reading(N%) ^ 3) + (.00000683511# * Reading(N%) ^
2) + (.0299110239# * Reading(N%)) + .84750304816#

ELSEIF N% = 3 THEN
ReadUnit!(N%, a%) = (.000000000015# * Reading(N%) ^ 4) + (-
.0000000243569# * Reading(N%) ^ 3) + (.0000093328718# * Reading(N%) ^
2) + (.0839055464682# * Reading(N%)) + .9916762321082#


ELSEIF N% = 4 THEN
ReadUnit!(N%, a%) = (.00000000000037# * Reading(N%) ^ 4) +
(.00000000201321# * Reading(N%) ^ 3) + (-.0000036896961# *
Reading(N%) ^ 2) + (.01704990185651# * Reading(N%)) +
.93883429070553#

ELSEIF N% = 5 THEN
ReadUnit!(N%, a%) = (8.0855D-14 * Reading(N%) ^ 4) +
(.00000000060899# * Reading(N%) ^ 3) + (.0000018148# * Reading(N%) ^
2) + (.028353 * Reading(N%)) + 2.2125

ELSEIF N% = 6 THEN
ReadUnit!(N%, a%) = (3.4096D-14 * Reading(N%) ^ 4) + (-
.00000000026226# * Reading(N%) ^ 3) + (.00000091797# * Reading(N%) ^
2) + (.02918 * Reading(N%)) + 2.0595
END IF

'IF State$ <> "paramadj" THEN
'VIEW: WINDOW
'COLOR C%(2)
'LOCATE 4, 73: PRINT USING "###.#"; ReadUnit!(2, a%)
'COLOR C%(3)
'LOCATE 7, 73: PRINT USING "###.#"; ReadUnit!(3, a%)
'COLOR C%(4)
'LOCATE 11, 73: PRINT USING "###.#"; ReadUnit!(4, a%)
'COLOR C%(5)
'LOCATE 14, 73: PRINT USING "###.#"; ReadUnit!(5, a%)
'COLOR C%(6)
'LOCATE 18, 73: PRINT USING "###.#"; ReadUnit!(6, a%)
'END IF
```

```
IF exp$ = "exp" THEN                    'calls sub that communicates with
                                        balance
 CALL Communication
 w(a% + 1) = VAL(w$)

END IF

IF State$ = "paramadj" THEN             'prints screen for
                                        parameter set up

LOCATE (4 + N%), 10
 COLOR 15
 IF N% = 2 THEN
 PRINT "PM Pressure"

 ELSEIF N% = 3 THEN
 PRINT "CF Pressure"

 ELSEIF N% = 4 THEN
 PRINT "Flow rate"

 ELSEIF N% = 5 THEN
 PRINT "Feed temperature"

 ELSEIF N% = 6 THEN
 PRINT "PM Temperature"
 END IF
LOCATE (4 + N%), 50
 PRINT USING "  #####"; Reading(N%);
 'PRINT USING "  #.###"; Reading(N%) * adscale;
 'PRINT USING "  ##.#"; ReadUnit!(N%, a%)
END IF
NEXT N%

FOR i% = 2 TO 6                         'This stores readings in
        SAVChan(i%) = SAVChan(i%) - chan(i%, 10)
                                        'an array, moving the
                                        values
        FOR g% = 10 TO 2 STEP -1        'along to give an average
                chan(i%, g%) = chan(i%, g% - 1)
                                        'of the last 10 values.
        NEXT g%
        chan(i%, 1) = ReadUnit!(i%, a%)
        SAVChan(i%) = SAVChan(i%) + chan(i%, 1)
        AvChan(i%) = SAVChan(i%) / 10
        LOCATE (4 + i%), 40
        COLOR 12
        IF State$ = "paramadj" THEN
         PRINT USING "##.#"; AvChan(i%) '* adscale
        END IF
NEXT i%

END SUB

SUB DataSave (Num, T())

Num = Num + 1                           'Creates data file
IF Num = 1 THEN
        X$ = LEFT$(TIME$, 2)
        y$ = RIGHT$(LEFT$(TIME$, 5), 2)
```

```
        tim$ = X$ + y$
END IF

m$ = LEFT$(DATE$, 2)

SELECT CASE m$
        CASE IS = "01"
                m$ = "Ja"
        CASE IS = "02"
                m$ = "Fe"
        CASE IS = "03"
                m$ = "Mr"
        CASE IS = "04"
                m$ = "Ap"
        CASE IS = "05"
                m$ = "My"
        CASE IS = "06"
                m$ = "Jn"
        CASE IS = "07"
                m$ = "Jl"
        CASE IS = "08"
                m$ = "Au"
        CASE IS = "09"
                m$ = "Se"
        CASE IS = "10"
                m$ = "Oc"
        CASE IS = "11"
                m$ = "No"
        CASE IS = "12"
                m$ = "De"
END SELECT

finame$ = "C:\Filtrate\Exdata\" + RIGHT$(LEFT$(DATE$, 5), 2) + m$ +
tim$ + ".sav"

OPEN finame$ FOR APPEND AS #5

IF Num = 1 THEN
        PRINT #5, "Time-(min) ";
        PRINT #5, "Total-Filtrate-mass-(g) ";
        PRINT #5, "Pre-membrane-pressure-(p.s.i) ";
        PRINT #5, "Post-membrane-pressure-(p.s.i) ";
        PRINT #5, "Crossflow-rate-(ml/s) ";
        PRINT #5, "Temperature-feed-tank-(øC) ";
        PRINT #5, "Temperature-feed-(øC) "
        PRINT #5,
END IF

IF TIMER - T0 < 5 THEN
      PRINT #5, T(60);              'Actual time of the
                                    measurement
      PRINT #5, w(62);
      FOR j% = 2 TO 6
        PRINT #5, a(j%, 62);        'Different parameters
                                    measured
      NEXT j%
      PRINT #5,
ELSE
'IF TIMER - T0 > 5 THEN
      FOR i% = 61 - a% TO 60
        PRINT #5, T(i% + a% - 60);  'Actual time of the
```

```
                                    measurement
        PRINT #5, w(i% + a% - 60);
      FOR j% = 2 TO 6
        PRINT #5, a(j%, i%);        'Different parameters
                                    measured
      NEXT j%
      PRINT #5,
      NEXT i%
END IF
CLOSE #5

END SUB

SUB Equipment (Jn%)                 'when parameters are
                                    defined in this way it
                                    ensures they are shared
                                    between the routines and
                                    programs in which they are
                                    stated

STATIC T%

IF T% = 0 THEN
        'dig% = INP(BASEADD + PIOA)
        'dig% = dig% AND 253        'Switch cold water off
        'OUT (BASEADD + PIOA), dig%

        dig% = INP(BASEADD + PIOA)
        dig% = dig% AND 254         'Switch hot water off
        OUT (BASEADD + PIOA), dig%
END IF

IF T% = 20 - Jn% THEN
        dig% = INP(BASEADD + PIOA)
        dig% = dig% OR 1            'Switch hot water on
        OUT (BASEADD + PIOA), dig%

END IF


T% = T% + 1                         'Counts from zero to ten
IF T% >= 20 THEN T% = 0             ensuring that control is
                                    actuated
END SUB

SUB EquipmentCold (jcn%)

STATIC Tc%

IF Tc% = 0 THEN
        dig% = INP(BASEADD + PIOA)
        dig% = dig% AND 253         'Switch cold water off
        OUT (BASEADD + PIOA), dig%
END IF

IF Tc% = 20 + jcn% THEN
        dig% = INP(BASEADD + PIOA)
        dig% = dig% OR 2            'Switch cold water on
        OUT (BASEADD + PIOA), dig%

END IF
```

```
Tc% = Tc% + 1                          'Counts from zero to ten
IF Tc% >= 20 THEN Tc% = 0              'ensuring that control is

END SUB

SUB Footnote

LOCATE 15, 5: COLOR 15
PRINT "Press F1 when you have completed parameter adjustment"
LOCATE 16, 5: COLOR 15
PRINT "to finish and return to the main menu."

END SUB

SUB FootNote1

LOCATE 15, 5: COLOR 15
PRINT "Press F2 when system has reached operating temperature,"
LOCATE 16, 5: COLOR 15
PRINT "to finish."

END SUB

SUB Footnote2

LOCATE 18, 5: COLOR 15
PRINT "Press F3 to return to the Main Menu."

END SUB

SUB FootNote3

LOCATE 15, 5: COLOR 15
PRINT "Press F2 when Experiment is Complete."

END SUB

SUB GraphDataSave (T())

CALL KeyWait

VIEW: WINDOW

IF exp$ = "exp" THEN
COLOR C%(1)
LOCATE 21, 73: PRINT USING "###.##"; w(a% + 1COLOR C%(7)
LOCATE 10, 10: PRINT USING "###.#"; T(a% + 1); : PRINT " min"
COLOR C%(7)
LOCATE 11, 11: PRINT USING "##.#"; a%; : PRINT " a%" 'WARNING this is
******

VIEW                                   'Indicate data that has not been
                                       saved
VIEW (47, 339)-(527, 349): WINDOW (0, 0)-(60, 1)

LINE (0, 0)-(60 - a%, 1), 8, BF        'Remove the last
a% = a% + 1                            'indicator

LINE (60 - (a% / (period% / period%)), 0)-(60, 1), 4, BF
                                       'Show the current
```

```
END IF

CALL KeyOnTS

END SUB

SUB GraphDraw (a(), ReadUnit!(), C%(), fsd(), T0, T())

CALL KeyWait

VIEW: WINDOW
                                    'Define a window for display of
                                    graph
VIEW (47, 19)-(527, 299): WINDOW (0, 0)-(60, 100)

IF TIMER - T0 < 5 THEN
   FOR j% = 2 TO 6                  'Assign data chan to a
      a(j%, 61) = a(j%, 62)
   NEXT j%
   a(1, 61) = w(62)
ELSE
   FOR j% = 2 TO 6                  'Assign data chan to a
      a(j%, 61) = AvChan(j%)  'ReadUnit!(j%, a%)
   NEXT j%
   a(1, 61) = w(a% + 1)
END IF

FOR i% = 0 TO 59                    'Erase old graph line and draw
                                    new graph line
 FOR j% = 1 TO 6
 LINE (i%, a(j%, i%) * 100 / fsd(j%))-(i% + 1, a(j%, i% + 1) * 100 /
fsd(j%)), 8
 LINE (i%, a(j%, i% + 1) * 100 / fsd(j%))-(i% + 1, a(j%, i% + 2) *
100 / fsd(j%)), C%(j%)
 NEXT j%
NEXT i%

                                    'Re-enforce graph line and shift
                                    to make the graph move
FOR j% = 1 TO 6
   LINE (0, a(j%, 1) * 100 / fsd(j%))-(1, a(j%, 2) * 100 / fsd(j%)),
C%(j%)
      FOR i% = 0 TO 60
          LINE -(i%, a(j%, i% + 1) * 100 / fsd(j%)), C%(j%)
          a(j%, i%) = a(j%, i% + 1)
                                    'shift
      NEXT i%
NEXT j%

LINE (0, 0)-(60, 100), 11, B        'Redraw the box for the chart
                                    graph, since the box is erased
                                    after each run

CALL KeyOnTS

END SUB

SUB GraphFrameSU (C%(), period%)

                                    'This is the warm-up temperature
```

```
                                    display graph
                                    'Draw frame for graph on screen 1
VIEW: WINDOW
IF exp$ = "" THEN
 LOCATE 1, 55: COLOR 6              'Put on an abort reminder
 PRINT "Press F2 to abort warm-up"
 LOCATE 1, 25: COLOR 11
 PRINT "Temp-Setup Graph"
ELSEIF exp$ = "exp" THEN
 LOCATE 1, 55: COLOR 6              'Put on a finish reminder
 PRINT "Press F2 to finish"
 LOCATE 1, 25: COLOR 11
 PRINT "Experimental Data"
END IF

LINE (47, 19)-(527, 299), 11, B     'Draw the outer frame
LINE (527, 19)-(639, 299), 11, B
LINE (48, 20)-(526, 298), 8, BF     'Background colour for the graph

FOR j% = 1 TO 5                     'Draw frames for parameter text
    LINE (527, j% * 280 / 6 + 22)-(639, j% * 280 / 6 + 22), 11
NEXT j%

FOR j% = 0 TO 10                    'Scale y-axis
    LINE (47, 19 + j% * 28)-(43, 19 + j% * 28), 11
NEXT j%

FOR j% = 100 TO 0 STEP -10          'Numbering of y-axis
    LOCATE 22 - j% / 5, 1: COLOR 11: PRINT j%
NEXT j%

LOCATE 1, 1: PRINT "f.s.d (%)"      'Title for y-axis

FOR j% = 0 TO 59                    'Scale x-axis (minor divisions)
    LINE (47 + j% * 8, 299)-(47 + j% * 8, 301), 11
NEXT j%

FOR j% = 0 TO 6                     '(Major divisions)
    LINE (47 + j% * 80, 299)-(47 + j% * 80, 303), 11
NEXT j%

FOR j% = 0 TO 6                     'Numbering of x-axis
LOCATE 23, 65 - j% * 10: PRINT j% * period% / 6
NEXT j%

LOCATE 24, 20
PRINT "Data Points (approx";        'Title for x-axis
PRINT period% / 60;
PRINT "min. intervals)";


                                    'Print the parameter name and the
                                    corresponding colour in the
                                    parameter frames

LOCATE 3, 68: COLOR C%(2): PRINT "PM Pressure";
       LOCATE 4, 68: PRINT "p.s.i."
LOCATE 6, 68: COLOR C%(3): PRINT "CF Pressure";
       LOCATE 7, 68: PRINT "p.s.i."
LOCATE 10, 68: COLOR C%(4): PRINT "Flow Rate"
       LOCATE 11, 68: PRINT "ml/s"
LOCATE 13, 68: COLOR C%(5): PRINT "Feed Temp"
```

```
        LOCATE 14, 68: PRINT CHR$(248); : PRINT "C"
LOCATE 17, 68: COLOR C%(6): PRINT "PM Temp"
        LOCATE 18, 68: PRINT CHR$(248); : PRINT "C"
IF exp$ = "exp" THEN

 LOCATE 20, 68: COLOR C%(1): PRINT "Weight"
 LOCATE 21, 68: COLOR C%(1): PRINT "g"
 VIEW                                'Saving reminder
 VIEW (47, 339)-(527, 349): WINDOW (0, 0)-(60, 1)
 LINE (0, 0)-(60, 1), 8, BF
 LOCATE 25, 68: COLOR 4: PRINT "Not saved";
 LOCATE 25, 1: COLOR 8: PRINT "Saved";
END IF

END SUB

SUB KeyDefine


ON KEY(1) GOSUB StartSetParam
ON KEY(2) GOSUB TempSetup
ON KEY(3) GOSUB Experiment
ON KEY(8) GOSUB WaterWarm
ON KEY(9) GOSUB refresh
ON KEY(10) GOSUB finish

END SUB

SUB KeyDefineEndEx

ON KEY(3) GOSUB EndExperiment

END SUB

SUB KeyDefineETS

ON KEY(3) GOSUB EndTempSetup

END SUB

SUB KeyDefineEx

ON KEY(2) GOSUB ScreenHold2


END SUB

SUB KeyDefineOff

ON KEY(1) GOSUB StopSetParam

END SUB

SUB KeyDefineTS

ON KEY(2) GOSUB Screenhold

END SUB

SUB KeyDefineWW
```

```
ON KEY(8) GOSUB WaterWarmEnd


END SUB

SUB KeyOff

KEY(1) OFF
KEY(2) OFF
KEY(3) OFF
KEY(4) OFF
KEY(5) OFF
KEY(6) OFF
KEY(7) OFF
KEY(8) OFF
KEY(9) OFF
KEY(10) OFF

ON KEY(1) GOSUB Dumb
ON KEY(2) GOSUB Dumb
ON KEY(3) GOSUB Dumb
ON KEY(4) GOSUB Dumb
ON KEY(5) GOSUB Dumb
ON KEY(6) GOSUB Dumb
ON KEY(7) GOSUB Dumb
ON KEY(8) GOSUB Dumb
ON KEY(9) GOSUB Dumb
ON KEY(10) GOSUB Dumb

END SUB

SUB KeyOn

KEY(1) ON
KEY(2) ON
KEY(3) ON
'KEY(4) ON
'KEY(5) ON
'KEY(6) ON
'KEY(7) ON
KEY(8) ON
KEY(9) ON
KEY(10) ON

END SUB

SUB KeyOnEndEx

KEY(3) ON

END SUB

SUB KeyOnETS

KEY(3) ON

END SUB

SUB KeyOnEx

KEY(2) ON
```

```
END SUB

SUB KeyOnTS

KEY(2) ON

END SUB

SUB KeyOnWW

KEY(8) ON

END SUB

SUB KeyWait

KEY(1) STOP
KEY(2) STOP
KEY(3) STOP
KEY(4) STOP
KEY(5) STOP
KEY(6) STOP
KEY(7) STOP
KEY(8) STOP
KEY(9) STOP
KEY(10) STOP

END SUB

SUB Menu

SCREEN 9, , 0, 0: COLOR 15, 0: CLS 0
LOCATE 1, 36: PRINT "MAIN MENU"
LOCATE 2, 36: PRINT "ÍÍÍÍÍÍÍÍÍ"
LOCATE 8, 15: PRINT "F1  =  Parameter Setup"
LOCATE 9, 15: PRINT "F2  =  Warmup Routine"
LOCATE 10, 15: PRINT "F3  =  Experiment Start"
LOCATE 11, 15: PRINT "F4  = "
LOCATE 12, 15: PRINT "F5  = "
LOCATE 13, 15: PRINT "F6  = "
LOCATE 14, 15: PRINT "F7  = "
LOCATE 15, 15: PRINT "F8  =  Run heat transfer water"
LOCATE 16, 15: PRINT "F9  =  Refresh screen"
LOCATE 17, 15: PRINT "F10 =  Exit"

END SUB

SUB Modifications

                                    '13/12/01       SJM
                                    Removed sections of program that
                                    were resetting the control
                                    parameters after setting up the
                                    equipment to steady state and
                                    before starting an experiment.
                                    Added a section to the Experiment
                                    GOSUB routine so that 10 seconds
                                    of readings are taken from the
                                    equipment before starting from
```

```
                                    time zero. This fills the
                                    averaging data array and
                                    therefore gives sensible/correct
                                    data readings at time zero.
                                    Corrected data readings so that
                                    at time zero the values at this
                                    time were recorded; before the
                                    data readings were offset by 30
                                    seconds.

END SUB

SUB PumpOff

dig% = INP(BASEADD + PIOA)
dig% = dig% AND 251
OUT (BASEADD + PIOA), dig%

END SUB

SUB PumpOn

dig% = INP(BASEADD + PIOA)
dig% = dig% OR 4
OUT (BASEADD + PIOA), dig%

END SUB

SUB SafeState

SCREEN 9, , 0, 0: COLOR 15, 0: CLS 0
LOCATE 1, 36: PRINT "S A F E  M O D E"
LOCATE 2, 36: PRINT "ÍÍÍÍÍÍÍÍÍÍÍÍÍÍÍÍ"
COLOR 7
LOCATE 4, 4
PRINT "Due to an error during the program execution, equipment has
been"
LOCATE 5, 4: PRINT "shut down."
LOCATE 7, 4: PRINT "Unrecoverable error"; ERR
END

END SUB

SUB Variprint

VIEW: WINDOW
COLOR C%(2)
LOCATE 4, 73: PRINT USING "###.#"; AvChan(2)   'ReadUnit!(2, A%)
COLOR C%(3)
LOCATE 7, 73: PRINT USING "###.#"; AvChan(3)   'ReadUnit!(3, A%)
COLOR C%(4)
LOCATE 11, 73: PRINT USING "###.#"; AvChan(4)  'ReadUnit!(4, A%)
COLOR C%(5)
LOCATE 14, 73: PRINT USING "###.#"; AvChan(5)  'ReadUnit!(5, A%)
COLOR C%(6)
LOCATE 18, 73: PRINT USING "###.#"; AvChan(6)  'ReadUnit!(6, A%)

END SUB

SUB Warning
```

```
LOCATE 4, 20: COLOR 12
PRINT "WARNING: 60 psi has been exceeded"

END SUB

SUB WaterWarm

dig% = INP(BASEADD + PIOA)
dig% = dig% OR 1                    'Switch hot water on
OUT (BASEADD + PIOA), dig%

dig% = INP(BASEADD + PIOA)
dig% = dig% OR 2                    'Switch cold water on
OUT (BASEADD + PIOA), dig%

END SUB

SUB WaterWarmOff

 dig% = INP(BASEADD + PIOA)
 dig% = dig% AND 253                'Switch cold water off
 OUT (BASEADD + PIOA), dig%

 dig% = INP(BASEADD + PIOA)
 dig% = dig% AND 254                'Switch hot water off
 OUT (BASEADD + PIOA), dig%


END SUB
```

A.6 Circuit and wiring diagrams for experimental equipment

A.6.1 Signal conditioner

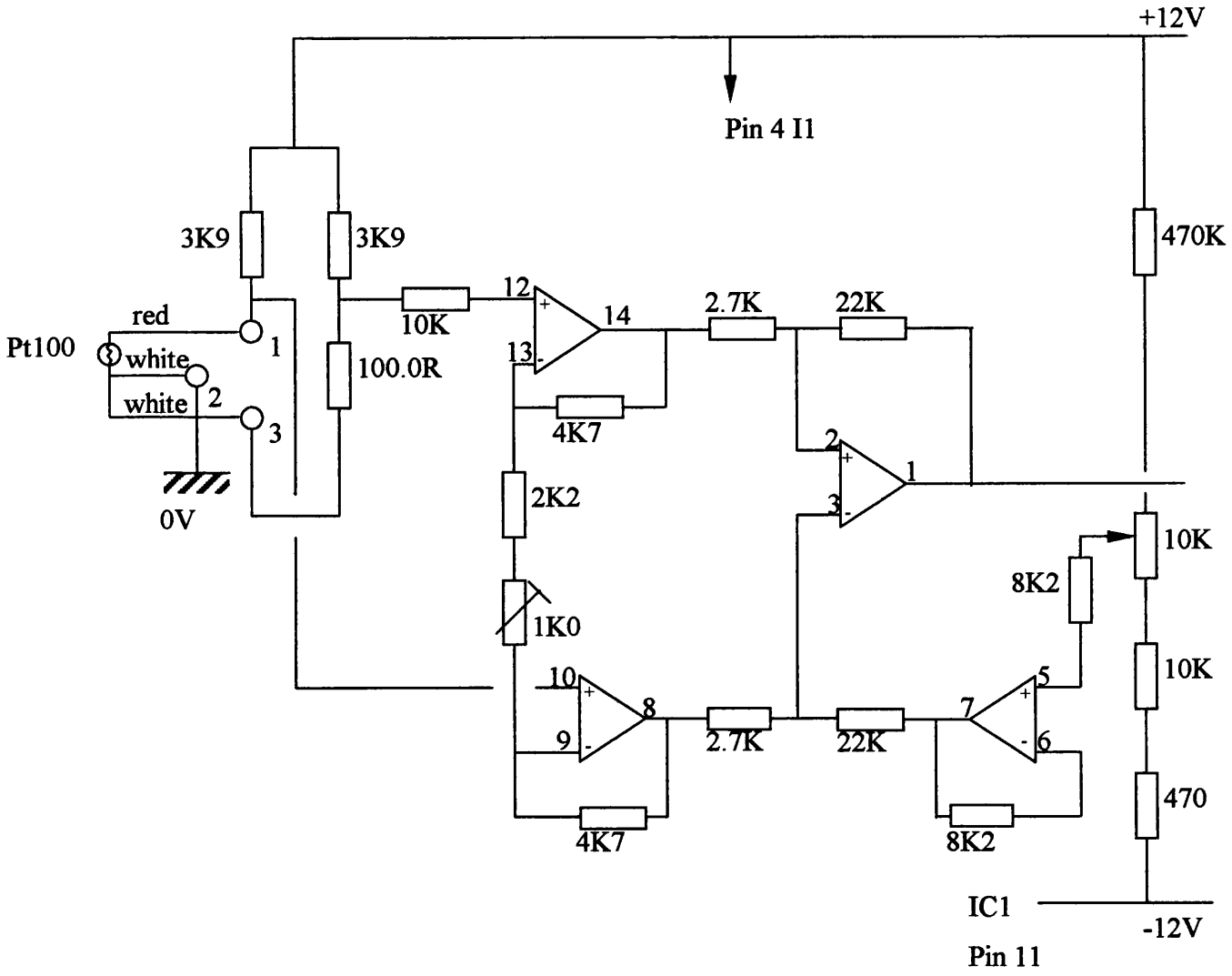

Figure A.6-1 Platinum resistance thermometer signal conditioner circuit

The circuit diagram shown in Figure A.6-1 conditions the voltage signal acquired from the platinum resistance thermometer such that it is recognisable by the DAC installed on the control and data logging PC. Similar circuits are used for flow and pressure signal conditioning.

A.6.2 Relay power control unit

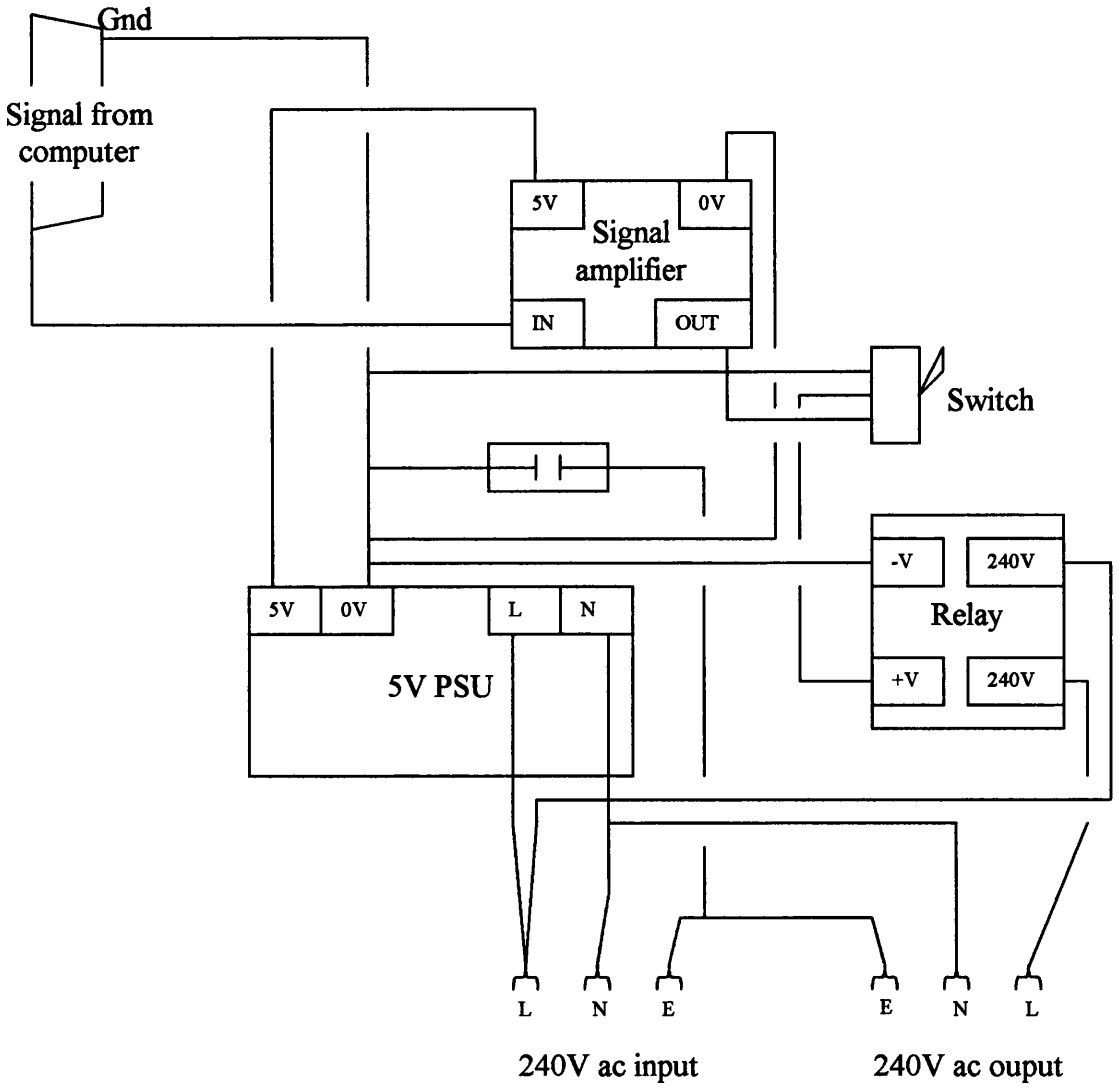

Figure A.6-2 Wiring diagram for relay control box

The wiring diagram shown in Figure A.6-2 converts a small signal voltage produced by the PC, via its on-board digital-analogue/analogue-digital converter, into a larger voltage suitable for switching the relay. The relay supplies mains (240V ac) power to the solenoid valves on the heat exchanger, and to the pump. This wiring diagram presents 1/3 of the contents of the relay unit, as three relays are operated.

A.7 Heat exchanger design

The pump is determined to have a heating effect of 0.032 kJ/s, thus at a average mass flow rate of 0.04 kg/s (4 ml/s) a temperature increase from 25°C to 26.915°C is possible (assuming water has a heat capacity of 4.177 kJ/kg K). To remove this energy a stream of cooling water supplied at 19°C and at a flow rate of 0.1 kg/s would have to be heated to a temperature of 19.077°C.

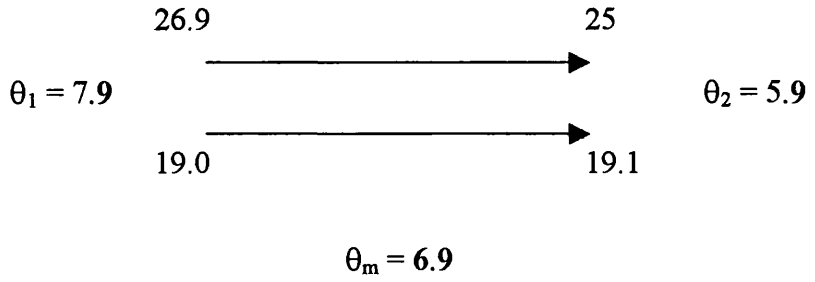

Figure A.7-1 Log-mean temperature difference of a co-current system (values in °C)

The diagram shown in Figure A.7-1 presents the calculation for the log mean temperature difference in a co-currently operated heat exchanger. Table A.7-1 shows the pipe dimensions and corresponding fluid velocities.

Pipe details (process fluid)		
Outside diameter	0.25	Inches
Wall thickness	0.035	Inches
Inside diameter	0.18	Inches
	0.0046	m
Cross sectional area	1.64E-05	m^2
Velocity (0.000004 m^3/s)	0.24	m/s

Table A.7-1Specification of process piping

The heat exchanger takes the form of a singular concentric tube layout with the process fluid flowing through the inner tube and the cooling/heating fluid flowing in the annulus between the inner and out pipes. At a mass flow rate of 0.1 kg/s the fluid velocity in the annulus is 0.70 m/s.

On the basis of the following equation for heat transfer,

$$Q = UA\Delta T \tag{1.10}$$

the area necessary for heat transfer, where the heat transfer coefficient is found to be 800 W/m^2 °C (Sinnot, 1993), is 0.0006 m^2, which equates to a heat exchanger that is 3.4 cm in length.

Since this is the heat transfer area required to remove only the heat provided by the pump and there were perceived to be instances where feed temperature was far from the set point value, a heat transfer area approximately ten times that required was used.